Title
The exploitation of nuclear functions by a group of cytoplasmic RNA viruses

Author
Flather, Dylan Paul

Publication Date
2018

Peer reviewed|Thesis/dissertation

UNIVERSITY OF CALIFORNIA,
IRVINE

The exploitation of nuclear functions by a group of cytoplasmic RNA viruses

DISSERTATION

Submitted in partial satisfaction of the requirements for the degree of

DOCTOR OF PHILOSOPHY

in Biomedical Sciences

by

Dylan Paul Flather

Dissertation Committee:
Professor Bert L. Semler, Chair
Professor Rozanne M. Sandri-Goldin
Professor Yongsheng Shi
Professor Michael McClelland

2018

TABLE OF CONTENTS

LIST OF FIGURES

LIST OF TABLES

ACKNOWLEDGMENTS

Scientific understanding can only be advanced through a community of scientists. I have been fortunate to be surrounded by many, both established and in training, in the Semler lab and in the department of Microbiology and Molecular Genetics at UC Irvine.

First and foremost I would like to acknowledge the fact that my advisor, Dr. Bert L. Semler, has been formative in my growth as a scientist. Not only did he provide an environment that promoted good science through open dialogue and collaboration, but just as importantly, he allowed me the independence to, at times, struggle through a meandering path of discovery. He has taught me that without self-motivation and determination, science is not a good career choice. His reductionist thinking and insistence on mechanistic understanding are ingrained in me and are qualities that I will carry with me in all my future research pursuits. I am deeply appreciative of his mentorship and the effort he has put toward making me the scientist I am today.

Former and current members of the Semler lab have also been influential in my scientific pursuits. Dr. Amanda Chase was my mentor when I was a first-year rotation student and I was only able to fully grasp the level of sacrifice this required when I mentored a student years later. Dr. Kerry Fitzgerald, Dr. Ilya Belalov, Dr. Richard Virgen-Slane, Dr. Andrea Cathcart, Dr. Sonia Maciejewski, Dr. Alexis Bouin, Eric Baggs, and Autumn Holmes have all offered their time and energy to help me grow as a scientist through training, suggestions during lab meetings, and providing their editorial skills. Dr. Nicolas Lévêque was one of my favorite people to work with in the lab and provided an outstanding example of how, when you truly care about your work and colleagues, not only will your science be first-rate, but the science around you will improve as well. I would also like to single out Wendy Ullmer. As a nontraditional graduate student she brought a level of expertise to the lab that was truly unmatched. If not for her (sometimes salty) suggestions I would very likely still be trying to perform a Western blot properly. She has made the science in the Semler lab higher quality. Finally, I would like to thank the two people that (along with Bert, of course) make the Semler lab what it is: Hung Nguyen and My Phuong Tran. Without these two tireless technicians very little research would get done. They are always willing to provide cells, offer advice, and share stories during long workdays.

I would also like to acknowledge the extensive work our collaborator, Dr. Paul D. Gershon performed in order to advance the project described in Chapter 3 of this dissertation. He performed all of the mass spectrometry analysis and allocated substantial time and effort to explain what this analysis meant. Moreover, he encouraged thoughtful discussion about enterovirus biology. Without his contributions, the project would have never gotten off the ground.

Adeela Syed trained me in the use of the confocal microscope which was used to generate the images of Chapter 3. I thank her for taking the time to assist me in this process.

I am also grateful for the critical comments and suggestions provided by my committee members: Dr. Rozanne M. Sandri-Goldin, Dr. Yongsheng Shi, and Dr. Michael McClelland. They have challenged me to more completely understand the biology of my projects and I have taken all of their suggestions to heart. I would like to specifically thank Dr. Michael McClelland for his incisive emails and discussions after many of my presentations; they have been of great benefit to my research and forced me to consider things I would not have otherwise.

Finally, I would like to acknowledge the Center for Virus Research for allowing me to meet and discuss life and science with virologists from across the United States, as well as for providing funding for my research through a National Institutes of Health training grant. It was through involvement in this research center that I became aware of the investigator whose lab I will be joining as postdoctoral researcher in the upcoming months. I thank Dr. Jo Ellen Brunner and Crystal Spitale for helping me navigate membership in the CVR.

The scientists in the Semler lab, in the department of Microbiology and Molecular Genetics, and at UC Irvine in general have provided me with numerous examples of how to conduct meaningful research. Furthermore, they have demonstrated the importance of mentoring young scientists. Training of students allows research communities to flourish, and I am grateful to have been part of a passionate and dedicated community during my time at UC Irvine.

CURRICULUM VITAE

Dylan P. Flather

University of California, Irvine
Medical Sciences I, B214
Irvine, CA 92697
(949) 824-6058
dflather@uci.edu

37 W Neapolitan Lane
Long Beach, CA 90803
(970) 227-5010
dylan.flather@gmail.com

EDUCATION

Ph.D., Biomedical Sciences. University of California, Irvine, School of Medicine. Department of Microbiology and Molecular Genetics. Principal Investigator: Bert L. Semler. July 2011- March 2018.

B.S., Chemical and Biological Engineering (Minor: Biochemistry), University of Colorado, Boulder. August 2005-May 2009.

FELLOWSHIPS

Molecular Biology of Eukaryotic Viruses. September 2012-August 2013, September 2014-August 2016. NIH Virology Training Grant (T32 AI 07319), National Institute of Allergy and Infectious Diseases.

HONORS AND AWARDS

Associated Graduate Students Travel Grant; Summer 2016
School of Medicine Student Travel Award; Spring 2014, Summer 2016, Spring 2017
Finalist, Stanley Behrens Fellows in Medicine Program; 2016
Student Travel Award Recipient, American Society for Virology; June 2014, June 2017

PROFESSIONAL AFFILIATIONS/MEMBERSHIPS

American Society for Virology. Member 2014-present
American Institute of Chemical Engineers. Member 2006-2009

PROFESSIONAL EXPERIENCE

Research Associate, Process Chemistry Group. SomaLogic, Inc. Boulder, CO. June 2009-May 2011. (Supervisor: Jeff Carter, Director of Process Chemistry)

PROFESSIONAL DEVELOPMENT EXPERIENCE

Graduate Student Representative. University of California, Irvine. August 2016-August 2017.

Ultracentrifuge Manager. University of California, Irvine. March 2013-January 2018.

Introduction to Biostatistics: an ICTS Research Methods Short Course. University of California, Irvine.

Organizer, Microbiology and Molecular Genetics department seminar series. University of California, Irvine. Academic year 2014-2015.

Mentor, Bridges to the Baccalaureate Program. University of California, Irvine. Summer 2014.

Integrated Training for High Containment BSL3 Laboratories. University of California, Irvine. June 10-14, 2013.

Graduate Student Representative, Preliminary Examination Preparation. University of California, Irvine. Spring 2013.

Summer Soil Institute. Colorado State University. July 8-21, 2012.

PRESENTATIONS

Flather, D., Im, J., Gershon, P. D., and Semler, B.L. 2017. American Society for Virology annual meeting workshop: *Quantitative Proteomics Reveals Novel Players in Human Rhinovirus Replication Through Altered Nuclear Redistribution Patterns.* University of Wisconsin, Madison, WI.

Flather, D., Gershon, P. D., and Semler, B.L. 2016. European Study Group on the Molecular Biology of Picornaviruses (EUROPIC) conference speaker: *Identification and Characterization of Novel Virus-Host Interactions Through Analysis of Nuclear Protein Efflux During Rhinovirus Infection*. Les Diablerets, Switzerland.

Flather, D. 2014, 2015, 2016, 2017. Research in progress seminar series: *Defining and Characterizing the Functional Role of Nuclear Proteins in Enterovirus Replication.* Department of Microbiology and Molecular Genetics, University of California, Irvine.

Flather, D. and Semler, B.L. 2014. American Society for Virology annual meeting workshop: *Isolation of Ribonucleoprotein Complexes Associated with Poliovirus RNA Replication.* Colorado State University, Fort Collins, CO.

Flather, D. and Semler, B.L. 2014. Department retreat poster session: *RNA Affinity-tagged Polioviruses for the Identification of Ribonucleoprotein Complexes Associated with viral RNA replication.* Lake Arrowhead, CA.

Process Chemistry Team, 2011. Seminar: *SOMAmer Synthesis, Scale-up, Research, Development, and Production*. SomaLogic, Inc., Boulder, CO.

PUBLICATIONS

Flather, D., Semler, B.L., and Gershon, P.D. “Quantitative proteomics reveals novel players in human rhinovirus replication through altered nuclear protein distribution patterns.” Manuscript in preparation.

Gilliam, A., Smith, J., **Flather, D.**, Johnston, K., Gansmiller, A., Fishman, D., Edgar, J., Balk, M., Majumdar, S., and Weiss, G. "Affinity-Guided Design of Caveolin-1 Ligands for Deoligomerization." *Journal of Medicinal Chemistry* (2016).

Flather, D., Cathcart, A.L., Cruz, C., Baggs, E., Ngo, T., Gershon, P.D., and Semler, B.L. “Generation of Recombinant Polioviruses Harboring RNA Affinity Tags in the 5′ and 3′ Noncoding Regions of Genomic RNAs.” *Viruses 8*.2 (2016): 39.

Flather, D., and Semler, B.L. “Picornaviruses and nuclear functions: targeting a cellular compartment distinct from the replication site of a positive-strand RNA virus.” *Frontiers in Microbiology* 6 (2015).

Gold, L., Ayers, D., Bertino, J., Bock, C., Bock, A., Brody, E., Carter, J., Cunningham, V., Dalby, A., Eaton, B., Fitzwater, T., **Flather, D.**, et al. “Aptamer-based multiplexed proteomic technology for biomarker discovery.” *PLoS One* 5.12 (2010).

ABSTRACT OF THE DISSERTATION

The exploitation of nuclear functions by cytoplasmic RNA viruses

By

Dylan Flather

Doctor of Philosophy in Biomedical Sciences

University of California, Irvine, 2018

Professor Bert L. Semler, Chair

Picornaviruses have small, positive-sense RNA genomes and are traditionally described as cytoplasmic because their replication is carried out in the cytoplasm of the infected cell. However, a growing body of evidence suggests that proteins that are normally localized to the nucleus of cells have important roles in the replication of viruses in this family. In fact, picornaviruses of the enterovirus genus encode proteinases that directly target the proteins that make up the nuclear pore complex for degradation, resulting in the redistribution of nuclear proteins into the cytoplasm. To better characterize the virus-host interactions that occur throughout the course of an enterovirus infection we utilized two experimental approaches. The first and most direct approach sought to determine the proteome of poliovirus replication complexes. We developed recombinant viruses containing aptamer tag insertions within their genome, for biochemical isolation of viral RNA and associated proteins from infected cells. Despite the stable insertion of exogenous sequence specific for positive- or negative-strand purification, we were unable to isolate these RNAs. However, this work provides a template for similar studies with superior isolation techniques. Through a more indirect approach, we used

quantitative protein mass spectrometry to identify proteins that both increase in abundance in the cytoplasm of human rhinovirus 16 (HRV16)-infected cells. We used molecular methods to validate the involvement of SFPQ in HRV16 replication, confirming that our cytoplasmic enrichment screen is an effective approach to reveal novel viral replication factors. In subsequent investigations, we aim to combine these distinct but complementary approaches to expand the known array of host proteins that may normally be found within the nucleus but are required for enterovirus replication. The work presented in this dissertation reinforces the idea that enteroviruses are not unambiguously cytoplasmic in nature, presents new methodologies for describing virus-host interactions in molecular detail, and provides direct evidence for a novel nuclear factor in the replication cycle of HRV16. Only through taking a more integrated view of the enterovirus-infected cell can we gain a deeper understanding of enterovirus biology and foster the development of treatments for a group of viruses that continue to burden society.

CHAPTER 1

Introduction: The interplay between picornaviruses and nuclear functions

Summary

The compartmentalization of DNA replication and gene transcription in the nucleus and protein production in the cytoplasm is a defining feature of eukaryotic cells. The nucleus functions to maintain the integrity of the nuclear genome of the cell and to control gene expression based on intracellular and environmental signals received from the cytoplasm. The spatial separation of the major processes that lead to the expression of protein-coding genes establishes the necessity of a transport network to allow biomolecules to translocate between these two regions of the cell. The nucleocytoplasmic transport network is therefore essential for regulating normal cellular function. The *Picornaviridae* virus family is one of many viral families that disrupt the nucleocytoplasmic trafficking of cells to promote viral replication. Picornaviruses possess positive-sense, single-stranded RNA genomes and replicate in the cytoplasm of infected cells. As a result of the limited coding capacity of these viruses, cellular proteins are required by these intracellular parasites for both translation and genomic RNA replication. Being of messenger RNA polarity, a picornavirus genome can immediately be translated upon entering the cell cytoplasm. However, the replication of viral RNA requires the activity of RNA-binding proteins, many of which function in host gene expression, and are consequently localized to the nucleus. As a result, picornaviruses disrupt nucleocytoplasmic trafficking to exploit protein functions normally localized to a different cellular compartment from which they translate their genome to facilitate efficient replication. Furthermore, dysregulation of nucleocytoplasmic trafficking

results in down-regulation of the innate antiviral response. Picornavirus proteins are also known to enter the nucleus of infected cells to limit host-cell transcription. The interactions of picornavirus proteins and host-cell nuclei are extensive, required for a productive infection, and are the focus of this chapter.

Background

Overview

In this section, we first provide a brief review of nucleocytoplasmic trafficking in uninfected eukaryotic cells, followed by an outline of the salient features of picornavirus gene expression and replication. In subsequent sections, we discuss the wide-ranging interactions between picornaviruses and the nucleus of the cells they infect. Refer to **Table 1.1** for acronyms used in this chapter and throughout the dissertation.

Table 1.1. Acronyms used in this chapter

Acronym	Definition
NPC	nuclear pore complex
Nup	nucleoporin
FG	phenylalanine-glycine-rich
NLS	nuclear localization signal
NES	nuclear export signal
NCR	noncoding region
IRES	internal ribosome entry site
S-L	stem-loop
ITAF	IRES trans-acting factors
RNP	ribonucleoprotein
EMCV	encephalomyocarditis virus
FMDV	foot and mouth disease virus
HRV	human rhinovirus
CVB3	coxsackievirus B3
EV71	enterovirus 71
TMEV	Theiler's murine encephalomyelitis virus
HAV	hepatitis A virus
EGFP	enhanced green fluorescent protein
PAMP	pathogen associated molecular pattern
ISG	interferon-stimulated gene
Pol	DNA-directed RNA polymerase
SFPQ	Splicing factor proline and glutamine rich

The nucleus and nucleocytoplasmic transport

The nucleus is surrounded by two phospholipid bilayers termed the nuclear envelope. The inner nuclear membrane is associated with a network of the scleroprotein lamin, comprising the nuclear lamina, and the outer nuclear membrane is an extension of the endoplasmic reticulum (Callan et al., 1949). The nuclear envelope functions as a physical barrier between the cytoplasm and the nucleus and is selectively permeable via nuclear pores, which average in number between 2000 and 5000 per nucleus in vertebrate cells (Grossman et al., 2012). Macromolecules traffic between the nucleus and cytoplasm through these pores that fuse the inner and outer nuclear envelope. A protein complex known as the nuclear pore complex (NPC) is integrated within the nuclear pores and acts as a gate that restricts the diffusion of larger biomolecules across the nuclear envelope. With an approximate mass of 125 MDa, the NPC is one of the largest and most intricate assemblages of proteins in the eukaryotic cell. The NPC is a dynamic and modular structure that contains both symmetrical and asymmetrical portions. The symmetrical portion can be divided into three recognizable ring-like structures surrounding the central channel of the nuclear pore which includes the cytoplasmic ring, the central spoke ring, and the nuclear ring (Frenkiel-Krispin et al., 2010). Attached to the cytoplasmic and nuclear rings are 8 proteinaceous filaments which extend into the cytoplasm and nucleus, respectively, with the nuclear filaments converging to form the nuclear basket (Cautain et al., 2015). These extended structures, together, make up the asymmetrical portion of the NPC.

The NPC is composed of approximately 30 different proteins called nucleoporins (Nups), with ~500–1000 individual Nups comprising a single NPC (Cronshaw et al., 2002; Hoelz et al., 2011; Reichelt et al., 1990). Nups are categorized as transmembrane, barrier, or scaffold Nups based upon their location within the NPC, amino acid sequence motifs, and structure (Grossman et al., 2012). Transmembrane Nups anchor the NPC to the nuclear envelope to form nuclear pores, barrier Nups facilitate active transport of cargoes, and scaffold Nups link the transmembrane Nups to the barrier Nups and provide the structural framework of the NPC (**Figure 1.1**). Barrier Nups contain repeated phenylalanine-glycine-rich (FG) sequences that form intrinsically disordered motifs and act as the major impediment to free diffusion through the main channel of the NPC (Cautain et al., 2015). Concomitantly, these FG Nups provide the only route for active transport of cargo biomolecules between the cytoplasm and nucleus by allowing multiple low-affinity interactions between nuclear transport receptors and the NPC itself (Ben-Efraim and Gerace, 2001; Ribbeck and Görlich, 2001). The actual translocation of biomolecules through the NPC is energy-independent as GTP hydrolysis is required only as a final step in the transport process (Schwoebel et al., 1998). The efficiency of nucleocytoplasmic transport is staggering: a single NPC has been proposed to be capable of transporting a 100 kDa protein at an average rate of 800 translocation events per second (Fried and Kutay, 2003; Ribbeck and Görlich, 2001).

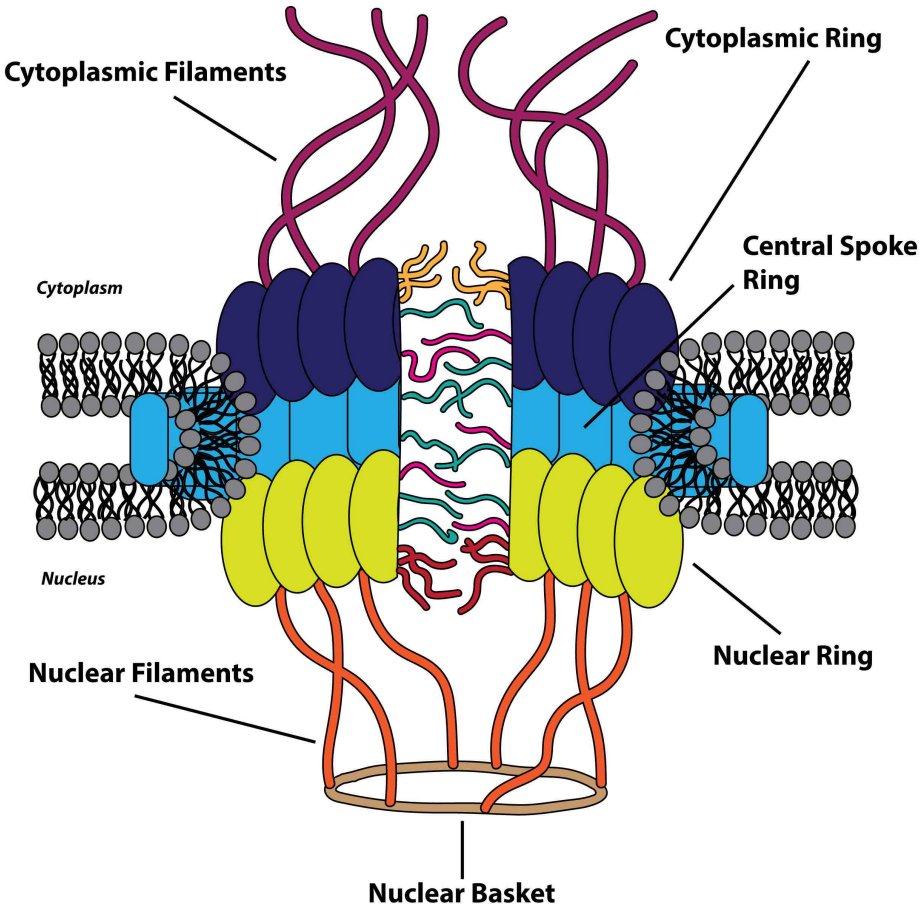

Figure 1.1. The nuclear pore complex. The cytoplasmic (dark blue), central spoke (light blue), and nuclear ring (chartreuse) structures constitute the symmetrical portion of the nuclear pore complex (NPC) that surrounds the central channel. Transmembrane and scaffold Nups (not labeled) form these three symmetrical ring-like structures of the NPC. The asymmetrical portion of the NPC is composed of cytoplasmic filaments (purple) on the cytoplasmic side and the nuclear filaments (orange) and nuclear basket (brown) on the nuclear side of the nuclear envelope. FG repeat containing barrier Nups are depicted as filaments within the central channel.

Small molecules including ions, metabolites, and proteins less than ~40 kDa are able to translocate between the cytoplasm and nucleus via passive diffusion, perhaps through channels peripheral to the major channel of the NPC (Hinshaw et al., 1992). In addition to allowing this energy-independent diffusion, the NPC simultaneously facilitates the selective, energy-dependent nucleocytoplasmic trafficking of large cellular molecules. This is generally accomplished via specific amino acid sequences present

on cargo proteins known as nuclear localization signals (NLSs) or nuclear export signals (NESs), depending on the directionality of transport. These signal sequences are recognized by the soluble nuclear transport receptors that bind cargo proteins and actively transport these molecules through the NPC. Many nuclear transport receptors belong to the karyopherin protein family, known as importins or exportins, and bind specific cargo proteins directly or through adaptor molecules to shuttle proteins from one side of the nuclear envelope to the other. The energy required for this process is provided by GTP hydrolysis carried out by the GTPase Ran, and the concentration gradient of Ran bound to GTP (Ran-GTP) imparts the directionality needed for the proper segregation of nuclear and cytoplasmic functions. Ran-GTP is abundant in the nucleus due to the presence of chromatin-bound Ran-guanine nucleotide exchange factor (Ran-GEF). Conversely, Ran-GDP is more abundant on the cytoplasmic side of the nuclear envelope as a result of the cytoplasmic filament-bound Ran-GTP-activating protein (Ran-GAP), which increases the GTPase activity of Ran, rapidly hydrolyzing bound GTP to GDP (Grossman et al., 2012). Accordingly, the Ran-GTP gradient provides directionality to nucleocytoplasmic transport because importins and exportins utilize the Ran-GTP gradient in a complementary fashion. Nuclear import complexes (importin(s)/cargo) assemble at low Ran-GTP concentrations in the cytoplasm and traverse the NPC through transient association-dissociation between importin and FG Nups. The cargo is then released by the interaction between the import complex and Ran-GTP in the nucleus (Görlich et al., 1996; Rexach and Blobel, 1995). Conversely, trimeric nuclear export complexes (exportin/cargo/Ran-GTP) assemble at high Ran-GTP concentrations in the nucleus, traverse the NPC, and dissociate upon

interconversion of Ran-GTP to Ran-GDP in the cytoplasm. Both importins and exportins bind Ran-GTP directly and utilize the metabolic energy provided by the Ran-GTPase system to relate directionality to transport (**Figure 1.2**). Nucleocytoplasmic transport is a highly regulated and effective process necessary for cellular homeostasis and, consequently, is the target of perturbation by many viral pathogens, including picornaviruses.

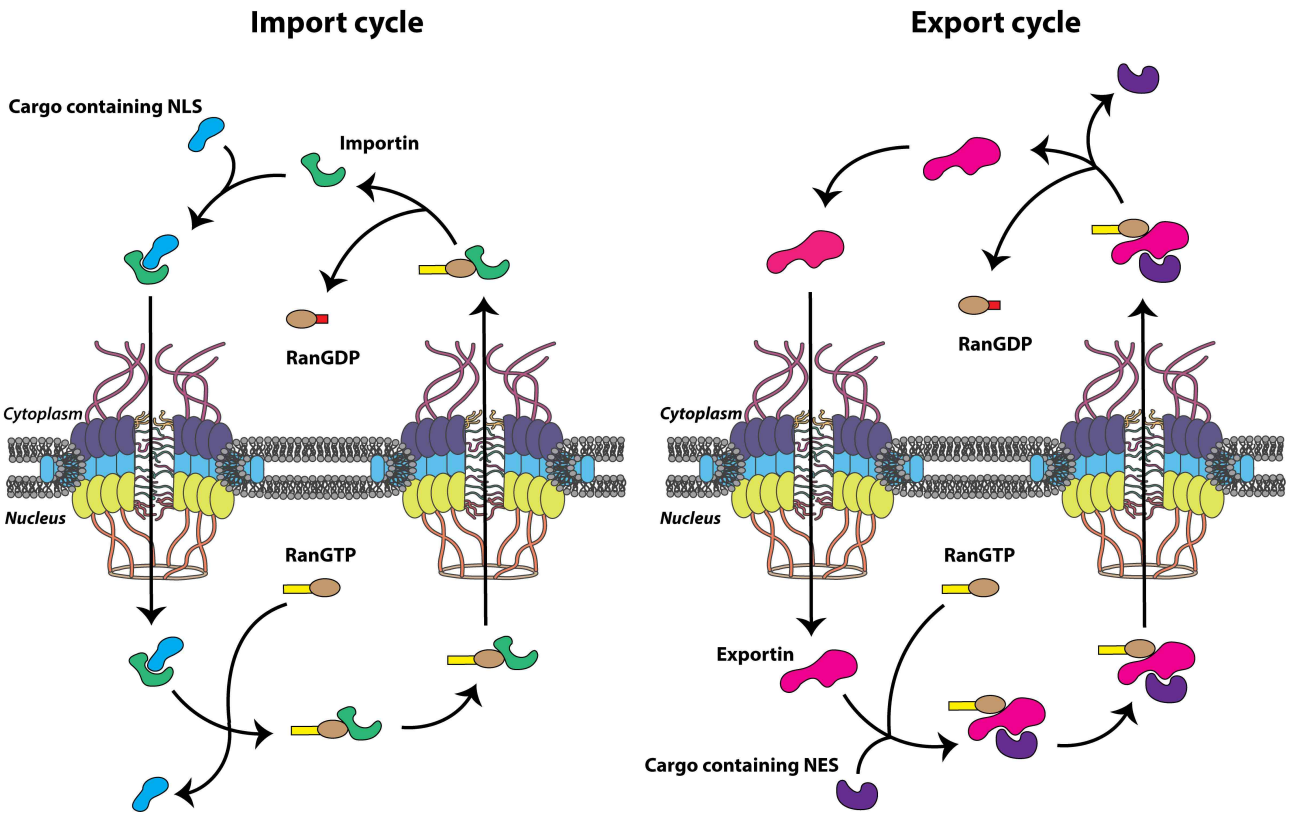

Figure 1.2. Nuclear transport cycles. Nuclear import and export cycles function in complementary fashion to recycle nuclear transport receptors, importins and exportins (green and pink, respectively), through the nuclear pore complex (NPC). Transport of biomolecules (cargo) containing a nuclear localization signal (NLS) (light blue) or nuclear export signal (NES) (purple) through the NPC itself is energy independent but the movement of nuclear transport receptors is dependent upon the hydrolysis of GTP.

Picornaviruses

The picornaviruses are a large group (35 genera currently recognized) of non-enveloped, small (~30 nm in diameter) viruses. The viral particle contains a positive-polarity, single-stranded RNA genome of ~7–10 kb in length with a viral protein (VPg) covalently attached to the 5'-terminus of the genome. These RNA molecules contain both 5′- and 3′-untranslated regions that function, in association with viral and host cell proteins, to facilitate both translation of the single open reading frame flanked by these regions, as well as RNA replication for genomic amplification. The long (~600–1500 nucleotide, including up to a ~500 nucleotide poly(C) tract for some aphthoviruses), highly structured, 5′-noncoding region (5'-NCR) contains an internal ribosome entry site (IRES) that directs the cap-independent translation of a large polyprotein from the viral genome (Martínez-Salas et al., 2015; Racaniello, 2013). This polyprotein is co- and post-translationally processed by viral proteinase 3C, as well as enteroviral 2A and leader proteinase L for aphthoviruses and erboviruses, to generate intermediate and mature viral proteins with distinct functions. Importantly, 3CD, the precursor to 3C and the RNA-directed RNA polymerase, 3D, is also an active proteinase and functions in polyprotein processing (Ypma-Wong et al., 1988). In addition to the highly structured IRES region, many picornaviruses also contain stem-loop (S-L) structures that allow for protein interactions that promote genome replication. S-L I, found on the 5'-terminus of RNA molecules, promotes the formation of ribonucleoprotein (RNP) complexes that serve to facilitate viral RNA replication. On the opposite terminus of the viral genome, the shorter (~50–650 nucleotide) 3′-NCR contains structured regions involved in viral RNA synthesis (though non-essential for infectivity), as well as an essential poly(A) tract

(Racaniello, 2013; Todd et al., 1997). 3D functions to replicate the viral genome through a negative-stranded intermediate, and is encoded within the P3 region of the polyprotein (**Figure 1.3**).

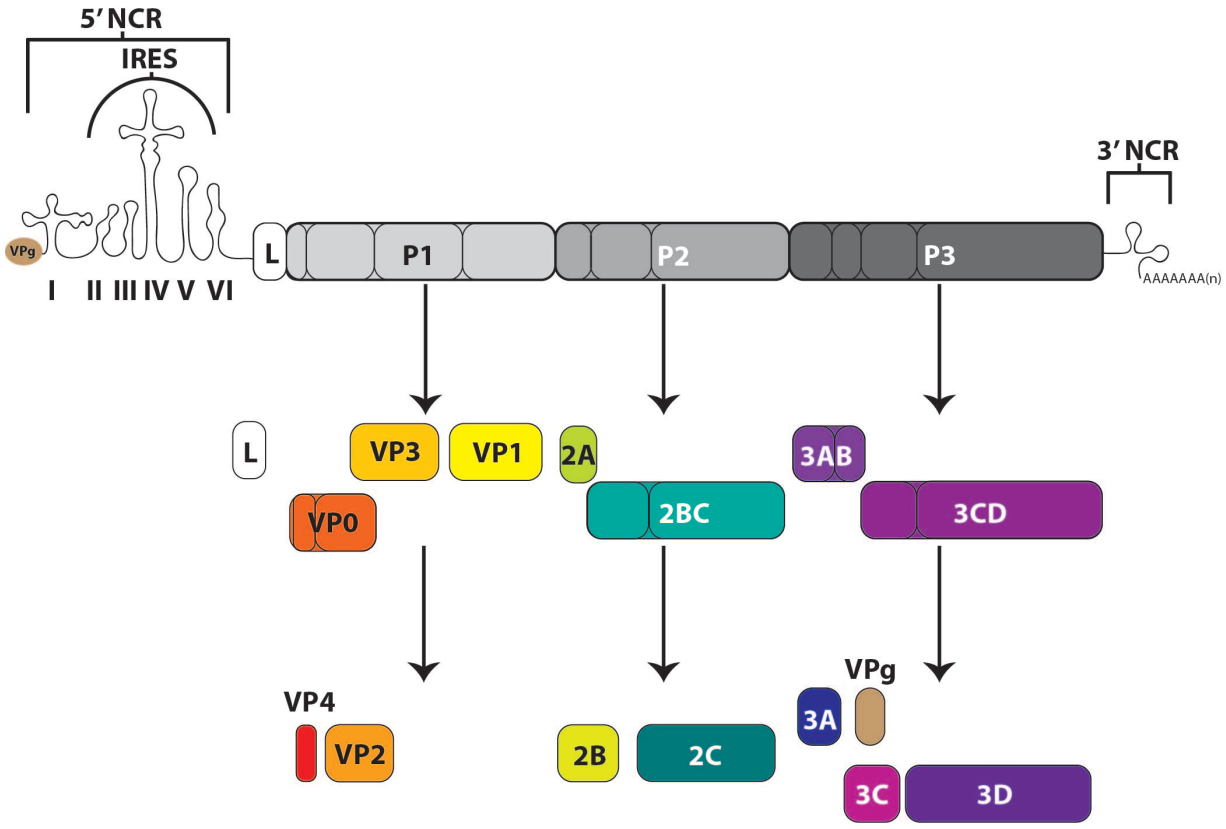

Figure 1.3. Picornavirus genome map and polyprotein cleavage cascade. The positive-sense RNA genomes of picornaviruses contain an internal ribosome entry site (IRES), within a 5'-noncoding region (5'-NCR), which drives the cap-independent translation of the downstream open reading frame. Roman numerals indicate distinct S-L structures. Viral gene products include functional precursors (some of which are depicted here) that are further processed by viral proteinases to produce mature viral proteins. The P1 region of the genome encodes structural proteins and the P2 and P3 regions encode non-structural proteins. Precursor 2BC as well as mature 2B and 2C are associated with host membrane rearrangements, membrane binding, and viral RNA replication. The 2A protein has proteinase activity, except in the case of cardioviruses. The precursor protein 3AB also associates with membranes and stimulates the function of 3CD and the RNA-directed RNA polymerase 3D. The proteolytically active 3CD precursor functions in VPg uridylylation and viral RNA replication through the formation of the ternary complex on the 5'-terminus of viral genomic RNA molecules. 3C functions in viral protein maturation through its proteinase activity. VPg (3B) acts as a protein primer for initiation of viral RNA synthesis. Leader protein (L) is not encoded by all picornaviruses and, and in some genera (including aphthoviruses), L has proteinase activity. The 3'-terminus of the genome contains a 3'-noncoding region as well as a genetically encoded poly(A) tract.

The infectious cycles of picornaviruses are initiated following viral attachment to specific cellular receptors, which vary depending on the particular virus species. The RNA genome is then released from the virion capsid and enters the cytoplasm of the target cell. Once in the cytoplasm, the picornavirus RNA molecule is used as a template for IRES-driven viral protein production. Aside from roles in polyprotein processing, the picornavirus proteinases that are produced target cellular proteins for cleavage, disrupting cellular functions and promoting different steps of the replication cycle. Enteroviral proteinase 2A targets phenylalanine-glycine (Phe-Gly) or tyrosine-glycine residues (Tyr-Gly), while the 3CD/3C recognition site consists primarily of glutamine-glycine (Gln-Gly) sites with an aliphatic side chain four positions proximal to the target site, but can also cleave at additional sites (Blair and Semler, 1991; Nicklin et al., 1986; Toyoda et al., 1986). An incompletely defined set of events that likely involve local concentrations of viral proteins and cleavage of specific host factors allows the same RNA template used for translation to be cleared of ribosomes and utilized for the production of a complementary, intermediate negative-sense (anti-genomic) RNA molecule. The first step of RNA replication produces a double-stranded RNA structure called the replicative form on membranous vesicles that are induced within the infected cell. The negative-sense RNA molecule is, in turn, used as a template for the production of multiple positive-sense RNA molecules simultaneously, generating a multiple-stranded RNA complex called the replicative intermediate. The nascent viral RNA molecules are then recycled back through the translation/replication process or packaged into progeny virions. Importantly, proteins that are predominantly localized to

the nucleus in uninfected cells are utilized by these cytoplasmic viruses from the very primary steps of the replication process.

Nuclear resident proteins are hijacked for picornavirus translation

The positive-sense RNA genome of a picornavirus is competent for immediate IRES-driven translation upon uncoating. In addition to picornavirus RNAs, it has been suggested that up to 10% of cellular mRNAs contain an IRES element (Spriggs et al., 2005). Somewhat counterintuitively, many of the proteins that mediate IRES-dependent translation of cellular and viral mRNAs, known as IRES trans-acting factors or ITAFs, are compartmentalized in the host cell nucleus or shuttle between the nucleus and the cytoplasm (Semler and Waterman, 2008). It is currently unclear whether ITAFs associate with cellular IRES elements during the biogenesis of mRNA transcripts in the nucleus and are subsequently transported to the cytoplasm as RNP complexes, or whether these ITAFs are redistributed to the cytoplasm, where IRES-containing mRNAs are already present, in response to signals stimulating IRES-driven translation. Regardless of the mechanism in which ITAFs associate with cellular IRES elements, the ITAFs utilized by picornaviruses are available at sufficient concentration in the cytoplasm upon infection, at least for the initial rounds of viral protein production. Picornaviruses subvert the host protein synthesis machinery through cleavage of canonical translation initiation factors, thereby inhibiting cellular translation and releasing ribosomes and associated proteins from their roles in cap-dependent translation. Here, for the purpose of discussion, nuclear resident proteins will be defined as those that are normally more concentrated in the nucleus than the cytoplasm, because all cellular proteins can be found to some extent in the cytoplasm during

biogenesis, and many shuttle between the nucleus and cytoplasm to perform their functions.

Nuclear resident/shuttling ITAFs often have RNA-binding capabilities and control many features of RNA biology and gene expression including: transcriptional regulation, splicing, and RNA transport and stability (Martínez-Salas et al., 2015). Furthermore, mammalian cells encode nearly 1000 RNA-binding proteins (although not all of these are nuclear resident) and as a result, the viral mRNAs of picornaviruses employ the functions of several of these RNA-binding and RNA-chaperone proteins to facilitate translation (Castello et al., 2012). All picornaviruses contain IRES elements within the 5'-NCR of their genomes to facilitate ribosome association and these elements are categorized into four separate types, I–IV, for the 12 best-studied picornavirus genera. IRES types are categorized depending upon primary RNA sequence, secondary RNA structure, location of translation initiation codon, and phylogeny. Type I structures are found in the genomes of enteroviruses; Type II in aphthoviruses, cardioviruses, erboviruses, kobuviruses, and parechoviruses; Type III in hepatoviruses; and Type IV in avihepatoviruses, sapeloviruses, senecaviruses, teschoviruses, and tremoviruses (Martínez-Salas et al., 2015; Palmenberg et al., 2010). The categorization of picornavirus IRES types is somewhat arbitrary and flexible, and ongoing work related to cap-independent translation from these viruses will likely result in changes to the currently recognized classifications. Recently, it has been proposed that the kobuvirus genus contains a distinct, fifth type of IRES, but there will be no further discussion within this chapter, as no nuclear resident ITAFs have been reported for this IRES type (Sweeney et al., 2012; Yu et al., 2011b). There is little sequence homology across the

four IRES types and, as a result, picornaviruses harboring different IRES structures likely utilize slightly different cohorts of ITAFs and in different ratios. However, there is at least some overlap in the identity of those nuclear proteins that are used as ITAFs for general picornavirus translation.

Polypyrimidine tract binding protein 1 (PTBP1)

Type I and Type II IRESs have been the most extensively studied of the picornavirus IRES elements and as a result, have been shown to associate with the greatest number of nuclear resident proteins compared to the other IRES Types. Polypyrimidine tract binding protein 1 (PTBP1, also known as hnRNP I) was the first host protein shown to interact with, and promote translation from, the IRES regions of encephalomyocarditis virus (EMCV), foot and mouth disease virus (FMDV), poliovirus, and human rhinovirus 2 (HRV2) (Hellen et al., 1993; Hunt and Jackson, 1999; Jang and Wimmer, 1990; Kaminski et al., 1995; Luz and Beck, 1991; Niepmann, 1996). PTBP1 contains four RNA recognition motifs distributed across a flexible structure, functions in the regulation of pre-mRNA splicing and transport, and has been shown to be predominantly localized to the nucleus while also shuttling to the cytoplasm (Ghetti et al., 1992; Oh et al., 1998; Sawicka et al., 2008). This protein is hypothesized to promote translation initiation on Type I IRESs by modulating an interaction between domain V of these structures and the C-terminal portion of translation initiation factor eIF4G, which is cleaved during infection with enteroviruses but retains some RNA binding capability, with the C-terminal fragment utilized for cap-independent translation (Buckley and Ehrenfeld, 1987; Kafasla et al., 2010; Ohlmann et al., 1995; Ohlmann et al., 1996). Coxsackievirus B3 (CVB3), which contains a Type I IRES element, also utilizes PTBP1

as an ITAF, and because it has been shown to bind both the 5'- and 3'-NCRs of CVB3 RNA, has been proposed to facilitate circularization of the RNA molecule to promote efficient translation (Verma et al., 2010). Furthermore, EMCV and FMDV Type II IRESs appear to require the binding of two copies of PTBP1, at two distinct regions, for maximal IRES activity, at least *in vitro* (Kafasla et al., 2009; Kolupaeva et al., 1996). Since poliovirus and EMCV translation is dependent upon the simultaneous interaction of three of the four RNA-binding domains found within this protein, and FMDV requires two of the four RNA-binding domains of PTBP1 for efficient IRES activity, PTBP1 likely acts as an RNA chaperone, stabilizing viral IRES structures to promote conformations conducive to translation (Kafasla et al., 2011; Song et al., 2005). Analysis of viral gene expression and propagation in cells has recapitulated the PTB1-dependence of Type I and Type II IRESs observed by *in vitro* methods (Florez et al., 2005). Finally, PTBP1 has been demonstrated to be the only ITAF (i.e., non- canonical translation factor) that is required for the translation of EMCV transcripts *in vitro* (Pestova et al., 1996).

Sjögren syndrome antigen B (SSB)

The nuclear protein Sjögren syndrome antigen B (SSB) (also known as Lupus La protein) has also been implicated in having a role in the cap-independent translation of type I and II IRESs. SSB has been shown to bind a portion of the poliovirus IRES as a dimer and enhance the production of poliovirus proteins (Craig et al., 1997; Meerovitch et al., 1989; Meerovitch et al., 1993). Similarly, SSB stimulates the translation of both CVB3 and EMCV RNA (Kim and Jang, 1999; Ray and Das, 2002). SSB stabilizes nascent RNA produced in cells. It binds the 3′ poly(U) termini of RNA polymerase III transcripts to protect them from degradation and to promote their maturation, and as a

result, is generally confined to the nucleus (Stefano, 1984). SSB has been proposed to mediate an interaction between the 40S ribosomal subunit and the poliovirus IRES *in vivo* (Costa-Mattioli et al., 2004). Importantly, SSB relocalizes to the cytoplasm of enterovirus-infected cells (Gustin and Sarnow, 2001, 2002; Shiroki et al., 1999).

Poly(rC) binding protein 2 (PCBP2)

Poly(rC) binding protein 2 (PCBP2) binds single-stranded nucleic acids through three hnRNP K-homologous domains (KH domains) and is involved in the stabilization of several cellular mRNAs (Holcik and Liebhaber, 1997; Siomi et al., 1994). Although predominantly nuclear, PCBP2 binds to both S-L IV and S-L I of the 5′-NCR within the poliovirus and CVB3 genomic RNA (Blyn et al., 1995; Blyn et al., 1996; Gamarnik and Andino, 1997; Leffers et al., 1995; Parsley et al., 1997; Sean et al., 2009; Silvera et al., 1999; Zell et al., 2008a; Zell et al., 2008b). S-L IV is located in the central portion of Type I IRES elements and alterations to the nucleic acid sequence identified as important for PCBP2 association decrease poliovirus translation *in vitro* (Blyn et al., 1995). Moreover, depletion of PCBP2 from cellular extracts results in inefficient poliovirus translation (Blyn et al., 1997). Although PCBP2 is required for translation of poliovirus, coxsackievirus, and HRV, it is not necessary for the translation of the type II IRES-containing RNAs of EMCV and FMDV (Walter et al., 1999). PCBP2 is the only ITAF shown to be required for the translation of poliovirus, enterovirus 71 (EV71), and bovine enterovirus (i.e., Type I IRESs) by *in vitro* reconstitution of translation initiation (Sweeney et al., 2014). However, as with PTBP1 and the EMCV IRES, whether these *in vitro* systems are representative of the conditions encountered within the cellular milieu during infection, or if other, non-essential, ITAFs enhance viral IRES- driven translation,

remains to be elucidated. It should be noted that PCBP1 can also bind the poliovirus IRES but PCBP2 appears to be essential for translation initiation (Gamarnik and Andino, 1997; Walter et al., 2002).

Serine and arginine rich splicing factor 3 (SRSF3)

Type I IRES structures also utilize serine and arginine rich splicing factor 3 (SRSF3 or SRp20) to promote cap-independent translation. The SR proteins comprise a group of splicing factors with a multitude of functions related to gene expression including: constitutive and alternative splicing, mRNA export and stability, and translation (Graveley, 2000; Huang et al., 2003; Huang and Steitz, 2001; Sanford et al., 2004). As a result of these functions, a subset of SR proteins including SRSF3 are considered shuttling proteins, although they most often accumulate in the cellular nucleus (Cáceres et al., 1998). Depletion of SRSF3 from cells or cellular extracts decreases the protein production from a reporter construct containing the poliovirus IRES (Bedard et al., 2007). In addition, SRSF3 and PCBP2 have been shown to act synergistically to increase the efficiency of IRES-mediated translation *in vitro* and in poliovirus-infected cells, with SRSF3 associating with S-L IV of the IRES via a PCBP2 bridge. Specifically, this enhancement in non-canonical translation is a result of SRSF3 interacting with the KH3 domain of PCBP2 to directly or indirectly recruit ribosomes to the viral RNA. Furthermore, both are found associated with translation initiation complexes in poliovirus-infected cells (Bedard et al., 2007; Fitzgerald and Semler, 2011). CVB3 and HRV16 also likely utilize SRSF3 to promote translation, as this protein is relocalized in cells expressing the 2A proteinase of these viruses (Fitzgerald et al., 2013).

Proliferation-associated protein 2G4 (PA2G4)

The SRSF3/PCBP2 cooperative enhancement to poliovirus IRES-driven translation initiation is mirrored by the interaction between PTBP1 and proliferation-associated protein 2G4 (PA2G4 or EBP1) with the FMDV IRES element. A chimeric Theiler's murine encephalomyelitis virus (TMEV, which also possesses a Type II IRES) containing the FMDV IRES element in place of the TMEV IRES was unable to replicate in mouse neurons, suggesting the absence of a necessary ITAF for minimal FMDV translation. This ITAF was identified as PA2G4 ("ITAF 45") in assaying for the formation of 48S initiation complexes through biochemical reconstitution and was shown to bind directly to viral RNA corresponding to the FMDV IRES through UV cross-linking (Pilipenko et al., 2000). PA2G4 and PTBP1 bind to distinct sites within the FMDV IRES, causing localized structural changes within these regions, thereby enhancing binding of the eIF4G/4A complex to the IRES structure. It has been proposed that unlike in the case of the TMEV IRES, PTBP1 alone is unable to promote the RNA structural modifications to the FMDV IRES necessary for ribosome association and translation initiation. This is likely due to differences in the nucleotide sequence within these Type II IRES structures and associated differences in the way in which PTBP1 binds and re-arranges these regions, forcing FMDV to rely on PA2G4 to shape a functionally competent IRES structure (Pilipenko et al., 2000). PA2G4 was also shown to interact with TMEV and EMCV RNA, so this protein likely binds RNA non-specifically. However, EMCV IRES-driven translation has been shown to be unaffected by the presence of PA2G4. Moreover, PA2G4 does not interact with PTBP1, corroborating the fact that translation initiation from the EMCV IRES is independent of PA2G4 (Monie et al., 2007).

Interestingly, despite the fact that FMDV and EMCV have different ITAF requirements, experiments comparing the sites of hydroxyl radical cleavage within the IRES structures from the eIF4G hub demonstrated that when these Type II IRESs interact with their cognate ITAFs, similar structural conformations are adopted (Yu et al., 2011a). This suggests that although these IRES sequences can vary by ~50%, their shared requirement for PTBP1 seems to lie in the fact that it acts as versatile adaptor protein, whether alone or in combination with other ITAFs, in translation initiation form Type II IRESs.

Minimal vs. stimulatory ITAFs

It is important to note that while there has been rather extensive study of the Type I and Type II IRESs and their associated ITAFs, there is some variability in the reported ITAF requirements across particular viral species. For the Type I IRES elements tested (poliovirus, HRV2, and CVB3), PTBP1 has been shown to be either required or unnecessary (Hunt and Jackson, 1999; Sweeney et al., 2014; Verma et al., 2010). Similarly, for viruses containing Type II IRES elements, there is discrepancy in the obligatory ITAFs reported. PTBP1 is required for FMDV translation, but the requirement for this ITAF in EMCV translation appears conditional upon the reporter and IRES variant utilized in experiments (Kaminski and Jackson, 1998). Additionally, translation from the TMEV IRES has been shown to be independent of, as well as strongly dependent on, PTBP1 (Kaminski et al., 1995; Pilipenko et al., 2001). As mentioned previously, the inconsistencies in reported ITAFs are likely a result of the assay used (*in vitro* compared to experiments in cells) as well as the use of different strains of virus/sequences of reporter constructs. These apparently discrepant results

point to the fact that there are some minimal ITAFs required for Type I and Type II IRES elements but a multitude of ITAFs that play some stimulatory or translation-enhancing role depending on the specific context of an infection. For example, it is possible that different ITAFs are utilized by viral IRES elements depending on the cell type infected (i.e., cell-type-specific ITAFs), as the availability of particular proteins that function in this regard likely dictate whether viral protein production and growth are supported, and to what extent (Chang et al., 1993; Wimmer et al., 1993). Cell-type-specific IRES function is exemplified by the fact that viral RNAs that initiate translation from the HRV2 IRES, but not the poliovirus IRES, are excluded from neuronal cell polysomes but not from those of glioma cells. This is thought to be the result of a specific protein heterodimer that inhibits HRV2 IRES-driven translation in neuronal but not glioma cells, as discussed below (Merrill and Gromeier, 2006).

Other ITAFs of type I IRESs

Other nuclear resident proteins that function as ITAFs of Type I IRESs have also been proposed, but less completely characterized. Nucleolin, which relocalizes to the cytoplasm of poliovirus-infected cells, has been shown to stimulate translation from constructs containing poliovirus and rhinovirus IRES structures *in vitro* and in cells, and the amino-terminal domain of this protein is required for this activity (Izumi et al., 2001; Waggoner and Sarnow, 1998). Heterogeneous nuclear ribonucleoprotein (hnRNP) A1 shuttles between the nucleus and the cytoplasm, functions in both pre-mRNA splicing and nuclear export of mRNA molecules, and has been shown to interact with S-L II and VI of the EV71 IRES via electrophoretic mobility shift assays. However, only when both hnRNP A1 and hnRNP A2 are knocked down is there a decrease in translation of a

reporter gene containing the EV71 IRES sequence, and an overall reduction in viral replication in these cells, suggesting a functional redundancy of these proteins for EV71 replication (Lin et al., 2009b). The HRV2 IRES region has also been shown to bind hnRNP A1 and promote translation following its relocalization into the cytoplasm of infected cells (Cammas et al., 2007). The EV71 IRES also interacts with far upstream element binding protein 1 (FUBP1, also known as FBP1) and KH RNA binding domain containing, signal transduction associated 1 (Sam68), both of which redistribute to the cytoplasm of infected cells and may promote translation from the EV71 IRES (Huang et al., 2011; Zhang et al., 2015). ELAV like RNA binding protein 1 (also known as HUR) and Argonaute 2, RISC Catalytic Component (AGO2) have also been shown to bind S-L II of EV71 RNA *in vitro* and suggested to promote IRES-driven translation; however, knockdown of these proteins resulted in no difference in viral RNA synthesis, a finding that is not consistent with the close association between viral translation and RNA replication, described in subsequent sections (Lin et al., 2015). As with EV71 infection, Sam68, which is a putative regulator of mRNA stability and mRNA nuclear export, moves from the nucleus to the cytoplasm in poliovirus-, HRV14-, HRV16-, and HRV2-infected cells and has been shown to interact with poliovirus 3D through yeast two-hybrid assays; however, the possible role that this protein may play in the viral RNA replication cycle is not clear (Coyle et al., 2003; Gustin and Sarnow, 2002; McBride et al., 1996; Walker et al., 2015). Type II IRES-containing FMDV may also utilize Sam68 to promote IRES-dependent protein production following 3C-dependent cleavage and subsequent cytoplasmic localization (Lawrence et al., 2012).

Nuclear resident proteins that inhibit picornavirus translation

In contrast to the discussion thus far, there are also examples of nuclear resident proteins that act to inhibit enterovirus translation. Interleukin enhancer-binding factor 3 (ILF3 also known as DRBP76) heterodimerizes with interleukin enhancer-binding factor 2 (ILF2 also known as NF45) and this heterodimer binds the HRV2 IRES. Together, these proteins inhibit translation initiation from the HRV2 IRES in neuronal cells. The recombinant oncolytic poliovirus PVS-RIPO exploits the incorporated HRV2 IRES to permit attenuated neurovirulence in the treatment of malignant glioma, possibly due to the presence of ILF3:ILF2 heterodimers in the cytoplasm of neuronal, but not glioma cells (Merrill et al., 2006; Merrill and Gromeier, 2006). Similarly, KH-type splicing regulatory protein (KHSRP, also known as far-upstream element-binding protein 2, FUBP2), which is involved in splicing and mRNA trafficking, inhibits EV71 IRES-driven translation (Chen et al., 2013; Lin et al., 2009a). AU-rich binding factor 1 (AUF1, also known as hnRNP D) also relocalizes from the nucleus during enterovirus infection and inhibits viral replication (Cathcart et al., 2013; Rozovics et al., 2012). FUBP2 and AUF1 are discussed in more detail in a subsequent section. Cytoplasmic proteins that function as ITAFs for picornavirus RNA translation have also been reported, as well as canonical elongation factors, but these are outside the scope of this review [for a recent review of picornavirus translation including the role of cytoplasmic proteins, see (Martínez-Salas et al., 2015)].

ITAFs of type III and type IV IRESs

There has been comparatively little study of type III and IV IRES elements, but several of the same nuclear resident proteins involved in IRES-driven translation of type

I and type II IRES structures have been implicated for type III structures as well. The type III IRES structure found in the genome of hepatitis A virus (HAV) interacts with, is stabilized by, and is stimulated by PTBP1 (Chang et al., 1993; Gosert et al., 2000a). Similarly, HAV IRES activity is increased in the presence of PCBP2. However, although this protein interacts with the 5'-NCR of the HAV genome, it does not bind to regions that correspond to the IRES structure (Graff et al., 1998). Interestingly, in contrast to its role in the functions of type I and type II IRESs, SSB suppresses translation from the HAV IRES (Cordes et al., 2008). Even less is known about the ITAF requirements of picornavirus type IV IRES elements, but as these IRES elements are very similar to those found in some flaviviruses, it is expected that at least some of the same ITAFs utilized by hepatitis C virus, for example, might also enhance the translation of sapelovirus, senecaviruses, teschoviruses, and tremoviruses.

Other nuclear resident proteins that interact with viral RNA molecules

Large-scale proteomic studies have identified a multitude of RNA-binding proteins that interact with poliovirus RNA isolated from infected cells, bind to biotin-labeled EV71 5'-NCR, as well as FMDV RNA *in vitro* (further confirming many of the associations mentioned above), but the specific role of each of these newly-identified proteins remains to be elucidated (Lenarcic et al., 2013; Lin et al., 2008; Lin et al., 2009a; Pacheco et al., 2008b). One protein identified as interacting with the FMDV IRES element through large-scale proteomic studies is gem nuclear organelle associated protein 5 (Gemin5), which was shown to inhibit FMDV translation, likely by competitively inhibiting PTBP1 binding (Pacheco et al., 2008a; Piñeiro et al., 2012a). Non-POU domain-containing octamer-binding protein (NONO) has been shown to

interact with poliovirus RNA through thiouracil cross-linking mass spectrometry and impact the generation of positive-sense RNA during infection. However, whether NONO is involved in translation or RNA replication is not clear (Lenarcic et al., 2013). Additionally, the poly(C) binding protein hnRNP K is redistributed to the cytoplasm in EV71-infected cells, binds the EV71 IRES, promotes viral RNA replication, and may be exploited in place of PCBP2 by EV71(Lin et al., 2008).

Another nuclear resident protein with a proposed role in picornavirus replication is DExH-Box Helicase 9 (DHX9, also known as RNA helicase A), which binds the 5'-NCR of FMDV genomic RNA and co-precipitates with the 2C and 3A proteins. Furthermore, knockdown of DHX9 results in decreased FMDV titers, suggestive of a proviral role in replication (Lawrence and Rieder, 2009). Although those proteins that act as ITAFs to mediate the translation of picornavirus RNA templates warrant further investigation, one commonality among the proteins mentioned above is that they are all RNA-binding proteins with the ability to form multimers. This suggests that they are able to interact with the viral IRESs in multiple locations and perhaps stabilize the structures of their associated IRESs to promote recognition by the translation machinery (Jackson et al., 1995; Kafasla et al., 2009) (**Table 1.2**).

Nuclear resident proteins function in template-usage switching

In addition to the roles that nuclear RNA binding proteins play in viral translation, they may also govern the template usage switch that occurs following the production of picornavirus proteins to transition to viral RNA replication. The same genomic template is used for both translation and RNA replication; however this RNA but cannot be traversed simultaneously by ribosomes and the viral polymerase, which travel in

opposite directions on the template. Thus, the RNA must be “reset” prior to RNA replication (Barton et al., 1999). The regulation of this switch is dependent, in part, upon the sufficient production of viral proteins, specifically proteinases, which subsequently target the ITAFs that acted to promote the translation of the proteinases themselves.

As mentioned previously, PCBP2 binds to both S-L I and S-L IV of poliovirus genomic RNA, but with much greater affinity to S-L IV in isolation (Gamarnik and Andino, 2000). However, upon cleavage by the viral 3CD/3C proteinase, the cleaved PCBP2 is unable to stimulate IRES-driven translation. 3CD/3C liberates the C-terminal KH3 domain, leaving the N-terminal portion of the protein unable to form a complex with S-L IV and therefore unable to aid in ribosome recruitment (Perera et al., 2007). The N-terminal portion of PCBP2 is, however, still capable of interacting with S-L I RNA structures, an interaction that is enhanced when the viral proteinase precursor 3CD is present on this 5’-terminal RNA structure (Gamarnik and Andino, 1998; Perera et al., 2007). The resulting ternary complex formed between S-L I RNA, PCBP2, and 3CD promotes viral RNA synthesis (Gamarnik and Andino, 2000; Parsley et al., 1997). There is also evidence to suggest that cleaved PCBP2 directly enhances poliovirus RNA replication *in vitro* (Chase et al., 2014). Although the interaction between PCBP2 and S-L I may aid in the stimulation of viral protein synthesis early during infection, it is the presence of 3CD and subsequent interactions with PCBP2 that allows the viral RNA replication process to proceed (Kempf and Barton, 2008).

Adding further regulation to the template usage switch orchestrated by poliovirus is the fact that PTBP1, another ITAF, is cleaved by 3CD/3C leading to inhibition of poliovirus translation. A decrease in viral translation corresponds closely to the

accumulation of truncated PTB isoforms *in vitro* indicative of a role for PTBP1 in mediating the switch to negative-strand RNA production during the replication cycle (Back et al., 2002). Similarly, cleavage of the nuclear shuttling poly(A)-binding protein 1 (PABP1), which functions in regulation of mRNA metabolism and is closely associated with RNA and mRNP complexes, has been proposed to be involved in the inhibition of poliovirus translation (Afonina et al., 1998). Expression of PABP1 resistant to poliovirus 3CD/3C mediated cleavage during infection increases viral protein synthesis from non-replicating reporter RNAs and reduces viral RNA accumulation compared to wild type PABP1 expression (Bonderoff et al., 2008). Ribosome-associated PABP1 is also preferentially targeted by enterovirus 3CD/3C (Kuyumcu-Martinez et al., 2002). Furthermore, PABP1 is cleaved by poliovirus and CVB3 2A proteinase (Joachims et al., 1999; Kerekatte et al., 1999). Taken together, the cleavage of PABP1 during enterovirus infection likely has the dual role of inhibition of cellular translation by disrupting mRNA circularization as well as supplementing the viral template usage switch. HAV likely utilizes a similar mechanism to suppress translation and promote RNA replication, since the 3CD/3C proteinase of this virus has been shown to cleave PCBP2 and PTBP1, resulting in reduced protein-RNA affinity and decreased viral translation (Kanda et al., 2010; Zhang et al., 2007). Increased viral protein accumulation and alterations to nuclear RNA-binding proteins are the mechanisms by which poliovirus and HAV RNA replication are able to proceed, but whether this mechanism to induce a template usage switch is broadly applicable to other picornaviruses is not clear. Indeed, a recent report demonstrated that three HRV serotypes do not induce the cleavage of PCBP2 or PTBP1 during infection of a human lung cell line, suggesting alternative

mechanisms must be used under theses experimental conditions (Chase and Semler, 2014).

A Nuclear resident protein removes VPg from viral genomic RNA molecules

Finally, in addition to the nuclear resident proteins utilized by picornaviruses to promote IRES-mediated protein production and the switch to RNA replication, another nuclear resident protein functions in RNA processing of poliovirus RNA. VPg, the viral protein covalently attached to the 5'-terminus of the viral RNA, is removed from viral RNAs found on polysomes (Ambros et al., 1978). This cleavage is performed by 5'-tyrosyl-DNA phosphodiesterase-2 (TDP2), a DNA repair enzyme that normally functions to remove covalent topoisomerase 2 adducts from DNA via hydrolysis of 5'-phosphodiester bonds, and which is relocalized to the cytoplasm during poliovirus infection (Virgen-Slane et al., 2012). TDP2 also appears to be important for the replication of CVB3 and HRV1a (Maciejewski et al., 2016). VPg serves as the protein primer for viral RNA synthesis and is present on encapsidated RNA molecules. The functional role of TDP2 in viral infection is not completely clear; although it has been hypothesized that exclusion of TDP2 from replication complexes at late times of infection may serve as a signal for RNA encapsidation (Langereis et al., 2013; Virgen-Slane et al., 2012). Independent of understanding the precise role of TDP2 during infection, this protein provides an additional example of nuclear resident proteins being used in diverse ways, even during the very initial steps in the infectious cycles of picornaviruses.

During the initial rounds of IRES-mediated translation, picornaviruses co-opt nuclear shuttling proteins that are encountered in the cytoplasm of an infected cell. As

genome amplification proceeds and further rounds of translation are initiated, increasing amounts of nuclear resident proteins are required in the cytoplasm of cells to facilitate a productive infectious cycle. To provide these critical nuclear factors to the sites of viral replication, alterations to nucleocytoplasmic trafficking and the normal compartmentalization of cellular proteins occurs, resulting in a large cytoplasmic stock of nuclear factors. How this is achieved is the focus of a subsequent section of this chapter. So, despite the fact that the early rounds of viral translation and genomic RNA replication can proceed utilizing the limited supply of nuclear resident proteins already in the cytoplasm, successive rounds require the selective loss of cellular protein compartmentalization allowing cellular factors to be available for viral replication processes. It is clear that nuclear resident proteins play a critical role in the regulation of picornavirus translation, despite that fact that these positive-sense RNA viruses complete their replication cycle in the cytoplasm of the infected cell.

Nuclear resident proteins utilized in the process of picornavirus RNA replication

Although picornaviruses encode their own RNA-directed RNA polymerase (3D), they utilize host cell factors to augment the function of this replicase enzyme. As with IRES- dependent translation, most of the factors utilized in the process of RNA synthesis are nuclear resident proteins with RNA-binding functions that can be used by the virus to facilitate the replication of viral RNA molecules. These host proteins act in the context of RNP complexes they form with picornavirus RNAs to impart replication specificity to the polymerase, as 3D is able to replicate RNA non-specifically when provided with a primed template *in vitro* (Tuschall et al., 1982). During an infection, however, 3D solely replicates picornavirus RNA despite the large excess of cellular

mRNA present. To make use of picornavirus RNA templates exclusively, complexes of picornavirus RNA, host nuclear resident proteins, and viral proteins are thought to act as recognition elements that enable template recognition by 3D and initiation of RNA synthesis. Particularly critical in the regulation of 3D appears to be 5'-3' intramolecular associations that yield functionally circularized templates. This section will focus on those nuclear resident proteins that are known to promote either the production of intermediate negative-sense RNA molecules or the amplification of positive-sense RNA molecules from this template.

As discussed previously, a template usage switch from translation to RNA replication occurs as viral proteins accumulate and, in some cases, proteinases cleave host cell factors functioning as ITAFs. Prior to this transition, it has been proposed that optimal translation of poliovirus RNA requires the circularization of the RNA molecule, likely allowing ribosomes to be efficiently reloaded on the template (Ogram et al., 2010). This finding supports the fact that picornavirus RNA molecules that are to be replicated must first be translated (Novak and Kirkegaard, 1994). Host proteins present on the viral RNA that allow for the initial circularization of the translation-competent template could enhance the circularization efficiency of the replication-competent template. This coupling between poliovirus translation and RNA replication has been suggested to be promoted by at least two proteins common to both translation and RNA replication: PABP1, which binds the 3'-poly(A) region, and PCBP2, which binds the 5'-NCR.

The possible role of nuclear resident proteins in promoting enterovirus genomic RNA circularization and negative-sense RNA production

The first step of enterovirus RNA replication is negative-sense or anti-genomic RNA production The 5'-NCRs of picornavirus RNAs contain structural elements that are required for the replication of these genomes by acting as scaffolds for protein interactions (Andino et al., 1990; Barton et al., 2001; Nagashima et al., 2008; Nateri et al., 2002; Parsley et al., 1997). Electrophoretic mobility shift assays incorporating recombinant proteins and subgenomic portions of poliovirus RNA molecules have been instrumental in identifying the components of RNP elements *in vitro* that may be important for the process of enterovirus RNA replication. The 5′ terminal structure of the poliovirus genome, known as S-L I or the cloverleaf, has been shown to be critical for the formation of RNP complexes that function in the initiation of RNA synthesis even though the 3D polymerase starts this process at the 3'-terminus of viral RNA (Andino et al., 1993). One of the proteins involved in this RNP formation is the nuclear resident PCBP2, which binds to the S-L I structure with increased affinity when the viral polymerase precursor, 3CD, is also present near the 5'-terminus of the RNA, forming a ternary complex (Gamarnik and Andino, 1997; Gamarnik and Andino, 2000; Parsley et al., 1997). On the opposite terminus of the poliovirus genome, PABP1 associates with the genetically encoded poly(A) tract. Through co-immunoprecipitation using antibodies directed against PABP1, it has been demonstrated that PCBP2 and PABP1 directly interact in poliovirus-infected cells. As a result, it has been proposed that PABP1 acts as a bridge to link both ends of the viral genome because it is able to simultaneously interact with the 3'-terminus of poliovirus genomic RNA as well as the ternary complex

(i.e., both 3CD and PCBP2), which is present on the 5'-terminus of the same RNA molecule (Herold and Andino, 2001) (**Figure 1.4A**). More recently it has been shown that PCBP2 binds to both the S-L I structure and to a C-rich spacer region that is found between S-L I and the IRES element of poliovirus RNA (Toyoda et al., 2007). Based on similar interactions between PCBP2 and CVB3 RNA, it is likely that PCBP2 modulates the RNA replication of this closely related virus (Zell et al., 2008a; Zell et al., 2008b).

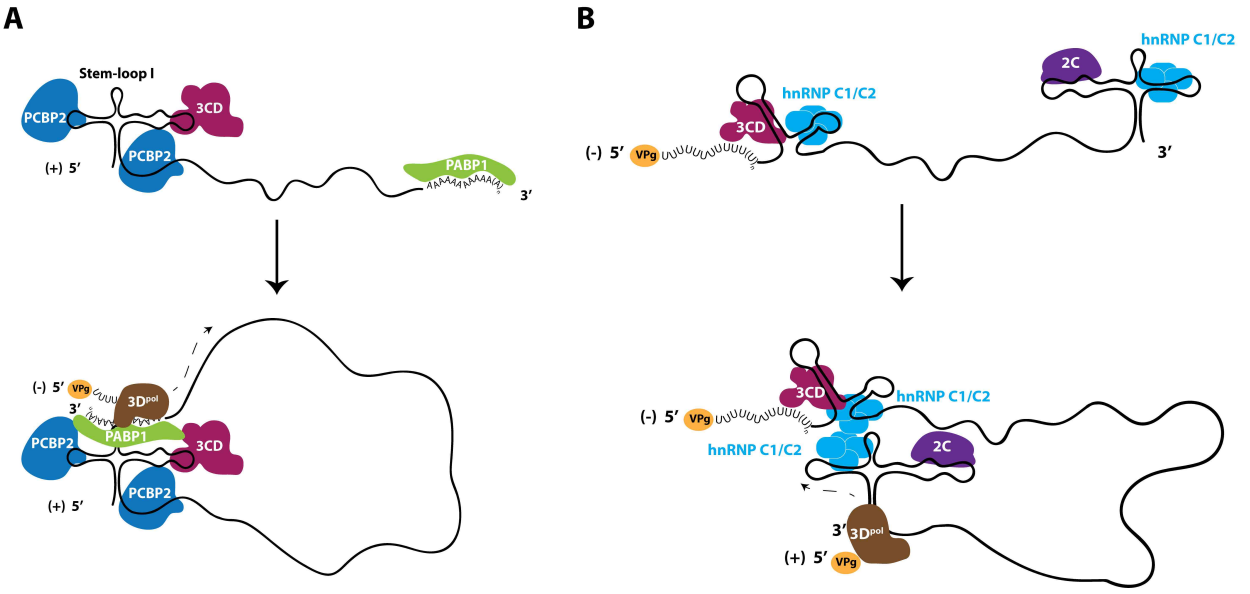

Figure 1.4. Ribonucleoproteins (RNPs) comprised of nuclear resident proteins facilitate enterovirus RNA replication. (**A**) Nuclear resident proteins PCBP2 (dark blue) and PABP1 (green) act in conjunction with viral protein 3CD (fuchsia) to circularize genomic RNA for use as templates to produce negative-sense RNA intermediates. (**B**) Nuclear protein hnRNP C1/C2 (light blue) interacts with both termini of negative-sense RNA molecules and is hypothesized to circularize the negative-sense template to promote genomic RNA production. Although likely in the form of double-stranded RNA, the negative-sense RNA is shown here as single stranded for clarity. Viral protein 2C (purple) interacts with the 5'-terminus of negative-sense RNA, although the direct function of this protein in viral RNA replication is unclear. The viral RNA-directed RNA polymerase $3D^{pol}$ (brown) is recruited to these circularized templates and initiates viral RNA synthesis. VPg (yellow), the viral protein that primes RNA synthesis, is found on RNA molecules that have not been translated.

A nuclear resident protein promotes enterovirus genomic RNA production

The production of negative-sense viral RNA from genomic templates results in the formation of a double-stranded RNA molecule called the replicative form. The replicative form contains the template for the production of genomic RNA, and therefore the duplexed RNA strands within this structure must be separated at the 3'-terminus of the negative- strand RNA to allow for 3D association and the initiation of RNA synthesis. A single host-cell protein, hnRNP C1/C2, has been demonstrated to promote the amplification of positive-strand poliovirus RNA from the negative-strand template and, as with many other host proteins involved in the infectious cycles of picornaviruses, is a nuclear resident protein. HnRNP C1 and C2 are produced by alternative splicing, with the C2 isoform containing 13 additional amino acids (Koloteva-Levine et al., 2002). Together, these hnRNP C1 and C2 proteins form a heterotetramer containing three copies of C1 and a single copy of C2 that bind pre-mRNA, regulate splicing, and nucleate the formation of 40S hnRNP particles (Barnett et al., 1989; Huang et al., 1994). Each C protein contains an RNA recognition motif, an oligomerization domain, a nuclear localization signal, and a nuclear retention signal (Görlach et al., 1992; McAfee et al., 1996; Nakielny and Dreyfuss, 1996; Wan et al., 2001). In contrast to many other hnRNP proteins, hnRNP C1/C2 appears to be restricted to the nucleus and does not shuttle to the cytoplasm in complex with mRNA (Piñol-Roma and Dreyfuss, 1992; Piñol-Roma and Dreyfuss, 1993). Polioviruses that lack the 3'-terminus of genomic RNA molecules, and therefore the 5'-terminus of anti-genomic RNAs, have been shown to have a defect in the initiation of positive-strand RNA synthesis, consistent with the idea that both termini of the negative-strand intermediate are important for genomic RNA production

(Brown et al., 2004). HnRNP C1/C2 can bind both the 3'-and 5'-termini of poliovirus negative-sense RNA intermediates (regions complementary to the 5'-NCR and 3'-NCR of genomic RNA, respectively) and has been proposed to play a role in poliovirus RNA replication by facilitating and/or stabilizing the terminal strand separation required for replication of this template (Brunner et al., 2005; Ertel et al., 2010; Roehl and Semler, 1995).

The association of hnRNP C1/C2 with both termini of the negative-sense RNA molecule may also allow for the end-to-end linkage of this RNA template via the multimerization of hnRNP C1/C2 tetramers, since the multimerization domain of this protein is required for efficient *in vitro* replication of poliovirus RNA (Ertel et al., 2010). Recombinant hnRNP C1/C2 is able to rescue positive-strand RNA synthesis in cellular extracts depleted of endogenous hnRNP C1/C2, supporting a critical role for this protein in the production of poliovirus genomic RNA (Brunner et al., 2005). It has also been demonstrated that hnRNP C1/C2 interacts with the poliovirus protein 3CD (the polymerase precursor) through glutathione S-transferase pull-down assays; therefore, hnRNP C1/C2 may aid in the recruitment of the 3D polymerase to the replication template (Brunner et al., 2005). Furthermore, reduced cellular levels of hnRNP C1/C2 cause a decrease in the kinetics of poliovirus RNA synthesis during infection (Brunner et al., 2010). Combined with the finding that an intact 3'-NCR of poliovirus genomic RNA contributes to positive-strand RNA synthesis efficiency through complementary elements conserved at the 5'-end of negative-sense strand, a model for positive-sense RNA synthesis has been proposed. Because hnRNP C1/C2 preferentially binds single-stranded RNA, it may be necessary for viral protein 2C (or 2BC) to bind the negative-

sense cloverleaf first, due to the presence of RNA duplexes and structures immediately following negative-sense RNA production (Brunner et al., 2005; Dreyfuss et al., 1993). This model is reminiscent of negative-sense RNA production, with both ends of the RNA template in close proximity, albeit in the form of a predominantly dsRNA molecule (Ertel et al., 2010). Due to the proximity of the ternary complex found on the 5'-end of the positive sense poliovirus RNA molecule, it is possible that at least one polymerase utilized in the synthesis of the positive-sense RNA is recruited directly from the ternary complex on the genomic RNA molecule to the negative-sense template, as suggested by the trans-initiation model (Vogt and Andino, 2010) (**Figure 1.4B**).

The circularization of RNA templates proposed to promote poliovirus RNA replication is made possible by nuclear resident proteins. Circularized templates may serve to function as a fidelity check on the RNA itself, to act in lieu of a true promoter region to enhance the initiation of RNA synthesis, and/or to provide a mechanism by which 3D specifically recognizes a polyadenylated mRNA of viral origin in an infected cell containing abundant polyadenylated mRNA transcripts. While there has been little exploration of the RNA replication process in genera beyond the enteroviruses, it is possible that, as with the handful of nuclear proteins that are considered picornavirus-general ITAFs, there is a minimal requirement of particular nuclear resident proteins to promote picornavirus RNA replication. At present, the three major players are PCBP2, PABP1, and hnRNP C1/C2, at least for enterovirus RNA replication, but it is possible that there are species-specific factors that act to further enhance the efficiency of RNA replication. As with translation, the cohort of proteins utilized for picornavirus RNA replication may also be dependent upon the availability of particular proteins within the

context of the cellular microenvironment where the viral RNA molecules are located. The different levels of enhancement provided to picornavirus RNA replication through the activities of different (or available) nuclear resident host-cell proteins may contribute to the variable ratios of positive- to negative-sense RNA ratios, which have been reported to range from 30:1 to 70:1 for poliovirus (Andino et al., 1990; Giachetti and Semler, 1991; Novak and Kirkegaard, 1991).

Nuclear protein involvement in the RNA replication cycle of other picornaviruses

There has been little study of the RNA replication cycle of non-enterovirus picornaviruses. It has been reported that PABP1 is cleaved in EMCV-infected cells and that this cleavage is mediated by 3C. However, even though viral RNA replication and viral titers were reduced in the presence of a non-cleavable PABP1, viral translation was unaffected which was not reconciled with what is known about the coupling between translation and RNA replication by the authors (Kobayashi et al., 2012). See **Table 1.2** for an accounting of the nuclear proteins that are closely associated with picornavirus RNA during the infectious cycle.

Table 1.2. Nuclear resident proteins directly involved in the picornavirus replication cycle

Cellular protein	Function in infectious cycle
PTBP1	Promotes translation through stabilization of RNA secondary structure (Type I, III, and III IRESs); contributes to template usage switch
SSB	Stimulates translation from Type I and Type II IRESs; suppresses translation from Type III IRESs
PCBP2	Stimulates translation from Type I and Type III IRESs but does not bind Type III IRES elements; contributes to template usage switch; involved in template circularization and RNA replication
SRSF3	Acts synergistically with PCBP2 to increase efficiency of poliovirus translation
PA2G4	Promotes FMDV translation in cooperation with PTBP1; not required for EMCV translation
Nucleolin	Stimulates translation of Type I IRESs
hnRNP A1/hnRNP A2	Interacts with Type I IRESs to promote translation
FUBP1	Promotes translation from the EV71 IRES
FUBP2	Negative regulator of EV71 translation
Sam68	Interacts with Type I and Type II IRESs to promote translation
HUR	Binds to the EV71 IRES, may promote translation
AGO2	Binds to the EV71 IRES, may promote translation
ILF3	Heterodimerizes with ILF2 and inhibits HRV2 translation
AUF1	Binds Type I IRES elements and inhibits translation; binds 3'-NCR of CVB3
Gemin5	Likely inhibits FMDV translation through competitive inhibition of PTB1 binding
NONO	Positive regulator of poliovirus replication
hnRNP K	Positive regulator of EV71 replication
DHX9	Positive regulator of FMDV replication
PABP1	Involved in circularization of poliovirus RNA to stimulate RNA replication, may be involved in template usage switch
TDP2	Removes VPg from viral RNA, possible role in encapsidation
hnRNP C1/C2	May act to circularize negative-sense templates; promotes genomic RNA synthesis

Alterations in nucleocytoplasmic trafficking causes the loss of normal subcellular localization of nuclear resident proteins and facilitates picornavirus replication

As discussed above, the initial rounds of picornavirus translation and RNA replication are dependent on nuclear resident proteins that are present in the cytoplasm of the infected cell as a result of their shuttling function or nascent biogenesis. As the replication process continues, there is amplification in both viral protein production and RNA replication as the number of viral RNA templates increase. The low concentration of nuclear proteins normally present in the cytoplasm is no longer sufficient to meet the increased demand for these proteins. As a result, picornaviruses alter

nucleocytoplasmic trafficking to provide the functions of normally nuclear resident proteins to the cytoplasm where viral replication takes place.

Enterovirus proteinases degrade the nucleoporin proteins of the NPC

Because the NPC is the main route by which the nucleus and cytoplasm exchange material, picornaviruses target the NPC specifically to disrupt normal protein trafficking, resulting in the cytoplasmic accumulation of nuclear proteins. Enterovirus (poliovirus or HRV14) infection alters both the classical import pathway, which relies on a heterodimer consisting of an importin-α (karyopherin α) adaptor protein that binds the arginine-lysine-rich NLS of the cargo protein and transport receptor importin-β (karyopherin β1), as well as the transportin-1 (karyopherin β2) pathway in which the import receptor transportin-1 recognizes a glycine-rich motif known as the M9 NLS [reviewed in (Cautain et al., 2015)]. In uninfected cells expressing enhanced green fluorescent protein (EGFP) linked to either a classical NLS derived from the large T antigen of simian virus 40 (SV40 TAg) or the M9 NLS of hnRNP A1, EGFP localizes to the nucleus. However, upon infection with poliovirus an accumulation of EGFP protein is observed in the cytoplasm, demonstrating a disruption in these two import pathways as a consequence of infection (Gustin and Sarnow, 2001). Additionally, hnRNP K, which contains a unique 40-amino acid motif NLS, known as K nuclear shuttling (KNS) domain, is also relocalized to the cytoplasm of poliovirus-infected cells, suggesting the import of proteins through the KNS-mediated pathway is prevented during infection (Gustin and Sarnow, 2001; Michael et al., 1997). HRV14 infection also causes cytoplasmic localization of EGFP fusion proteins containing a classical or M9 NLS, albeit at later times during infection than observed for poliovirus (Gustin and Sarnow,

2002). Conversely, an EGFP fusion protein containing an NLS that mediates nuclear import through a hormone-dependent but unknown importin-α-independent pathway remains localized to the nucleus upon poliovirus infection. This suggests that specific import pathways are targeted by poliovirus, while some import pathways remain functional (also see transportin-3 discussion, below). By analyzing the reverse of nuclear import, it has also been shown that at least one NES pathway remains intact during poliovirus infection. An EGFP fusion protein containing a leucine-rich NES recognized by the exportin-1 (also known as chromosome region maintenance 1, CRM1) export receptor is localized to the cytoplasm during infection, and a small molecule inhibitor of exportin-1 causes retention of the EGFP fusion protein in the nucleus, suggesting that this export pathway is unaltered in poliovirus-infected cells (Gustin and Sarnow, 2001). However, exportin-1-dependent export does seem to be disrupted by ectopic expression of rhinovirus 2A proteinases or infection with HRV16 (Watters et al., 2017). **Table 1.3** summarizes what is known about the dysregulation of nucleocytoplasmic trafficking during picornavirus infections, causing the cytoplasmic accumulation of proteins that use these pathways to translocate to the nucleus following biogenesis.

Table 1.3. Nucleocytoplasmic trafficking pathways disrupted during enterovirus or cardiovirus infections

Importin/exportin	Type of signal sequence	Example protein	Nups utilized
Importin-α/β	Classical/SV40 TAg-like	cyclin B1	54, 58, 62, 98, 153, 214, 358, TPR
Transportin-1	M9 NLS-like	hnRNP A1	62, 98, 153, 214, 358
Transportin-3	RS NLS-like	SRSF1	?
Exportin-1	PKI NES-like/leucine-rich NES	snurportin 1	62, 98, 153, 214
Exportin-2	?	importin-α	?
?	KNS domain	hnRNP K	?

Note: references in main text and (Cautain et al., 2015; Ryan and Wente, 2000)

Like poliovirus, CVB3 also causes the relocalization of GFP fused with a classical NLS, indicating that alterations to nucleocytoplasmic transport pathways are a general feature of enteroviruses (Belov et al., 2000). However, the use of Timer proteins that change emission fluorescence based on their age has shown that the accumulation of nuclear proteins in the cytoplasm of enterovirus-infected cells is, in part, a result of increased efflux of “old” proteins from the nucleus, rather than simply a block to the import of newly-synthesized proteins (Belov et al., 2004). It should also be noted that cellular cap-dependent translation is inhibited early during enterovirus infection, through proteinase-induced cleavage of canonical initiation factors (Dougherty et al., 2010). This indicates that although enteroviruses cause dysregulation of some nuclear import pathways, there is not a continuous buildup of newly synthesized proteins in the cytoplasm throughout the course of infection, as cellular translation is effectively shutdown early in the infectious cycle.

The finding that nuclear resident proteins accumulate in the cytoplasm of cells upon picornavirus infection as a result of increased protein efflux from the nucleus appears at odds with the observation that picornavirus-induced disruptions in nuclear import cause cytoplasmic retention of newly synthesized nuclear resident proteins. However, these seemingly disparate findings can be reconciled upon closer examination of the particular alterations made to the NPC during infection. The increased permeability of, and inability to import proteins through the NPC during enterovirus infection is the result of changes made to Nup proteins that comprise the NPC itself. Electron microscopy of poliovirus-infected cells shows structural alterations to the nuclear envelopes and nuclear pores, specifically the loss of an obstructing bar-

like structure in the central channel, which is at least partially caused by the viral proteinase 2A. General inhibitors of the 2A proteinase suppress the efflux of marker proteins from the nucleus during infection. In addition, transfection of a wild type 2A expression construct, but not a construct encoding an inactive 2A, into cells yields cytoplasmic relocalization of stably expressed GFP-NLS proteins (Belov et al., 2004). Structural data from electron microscopy studies showing destruction of the NPC and products of proteolysis within the pore bolster biochemical data that demonstrates the degradation of Nup 153 and Nup 62 in cells infected with either poliovirus or rhinovirus. Moreover, immunofluorescence microscopy indicates a decrease in overall levels of these Nups as the course of an enterovirus infection proceeds (Gustin and Sarnow, 2001, 2002).

Prior to the proteolysis of Nup 153 and Nup 62, Nup 98 is degraded by 2A in poliovirus-infected cells. The cleavage of Nup 98 is insensitive to guanidine hydrochloride treatment, which inhibits enterovirus RNA replication and results in reduced viral protein production, whereas the cleavage of Nup 153 and Nup 62 is sensitive to the presence of guanidine. Together with the fast kinetics of this cleavage (within 1 h post-infection), this suggests that Nup 98 is cleaved even when there is a very low concentration of viral protein present within the infected cell. This also suggests that poliovirus (and perhaps other enteroviruses) may target specific Nups and trafficking pathways at different times in the infectious cycle to facilitate viral replication (Park et al., 2008). The addition of purified HRV2 2A to whole cell lysates causes the cleavage of Nup 98 while the expression of poliovirus 2A in cells results in the degradation of Nup 62, Nup 98, and Nup 153, demonstrating that 2A is able to alter

components of the NPC (Castelló et al., 2009; Park et al., 2008). In agreement with what was observed for HRV2, expression of poliovirus 2A in HeLa cells results in the degradation of Nup 62, Nup 98, and Nup 153 (Fitzgerald et al., 2013). Furthermore, purified HRV2 2A is able to cleave recombinant Nup 62 *in vitro*. HRV2 2A-dependent cleavage of Nup 98 (Gly-374 and Gly-552) and Nup 62 (Ala-103) liberates the FG-rich regions from these proteins, a domain important for nuclear transport receptor association during translocation through the NPC (Park et al., 2015; Park et al., 2010). Interestingly, experiments utilizing recombinant 2A from the three different HRV species, live-cell imaging of cells stably expressing mCherry marker proteins linked to NLS or NES sequences, or through Western blot analysis of lysates from HRV-infected cells demonstrated that these proteinases cleave Nup 62, Nup 98, and Nup 153 at distinct sites and with variable rates, causing commensurate mislocalization of proteins (Walker et al., 2015; Watters et al., 2017; Watters and Palmenberg, 2011). This suggests that following infection there are species-specific nuclear protein relocalization patterns.

Enterovirus 2A has an obvious role in Nup proteolysis during infection; however, two additional Nups, Nup 214 and Nup 358, as well as the previously mentioned Nup 153, are degraded in cells transfected with HRV16 3C or 3CD expression constructs, suggesting that the proteolytic activity of 2A alone does not account for all Nup degradation in enterovirus-infected cells (Ghildyal et al., 2009). In support of this idea, Nup 62 does not contain a 2A specific Tyr-Gly cleavage site and the sizes of Nup 153 cleavage products from poliovirus-infected cells do not correspond to those expected if 2A does degrade this Nup (Belov et al., 2004). Moreover, high concentrations of purified

HRV14 3C are able to induce the partial cleavage of Nup 62 *in vitro* (Park et al., 2010). Ectopic expression of active or inactive HRV16 3C proteinase in HeLa cells suggests that 3CD/3C likely mediates the cleavage of Nup 153, while Nup 62 and Nup 98 are more likely targeted by the 2A proteinase of this virus (**Table 1.4**). Importantly, structural components of the NPC, Nup 93 and Nup 133, are not degraded in enterovirus-infected cells, suggesting some level of specificity to those Nups that are targeted during enterovirus infection (Walker et al., 2013). During a natural infection, enterovirus proteinases likely act cooperatively to degrade Nup proteins, a process that is difficult to recapitulate *in vitro*.

Table 1.4. Alterations to nucleoporin proteins that result in nucleocytoplasmic trafficking disruptions during enterovirus and cardiovirus infections

Nup	Viral protein	Outcome
62	enterovirus 2A	degradation
	enterovirus 3CD/3C	degradation
	cardiovirus L	hyperphosphorylation
98	enterovirus 2A	degradation
	cardiovirus L	hyperphosphorylation
153	enterovirus 3CD/3C	degradation
	enterovirus 2A	degradation
	cardiovirus L	hyperphosphorylation
214	enterovirus 3CD/3C	degradation
	cardiovirus L	hyperphosphorylation
358	enterovirus 3CD/3C	degradation

Note: proteinases in grey text can cleave associated Nups in vitro or via ectopic expression, but likely have a more limited role during infection; hyperphosphorylation of Nups during cardiovirus infection is carried out through a Ran-dependent, mitogen-activated protein kinase cascade, not L directly.

Cardiovirus infection induces the hyper-phosphorylation of nucleoporin proteins

Like enteroviruses, the cardiovirus EMCV breaks down the specificity of bidirectional protein traffic through the NPC in infected cells by directly modifying the architecture of the NPC (Lidsky et al., 2006). The 2A proteins of cardioviruses lack proteinase activity, and Nup 62 as well as Nup 153 are stable in mengovirus-infected cells (Lidsky et al., 2006). Despite the lack of degradation of these Nups, mengovirus

and EMCV promote the redistribution of stably-expressed EGFP proteins containing the classical NLS of the SV40 TAg to the cytoplasm and normally cytoplasmic-resident proteins such as cyclin-B1 to the nucleus (Lidsky et al., 2006) (**Table 1.3**). The normal subcellular partitioning of proteins in cardiovirus-infected cells, like that of enterovirus-infected cells, is disrupted by dysregulation of bidirectional nucleocytoplasmic trafficking. Unlike enteroviruses, however, cardioviruses achieve this dysregulation through the action of the leader (L) protein. Mengovirus mutants lacking the leader protein coding sequence or encoding an L protein with a mutated zinc finger domain are unable to trigger the cytoplasmic redistribution of a stably expressed GFP-NLS fusion protein in cells. Furthermore, phosphorylation of a threonine residue at position 47 of the L-protein of mengovirus has also been suggested to play a functional role in L-dependent alterations to nuclear resident protein localization (Lidsky et al., 2006). Mutations to the L protein of TMEV, specifically disruptions made to the zinc-finger domain of this protein, also fail to facilitate the relocalization of endogenous nuclear proteins to the cytoplasm that are relocalized during infection with wild type TMEV (Delhaye et al., 2004). Protease inhibitors fail to suppress the cytoplasmic redistribution of stably expressed EGFP-NLS fusion proteins in EMCV-infected cellular extracts. Additionally, EMCV replicons containing mutations to the 2A coding sequence do not affect the nuclear envelope leakiness observed during EMCV infection. Taken together, these studies demonstrate that cardioviruses do not utilize a proteinase or viral protein 2A specifically to promote alterations to nucleocytoplasmic trafficking.

In the absence of other cardiovirus proteins, recombinant EMCV L alone is able to disrupt normal nuclear localization of a transiently transfected GFP-NLS, and an

intact zinc-finger domain within the L protein is specifically required for the observed increase in permeability of the nuclear envelope. A cellular phosphorylation pathway is also required to induce nuclear envelope leakiness, because L protein does not possess kinase activity. Additionally, the protein kinase inhibitor staurosporine can rescue nuclear import/export activity from L-dependent inhibition (Porter and Palmenberg, 2009). Nup 62, Nup 153, and Nup 214 each become hyperphosphorylated in an L-dependent manner as shown by phosphoprotein staining during infection with EMCV, and similarly, Nup 62 and Nup 98 are hyperphosphorylated in mengovirus and TMEV-infected cells, respectively, as shown by assaying for gel migration shifts following alkaline phosphatase treatment (Bardina et al., 2009; Porter and Palmenberg, 2009; Ricour et al., 2009b). The phosphorylation of Nup 62 and 98 in mengovirus and TMEV-infected cells, respectively, is also dependent upon the zinc- finger domain of L (Bardina et al., 2009; Ricour et al., 2009b). Interestingly, there is no phosphorylation level change of Nup 358 during cardiovirus infection, a Nup that is cleaved during enterovirus infection, (Porter and Palmenberg, 2009). As is the case with enteroviruses, there does appear to be specificity to the Nups that are targeted during cardiovirus infections. This is exemplified by the fact that Nup 50 is not phosphorylated by an L protein-dependent mechanism (Ciomperlik et al., 2015) (**Table 1.4**).

Direct architectural changes to the NPC can be observed through electron microscopy of NPC cross-sections from cardiovirus-infected cells. The central channel of nuclear pores is less electron dense in infected compared to uninfected cells, similar to what is observed in poliovirus-infected cells. How phosphorylation of Nups achieves un-blocking of these pores is not clear (Bardina et al., 2009; Lidsky et al., 2006). One

possibility is that phosphorylation increases the negative charge present on FG motif containing fibrils within the pores that normally act to block passive diffusion of macromolecules, and could promote retraction of fibrils to the NPC scaffold leaving the pore less inhibitory to diffusion (Cohen et al., 2012). Through screening a panel of kinase inhibitors, Nup hyperphosphorylation appears to be carried out via two mitotic terminal kinase effectors within the mitogen activated protein kinase cascade: extracellular signal-regulated receptor kinase (ERK also known as mitogen-activated protein kinase 1) and p38 mitogen-activated protein kinase (p38 also known as mitogen-activated protein kinase 14), although the exact mechanism by which L co-opts these kinases is not known (Porter et al., 2010). A C-terminal acidic domain within the L protein is also important for the Nup hyperphosphorylation, perhaps via interactions with MAPK pathway regulatory proteins (Porter et al., 2010). Another kinase that may have a role in L-dependent alterations to nucleocytoplasmic trafficking is casein kinase II (CK-2), as it has been shown to phosphorylate Thr-47 of mengovirus L, a phosphorylation event that has a functional role in nuclear protein efflux (Lidsky et al., 2006; Zoll et al., 2002). More recent studies have shown that CK-2 does indeed phosphorylate Thr-47 and spleen associated tyrosine kinase (syk) phosphorylates Tyr-41 of the EMCV L protein, although there appears to be variability in the kinases utilized during infection with other Cardioviruses (Basta et al., 2014; Basta and Palmenberg, 2014). The L protein of cardioviruses has also been shown to bind directly to Ran-GTPase (the concentration of which provides the gradient that imparts directionality to transport) as well as exportin-1 and exportin-2 (also known as CAS and CSE1L), suggesting cardioviruses may utilize multiple strategies to inhibit homeostatic nucleocytoplasmic

trafficking (Bacot-Davis et al., 2014; Bacot-Davis and Palmenberg, 2013; Ciomperlik et al., 2016; Porter et al., 2006). mRNA export has also been reported to be inhibited in cells expressing TMEV L protein by assaying for poly(A) transcript retention in the nucleus of cells via *in situ* hybridization (Ricour et al., 2009b). **(Table 1.3)**

FMDV infection does not cause dysregulation of nucleocytoplasmic trafficking

Interestingly, another picornavirus of the aphthovirus genus, FMDV, which encodes a proteolytic L-protein, does not appear to target Nups for degradation (Castelló et al., 2009). Moreover, infection with FMDV has not been reported to alter general nucleocytoplasmic trafficking, although some nuclear resident proteins are redistributed to the cytoplasm of infected cells, likely through a more cellular protein-specific directed approach (Lawrence and Rieder, 2009; Lawrence et al., 2012).

Alterations to NPC components are not a result of apoptosis

Apoptotic cell death has been shown to cause damage to the nuclear envelope barrier, including cleavage of Nup 153, through the actions of cellular caspase-9 (Buendia et al., 1999; Faleiro and Lazebnik, 2000). Because enteroviruses can promote apoptotic cell death, it is theoretically possible that the increases in NPC permeability observed during picornavirus infection are due to caspase-9 induction rather than the direct actions of viral proteins themselves [reviewed in (Buenz and Howe, 2006)]. Indeed, poliovirus can cause the initiation of an apoptotic program through caspase-9, and expression of 2A alone can cause cell death through apoptosis (Agol et al., 1998; Belov et al., 2003; Goldstaub et al., 2000; Tolskaya et al., 1995). However, cells deficient in caspase-9 (as well as associated caspase-3) did not show differences in NPC permeability compared to cells expressing normal levels of caspases when

infected with poliovirus, suggesting that the increased permeability of the NPC during picornavirus infection is independent of the action of pro-apoptotic caspases (Belov et al., 2004). Similar results have been observed using the small molecule pan-caspase inhibitor benzyloxycarbonyl-Val-Ala-Asp-(OMe) fluoromethyl ketone (zVAD-FMK) (Belov et al., 2000; Belov et al., 2004). In the presence of zVAD-FMK, nuclear protein efflux was delayed during poliovirus infection; however, this is likely because zVAD-FMK can inhibit the activity of enterovirus proteinases, with consequences to the kinetics of the infectious cycle (Deszcz et al., 2004; Martin et al., 2007). Moreover, Nup 62 destruction is a marker of picornavirus-infected cells but not apoptotic cells (Buendia et al., 1999; Gustin and Sarnow, 2001, 2002).

Like poliovirus, HAV, CVB3, and TMEV can induce apoptosis, but the multitude of ways in which picornaviruses are known to inhibit apoptotic pathways to allow for their replication has been well documented [reviewed in (Croft et al., 2017)]. The consistent relocalization of cellular proteins to different cellular compartments seen during infection cannot be solely attributed to pathways involved in programmed cell death (Belov et al., 2003; Gosert et al., 2000b; Henke et al., 2001; Jelachich and Lipton, 2001; Neznanov et al., 2001; Romanova et al., 2009; Tolskaya et al., 1995).

Picornavirus-induced alterations to nucleocytoplasmic trafficking result in the redistribution of cellular proteins

Although both increased efflux of nuclear resident proteins as a result of the dysregulation of the barrier function of the nuclear envelope as well as impediments to nuclear import of nascently produced cellular proteins in the cytoplasm (i.e., prior to host protein translation inhibition by viral infection) have been demonstrated to occur in

picornavirus-infected cells, these mechanisms are not mutually exclusive. Enterovirus-induced cleavage of Nups 62, 98, 153, 214, and 358 by the 2A and 3CD/3C proteinases, or cardiovirus-induced hyper-phosphorylation of Nups 62, 98, 153, and 214 through actions of the Leader protein, is directly responsible for both the increased "leakiness" of the nuclear envelope and the lack of nuclear import receptor–cargo complex docking at the cytoplasmic face of the NPC. Nucleocytoplasmic trafficking is an intricate and tightly regulated process allowing for precise control of gene expression. As a result, drastic alterations to the components of the NPC, the gateway between the two major compartments of the eukaryotic cell, will have diverse and far-reaching consequences on trafficking pathways. Indeed, enterovirus- and cardiovirus-induced alterations to the NPC can cause the loss of normal protein partitioning not only for nuclear resident proteins but also for some cytoplasmic-resident proteins (Belov et al., 2004; Lidsky et al., 2006). The picornaviruses have evolved to take advantage of this important regulatory node to supply nuclear resident proteins, and therefore an increased functional repertoire, within the cytoplasmic site of their replication.

All of the Nup proteins that are the targets of alteration by picornavirus proteins have critical roles in shuttling macromolecules through the NPC (**Figure 1.5**). Nup 214 and 358 are positioned on the cytoplasmic side of the NPC, with Nup 358 making up cytoplasmic filaments of the NPC, and Nup 214 residing on the cytoplasmic face of the NPC. Nup 62 is localized to the central pore of the NPC and Nup 153 is a component of the nuclear basket. Nup 98 is found within and on both sides of the NPC and can function, to some degree, independently of the NPC due to its mobile nature (Griffis et al., 2002). All five of these Nups contain FG repeat domains, indicative of their direct

role in nucleocytoplasmic transport [reviewed in (Chatel and Fahrenkrog, 2011)]. Nup 62, in association with other Nups, forms a central “plug” in the channel of the NPC, and the cleavage of this protein by enteroviral proteinases has been suggested to account for the loss of the electron-dense material within the NPC and appearance of “granules” likely corresponding to Nup cleavage products, as observed via electron microscopy (Bardina et al., 2009). This particular alteration could allow for the diffusion of proteins in and out of the nucleus, accounting for the increased “leakiness” of the nuclear envelope observed as a result of infection (Belov et al., 2004). Interestingly, it appears that the alterations made to these proteins individually are not sufficient to promote a loss of normal cellular protein partitioning and that inhibition of nuclear import can only occur in cells with a composite of Nup alterations (Park et al., 2008). **Table 1.4** summarizes what is known about picornavirus-induced alterations to Nup proteins.

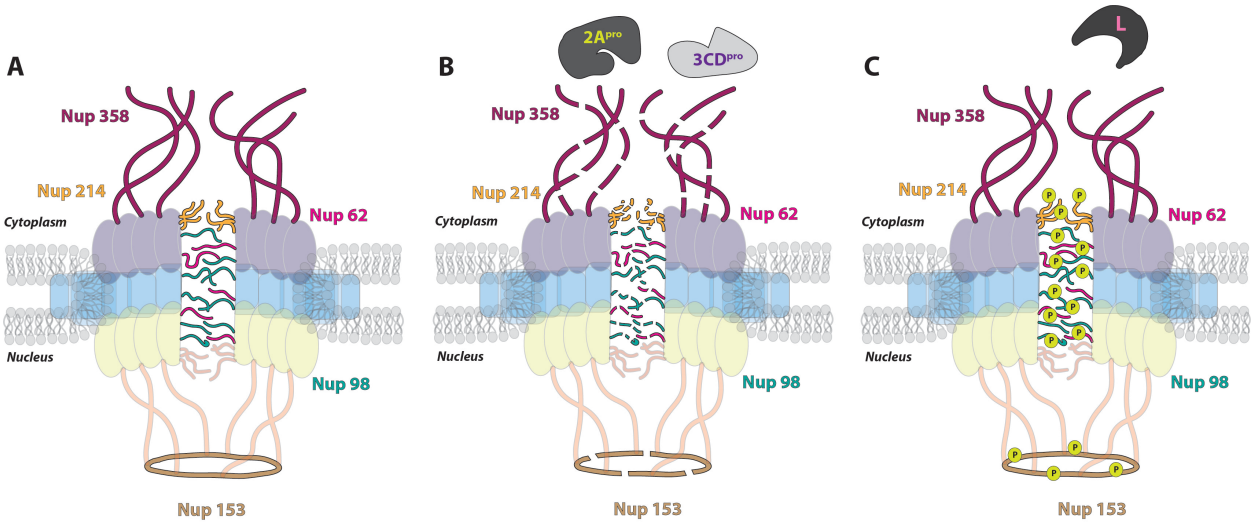

Figure 1.5. Picornavirus-induced alterations to the nuclear pore complex. (**A**) Localization of the regions within the NPC where the five Nup proteins targeted by picornavirus proteins during infection. (**B**) Enterovirus proteinase 3CD/3C ($3CD^{pro}$) cleaves Nup358 (purple) and Nup153 (brown), which are components of the cytoplasmic filaments and nuclear basket, respectively. The cytoplasmic Nup214 (yellow), is also targeted by $3CD^{pro}$.The 2A proteinase ($2A^{pro}$) of enteroviruses degrades FG repeat containing barrier Nups of the central channel, including Nup62 and Nup98 (pink and green, respectively). **C.** Cardiovirus infection induces the hyper-phosphorylation (P within chartreuse circle) of the same Nups targeted by enteroviruses, excluding Nup358, through actions of the Leader protein (L) but is dependent on a cellular kinase cascade since L has not kinase activity.

Nup 153 has been reported to interact with importin α/β and transportin-1; therefore, alterations to Nup 153 are at least partially able to account for the inhibition of the nucleocytoplasmic trafficking pathways that rely on these receptors (i.e., classical SV40 TAg-like and M9 NLS-like) (Nakielny et al., 1999; Shah et al., 1998). Although Nup 98 has been implicated in mRNA export from the nucleus, alterations made to this Nup during enterovirus infection do not inhibit cellular mRNA export, in contrast to the mRNA export inhibition observed in cardiovirus-infected cells (Griffis et al., 2003; Park et al., 2008; Porter et al., 2006; Powers et al., 1997; Ricour et al., 2009b). Notably, however, a study in which an enteroviral 2A expression construct was electroporated into cells demonstrated that nuclear export of mRNAs, U snRNAs, and rRNAs but not tRNAs was blocked when 2A was expressed (Castelló et al., 2009). In addition to FG domains present in Nup 358 and Nup 153, these Nups also contain Ran binding domains and as a result, picornavirus targeting of these proteins could conceivably have profound consequences on the compartmentalization of cellular proteins by disruption of the Ran gradient (Wente and Rout, 2010). The L-protein of EMCV, and likely cardioviruses in general, is simultaneously able to disrupt the differential Ran gradient across the nuclear envelope by directly binding and sequestering Ran (Porter et al., 2006).

The picornavirus-mediated changes to components of the NPC critical to nucleocytoplasmic trafficking increase the bidirectional transport of proteins within the infected cell, thus causing a massive dysregulation of the transport process as a whole. However, as mentioned previously, there appears to be some level of specificity to which import and export pathways are affected, as a subset of nuclear resident proteins

relocalize while others do not. For example, nuclear resident proteins fibrillarin, TATA-box binding protein (TBP), lamin A/C, and serine and arginine-rich splicing factor 2 (SRSF2 or SC35) do not relocalize from the nucleus to the cytoplasm during enterovirus infection (Gustin and Sarnow, 2001; McBride et al., 1996; Meerovitch et al., 1993; Waggoner and Sarnow, 1998; Walker et al., 2013). SRSF2 is imported into the nucleus through the transportin-3 (also known as transportin-SR) import receptor, so it is possible that this pathway is unaffected by infection with some picornaviruses (Kataoka et al., 1999). In contrast, it has recently been demonstrated that ectopic expression of rhinovirus 2A proteinases causes the disruption of the transportin-3 import pathway (Watters et al., 2017). **(Table 1.3)**

Because picornavirus infection halts cellular translation in the early stages of infection, the persistence of some nuclear resident proteins in the nucleus cannot be solely attributed to continued transport of newly synthesized proteins to this subcellular compartment. Nuclear shuttling proteins, however, could be inhibited from re-entering the nucleus by picornavirus-mediated disruptions to trafficking pathways, trapping these proteins in the cytoplasm. Protein-specific nuclear retention signals (NRSs) may allow some proteins to maintain normal localization throughout the course of infection, although not all proteins that contain NRSs remain in the nucleus, as even the strongly nuclear resident hnRNP C1/C2 is relocalized to the cytoplasm between following infection with enteroviruses (Gustin and Sarnow, 2001; Walker et al., 2015). Further complicating attempts to fully explain how picornavirus infection affects the subcellular localization of endogenous proteins is the fact that some normally-nuclear resident proteins such as nucleolin, SSB, Sam68, hnRNP A1, hnRNP K, and hnRNP C1/C2

have been observed almost completely relocalized to the cytoplasm upon enterovirus infection (as observed by immunofluorescence microscopy), even though a general increase in bidirectional trafficking through the nuclear envelope would predict a uniform distribution of these proteins between the nucleus and cytoplasm (Gustin and Sarnow, 2001, 2002).

It is possible that the apparent uneven redistribution of some proteins between the nucleus and cytoplasm in spite of picornavirus-induced disruptions to nucleocytoplasmic trafficking can be interpreted as these proteins being associated with specific cellular or viral structures that retain their subcellular location throughout infection. For example, retention of nuclear resident proteins within the nucleus following infection could be explained by these proteins having strong associations with DNA, which remains in the nucleus regardless of virus-induced nuclear pore modifications. Interestingly, serum response factor (SRF) relocalizes to the cytoplasm of CVB3-infected cells following 2A-mediated cleavage, likely as a result of liberating its transactivation domain from its DNA-binding domain, although SRF does not appear to play a role in viral replication (Wong et al., 2012).

Many proteins, including nucleolin, hnRNP A1, PTBP1, SSB, Sam68, hnRNP K, hnRNP C1/C2, SRSF3, and TDP2, that are relocalized as a result of picornavirus infection have direct effects on the replication cycle of picornaviruses (Back et al., 2002; Fitzgerald et al., 2013; Fitzgerald and Semler, 2011; Gustin and Sarnow, 2001, 2002; Lin et al., 2008; McBride et al., 1996; Meerovitch et al., 1993; Ricour et al., 2009a; Virgen-Slane et al., 2012; Waggoner and Sarnow, 1998; Zhang et al., 2015). Additionally, TAR DNA binding protein (TARDBP also known as TDP-43) has been

shown to translocate from the nucleus to the cytoplasm in a 2A-dependent manner following CVB3 infection and to be cleaved by CVB3 3C *in vitro*. Knockdown of TARDBP was also shown to increase titers of CVB3, suggesting it may impact viral replication (Fung et al., 2015). Recently, the nuclear protein hnRNP M has been shown to redistribute to the cytoplasm of poliovirus- and CVB3-infected cells. This protein is the target of 3CD/3C-induced cleavage at Gln389-Gly390 *in vitro* and *in vivo*. Depletion of hnRNP M via small interfering RNA knockdown resulted in reduced titers of both poliovirus and CVB3. However, hnRNP M knockdown did not affect poliovirus IRES-driven translation or viral RNA stability. Although the precise mechanism by which hnRNP M promotes enterovirus replication is not known, this study demonstrates that even relocalized nuclear proteins that are the target of viral proteinases can have proviral roles during infection (Jagdeo et al., 2015).

Aside from direct roles in picornavirus replication, redistribution of nuclear proteins also has consequences on cellular homeostasis. For example, because Sam68 functions in cell cycle transitions, the redistribution of this protein as a result of infection could disrupt the cell cycle. Other proteins, including various splicing factors which appear to have no role in viral replication, have also been shown to redistribute to the cytoplasm of poliovirus 2A expressing cells, likely as a mechanism to further disrupt host-cell gene expression, which will be discussed in a subsequent section (Alvarez et al., 2013; Álvarez et al., 2011).

While the relocalization of most cellular proteins utilized by picornaviruses during infection can be attributed to disruption of homeostatic nucleocytoplasmic trafficking, some other proteins are relocalized, at least partially, through direct cleavage by viral

proteinases and the subsequent loss or alteration of functional NLS regions within these proteins. Cleavage of PTBP1 and SSB, both of which contain a bipartite NLS, by poliovirus 3CD/3C exemplifies this phenomenon (Back et al., 2002; Romanelli et al., 1997; Shiroki et al., 1999; Simons et al., 1996). Sam68 is also relocalized to the cytoplasm of FMDV-infected cells, due to 3CD/3C-induced cleavage, which liberates the NLS-containing domain, preventing the re-importation of cleaved Sam68 to the nucleus. Cleaved Sam68 then binds regions within the FMDV IRES and likely has a role in viral translation, but it also may be utilized for RNA replication (Lawrence et al., 2012; Rai et al., 2015). DHX9, which likely functions in aphthovirus RNA replication, is also mislocalized in FMDV-infected cells. This relocalization has been attributed to the demethylation of DHX9 (Lawrence and Rieder, 2009). Furthermore, the nuclear efflux of DHX9 occurs with a concomitant influx of Jumonji C-domain containing protein 6, a demethylating protein that may act on DHX9 (Lawrence et al., 2014). This suggests that because FMDV does not degrade Nup proteins directly, it may have more precise control over cellular protein trafficking compared to general disruptions in trafficking pathways observed with other picornaviruses.

Virus-induced NPC alterations lead to interference with host antiviral defenses

In addition to concentrating proteins with functions that are co-opted by picornaviruses for replication in the cytoplasm, alterations to nucleocytoplasmic trafficking can also disable innate antiviral signaling cascades in infected cells. One of the earliest host responses to viral infection, the innate antiviral response, is mediated primarily by the action of Type-I interferons (IFNs). This response is activated by the cellular recognition of viral molecules called pathogen associated molecular patterns

(PAMPs). One major receptor of intracellular PAMPs that recognize picornavirus family members is interferon induced with helicase C domain 1 (also known as melanoma differentiation-associated protein 5 or MDA5) (Feng et al., 2012; Kato et al., 2006). Upon PAMP recognition, cytoplasmic receptors such as MDA5 initiate a cascade of events that results in the activation of transcription factors such as IFN regulatory factor 3 (IRF-3), IRF-7, and nuclear factor (NF)-κB. Importins then act in transporting these transcription factors through the NPC to the nucleus, which, in turn, activates the transcription of type I interferons (IFN-α/β) and interferon-stimulated genes (ISGs). The resultant IFN mRNA is exported to the cytoplasm where it is translated and its protein product is then secreted, inducing a secondary response in an autocrine and paracrine manner. This results in the activation of a second signaling cascade involving many effectors and transcription factors such as signal transducer and activator of transcription (STAT) proteins, which translocate to the nucleus. Within the nucleus, these proteins activate transcription of additional ISGs. These IFN stimulated gene products target the pathogen for destruction (Younessi et al., 2012).

Changes made to the NPC by picornaviruses can lead to disruptions in translocation of transcription factors (e.g. IRF-3) to the nucleus and subsequent attenuation in ISG expression and the associated antiviral response. Nup 98 is cleaved much more rapidly than the other Nup targets in poliovirus-infected cells, and this has been suggested to be an early target of picornavirus proteins to diminish induction of antiviral gene transcription. Experiments utilizing guanidine hydrochloride, which inhibits enterovirus RNA replication and, as a result, normal levels of viral protein production, have shown that cleavage of Nup 98 in poliovirus-infected cells is not sufficient to cause

relocalization of proteins like nucleolin and that high concentrations of viral proteins are needed to degrade other Nup targets to allow the widespread redistribution of nuclear resident proteins to the cytoplasm (Park et al., 2008). Nup 98 is a component of the NPC but can also be found dissociated from this complex both in the nucleus and the cytoplasm. Enteroviral 2A may be capable of targeting free Nup 98 prior to direct cap-dependent translation inhibition (when viral proteins begin to accumulate to sufficient levels) and transcriptional shutoff, which occurs when 3C precursors enter the nucleus of infected cells (discussed in a subsequent section), and interfere with signaling to the nucleus and/or the export of ISG transcripts. As a result, the virus may be able to avoid inducing an early antiviral response within the cell and promote maximal viral amplification (Park et al., 2008). Interestingly, Nup 98 has recently been shown to act as a transcriptional regulator and induce the expression of antiviral defense genes in *Drosophila* (Panda et al., 2014). Therefore, the rapid degradation of Nup 98 in infected cells could allow enteroviruses to limit innate antiviral responses as well as set the stage for dysregulation of nucleocytoplasmic trafficking early during infection.

In a recent study of rhinovirus 2A proteinases, A- and C-species displayed slower kinetics than B-species in disrupting nuclear import. Applying this to patient infections, the authors hypothesize that it is possible that some antiviral signaling might occur with the A and C viruses before full nuclear transport shutoff, thus promoting pro-inflammatory immune responses that could cause the more severe illness associated with rhinovirus A and rhinovirus C infections (Watters et al., 2017). The importance of restricting the production of IFN-α/β during picornavirus infection is substantiated by the fact that pre-treatment of cells with IFN- α/β inhibits picornavirus replication, confirming

that once ISG products are expressed they cannot be overcome (Chinsangaram et al., 2001). As corroboration of this phenomenon, various studies have demonstrated that poliovirus, HRV14, and HRV1a infection fails to induce a strong type I interferon response by blocking the activation of IRF-3, and enterovirus D68 3CD/3C cleaves the related IRF-7, to limit host antiviral defenses (Drahos and Racaniello, 2009; Kotla and Gustin, 2015; Kotla et al., 2008; Xiang et al., 2016). EV71 similarly interferes with IRF-3 activation but also targets the NF-κB pathway to limit host cell antiviral defenses (Kuo et al., 2013; Zheng et al., 2011).Taken together, enteroviruses limit the nucleocytoplasmic trafficking of regulators important for innate immune responses by targeting the relevant transcription factors directly, specific Nup proteins which subsequently cannot import transcription factors into the nucleus to drive the expression of ISGs, and even importins themselves (Wang et al., 2017).

As mentioned above, the cardiovirus TMEV L protein prevents export of cellular mRNAs from the nucleus. Furthermore, the TMEV L protein inhibits the transcription of cytokine and chemokine genes that are ordinarily activated upon viral infection (Van Pesch et al., 2001). This inhibition can be attributed to the fact that TMEV infection inhibits the formation of IRF-3 dimers, which normally translocate to the nucleus to regulate transcription of antiviral genes (IFN-α/β as well as ISGs), in response to infection. Because infection with TMEV containing a mutation in the zinc finger motif of L or a partial deletion of L allows the dimerization of IRF-3 but wild type TMEV infection does not, the inability of this nuclear translocation and subsequent antiviral protein production can be attributed to antagonizing this pathway by the L protein. Moreover, disruptions in nucleocytoplasmic trafficking and the block to mRNA export from the

nucleus correlate with Nup 98 hyper-phosphorylation (Ricour et al., 2009a). The leader protein of mengovirus has also been demonstrated to inhibit IFN-α/β expression in infected cells by suppressing the activation of NF-κB, a suppression dependent upon phosphorylation of Thr-47 in the L protein (Zoll et al., 2002). Interestingly, negative-sense RNA complementary to the L coding region of the EMCV genome was shown to be a determinant of MDA5 mediated interferon production (Deddouche et al., 2014). Finally, the L proteinase of FMDV functions in the inhibition of IFN-β mRNA induction. However, this inhibition is not dependent upon the dysregulation of cellular nucleocytoplasmic trafficking because FMDV does not target these pathways. Instead, the FMDV L proteinase promotes the degradation of an NF-κB component (De Los Santos et al., 2006; De Los Santos et al., 2007).

The redistribution of cellular proteins as a result of infection is not necessarily beneficial to viral replication

Because fundamental components and regulatory mechanisms of nucleocytoplasmic trafficking are disrupted during picornavirus infection, some proteins that relocalize to the cytoplasm of infected cells have no known function in viral replication, and in some instances have adverse effects on virus replication. AUF1 binds with high affinity to RNA molecules containing AU-rich elements (usually in the 3′-non-translated region), is a predominantly nuclear resident protein that shuttles to the cytoplasm, and promotes mRNA turnover [reviewed in (Gratacós and Brewer, 2010)]. AUF1 relocalizes from the nucleus to the cytoplasm of poliovirus, HRV14, and HRV16-infected cells in a 2A-driven manner and binds to S-L IV of the poliovirus IRES and within the 5’-NCR of HRV16 RNA (Cathcart et al., 2013; Rozovics et al., 2012; Spurrell

et al., 2005). The presence of this protein inhibits poliovirus translation in a dose-dependent manner *in vitro*, and cells lacking AUF1 produce higher titers of poliovirus, CVB3, and HRV1a. The enteroviral proteinase precursor 3CD and mature 3C cleave AUF1 *in vitro*, leading to a decrease in the affinity of AUF1 for poliovirus S-L IV (Cathcart et al., 2013; Rozovics et al., 2012). A similar phenomenon has been demonstrated during CVB3 infection; however, AUF1 binds the 3'-NCR of CVB3 RNA, and this protein was suggested to act as a restriction factor by destabilizing viral RNA (Wong et al., 2013). Analogous results have been observed with EV71, although AUF1 appears to bind S-L II of the EV71 IRES (Lin et al., 2014). Interestingly, AUF1 also relocalizes from the nucleus during cardiovirus infection but does not have a negative effect on EMCV amplification in mouse cells and is not degraded during infection (Cathcart and Semler, 2014). Although enteroviral infection and resultant NPC degradation causes the relocalization of this negative regulator of viral replication, the subsequent action by viral proteinases may ameliorate the antiviral effect of AUF1.

FUBP2 relocalizes from the nucleus to the cytoplasm of EV71-infected cells, interacts with the EV71 IRES, and appears to inhibit translation in bicistronic reporter assays. The ITAF FUBP1 has been suggested to outcompete FUBP2 for binding to the EV71 IRES, possibly allowing virus translation to proceed, even with FUBP2 present in the cytoplasm. However, FUBP2 knockdown did not affect viral RNA accumulation during EV71 infection, a finding that has not been reconciled with the fact that RNA replication is highly dependent upon the levels of viral proteins produced during an infection (Lin et al., 2009a). The fact that proteins that are negative regulators of virus translation relocalize to the cytoplasm in enterovirus-infected cells demonstrates that

nucleocytoplasmic trafficking disturbances can cause redistribution of a broad subset of nuclear resident proteins that do not necessarily benefit viral replication, but that picornaviruses have evolved to ways to mitigate the effects of these mislocalized restriction factors.

Although cardioviruses and enteroviruses target many of the same Nup proteins, the mechanisms that cause cytoplasmic accumulation of nuclear proteins are distinct. Enteroviral proteinases degrade FG repeat containing Nups while cardioviruses direct host kinases to phosphorylate these Nups. Nonetheless, the consequences of Nup alterations by picornaviruses are equivalent: the proteins that facilitate viral replication redistribute to the site of viral replication in the cytoplasm. Additionally, degradation of NPC components functions as a mechanism to limit signal transduction to the nucleus and thereby attenuate host antiviral defense pathways. Although to what degree picornaviruses are able to specifically orchestrate different nucleocytoplasmic trafficking pathways is unclear, increased NPC leakiness (i.e., increased export of macromolecules from the nucleus and the restriction of inbound cargo from the cytoplasm) is a functionally significant event that many picornaviruses have evolved to achieve in order to mount effective cytoplasmic replication strategies.

Picornavirus proteins enter the nucleus to limit cellular gene expression

In addition to shutting down most host-cell translation through actions in the cytoplasm, some picornaviruses also target the transcriptional components of cellular gene expression. Picornavirus infection has long been known to greatly reduce the initiation rate of cellular RNA synthesis (Baltimore and Franklin, 1962). This occurs despite the fact that cellular DNA-directed RNA polymerase (Pol) II itself is functional

during infection. However, at least one factor required for Pol II transcription is deficient in picornavirus-infected cells (Apriletti and Penhoet, 1978; Crawford et al., 1981). Viral protein synthesis is required to induce this cellular transcription inhibition, and cytoplasmic extracts of poliovirus-infected cells inhibit RNA synthesis in isolated nuclei (Balandin and Franklin, 1964; Bossart et al., 1982; Franklin and Baltimore, 1962). This early work prompted the question of whether picornavirus proteins are able to enter the infected cell nucleus to carry out this inhibitory task. Subsequent studies demonstrated that radiolabeled viral proteins do in fact enter the cell nucleus (Bienz et al., 1982; Fernández-Tomás, 1982). **Figure 1.6** summarizes what is known about picornavirus proteins entering the nucleus of infected cells.

Picornavirus infection results in the termination of cellular transcription

Enterovirus infection interferes with transcription driven by all three DNA-dependent RNA polymerases of mammalian cells. Pol I synthesizes ribosomal RNA (except 5S rRNA), which accounts for over half the RNA produced in the cell, and is carried out in the nucleolus (Russell and Zomerdijk, 2006). The Pol I transcription machinery is made up of two major transcription factor complexes: upstream binding factor (UBF) and selectivity factor 1 (SL1). Poliovirus infection was first shown to alter Pol I driven transcription using *in vitro* transcription assays in combination with lysates from uninfected cells or poliovirus-infected cells. Incubation of oligonucleotides containing the Pol I promoter element with extracts from poliovirus-infected HeLa cells resulted in faster migrating complexes by electrophoretic mobility shift assays compared to the same oligonucleotides incubated with extracts from uninfected cells. Incubation of poliovirus 3C with extracts from mock-infected cells recapitulated this result, suggesting

that this viral proteinase is responsible for cleavage of host factors required for Pol I driven transcription. This claim was verified when incubation of purified poliovirus 3C with cellular extracts was shown to produce near total inhibition of Pol I transcription (Rubinstein et al., 1992). The inhibition of Pol I transcription during poliovirus infection has been attributed to the inactivation of both UBF and SL1, two components of the Pol I transcription initiation complex. *In vitro* restoration of rRNA transcription requires the addition of both UBF and SL1 to extracts from poliovirus-infected cells. Poliovirus 3CD/3C is now known to cleave TATA-box binding protein associated factor, RNA polymerase I subunit C (TAF1C or TAF110), a component of SL1. Although UBF is not targeted by 3C *in vitro*, it does appear to be modified by a 3C-dependent mechanism within poliovirus-infected cells (Banerjee et al., 2005).

The Pol II transcription complex is responsible for the production of messenger RNA within eukaryotic cells. TFIID binding to the TATA box DNA sequence is the initial transcription step in the formation of the preinitiation complex and is performed by TBP, a component of TFIID. TFIID activity in poliovirus-infected cells is greatly decreased compared to mock-infected cells, and only TFIID is capable of restoring basal Pol II transcription *in vitro* (Kliewer and Dasgupta, 1988; Yalamanchili et al., 1996). The decrease in TFIID activity during poliovirus infection has also been attributed to 3CD/3C, as extracts from cells infected with a poliovirus encoding 3C with reduced activity is less effective at inhibiting Pol II transcription *in vitro*. Further experiments involving the co-transfection of constructs encoding poliovirus 3C and plasmids competent for Pol II transcription demonstrated that 3C is sufficient to inhibit Pol II transcription within cells (Yalamanchili et al., 1996). Poliovirus proteinases also target

TBP for cleavage during infection, and incubation of TBP with poliovirus 3C or 2A recapitulate the degradation of TBP *in vitro* (Clark et al., 1993; Das and Dasgupta, 1993; Yalamanchili et al., 1997a). However, 2A was unable to inhibit RNA Pol II transcription *in vitro*, suggesting that shutoff of Pol II transcription is mediated by 3CD/3C during infection (Kundu et al., 2005; Yalamanchili et al., 1997a). Furthermore, poliovirus inhibits activator-dependent Pol II transcription by cleaving and promoting the dephosphorylation of CAMP responsive element binding protein 1 (CREB1), leading to inhibition of CREB1-activated transcription in poliovirus-infected cells (Kliewer et al., 1990; Yalamanchili et al., 1997b). POU class 2 homeobox 1 (POU2F1, also known as octamer-binding transcription factor 1 or Oct-1) is also specifically cleaved in poliovirus-infected cells and by 3C *in vitro*, and cleaved POU2F1 is unable to support activated transcription (Yalamanchili et al., 1997c).

Finally, the Pol III transcription machinery, which controls the production of tRNA and 5S rRNA within eukaryotic cells, is also altered in poliovirus-infected cells. Studies similar to those discussed above demonstrated that 3C is responsible for cleaving the general transcription factor IIIC subunit 1 (GTF3C1 also known as TFIIIC), leading to reduced activity of this transcription factor and subsequent inhibition of Pol III transcription (Clark and Dasgupta, 1990; Clark et al., 1991; Fradkin et al., 1987; Shen et al., 1996).

Although most work focusing on enterovirus-induced alterations to cellular transcription has implicated 3C, 2A also functions in this regard. Transient expression of poliovirus 2A in cells leads to reductions in DNA replication, Pol II transcription, as well as cap-dependent translation demonstrating that both enteroviral proteinases function in

transcriptional repression (Davies et al., 1991). DEAD-box helicase 20 (DDX20, also known as Gemin3), a protein found in both the nucleus and cytoplasm of cells and which functions in biogenesis of spliceosomal complexes, is also proteolyzed in poliovirus-infected cells. The cleavage of this protein can be recapitulated *in vitro* using poliovirus 2A, and ectopic expression of 2A results in DDX20 cleavage in cells. Although the functional significance of this cleavage event during infection is not clear, the assembly of spliceosomal complexes is reduced in infected cells and correlates with DDX20 degradation and the loss of DDX20 localization to the nucleus. Therefore, it is likely that cellular splicing is also targeted by enteroviruses during infection to further inhibit cellular gene expression (Almstead and Sarnow, 2007). Similarly, the FMDV L proteinase cleaves Gemin5 during infection, suggesting that a wide range of picornaviruses target cellular splicing for inhibition, specifically at the survival of motor neuron (SMN) complex hub (Piñeiro et al., 2012b).

Picornavirus proteins translocate to the nucleus of infected cells

To enter the nucleus of an infected cell and alter cellular transcription, poliovirus proteinase 3C utilizes an NLS present within the 3D polymerase domain and thus accesses the nucleus in the form of the 3CD precursor protein. The single, basic-type NLS present in 3D consists of amino acids 125–129, with the sequence KKKRD, which is a motif that is highly conserved within the enteroviruses. Interestingly, although 3D contains an NLS, this signal is necessary but not sufficient to allow the transport of 3CD into the nucleus. Plasmid constructs encoding poliovirus 3C, 3D, 3CD, or a mutated 3CD that is not capable of autoproteolysis, fused to EGFP, were transfected into cells and these cells were then infected with poliovirus or mock-infected. Despite the

presence of the NLS in 3D, 3D-containing proteins were only present in the nucleus of infected cells (Sharma et al., 2004). Mutation of the putative NLS sequence in 3D eliminates the nuclear localization of 3D-containing proteins, even in infected cells, demonstrating that the NLS is necessary for 3CD entry into the nucleus, and that it does not enter the nucleus as a result of passive diffusion. Autoproteolysis of 3CD or trans-cleavage of one 3CD molecule by another, once within the nucleus, liberates 3C which then targets various transcription factors as discussed above. It should be noted that because 3CD is an active proteinase and is more abundant than 3C in infected cells, this precursor and physiologically significant form of 3C is also likely involved in the cleavage of host-cell proteins in the nucleus. Importantly, an NLS is required for 3CD to translocate to the nucleus, suggesting that the nuclear import pathway utilized by this viral precursor protein remains operational even in the face of the multiple alterations made to the NPC and nucleocytoplasmic trafficking in general during poliovirus infection. This provides further evidence that not all nuclear resident proteins relocalize to the cytoplasm of poliovirus-infected cells, possibly including those which utilize transportin-3 import receptors such as SRSF2 (Gustin and Sarnow, 2001). However, the fact that the NLS of 3D most closely resembles a classical NLS while the import of proteins containing this type of NLS is altered in picornavirus-infected cells remains to be reconciled.

Recent evidence demonstrates that 3D of EV71 and poliovirus also functions in alterations of host cell gene expression within the nucleus. Once 3CD enters the nucleus and self-cleaves, 3D associates with the pre-mRNA processing factor 8 (PRPF8, also known as Prp8), a central component of the spliceosome, causing

interference with pre-mRNA splicing and mRNA synthesis (Liu et al., 2014). Specifically, 3D interacts with the C-terminal region of PRPF8, resulting in lariat forms of the splicing intermediate accumulating within poliovirus- infected cell nuclei.

Studies focused on other enteroviruses have revealed similar insights into the translocation of viral proteins to the nucleus during infection. Cells infected with HRV16, probed with antibodies against 3C (which also recognize 3C precursors), then imaged via confocal microscopy demonstrated that proteins containing HRV16 3C accumulate in the nucleus of infected cells, similar to what was observed with poliovirus 3C (Amineva et al., 2004). The NLS of HRV16 3D is likely located in the N-terminal portion of the polymerase, since a transfected RNA construct encoding 3D with a 371 amino acid deletion from the C-terminus is still able to localize to the nucleus. However, the nuclear localization of the truncated 3CD and full-length 3CD was observed in the absence of infection, in contrast to previous work with poliovirus. Much like poliovirus, HRV16 3CD also degrades POU2F1 in infected cells (Amineva et al., 2004; Yalamanchili et al., 1997c). Cells infected with EV71 show decreased expression of cleavage stimulation factor subunit 2 (CSTF2, also known as CstF-64), which correlates, with the production of EV71 3C. Furthermore, 3C cleaves recombinant CSTF2 and inhibits cellular 3'-end pre-mRNA processing and polyadenylation *in vitro*. Interestingly, CSTF2 appears to remain within the nucleus throughout the course of infection with EV71, another indication that 3CD/3C in fact enters the nucleus and that CSTF2 itself is not utilized for replication directly. The accumulation of unprocessed pre-mRNA and reductions in mature mRNA are also observed in EV71-infected cells, suggesting that host-cell polyadenylation is targeted during enterovirus infection,

exemplifying another way in which picornaviruses redirect metabolic energy and cellular factors to support their replication (Weng et al., 2009).

There is also evidence for the presence of enteroviral 2A within the nucleus of infected cells. Aside from the aforementioned DDX20, this proteinase targets nuclear SRF for cleavage, resulting in the redistribution of SRF to the cytoplasm during CVB3 infection (Wong et al., 2012). Ectopically expressed poliovirus and HRV16 mCherry-tagged 2A proteins have also been observed localizing to the nucleus (Tian et al., 2011; Walker et al., 2016). However, infection with HRV1a results in a purely cytoplasmic distribution of the 2A proteinase as observed by immunofluorescence microscopy (Amineva et al., 2011). Interestingly, the presence of the enteroviral 2A proteinase seems to be required for the translocation of 3CD into the nucleus, as demonstrated by co-transfection experiments, which could explain the requirement of infection for poliovirus 3CD to enter the nucleus discussed above (Tian et al., 2011; Walker et al., 2016). This is also further evidence that during a natural infection, the viral proteinases likely act synergistically to degrade Nup proteins.

Although the functional importance of a capsid protein present in the nucleus is not clear, ectopic expression of CVB3 EGFP-VP1 has been demonstrated to result in the nuclear localization of this overexpressed protein, possibly through an NLS present in the C-terminus of VP1. However, this phenomenon has not been shown to occur during a CVB3 infection (Wang et al., 2012).

Cardiovirus proteins also enter the nuclei of infected cells. Immunofluorescence microscopy revealed that 2A, VPg (3B), 3C, and 3D localize to the nucleus (specifically to the nucleolus) of EMCV and mengovirus-infected cells (Aminev et al., 2003a).

Cardiovirus 2A contains a short motif (KRVRPFRLP) that closely resembles an NLS found in yeast ribosomal proteins, and deletions within this sequence result in the loss of nucleolar localization (Aminev et al., 2003a; Groppo et al., 2011; Svitkin et al., 1998). Similar to observations of rhinovirus 3CD protein translocations to the nucleus, cardiovirus 2A is capable of entering the nucleus in the absence of infection. Cardiovirus 2A colocalizes with nucleophosmin 1 (NPM1, also known as nucleolar phosphoprotein B23), a nuclear shuttling chaperone protein that, among other things, functions in ribosome biogenesis, a phenomenon that was also observed with rhinovirus 3C (Amineva et al., 2004). The nucleolar localization motif present within cardiovirus 2A and the consistent colocalization of 2A and NPM1 has led to the hypothesis that NPM1 associates with 2A and aids in the nucleolar localization of this picornavirus protein. This would allow cardiovirus 2A to enter the nucleus camouflaged as a ribosomal protein, where Pol I transcribes rRNA genes and ribosomal subunit assembly occurs (Aminev et al., 2003a). 2A may target the nucleolus to alter ribosomal biogenesis in some way, promoting viral IRES- dependent translation and/or 2A inclusion within ribosomes (Medvedkina et al., 1974). The EMCV 3BCD minor precursor protein has also been shown to associate with NPM1 and enter the nucleolar compartment via an NLS present in the 3D amino acid sequence, independent of infection (Aminev et al., 2003b). In agreement with studies of HRV16, this NLS is located at the very N-terminus of 3D and mimics a yeast ribosomal protein NLS rather than the basic NLS suggested for poliovirus.

FMDV has unique interactions with the nucleus

A large number of mature and precursor FMDV proteins have been shown to enter the nucleus of BHK-21 cells, although the functional consequence of the presence of the proteins in the nucleus has not been completely explored (García-Briones et al., 2006). FMDV has been shown to have distinct interactions with the transcription apparatus of cells. In contrast to other picornaviruses, FMDV modulates cellular transcription by targeting the regulation of transcriptionally active chromatin through the cleavage of the nucleosome component histone H3 (Griger and Tisminetzky, 1984). The FMDV 3CD/3C proteinase is capable of histone H3 cleavage *in vitro*, which has likely consequences for cellular transcription (Falk et al., 1990; Tesar and Marquardt, 1990). Transient transfection of FMDV 3ABC precursor protein expression constructs causes histone H3 degradation; however, a recent report suggests that the NLS motif MRKTKLAPT present in FMDV 3D is responsible for transporting 3CD to the nucleus, as well as GFP fused to this NLS, in the absence of infection (Capozzo et al., 2002; Sanchez-Aparicio et al., 2013). It is possible that the cleavage observed upon transfection of FMDV 3ABC was attributable to infection with vaccinia virus encoding a T7 RNA polymerase prior to transfection to facilitate 3ABC expression from the T7 promoter-containing plasmid. Nonetheless, it appears that similar to the enteroviruses, FMDV 3CD enters the nucleus via an NLS present in the 3D amino acid sequence, allowing proteinase functions to target cellular proteins within the nucleus.

The L proteinase of FMDV has also been shown to localize to the nucleus of porcine cells during wild type FMDV infection (De Los Santos et al., 2007). As noted above, FMDV L entry into the nucleus correlates with a decrease in the transcription of

antiviral IFN-β mRNA (De Los Santos et al., 2006). The motif present within FMDV L responsible for imparting nuclear localization was mapped to a SAF-A/B, Acinus, and PIAS (SAP) domain within L, a protein domain that is associated with nuclear retention of some proteins involved in transcriptional control. Virus containing a double mutation in the SAP region of L showed altered nuclear localization upon infection (De Los Santos et al., 2009) (**Figure 1.6**).

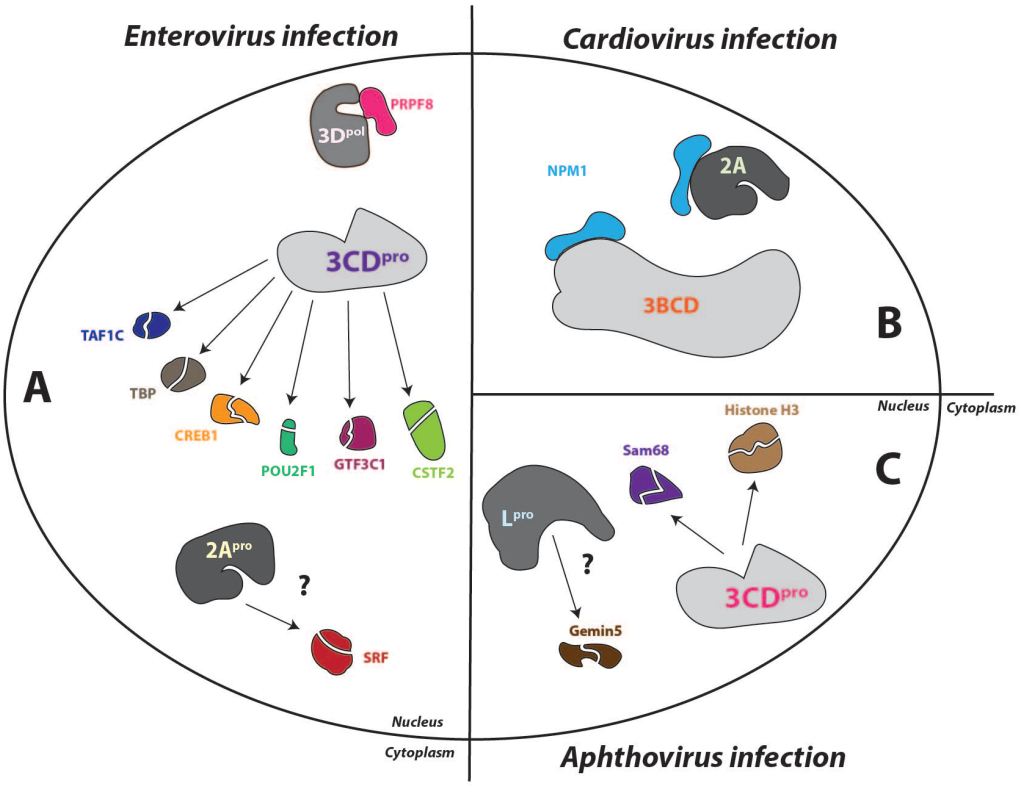

Figure 1.6. Picornavirus proteins enter the nucleus and associate with or proteolyze nuclear resident proteins. In this schematic, the large circle represents the nucleus. (**A**) During enterovirus infections, the viral proteinase 3CD/3C ($3CD^{pro}$) enters the nucleus and degrades TATA-box binding protein associated factor, RNA polymerase I subunit C (TAF1C), leading to inhibition of RNA Polymerase I (Pol I) transcription. Pol II transcription, including cellular mRNA production, is terminated in enterovirus-infected cells through cleavage of TATA-box binding protein (TBP), CAMP responsive element binding protein 1 (CREB1), and POU class 2 homeobox 1 (POU2F1) by $3CD^{pro}$. Pol III-driven transcription is also inhibited by $3CD^{pro}$, through cleavage of general transcription factor IIIC subunit 1 (GTF3C1). Cleavage stimulation factor subunit 2 (CSTF2) is also degraded in a 3CDpro dependent manner during enterovirus infections causing alterations in pre-mRNA processing. Furthermore, the enteroviral polymerase 3D ($3D^{pol}$) associates with the splicing factor pre-mRNA processing factor 8 (PRPF8), causing dysregulation of splicing. The 2A proteinase ($2A^{pro}$) of CVB3 cleaves serum response factor (SRF) during infection, but it is not clear if this occurs in the nucleus. (**B**) Cardiovirus infection causes the nuclear localization of both 2A and protein precursor 3BCD, both of which may associate with nucleophosmin 1 (NPM1). (**C**) Infection with FMDV causes the cleavage of both Histone H3 as well as Sam68 within the nucleus, following the entry of $3CD^{pro}$. L^{pro}, which also enters the nucleus of infected cells, targets Gemin5 for cleavage, but it is not clear if this occurs in the nucleus of infected cells. Note that although we have indicated $3CD^{pro}$ as the proteinase carrying out cleavage of nuclear proteins, it may be that $3CD^{pro}$ enters the nucleus, undergoes autoproteolysis, and mature $3C^{pro}$ is the species that performs the cleavages indicated.

The inhibition of cellular gene expression by picornaviruses is carried out in diverse ways that target translation as well as splicing and transcription. To affect the latter two processes, some picornavirus proteins enter the nucleus of the infected cell. The proviral effects of reduced cellular gene expression are two- fold: to liberate cellular proteins with functions advantageous to viral replication and to re-route metabolic energy from cell-specific to viral-centric functions. It is somewhat surprising that the 3D polymerase of many picornaviruses becomes localized to the nucleus of infected cells, because it would seem that maximizing viral RNA production in the cytoplasm would be prioritized during the infectious cycle. The fact that many picornavirus 3D proteins contain an NLS suggests that there are specific functions of 3D and/or the precursor 3CD in the nucleus, some of which remain to be uncovered, which are balanced with the polymerase function of 3D in the cytoplasm. Further experimentation will continue to reveal the elegant ways in which picornaviruses alter the cellular functions that occur in the nucleus and in which viral proteins are able to infiltrate the command center of the cell to appropriate cellular components and functions for their benefit.

Conclusions

Picornaviruses have traditionally been labeled as “cytoplasmic” RNA viruses as a result of the subcellular region in which these viruses produce viral proteins and replicate their genomic RNA molecules. Indeed, picornaviruses are able to complete the replicative cycle and produce infectious progeny in nucleus-free cytoplasts and cytoplasmic extracts (Barton and Flanegan, 1993; Follett et al., 1975; Molla et al., 1991; Pollack and Goldman, 1973; Svitkin and Sonenberg, 2003). However, it is not clear that enucleation treatments, e.g., with cytochalasin B, do not disrupt the nuclear envelope

and allow the escape of nuclear resident proteins or that cytoplasmic extracts do not contain significant concentrations of nuclear shuttling or nuclear resident proteins as a result of nuclear envelope leakage during cellular fractionation. It is significant that following cytochalasin B enucleation treatment, poliovirus capsid synthesis and virus growth are less efficient compared to infection of nucleated, untreated cells with a final yield from enucleated cells one-fifth of that from nucleated cells (Pollack and Goldman, 1973). Some studies have even provided evidence of a nuclear requirement of poliovirus early in infection, as virion RNA is able to replicate in the absence of a cell nucleus, but transfection of replicative form RNA into enucleated cells produced no detectable viral progeny (Detjen et al., 1978).

It is clear that picornaviruses make extensive use of nuclear resident and nuclear shuttling proteins to promote viral replication. The nuclear shuttling proteins PCBP2 and PTBP1 are particularly important for enterovirus translation as well as mediating the template usage switch required for RNA replication to proceed. Furthermore, PCBP2 and PABP1 may function in the circularization of genomic RNA templates to facilitate negative-sense intermediate RNA production. Additionally, the nuclear resident hnRNP C1/C2 is necessary for the efficient synthesis of poliovirus genomic RNA molecules from negative- sense intermediate RNA forms. Following the early rounds of translation in which the limited quantities of nuclear proteins in the cytoplasm are sufficient for viral protein production, picornavirus proteins 3CD/3C, 2A, and L induce alterations to the NPC. Cleavage of Nups by enteroviral 2A and 3CD/3C or hyperphosphorylation of Nups triggered by cardiovirus L results in dysregulation of nucleocytoplasmic trafficking and subsequent loss of nuclear compartmentalization of particular proteins within

picornavirus-infected cells. The presence of these nuclear proteins with functions critical to viral replication (including RNA-binding capabilities) allows for the amplification of viral progeny. Also as a result of deviations from standard nucleocytoplasmic trafficking, picornaviruses are able to disrupt the proper signaling pathways that allow for a strong innate immune response, including interferon production. Finally, picornavirus proteins enter the nucleus of infected cells to carry out functions related to host-cell transcription inhibition and disruptions in splicing, such as degradation of transcription factors, allowing metabolic energy and proteins sequestered in cellular roles to be redirected to virus-centric demands. Picornaviruses display a prominent level of direct and indirect interactions with the nucleus, interactions that have the potential to reveal pathogenic mechanisms and unique antiviral strategies as well as insights into cell biology through more detailed study. The fact that viruses of the Picornaviridae family have evolved to orchestrate a well-balanced promotion of viral replication with host-cell attenuation of nucleocytoplasmic trafficking demonstrates that interactions with the nucleus are functional and that these coding-capacity-limited cytoplasmic RNA viruses are master manipulators of even the most complex of cellular processes.

The remainder of this dissertation will focus on attempts to better define the cellular proteins, and in particular the nuclear proteins, that are closely associated with enterovirus replication. The two experimental approaches we take can be broadly categorized as either direct or indirect methods. The direct approach involved the generation of recombinant polioviruses harboring exogenous RNA to exploit as a biochemical handle for the isolation of viral RNA and associated proteins during infection and is discussed in Chapter 2. A parallel and more indirect approach involved

identifying proteins that increase in abundance in the cytoplasm of HRV16-infected cells, through quantitative protein mass spectrometry, followed by functional validation and is presented in Chapter 3. The goal of this work was to more fully describe the virus-host interactions that occur during infection with enteroviruses, in molecular detail. Basic research focused on host proteins that are involved in viral replication but are normally confined to the nucleus, allows for the possible identification of antiviral targets, if, for example, infection-induced relocalization of particular proteins can be inhibited resulting in suppression of viral replication.

CHAPTER 2

Generation of recombinant polioviruses harboring RNA affinity tags in the 5’-noncoding regions of genomic RNAs

Summary

Despite being intensely studied for more than 50 years, a complete understanding of the enterovirus replication cycle remains elusive. Specifically, only a handful of cellular proteins have been shown to be involved in the RNA replication cycle of these viruses. In an effort to isolate and identify additional cellular proteins, including nuclear resident proteins, that function in enteroviral RNA replication, we have generated multiple recombinant polioviruses containing RNA affinity tags within the 5’-noncoding region of the genome. These recombinant viruses retained RNA affinity sequences within the genome while remaining viable and infectious over multiple passages in cell culture. Further characterization of these viruses demonstrated that viral protein production and growth kinetics were unchanged or only slightly altered relative to wild type poliovirus. However, attempts to isolate these genetically-tagged viral genomes from infected cells have been hindered by high levels of co-purification of nonspecific proteins and the limited matrix-binding efficiency of RNA affinity sequences. Regardless, these recombinant viruses represent a step toward more thorough characterization of enterovirus ribonucleoprotein complexes involved in RNA replication.

Introduction

As discussed in Chapter 1, due to the inherent limited protein coding capacity of their small RNA genomes, enteroviruses require the functions of cellular proteins to complete their infectious cycle. Because enteroviral replication is composed of a series

of discrete steps that demand particular protein functions, there are dynamic changes to the composition of ribonucleoprotein (RNP) complexes throughout this cycle.

Much of what is known about the identity of cellular proteins that are usurped during the replication cycle of enteroviruses is a result of studies involving poliovirus. The poliovirus genome consists of a small viral protein (VPg) covalently linked to the RNA at the very 5′ terminus followed by a relatively long (742 nucleotide) and highly structured 5'-noncoding region (5'-NCR). There are six stem-loop (S-L I-VI) structures within the 5'-NCR, with the internal ribosome entry site (IRES) comprised of S-L II-VI. Downstream of the 5'-NCR the poliovirus genome encodes a single open reading frame. The 3'-region of the genome contains the ~75 nucleotide 3'-noncoding region (3'-NCR), made up of two predicted stem-loop structures called X and Y, and the genetically encoded poly(A) tract of ~60 nucleotides (Pilipenko et al., 1992b). The function of the 3'-NCR is not clear, but the poly(A) tract is required for infectivity and is the putative binding site for the viral RNA-directed RNA polymerase (3D) during initiation of negative-sense RNA synthesis (Sarnow, 1989; Spector and Baltimore, 1974).

Following cellular entry and uncoating, the initial step in the replication cycle of poliovirus is the translation of the ~7500 nucleotide genomic RNA molecule in the cytoplasm of the infected cell. Unlike cellular mRNAs, the poliovirus genome lacks a 5′ 7-methylguanosine cap structure and relies on cap-independent, IRES-mediated translation resulting in the production of a single 250-kDa polyprotein. The polyprotein is proteolytically processed by viral proteinases to produce 11 mature proteins, as well as intermediate precursor proteins, which have distinct functions. In addition to generating the proteins required for viral RNA replication directly, translation of the viral genome

also produces proteins that alter the infected cell to support conditions required for viral RNA synthesis. This includes induction of membranous structures that originate from the secretory pathway and/or autophagosomal pathways during infection (Belov et al., 2012; Bienz et al., 1987; Jackson et al., 2005; Kallman et al., 1958; Rust et al., 2001; Schlegel et al., 1996; Suhy et al., 2000). Viral RNA is synthesized in close association with these membranous structures induced during infection, and together are known as replication complexes (Caliguiri and Tamm, 1969).

Poliovirus RNA replication is dependent upon the formation of ribonucleoprotein (RNP) complexes that result from interactions between structured regions of the viral RNA molecule and proteins of host and viral origin (see Chapter 1). The RNA structures that nucleate various RNP complexes are found in the positive-sense RNA within in the 5'-NCR, the *cis*-acting replication element (cre) (a hairpin structure found within the coding region of 2C involved in the initiation of RNA synthesis), and the 3'-NCR. RNP complexes function in stimulating viral RNA replication, through direct or indirect recruitment of 3D, and are thought to be the determinants of 3D template specificity

End-to-end interaction is predicted to bring 3D (perhaps in the form of 3CD that is bound to S-L I) into close proximity to the site of replication initiation at the 3′ terminus of the template RNA. Many features of this model have been verified *in vitro*, and the specificity of 3D for viral RNA templates containing these RNP complexes is bolstered by the requirement for translation in *cis*, i.e., a viral RNA template must be translated before being used for RNA replication. As a result, RNA templates enter the replication cycle already associated with various cellular proteins that function in the translation of the viral genome, and may also be required for efficient RNA replication (Novak and

Kirkegaard, 1994). Because negative-sense RNA templates are not translated, they likely have a unique set of viral and host protein requirements compared to their genomic RNA counterparts.

Studies that have contributed to our understanding of enterovirus RNA replication have defined several proteins that interact directly with poliovirus RNA during the process of viral RNA production. However, previous work has relied heavily on *in vitro* assays and subgenomic poliovirus RNA constructs. To define the RNP complexes using full length genomic RNA in the context of infection, we have generated recombinant polioviruses containing RNA affinity tags within the noncoding region of the genome. The use of polioviruses possessing stable, specifically isolatable genomes could ultimately allow for strand-specific RNP complex characterization directly from infected cells, throughout the course of infection.

Work performed by Dr. Andrea Cathcart, a previous member of the Semler laboratory, focused on the generation of a recombinant poliovirus containing RNA sequence corresponding to tandem bacteriophage MS2 hairpins in place of the 3'-NCR of the genome. This region was chosen as a site for exogenous sequence insertion because the 3'-NCR of poliovirus is not required for viral replication, as a mutant poliovirus lacking this entire region is infectious and stable (Brown et al., 2005; Todd et al., 1997). The MS2 affinity purification assay is a well-established method for the purification of RNA-protein complexes via the high affinity (K_d ~1-3 × 10^{-9} M) interaction between the bacteriophage MS2 coat protein and a stem-loop structure within the phage genome, known as the operator or MS2 hairpin, and has been utilized for the purification of RNP complexes associated with long RNAs from cellular extracts

(Bardwell and Wickens, 1990; Keryer-Bibens et al., 2008; Tsai et al., 2011). Insertion of the tandem MS2 hairpins, the sequence of which is of similar length to the 3'-NCR itself, in place of the 3'-NCR resulted in the infectious, recombinant virus PV1-3'-MS2. While the MS2 hairpins were stable in the genome for at least six passages in cell culture, the growth kinetics of these viruses were significantly delayed, and total virus yields of PV1-3'-MS2 were reduced ~2 $\log_{10}$ units (~100 fold) compared to wild type poliovirus. Furthermore, although MS2-tagged RNA affinity purification to isolate MS2-tagged viral RNA from infected cells allowed for co-purification of proteins known to be involved in poliovirus replication, it also resulted in high levels of co-purification of nonspecific proteins, precluding identification of novel interactors by mass spectrometry analysis (Flather et al., 2016).

Here we present a biological characterization of a set of recombinant viruses containing aptamer tags within the 5'-NCR, which were generated in attempt to compensate for the shortcomings of the PV1-3'-MS2 virus. We demonstrate that these exogenous sequence insertions are also stable in the poliovirus genome for multiple passages in cell culture, while maintaining wild type-like growth kinetics. Our initial attempts to isolate these genetically-tagged viral RNAs and associated proteins from infected cells have been hampered by the limited binding efficiency between RNA affinity sequences and their respective matrices. Nonetheless, our results provide a foundation for the generation of enteroviruses that could eventually allow for a description of the dynamic changes in protein composition of viral RNP complexes that occur throughout the course of infection, and that reflect the distinct steps of the viral RNA replication cycle.

Results

Recombinant poliovirus RNAs containing aptamer sequences produce *in vitro* translation products equivalent to those produced by wild type poliovirus RNA

As a result of the lack of specificity we observed during purifications of poliovirus RNP complexes associated with PV1-3′MS2 RNA via MS2 affinity, we pursued alternate RNA affinity tags for the isolation of recombinant viral genomes and accompanying proteins. Aptamers developed to specifically bind streptavidin or Sephadex, a cross-linked dextran gel used in size-exclusion chromatography, were selected as affinity sequences for subsequent purifications. These RNA sequences are short: the consensus S1, streptavidin-binding aptamer is 44 nucleotides in length and the D8, Sephadex-binding aptamer is 33 nucleotides long (Srisawat and Engelke, 2001; Srisawat et al., 2001). Because large sequence insertions presumably incur a fitness cost on recombinant viral genomes, and because we were interested in generating viruses with as close to wild type replication kinetics as possible, the length of the sequence was a major determinant in our selection of affinity tag. These aptamer tags were also appealing because of their high affinity (K_d ~50-70 × 10^{-9} M) and potential for RNP complex isolation and subsequent characterization, as has been previously demonstrated for cellular mRNAs and rRNAs (Dienstbier et al., 2009; Dix et al., 2013; Iioka et al., 2011; Leonov et al., 2003; Li and Altman, 2002; Srisawat and Engelke, 2002; Vasudevan and Steitz, 2007; Vasudevan et al., 2007).

There are four known regions within the 5'-NCR of the poliovirus genome that have previously been shown to tolerate major sequence alterations: S-L III, S-L VI, nucleotide position 600 through 726 (including a portion of S-L VI), and just downstream

of nucleotide position 702 (Dildine and Semler, 1989; Haller and Semler, 1992; Kuge et al., 1989; Kuge and Nomoto, 1987). Deletions of these S-L regions or insertions of up to 72 nucleotides at position 702 produce mutant viruses that have essentially wild type growth kinetics and yields, with only slight delays in RNA synthesis. Based on the results of these previous studies, we separately introduced the minimal D8 and S1 motifs into three different locations within the poliovirus 5'-NCR: in place of S-L III, in place of S-L VI, or at nucleotide position 702 (**Figure 2.1**). These aptamer tags were engineered into these sites in a forward or reverse orientation within a poliovirus cDNA construct, subsequently allowing for the D8 or S1 RNA sequence motif to be present in the viral positive- or negative-strand RNA, respectively, potentially allowing for strand-specific RNP complex isolation. This resulted in the production of 12 plasmid constructs: three constructs harboring the D8 tag at the three separate sites for positive-strand isolation (D8+S-LIII, D8+S-LVI, D8+702), three constructs harboring the D8 tag for negative-strand isolation (D8−S-LIII, D8−S-LVI, D8−702), and the corresponding six constructs containing the S1 nucleotide sequence (S1+S-LIII, S1+S-LVI, S1+702, S1−S-LIII, S1−S-LVI, S1−702).

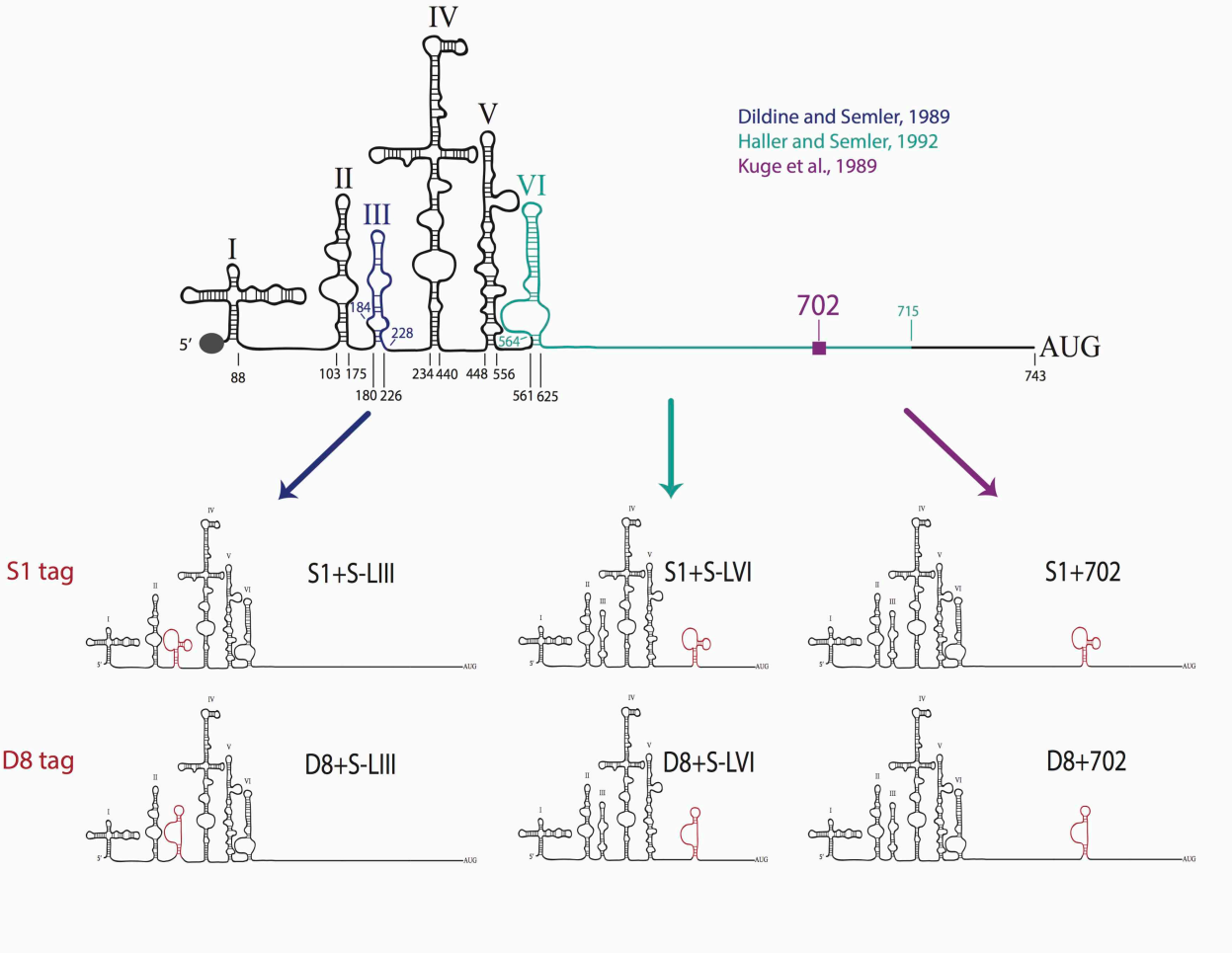

Figure 2.1. Schematic of poliovirus genomic RNAs containing S1 and D8 aptamer tags within the highly structured 5'-NCR, for positive-strand isolation. Insertion of either the S1 streptavidin-binding or D8 Sephadex-binding aptamer sequence within three regions of the poliovirus 5'-NCR resulted in the production of 12 poliovirus cDNA constructs. Tag insertions in place of S-L III (blue), in place of S-L VI (green), or at nucleotide position 702 (purple) are depicted on the left, middle, and right, respectively. Constructs for negative-strand isolation (aptamers inserted in a reverse orientation) are not shown.

Recombinant poliovirus cDNAs were linearized and transcribed *in vitro* to generate RNA corresponding to full-length poliovirus RNA with incorporated RNA affinity tag sequences. Tagged RNAs were subjected to an *in vitro* translation assay, making use of HeLa cell cytoplasmic extracts in the presence of ^{35}S-methionine to produce radiolabeled viral proteins. Only those constructs containing affinity tag sequence at nucleotide position 702 produced levels of viral proteins similar to wild type

poliovirus RNA (**Figure 2.2**). In agreement with previous studies that suggest the introduction of an AUG triplet into the highly variable region between S-L VI and the start codon of the poliovirus genome is deleterious for viral replication, the S1+702 construct, which contains an AUG triplet in-frame with the translation start codon at position 743, showed an altered protein profile compared to wild type poliovirus RNA translation (Kuge et al., 1989). This in-frame AUG triplet likely leads to alterations in authentic translation initiation, producing amino-terminal extensions on viral proteins P1, 1ABC, and VP0. Interestingly, however, the presence of an AUG triplet within the sequence of the S1 tag for negative-strand isolation, which is out-of-frame with the initiator codon, does not cause alterations to viral protein production compared to wild type RNA sequence.

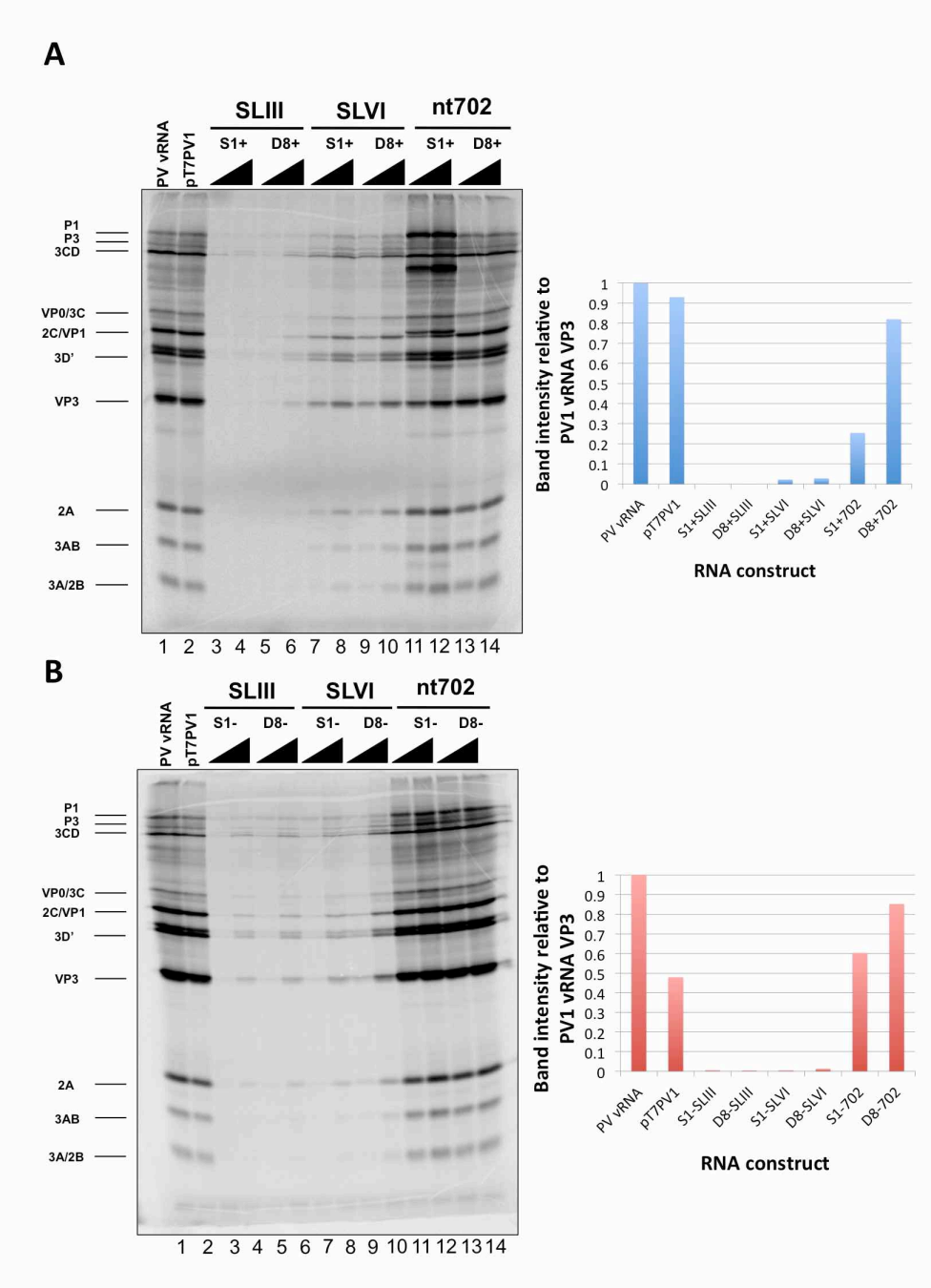

Figure 2.2. *In vitro* translation assays of poliovirus RNA constructs containing aptamer tags within the 5'-NCR. *In vitro* transcribed recombinant poliovirus RNA molecules containing RNA affinity tags for positive-strand isolation (**A**) or negative-strand isolation (**B**) were subjected to an *in vitro* translation assay utilizing HeLa cell cytoplasmic extracts and ^{35}S-methionine to label viral proteins. Translation products from wild type poliovirus RNA isolated from poliovirus virions (PV vRNA) and an *in vitro* transcribed poliovirus cDNA construct containing a T7 promoter (pT7PV1) are shown in lanes 1 and 2, respectively. Constructs containing either the S1 or D8 aptamer tags in place of S-L III, S-L VI, or at position 702 of the genome are shown in lanes 3–14, with either 250 or 500 ng of RNA (increasing RNA amounts are indicated with triangles). Viral translation products are indicated on the left of the images. Quantification of the intensity of the VP3 band observed in assays containing 250 ng of each RNA construct relative to PV vRNA is shown adjacent to each autoradiograph.

Recombinant polioviruses containing aptamer tags at genomic position 702 of the 5'-NCR are viable and have growth kinetics indistinguishable from those of wild type poliovirus

Because only those RNA constructs containing aptamer tag sequence insertions at nucleotide position 702 of the 5'-NCR produced viral proteins in amounts similar to wild type poliovirus via the *in vitro* translation assay, these constructs were transfected into HeLa cell monolayers for the generation of recombinant virus. To generate a recombinant poliovirus containing these RNA affinity sequences within the genome, RNA was transcribed *in vitro* and transfected into HeLa cell monolayers with a liquid overlay. Overlays were harvested upon the observation of cytopathic effects and used to infect HeLa cells for plaque purification and screening. Recombinant viruses containing the aptamers were isolated and virus stocks were generated by amplification in cell culture. Recombinant viral genomes were subjected to RT-PCR with primers designed to amplify the 5'-NCR and sequenced to examine the stability of the tag insertions after the second and third passage in cell culture. D8+702PV1, D8−702PV1, and S1-702PV1 viruses contained intact aptamer sequence after both the second and third passage in cell culture, with no other alterations to the 5'-NCR. The S1+ 702PV1 recombinant virus, in contrast, did not retain the S1 streptavidin affinity tag sequence without alterations. The in-frame AUG triplet within the S1 aptamer sequence was selected against during infection, with three distinct alterations to the AUG triplet observed in four separate isolates. Importantly, only the adenosine residue of the AUG triplet within the S1 aptamer sequence is conserved within the consensus sequence of the multiple streptavidin-binding aptamer sequences first identified (Srisawat and

Engelke, 2001). Thus, a viral isolate containing a single nucleotide change, a guanosine-to-uridine transversion at the third position of the triplet (S1+702AUUPV1), was selected as the recombinant virus possessing a streptavidin-binding genome to use in subsequent assays. This single nucleotide alteration within the S1 tag was stable within the poliovirus genome through three passages in cell culture, demonstrated by sequencing progressive passages of virus isolates. *In vitro* translation assays incorporating an S1+702 *in vitro* transcribed RNA containing the transversion observed within the S1+702AUUPV1 genome showed a wild type protein profile for this altered construct (data not shown), supporting the idea that the insertion of an in-frame AUG is unfavorable for viral protein production. We also generated recombinant virus from the RNA construct containing the D8 tag for negative-strand isolation in place of S-L VI. However, after a single passage in cell culture, sequencing cDNA generated from viral genomes revealed over half of the nucleotides within the tag sequence had been deleted, as well as 20–25 nucleotides of the genome downstream of the insertion site, providing further evidence that S-L VI is not a viable option for exogenous sequence insertion.

To characterize the growth properties of these recombinant viruses, single-cycle growth analyses were performed. Third passage stocks of virus were used to infect HeLa cell monolayers, then liquid overlay and cells were collected at intervals and subjected to plaque assays to determine viral titers. The single-cycle growth curves demonstrate that all recombinant viruses have essentially wild type growth kinetics, with maximum virus production reached 4 h following infection (**Figure 2.3A and B**). No significant differences in plaque morphology between wild type poliovirus and

recombinant viruses containing RNA affinity tag sequences were observed (**Figure 2.3C**). Furthermore, complete sequencing of third passage stocks of these recombinant viral genomes demonstrated that only a handful of changes to the third position of codons had occurred, resulting in synonymous mutations to amino acid sequences. A threonine-to-isoleucine mutation at amino acid position 93 of 3D was also identified, but this alteration was also present in wild type poliovirus generated from transfections of the pT7PV1 cDNA backbone, and therefore not a mutation compensatory for the presence of aptamer tag within the 5'-NCR.

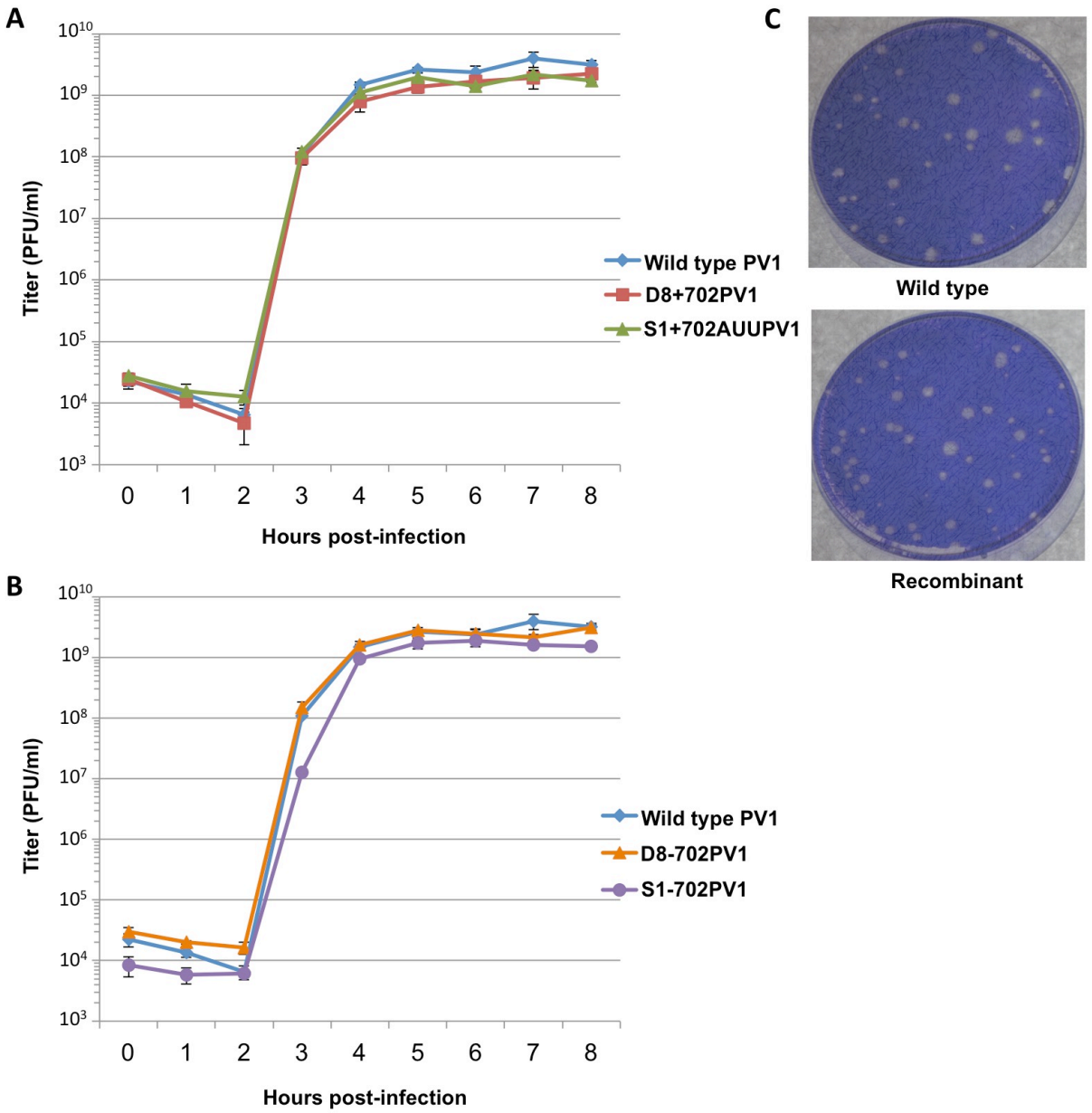

Figure 2.3. Single-cycle growth kinetics and plaque morphology of recombinant polioviruses containing aptamer tag sequence at nucleotide position 702 of the 5'-NCR. (**A**) A single-cycle growth analysis was carried out in HeLa cell monolayers infected with wild type poliovirus (PV1) or recombinant viruses containing aptamer tag for positive-strand isolation (D8+702PV1 or S1+702AUUPV1) at an MOI of 20. Cells and supernatant were harvested at 1 h intervals beginning at 0 h post-infection until 8 h post-infection, in triplicate. Virus yield was determined by plaque assay and plotted. (**B**) The same analysis as in (**A**) but comparing recombinant viruses containing aptamer tag for negative-strand isolation (D8-702PV1 or S1-702PV1) to wild type poliovirus. (**C**) Plaque morphology of wild type virus compared to representative recombinant virus (S1+702AUUPV1). Titer is given in plaque forming units (PFU) per milliliter. Error bars represent one standard deviation above and below the mean.

Poliovirus cDNA constructs transcribed *in vitro* can be enriched via RNA affinity tags but recombinant viral RNA isolation from infected cells is inefficient

After confirming the stability of affinity tag sequences within viral genomes and characterizing the growth kinetics of recombinant polioviruses, affinity purification procedures were tested. Aptamer-tagged RNA isolation was first performed *in vitro*, as previously described (Walker et al., 2008) (**Figure 2.4A**). *In vitro* transcribed poliovirus RNAs for positive-strand isolation were generated and renatured by heating and slow cooling. Aptamer binding was carried out under rotation at 4°C for 4 h, followed by separation of matrix material through centrifugation, and then the Sephadex or streptavidin-conjugated bead matrix was washed multiple times. RNA associations with insoluble matrix were determined by direct loading of the matrix onto an agarose gel containing ethidium bromide and performing electrophoresis (**Figure 2.4B**). The specificity of each construct containing the relevant aptamer tag insertion parallels the level of viral proteins produced in the *in vitro* translation assay shown in **Figure 2.2**. This suggests that not only is the nucleotide position 702 insertion site most favorable for the generation of a viable, genetically-tagged virus, but also for matrix accessibility and, as a result, most efficient isolation. Importantly, non-specific interactions between the RNA containing an irrelevant affinity sequence and no affinity sequence (i.e., wild type RNA) were limited (lanes 4 and 5 in both panels of **Figure 2.4B**), with the Sephadex matrix showing less background RNA associations than streptavidin beads. Although there appears to be specific association between aptamer-tagged RNAs and the respective matrix, the binding efficiency of these aptamers is very low, as the flow-through from tagged RNA purifications contains similar amounts of RNA compared to untagged, wild

type RNA (see lanes 6 and 7 in **Figure 2.4B**). Furthermore, elution of tagged RNAs from either matrix is limited, likely due to the minimal amount of tagged RNA associated with the matrix following binding and wash steps (data not shown).

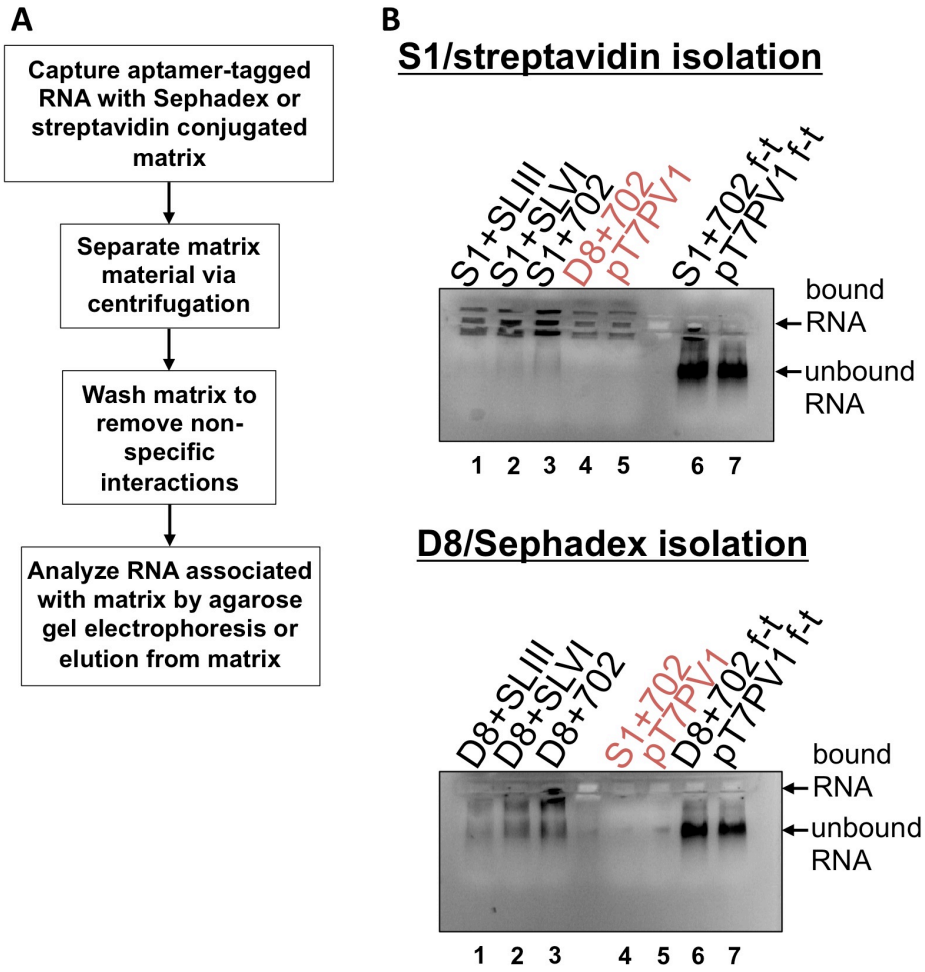

Figure 2.4. *In vitro* transcribed affinity-tagged RNA isolation. (**A**) Diagram of the RNA isolation procedure based on the use of S1 and D8 aptamer tags. Aptamer-tagged RNAs were captured by the respective matrix via incubation for 4 h at 4 °C, under rotation. The matrix material was then separated by centrifugation and washed 3–5 times to remove non-specific associations to the matrix. Finally, the matrix material was analyzed by agarose gel electrophoresis or incubated with dextran or biotin to elute aptamer-tagged poliovirus RNA. (**B**) Matrix material and associated RNA was loaded on a 1% agarose gel containing ethidium bromide and subjected to electrophoresis. Relative levels of RNA association are depicted as increased staining intensity within the wells of the agarose gel. Red labels of lanes 4 and 5 indicate negative controls: either wild type RNA (pT7PV1) or RNA containing an irrelevant tag for the matrix. Lanes 6 and 7 labeled as "f-t" are flow-through fractions that were loaded with the supernatant removed following the initial centrifugation, prior to the first matrix wash step. Unbound RNA migrates into the gel itself. Levels of unbound RNA present in samples removed following coupling step were similar between aptamer-tagged RNAs and wild type RNA, demonstrating the limited binding efficiency of these aptamers within the context of the 7.5 kb poliovirus RNA.

Subsequently, we attempted isolations of affinity-tagged viral RNA from infected HeLa cells. Third passage stocks of recombinant viruses containing aptamer tags for positive-strand isolation were used due to the greater abundance of positive-sense RNA relative to negative-sense RNA in infected cells. Wild type virus infections were used as controls. At 4 h post-infection, cells were harvested and infected cell pellets were resuspended and lysed. Pre-cleared lysates were purified as described above. Although we were able to observe specific isolation of genomes containing S1+ or D8+ tags compared to wild type poliovirus, the binding and elution efficiency associated with these RNAs was reduced compared to the *in vitro* transcribed RNA constructs. Furthermore, no proteins co-isolated with viral RNA were detected in elution fractions by electrophoresis in SDS-containing 12.5% polyacrylamide gels followed by SYPRO staining (data not shown). In addition, during infections with recombinant polioviruses, a formaldehyde cross-linking step was tested (Niranjanakumari et al., 2002); however, formaldehyde cross-linking abolished enrichment of recombinant viral genomes (data not shown).

Recombinant viral genomes containing modified S1 or D8 aptamer tags

In an attempt to increase the limited binding efficiency of S1 and D8 aptamers that we and others have observed (Leppek and Stoecklin, 2014), we engineered viral genomes with single S1 or D8 tags (in forward and reverse orientations for strand-specific isolation) that contain increased stem length to promote aptamer/matrix interactions for isolation of RNPs. The modified S1 and D8 tags (S1m and D8m) are 60 and 49 nucleotides in length, respectively. RNA constructs containing S1m or D8m at nucleotide position 702 of the genome were generated and characterized as previously

described. RNA constructs were first subjected to an *in vitro* translation assay to examine viral protein production from these RNAs (**Figure 2.5**). All modified D8 tag-containing constructs translated with similar efficiencies compared to the original D8 containing constructs and wild type poliovirus RNA (**Figure 2.5A**). Conversely, constructs containing the modified S1 containing tags, including a construct containing two S1m aptamers in series (S1m+(x2)702), produced limited levels of translation products (**Figure 2.5B**). Unlike the minimal S1 aptamer tags, no in-frame AUG sequences were present within these tags, so the limited protein production is likely a result of an inhibitory activity associated with ribosomal recognition or scanning.

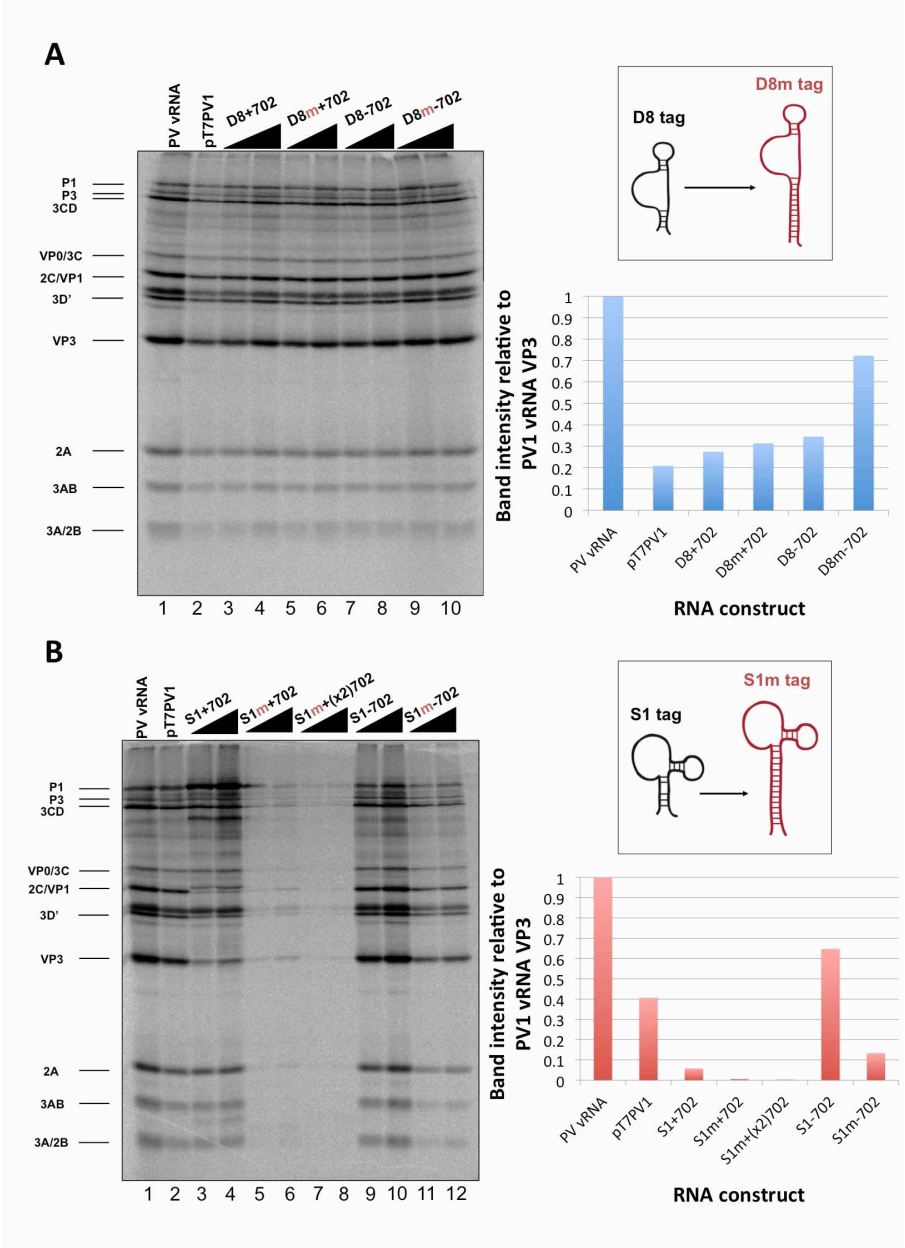

Figure 2.5. *In vitro* translation of poliovirus RNAs containing modified aptamers for RNA affinity isolation. (**A**) *In vitro* translation of RNA constructs containing original or modified D8 (denoted by a red "m") aptamers at nucleotide position 702 of the 5'-NCR show very similar levels of protein production compared to wild type RNA (lane 1 and 2). Quantification of the intensity of the band corresponding to VP3, relative to that of poliovirus virion RNA, is shown on the right hand side of the panel. A schematic of the alterations to the tag itself is shown above the quantification. (**B**) *In vitro* translation of RNA constructs containing original or modified S1 aptamers at nucleotide position 702 of the 5'-NCR show variable levels of protein production. The RNA construct containing modified S1 tag for positive-strand isolation (lanes 5 and 6) and an RNA construct containing two modified S1 tags in series (lanes 7 and 8) show very little protein production, but the RNA construct containing modified S1 tag for negative-strand isolation (lanes 11 and 12) translates at an intermediate level compared to the original S1 tag-containing constructs. Quantification of the intensity of the band corresponding to VP3 is shown on the right hand side of the panel, and a schematic of the alterations to the tag itself is shown above the quantification. Increasing RNA amounts (250 to 500 ng) are indicated with triangles above the autoradiographs. Bands corresponding to viral protein products are labeled.

Based on the translation product profiles, we focused on genomes containing modified Sephadex-binding tags for subsequent work. Recombinant polioviruses containing modified D8 aptamer tags in the forward or reverse orientation were generated as previously described. *In vitro* transcribed RNAs were transfected into HeLa cells and resulting recombinant viruses were plaque purified and amplified in cell culture. The stability of the tag sequence was verified by performing RT-PCR followed by sequencing of the 5'-NCR of these viruses. As was observed with viruses containing the original D8 tag, the D8m+702PV1 and D8m-702PV1 recombinant polioviruses retained an intact tag within the 5'-NCR with no alterations after three passages in cell culture, indicating that these genomic insertions were stable. The growth kinetics of these viruses were then characterized via single-cycle growth analyses (**Figure 2.6**). The recombinant polioviruses containing D8 tags of increased length had slight delays in virus production, but very similar titers were observed by the end of the infectious cycle compared to wild type poliovirus. These results suggested that recombinant polioviruses containing modified Sephadex-binding aptamers at nucleotide position 702 of the 5'-NCR could be used for the identification of RNP complexes associated with poliovirus RNA replication during the infectious cycle. However, attempts to isolate D8m+702PV1 RNA following infection have not yet been successful.

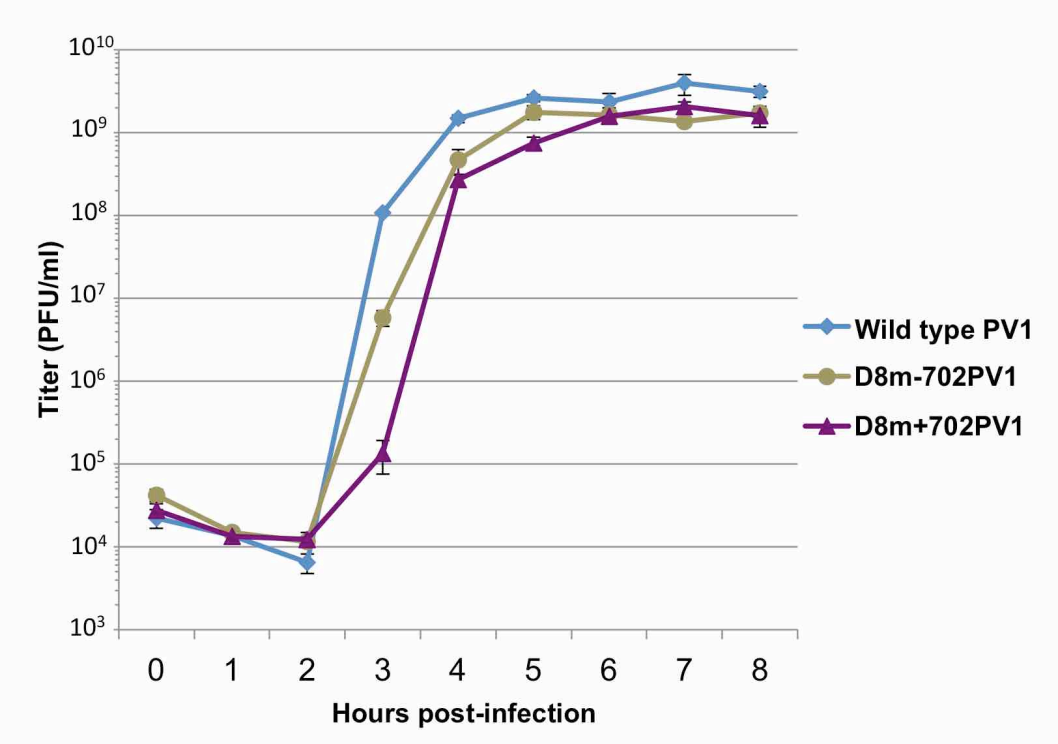

Figure 2.6. Single-cycle growth analysis of recombinant polioviruses containing modified D8 affinity tags. A single-cycle growth analysis was carried out in HeLa cell monolayers infected with wild type poliovirus (PV1), recombinant virus containing modified aptamer tag for positive-strand isolation (D8+m702PV1), or recombinant virus containing modified aptamer for negative-strand isolation (D8m-702PV1) at an MOI of 20. Cells and supernatant were harvested at 1 h intervals beginning at 0 h post-infection until 8 h post-infection, in triplicate. Virus yield was determined by plaque assay and plotted. Titer is given in plaque forming units (PFU) per milliliter. Error bars represent one standard deviation above and below the mean.

Discussion

In an effort to isolate intact enteroviral RNA replication complexes from infected cells at different times following infection and to identify the novel cellular components of these complexes that correspond to the discrete steps of the RNA replication process, we have generated recombinant polioviruses containing genetically encoded RNA affinity tags. Despite promising results related to the co-isolation of host proteins known to be involved in the replication cycle of poliovirus through MS2 affinity purification of viral RNA, the recombinant PV1-3′MS2 proved to be inadequate for the identification of novel host proteins involved in poliovirus RNA replication. This was in large part due to

the sensitivity of mass spectrometry analysis, as significant co-isolation of proteins from negative control purifications (i.e., from wild type poliovirus infections) resulted in poor signal-to-noise ratios.

Due to the lack of specificity we observed during isolations of viral RNP complexes from cells infected with PV1-3′MS2, we turned to alternate affinity tags that could increase the specificity of viral RNA isolations. In addition to adjusting affinity sequences from MS2 hairpins to aptamers, we also explored alternative genomic locations to the 3'-NCR for insertion of these purification tags. The replication defect of polioviruses lacking the 3'-NCR of the genome, including PV1-3′MS2, is thought to be a result of the absence of the complementary 5′ terminal region within the negative-sense intermediate RNA. This region, although not strictly required for viral replication, has been proposed to be a binding site for hnRNP C1/C2, allowing for efficient positive-sense RNA synthesis to take place (Ertel et al., 2010). Therefore, this recombinant virus was not ideal for identifying other proteins that may bind to these regions alongside hnRNP C1/C2. Moreover, the coding region of the poliovirus genome is obviously restricted in its ability to tolerate exogenous nucleic acid insertions throughout its length due to the potential of altered viral protein production from disruptions to translation reading frame and/or irregular polyprotein processing. While there are examples of viable, recombinant polioviruses containing nucleic acid sequence insertions within the coding region of genomes to generate fusion or tagged viral proteins, these genomes are only quasi-stable (Mueller and Wimmer, 1998; Teterina et al., 2010). To overcome the replication defect observed with PV1-3′MS2, the inherent deficiency this recombinant virus might offer in identifying proteins that interact with the genomic 3'-

NCR or negative-strand intermediate 5′-terminal region, and to promote the generation of a stable genome that could allow for growth kinetics that more closely matched wild type poliovirus, we focused on the 5'-NCR to identify potential aptamer tag sequence insertion sites. While interference with regulatory RNA regions within the 5'-NCR was a concern, there are several regions within the 5'-NCR of the poliovirus genome that have previously been shown to tolerate sequence alterations with limited effects to viral replication processes. Nucleic acid sequences generated via systematic evolution of ligands by exponential enrichment (SELEX) to bind with high affinity to streptavidin (S1) or Sephadex (D8) were selected due to their short length and demonstrated potential for RNP complex isolation. We tested three separate sites within the 5'-NCR of the poliovirus genome: S-L III, S-L VI, and nucleotide position 702 for their capacity to tolerate aptamer insertions while maintaining biological activity. Making use of these regions, we generated poliovirus RNA constructs containing either of the two aptamer tags within the 5'-NCR, in either a forward or reverse orientation to allow for aptamer sequences to be present in viral genomic RNAs or replication intermediate negative-strand RNAs and to permit strand-specific isolation from infected cells.

We initiated the RNP complex isolation study focused on the minimal, consensus sequences of the D8 and S1 aptamer tags with the rationale that their short length would be amenable to the production of recombinant virus containing a stable, RNA affinity-tagged genome. However, we observed insufficient RNA isolation efficiency associated with the S1 and D8 RNA affinity tags, and a loss of all specificity associated with these tags upon formaldehyde treatment. The minimal nature of these tags, particularly in the context of the relatively long poliovirus genomic RNA, likely limits the

amount of affinity-tagged RNA that can be isolated. Our results agreed with the recent finding that the binding efficiency of the minimal S1 aptamer offers almost no specificity of isolation relative to an untagged RNA construct (Leppek and Stoecklin, 2014). The authors of this latter study presented modified aptamer structures and tandem conformations that allow for up to 15-fold increases in binding efficiencies. However, the best binding efficiencies reported correspond to the inclusion of multiple tags of increased nucleotide length, likely preventing the generation of stable, recombinant poliovirus genomes containing these tags. In an attempt to increase the binding efficiency of the aptamer tags within the poliovirus 5'-NCR, while maintaining the stability of the tags through multiple passages, we increased the stem length of both the D8 and S1 by 16 nucleotides to promote the accessibility of RNA affinity sequence to matrix. However, increasing the stem length of the aptamer tags also proved to be insufficient for isolating poliovirus RNP complexes from infected cells.

Aside from the identification of the 3'-NCR and nucleotide position 702 of the poliovirus genome as amenable sites for the insertion of RNA affinity tags, the generation of recombinant viruses containing these tags, while not yet optimized for RNP complex isolation, revealed insights into the biology of the poliovirus genome. The Mahoney strain of the poliovirus 1 genome contains eight AUG triplets upstream of the authentic translation initiation site at nucleotide position 743, within the 5'-NCR. Kuge and colleagues have previously demonstrated that insertions into the poliovirus genome that contain an AUG triplet resulted in base substitutions to the AUG triplet alone, with no other alterations to the insertion sequence (Kuge et al., 1989). Our results partially support this finding, in that the AUG triplet present in the S1 aptamer sequence was not

tolerated in any of the viral isolates that were sequenced, with single nucleotide changes to this triplet sequence present in all cases. However, the sequence coding for the presence of the S1 aptamer within negative-sense RNA (S1−) also contains an AUG triplet (when present in the genomic RNA molecule) that is out-of-frame with authentic AUG start site. Interestingly, no alterations to protein production levels or polyprotein processing were observed upon *in vitro* translation of this construct compared to wild type RNA sequence. Whether this can be explained by the presence of a UAA stop codon in-frame with this AUG triplet remains to be seen. Other investigations have suggested that the translational efficiency of picornaviruses depends on the particular spacing between a polypyrimidine tract at nucleotide 558 of the 5'-NCR and one of the cryptic AUG triplets at nucleotide position 586, as well as whether AUG triplets are present within structured or unstructured elements (Jang et al., 1989; Pilipenko et al., 1992a; Sweeney et al., 2014). The function of the multiple AUG sequences upstream of the authentic translation initiation start site remains uncertain, but our work suggests that an additional AUG inserted into the poliovirus genome downstream of nucleotide position 586 is only selected against when this triplet is in-frame with the start codon, even when this AUG is within the structured region of an aptamer.

Our work also indicates that very short oligonucleotide sequences may not be adequate for stringent isolation of the RNA when they occur within the context of a long, structured viral genome. Although the region between S-L VI and the translation start site of the poliovirus genome (including nucleotide position 702) is often considered more-or-less unstructured, recent global RNA structure analysis has suggested that this region of the genome may in fact contain higher-order structures (Burrill et al., 2013b).

Incorporating aptamer tags within a structured RNA will impact the native structure of that region, and may impact the way in which the inserted sequences are able to make intramolecular contacts, possibly affecting proper secondary structure formation of the tags themselves. It is also possible that RNA affinity tags incorporated into the 5'-NCR of the poliovirus genome are sterically blocked from interacting with affinity matrices due to the highly structured nature of this region. Furthermore, the fact that this region interacts with many different protein species, which promote both viral translation and RNA replication, could lead to further masking of RNA affinity tags, thus blocking these RNA sequences from interacting with the matrix. MS2 coat protein RNA affinity tags within the 3'-NCR of the poliovirus genome should be sufficiently separated from RNA structural elements within the genome, which may aid in the isolation of the tagged RNA, but our work suggests the MS2 RNA affinity purification scheme itself allows for untenable levels of non-specific protein co-isolation. Adding complexity is the fact that poliovirus RNA is at least partially duplexed during RNA replication, obstructing affinity matrix/tag interactions and further complicating isolation schemes.

Leppek and Stoecklin have demonstrated increased isolation efficiencies with the S1 aptamer by increasing both the stem length of this aptamer as well as the number of tags incorporated into the RNA of interest. Although it would no doubt be advantageous to incorporate multiple aptamer tags in series (and/or at the apex of a stem-loop structure) we were limited in our choice of sequence length and insertion site, due to the constraint that recombinant viral genomes containing RNA affinity tags must recapitulate the biological activities of the wild type poliovirus genome. The fact that there is a maximum size threshold for exogenous sequence insertions into the

poliovirus genome before biological activity is affected was evidenced by cloning two modified streptavidin-binding aptamers into the nucleotide 702 region. This construct, S1m+(x2)702, produced the lowest levels of viral proteins of all constructs that were assayed by *in vitro* translation (**Figure 2.5**). A recent study that was published while our aptamer-based isolation attempts were ongoing has demonstrated the purification of poliovirus RNA through infection of a cell line stably expressing uracil phosphoribosyltransferase followed by UV cross-linking and oligonucleotide-directed poly(A) isolation (Lenarcic et al., 2013). This suggests that isolation of poliovirus RNA may be more tractable when using complementary oligonucleotide sequences rather than RNA affinity tags. Complementary oligonucleotide-based isolation of viral RNP isolation could also target negative-strand intermediates, as we attempted here, if oligonucleotides specific to this RNA were used in place of the oligo(dT) that was used for positive-strand isolation.

Overall, we have demonstrated that recombinant polioviruses containing RNA affinity tags within the noncoding regions of their genome are viable, and that these exogenous sequence insertions are stable for multiple passages in cell culture. Furthermore, we did not identify any significant compensatory mutations throughout the genomes of recombinant viruses as a result of these exogenous sequence insertions. Although recombinant flaviviruses and enteroviruses with stable epitope-tagged, fluorescent protein, or luciferase genes incorporated into their genome have been previously demonstrated, to our knowledge, these are the first examples of recombinant RNA viruses containing stable exogenous sequence insertions for biochemical isolation (Eyre et al., 2017; Lanke et al., 2009; Liu et al., 2010; Tamura et al., 2018; Zou et al.,

2011). Additionally, many of the recombinant viruses previously generated have significant impairments in replication compared to respective wild type viruses, unlike what we observed for some recombinant polioviruses containing aptamer-tagged genomes. Although we were able to specifically isolate RNA containing these affinity tags from cells infected with recombinant viruses, the efficiency of RNA affinity tag/matrix associations and isolation specificities were not sufficient to allow for the identification of novel cellular proteins that play roles in the RNA replication cycle of enteroviruses. However, the use of different affinity tags in the genomic positions discussed here could allow for this objective to be met in the future. Additionally, it is possible that these recombinant viruses have utility in other applications, such as in visualization of the production of specific polarities of RNA during the infectious cycle via the use of fluorescently labeled oligonucleotides complementary to tag sequences present in genomic RNAs or negative-strand intermediates (Walker et al., 2011). In summary, the viruses and methods described here represent an initial step toward the isolation of RNP complexes associated with enterovirus RNA replication directly from infected cells, in a strand-specific manner. Investigations utilizing these tools could eventually aid in the identification of cellular proteins that could be specifically targeted by anti-enteroviral therapeutics.

Materials and Methods

Cell culture and DNA constructs

HeLa cells were grown as monolayers in Dulbecco's Modified Eagle's Medium (DMEM) or in suspension culture in Spinner Minimal Essential Medium (S-MEM), both supplemented with 8% newborn calf serum (NCS). To generate plasmids encoding

either the S1 or D8 aptamer tags in forward or reverse orientation, or the modified forms of these aptamers, within the 5'-NCR of the poliovirus genome, three separate vectors were used. For constructs containing aptamer tag in place of S-L VI, the X585R plasmid (Haller and Semler, 1992) was engineered to contain an XhoI site at nucleotide position 564 (X585RXhoI). For generating aptamer tags in place of S-L III, and at nucleotide position 702, pT7PV1 (Haller and Semler, 1992) was digested with HincII and re-ligated to generate a subclone of this vector. XhoI sites were inserted flanking S-L III or at nucleotide position 702. These subclones, and X585RXhoI, were digested with XhoI then ligated with double stranded oligonucleotides corresponding to each one of the tag sequences containing XhoI recognition sites (**Table 2.1**). Tagged subclones were then ligated into full-length poliovirus cDNA constructs.

Table 2.1. Oligonucleotides corresponding to aptamer tag sequences incorporated into the 5′ noncoding region (5'-NCR) of the poliovirus genomic cDNA.

Affinity Tag	Oligonucleotide Sequence (5′–3′)
S1+	top: TCGAACCGACCAGAATCATGCAAGTGCGTAAGATAGTCGCGGGCCGGG bottom: TCGACCCGGCCCGCGACTATCTTACGCACTTGCATGATTCTGGTCGGT
S1−	top: TCGACCCGGCCCGCGACTATCTTACGCACTTGCATGATTCTGGTCGGT bottom: TCGAACCGACCAGAATCATGCAAGTGCGTAAGATAGTCGCGGGCCGGG
S1m+	top: TCGAAAGCGGCCGCCGACCAGAATCATGCAAGTGCGTAAGATAGTCGCGGG TCGGCGGCCGCTT bottom: TCGAAAGCGGCCGCCGACCCGCGACTATCTTACGCACTTGCATGATTCT GGTCGGCGGCCGCTT
S1m−	top: TCGAAAGCGGCCGCCGACCCGCGACTATCTTACGCACTTGCATGATTCTGGT CGGCGGCCGCTT bottom: TCGAAAGCGGCCGCCGACCAGAATCATGCAAGTGCGTAAGATAGTCGCG GGTCGGCGGCCGCTT
D8+	top: TCGATCCGAGTAATTTACGTTTTGATACGGTTGCGGA bottom: TCGATCCGCAACCGTATCAAAACGTAAATTACTCGGA
D8−	top: TCGATCCGCAACCGTATCAAAACGTAAATTACTCGGA bottom: TCGATCCGAGTAATTTACGTTTTGATACGGTTGCGGA
D8m+	top: TCGAAAGCGGCCTCCGAGTAATTTACGTTTTGATACGGTTGCGGAGGCCGCTT bottom: TCGAAAGCGGCCTCCGCAACCGTATCAAAACGTAAATTACTCGGAGGCC GCTT
D8m−	top: TCGAAAGCGGCCTCCGCAACCGTATCAAAACGTAAATTACTCGGAGGCCGCTT bottom: TCGAAAGCGGCCTCCGAGTAATTTACGTTTTGATACGGTTGCGGAGGCC GCTT

RNA constructs and virus stocks

RNA corresponding to full-length PV1 harboring aptamer tags within the 5'-NCR was generated by *in vitro* transcription of plasmids linearized with EcoRI using the MEGAscript T7 transcription kit (Ambion). Following transcription, RNA was purified by phenol/chloroform extraction followed by two rounds of ethanol precipitation in the presence of 700 mM ammonium acetate or by using the RNeasy Mini kit (Qiagen). For transfection of RNA into HeLa cells, 1 µg of transcribed RNA was incubated with TS buffer (137 mM NaCl, 4.4 mM KCl, 0.7 mM Na_2HPO_4, 0.5 mM $MgCl_2$, 0.68 mM $CaCl_2$, 25 mM Tris, pH 7.5) and 1 mg/mL DEAE-Dextran. Cells were washed twice with phosphate buffered saline (PBS) and 250 µL of Diethylaminoethyl(DEAE)-Dextran transfection mixture was added per 20 cm^2 plate of HeLa cells. After 30 min incubation at room temperature, DMEM-8% NCS was added and cells were incubated at 37 °C and monitored for cytopathic effects (CPE). CPE was observed after 1 day for RNAs containing aptamer tags in the 5'-NCR. Following detection of CPE, cells and supernatant were collected, subjected to 3-5 freeze-thaw cycles, and used to infect HeLa cell monolayers with a semi-solid agar overlay (DMEM-6% NCS, 0.45% agarose). Single plaque isolates were recovered at 2 days post-infection and used to infect fresh HeLa cell monolayers. The resulting virus was designated as passage 1. Virus was amplified by serial passage at a multiplicity of infection (MOI) of 20 in HeLa cell monolayers. Large-scale preparations of D8+/D8−/S1+/S1−/D8m+/D8m−702PV1 were generated for passage 3 stocks using HeLa suspension cells (1 liter). Cells were pelleted, washed once with PBS, resuspended with S-MEM and infected at an MOI of 20. After 30 min adsorption at room temperature, NCS was added to 8% by volume and

infection was allowed to proceed for 8 h. Cell cultures and fluids were subjected to three freeze-thaw cycles prior to centrifugation at ~1500 relative centrifugal units (rcf). For single-cycle growth analysis, HeLa cell monolayers were washed twice with PBS and infected with wild type PV1, PV1-3′MS2, or D8+/D8−/S1+/S1−/D8m+/D8m−702PV1 at an MOI of 20 for 30 min at room temperature. Cells were washed twice in PBS, overlaid with DMEM-8% NCS, and incubated at 37 °C. At times indicated, cells and supernatant were collected, subjected to 3–5 freeze-thaw cycles to release virus, and virus yields were determined in HeLa cells by plaque assay.

RT-PCR assays

For sequencing of viral RNA, HeLa cells were infected at an MOI of 20 for 4 h (D8+/D8−/S1+/S1−/D8m+/D8m−702PV1) and total cellular RNA was extracted using TriReagent (Molecular Research Center, Inc.) or TRIzol (Invitrogen). Reverse transcription was performed using avian myeloblastosis virus (AMV) reverse transcriptase (Life Sciences, Inc.). PCR amplification was performed using PfuTurbo (Stratagene) and PCR products were purified with QIAquick PCR purification kit (Qiagen) prior to sequencing (Laguna Scientific). RNA primers listed in (Burrill et al., 2013a) were used for D8+/D8−/S1+/S1−/D8m+/D8m−702PV1 and wild type poliovirus. For sequencing the 5'-NCR of D8+/D8−/S1+/S1−/D8m+/D8m−702PV1 viruses, PV17+(5′-GTTGTACCCACCCCAGAGG-3′) and PV895−(5'-CCTTGATGGGCTCGGTGAACTTG-3′) primers were used for RT-PCR.

In vitro translation of viral proteins

For *in vitro* translation assays, HeLa cell S10 cytoplasmic extracts were generated as described elsewhere (Walter et al., 2002). HeLa S10 (60% of total

volume) was incubated with 250 or 500 ng of *in vitro* transcribed RNA constructs corresponding to aptamer-tagged viral genomes or poliovirus virion RNA (vRNA), ^{35}S-methionine (PerkinElmer), and all-four buffer (1 mM ATP, 0.25 mM GTP, 0.25 mM UTP, 0.25 mM CTP, 60 mM potassium acetate, 30 mM creatine phosphate, 0.4 mg/mL creatine kinase, 15.5 mM HEPES-KOH [pH 7.4]). Translation was allowed to proceed at 30 °C for 5–6 h. 2X Laemmli sample buffer (LSB) was added to an equal volume of translation reaction and boiled for 3 min. Samples were then subjected to electrophoresis on an SDS-containing 12.5% polyacrylamide gel. Proteins were visualized by autoradiography following fluorography. Quantity One software (Bio-Rad Laboratories) was used to quantify VP3 band intensity of *in vitro* translation reactions that contained 250 ng of RNA relative to the band intensity of the poliovirus vRNA translation.

S1 and D8 aptamer affinity purification

RNA affinity purification utilizing S1 and D8 aptamers was performed as described in (Leppek and Stoecklin, 2014; Walker et al., 2008). *In vitro* transcribed RNA (11 µg) was renatured in TE buffer (10 mM Tris-HCl pH 7.5, 1 mM EDTA) by heating at 56 °C for 5 min, 37 °C for 10 min, and incubating at room temperature for 15 min. Streptavidin-agarose (Sigma-Aldrich,) was prepared by washing 10 times in lysis buffer (50 mM HEPES pH 7.4, 10 mM $MgCl_2$, 100 mM NaCl, 1 mM DTT, 0.1% Triton X-100, 10% glycerol), Complete protease inhibitors (Roche) and resuspended to 50% slurry in lysis buffer. Sephadex matrix was prepared by swelling 0.5 g Sephadex G-200 (Sigma-Aldrich) in 40 mL lysis buffer overnight at room temperature. The Sephadex was then washed 3 times with lysis buffer and resuspended to 50% slurry. RNA (1 µg) was

subjected to electrophoresis on a 1% agarose gel in Tris/Borate/EDTA (TBE) buffer to confirm an intact, homogenous RNA population. The remaining 10 µg of RNA was combined with 100 µL prepared streptavidin beads or Sephadex G-200 and 500 µL of lysis buffer. Samples were allowed to rotate at 4 °C for 4 h then subjected to centrifugation at ~25 rcf for 1 min to separate matrix, and supernatant was removed. Matrices were washed 5 times with 500 µL of lysis buffer, with rotation at 4 °C for 10 min. The matrix slurry was loaded directly onto a 1% TBE agarose gel containing ethidium bromide and subjected to electrophoresis to visualize RNA associated with matrix. As a comparison, the supernatant from the initial matrix separation (i.e., the flow-through) was also subjected to electrophoresis on the agarose gel. Elution of aptamer-tagged RNA was also carried-out by transferring matrix material slurry, following wash steps, to Ultrafree-MC HV centrifugal filter units (0.45 µm pore size (Millipore)) with 10 mM biotin (Sigma-Aldrich) or 50 mg/mL dextran (average molecular weight 9000–11,000 Da (Sigma-Aldrich)) in lysis buffer. Filter units were subjected to rotation at 4 °C for 1.5 h then subjected to centrifugation at ~7500 rcf for 2.5 min.

Isolation of recombinant viral RNA from infected cells was carried-out as described above, but the streptavidin matrix was first blocked with 10 µg avidin from egg white (Sigma-Aldrich). To generate lysates from infected cells, two 150 mm plates of HeLa cell monolayers were infected with wild type PV1, D8+702PV1, or S1+702PV1 at an MOI of 20 following two washes with PBS. After 30 min adsorption, DMEM-8% NCS was added to cells which were then placed in 37 °C incubator for 4 h. Formaldehyde cross-linking was incorporated where indicated as described in [35]: infected cells were washed twice with PBS then cross-linked with 0.2%–1% formaldehyde in PBS for 10

min at room temperature with shaking. Formaldehyde was quenched with 0.25 M glycine for 5 min at room temperature. Infected cells or infected and cross-linked cells were collected by scraping and pelleted at ~1500 rcf for 5 min, followed by washing twice with ice cold PBS. Pellets were resuspended in lysis buffer containing 20 U/mL RNasin (Promega). Cells were lysed by three rounds of sonication for 10 s followed by incubation on ice for 2 min. Lysates were pre-cleared by centrifugation and supernatant was incorporated into the isolation procedure.

CHAPTER 3

Quantitative proteomics reveals novel players in human rhinovirus replication through altered nuclear protein distribution patterns

Summary

The enteroviruses are a genus of quintessentially cytoplasmic RNA viruses. Viral protein production, genome replication, and virion assembly all occur within the cytoplasm of the infected cell. However, a growing body of evidence suggests host proteins that are predominantly localized within the cell nucleus facilitate enterovirus replication. In an effort to identify novel nuclear resident proteins involved in this process, we focused on proteins that increase in abundance in the cytoplasm of HeLa cells infected with human rhinovirus 16 (HRV16) via quantitative protein mass spectrometry. Through this approach we identified the multifunctional splicing factor proline and glutamine rich (SFPQ) as a protein, among many others, that redistributes from the nucleus to the cytoplasm during HRV16 infection. We show that SFPQ is targeted for proteolysis within the nucleus by viral proteinase 3CD/3C and that a fragment of SFPQ migrates into the cytoplasm during the later stages of infection. Knocking down SFPQ expression resulted in a significant reduction of HRV16 titer, viral protein production, and viral RNA accumulation, suggesting that SFPQ is a proviral factor. As a result of sequestration within the nucleus at early times of infection, it is unlikely that SFPQ is involved in HRV16 translation, but the truncated form of SFPQ that moves into the cytoplasm is able to bind, directly or indirectly, to HRV16 RNA. We propose that HRV16 targets SFPQ for cleavage and the truncated form of this protein facilitates HRV16 replication by directly promoting RNA replication, RNA stability, or

virion morphogenesis. Our findings reveal a more nuanced view of the enterovirus infectious cycle that incorporates the functions of proteins not normally found within the cytoplasmic site of replication.

Introduction

Viruses of the *Picornaviridae* family are characterized by a positive polarity, single-stranded RNA genome of 7-10 kb within a non-enveloped icosahedral capsid. The genome contains a single open reading frame flanked by a long (>500 nucleotide) 5'-noncoding region (NCR), a shorter 3'-NCR, and a 3'-terminal poly(A) tract. Although not unique to picornaviruses, another feature of these viruses is the use of the viral protein VPg to prime viral RNA synthesis. As a result, VPg is covalently linked to the 5'-terminus of the viral RNA and is the only viral protein known to be encapsidated. Being of mRNA polarity, the viral genome is translated immediately following virus attachment, uncoating, and release into the cell cytoplasm. The 5'-NCR contains extensive secondary structure (explored in Chapter 2), including an internal ribosome entry site (IRES), which drives the cap-independent translation of the viral genome. The multiple stem-loop structures of the IRES interact with cellular proteins to recruit ribosomes, initiating the synthesis of a polyprotein, which is co-translationally processed by viral proteinases 2A and 3CD/3C to produce both incompletely processed functional precursors and mature viral proteins (Bedard and Semler, 2004; Blyn et al., 1996; Fitzgerald and Semler, 2011). Viral RNA replication employs the newly synthesized RNA-directed RNA polymerase, 3D. Elements of secondary structure present at the termini of both polarities of viral RNA are also utilized for the process of genome replication. These structures serve as sites for interaction with cellular RNA-binding

proteins that are thought to promote intermolecular architectures conducive to this process, which, like translation, occurs in the cytoplasm of infected cells (Brunner et al., 2005; Herold and Andino, 2001; Parsley et al., 1997). RNA synthesis initially yields RNA intermediates of negative polarity, which then serve as templates for the production of genomic RNA. These nascent RNA molecules can then be used as templates for further rounds of translation and RNA replication and, upon production of sufficient viral protein, are encapsidated to yield mature, infectious virions. The resulting viral progeny then exit the cell via lysis and/or non-lytic release within extracellular vesicles (Altan-Bonnet, 2016).

Rhinoviruses, members of the enterovirus genus within the *Picornaviridae* family, are the causative agents of a plurality of all human respiratory infections (Mäkelä et al., 1998; Monto, 1994). Although most rhinovirus infections in healthy individuals cause relatively benign and self-limiting upper respiratory disease (i.e., the common cold), these infections can have more serious effects in some groups. For example, severe lower respiratory tract infections can occur in individuals with asthma, and acute exacerbations can arise in those with chronic obstructive pulmonary disease. In some instances, rhinovirus infection can also result in fatal pneumonia in the immunocompromised and the elderly (Corne et al., 2002; Gern et al., 1997; Hicks et al., 2006; Mallia et al., 2011). Rhinoviruses are categorized into three species (A, B, and C) comprising over 150 genotypes with broad (>12%) sequence divergence in the VP1 capsid gene (McIntyre et al., 2013; Royston and Tapparel, 2016). Attempts at vaccine development have been hindered by the resulting high antigenic diversity, consistent with which, no rhinovirus vaccines have been evaluated in clinical trials since the 1970s

(McLean, 2014; Papi and Contoli, 2011; Rohde, 2011). Moreover, antiviral agents for the treatment or prevention of rhinovirus infection have shown limited efficacy, and/or toxicity (De Palma et al., 2008; Jacobs et al., 2013). Despite the rarity of severe disease associated with rhinovirus infection, there is a substantial economic burden associated with the common cold. A survey of over 4,000 households in the USA allowed for an annual estimate of $17 billion in direct costs (e.g., visits to the doctor, prescription and over-the-counter drugs) and $23 billion in indirect costs (e.g., absence from work) of non-influenza-related respiratory tract infections. Somewhat startlingly, it was also estimated that more than $1 billion is spent annually on over 40 million irrelevant antibiotic prescriptions for those with non-influenza-related viral respiratory tract infections (Fendrick et al., 2003). Despite extensive study, largely in the poliovirus model, aspects of the enterovirus life cycle remain poorly understood. Insights into the rhinovirus replication cycle could provide opportunities for the development of effective antivirals and relief from the significant health and economic burden associated with these infections.

An underappreciated feature of the enterovirus replication cycle is the alteration in the bidirectional movement of biomolecules through the nuclear pore complex (NPC), a highly organized protein structure that regulates free diffusion through the nuclear pore [see Chapter 1 and reviewed in (Flather and Semler, 2015)]. This disruption in nucleocytoplasmic trafficking is mediated by viral proteinases, which target nucleoporin (Nup) proteins, the components of the NPC, for degradation. Nups containing phenylalanine-glycine (FG) repeats are specifically proteolyzed, as these FG-Nups occupy the central channel of the NPC and contain unstructured regions that serve as

contacts for the soluble transport receptors (called karyopherins) that ferry cargo biomolecules through the pore [reviewed in (Hoelz et al., 2011)]. Experiments using recombinant proteinases *in vitro* or transfection of proteinase expression constructs into cells, have shown that Nup62, 98, and 153 are targeted by enterovirus proteinase 2A, and Nup62, 153, 214, and 358 are targets for proteinase 3CD/3C (Ghildyal et al., 2009; Gustin and Sarnow, 2001, 2002; Park et al., 2008; Park et al., 2010; Walker et al., 2013; Watters and Palmenberg, 2011). However, during a natural infection, it is likely that the viral proteinases act synergistically to degrade these FG-Nups that are directly involved in nucleocytoplasmic transport (Cautain et al., 2015; Walker et al., 2016). Enterovirus-induced Nup cleavage causes a breakdown in the conduit by which proteins translocate between the cytoplasm and nucleus, as well as a dysregulation in the barrier function of the NPC, which together result in the mislocalization of nuclear proteins as the infectious cycle progresses (Belov et al., 2004; Gustin and Sarnow, 2001, 2002).

Nucleic acid binding proteins facilitate RNA virus replication, but the diversity and abundance of these proteins within the cytoplasmic space of cells may not necessarily be conducive to direct viral utilization upon infection. Targeting the NPC causes a defect in the process of normal protein partitioning within the cell, effectively expanding the repertoire of protein functions available where viral replication is carried out. Cellular proteins involved in enterovirus translation include nuclear shuttling proteins such as such as polypyrimidine tract binding protein 1 (PTBP1) and poly(r)C binding protein 2 (PCBP2). As a consequence of their normal cellular functions these proteins are present in the cytoplasm of uninfected cells and therefore can be exploited immediately upon viral infection (Blyn et al., 1997; Hellen et al., 1993; Hunt and Jackson, 1999). As

the infectious cycle progresses, the NPC is degraded, and proteins normally partitioned to the nucleus can be found within the cytoplasm. These nuclear resident proteins have unique functions that can be hijacked to promote efficient viral RNA replication. One protein that functions in enterovirus RNA replication is heterogeneous nuclear ribonucleoprotein C1/C2 (hnRNP C1/C2) (Brunner et al., 2005; Ertel et al., 2010; Roehl and Semler, 1995). This protein functions in pre-mRNA processing and is restricted to the nucleus of uninfected cells (Piñol-Roma and Dreyfuss, 1992; Piñol-Roma and Dreyfuss, 1993). However, upon infection with poliovirus, hnRNP C1/C2 redistributes to the cytoplasm where it promotes RNA replication, possibly through circularization of the negative strand intermediate RNA and recruitment of 3D (Brunner et al., 2010; Ertel et al., 2010).

We hypothesized that the identification of nuclear proteins that relocalize to the cytoplasm during the infectious cycle could reveal novel factors involved in enterovirus replication. To identify these putative replication factors, we screened for proteins that become enriched in the cytoplasm of HeLa cells during human rhinovirus 16 (HRV16, also known as rhinovirus A16) infection, using quantitative protein mass spectrometry. One of the proteins identified was splicing factor proline and glutamine rich (SFPQ), a C-terminal cleavage fragment of which appeared in the nucleus at mid-times during infection and subsequently relocalized to the cytoplasm. This cleavage was independent of caspase activity, and a predicted HRV16 3CD/3C proteinase cleavage site was identified within SFPQ. Knockdown of SFPQ through an siRNA-mediated approach resulted in reduced viral titers, protein production, and RNA accumulation, indicating that SFPQ is a proviral factor for HRV16. We also show that the C-terminal

fragment of SFPQ, present in the cytoplasm of infected cells, is able to bind *in vitro* transcribed HRV16 RNA. These results broaden our understanding of the importance of nuclear resident proteins in the life cycle of a cytoplasmic RNA virus.

Results

HRV16 induces a coordinated redistribution of proteins into the cytoplasm of infected cells.

To identify cellular proteins that become enriched in the cytoplasm during HRV16 infection of HeLa cells, we fractionated mock- and HRV16-infected cells at mid- (4 hours) and late- (8 hours) times of infection (**Figure 3.1A**). Nuclear and cytoplasmic fractions were generated by hypotonic swelling of cells followed by Dounce homogenization and centrifugation (Penman, 1966). Compartmental separation was confirmed by assaying for the cytoskeletal protein vinculin and the nuclear matrix protein lamin A/C (**Figure 3.1B**). By 4 hours post-infection (hpi) viral proteinase 3CD was detected in cytoplasmic fractions and by 8 hpi the viral RNA-directed RNA polymerase 3D was present in both cytoplasmic and nuclear fractions, consistent with a productive infection of cells prior to fractionation (**Figure 3.1B**). The presence of HRV16 3CD within the nucleus has been reported previously (Amineva et al., 2004). The above fractions were separately digested with trypsin, and the resulting tryptic peptides were tagged with light, intermediate, and heavy dimethyl isotope labels. Labeled fractions were combined and subjected to strong cation exchange (SCX) chromatography followed by nanoLC-MS/MS of active SCX fractions. As a result of the limited impact infection had on protein redistribution at 4 hours post-infection (data not shown), we

focused primarily on a comparison of protein abundance in mock- and HRV16-infected cells at 8 hours post-infection (8hpi:mock abundance ratios).

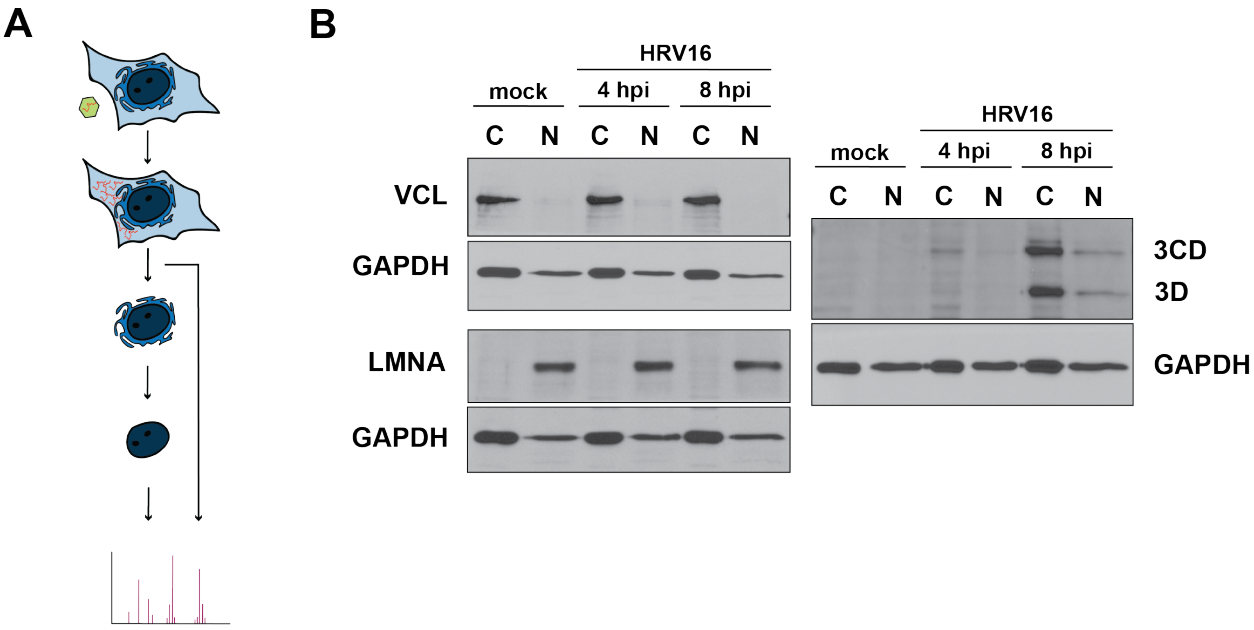

Figure 3.1. Subcellular fractionation of HRV16-infected HeLa cells for protein distribution analysis. (**A**) Schematic of mass spectrometry analysis of protein distribution. Mock- or HRV16-infected HeLa cells were separated into cytoplasmic and nuclear fractions, digested with trypsin, isotopically labeled, pooled, and subjected to nanoLC-MS/MS. (**B**) Fractionation of HeLa cells following mock, 4, or 8 hours post-HRV16 infection was confirmed by Western blot analysis. Vinculin (VCL) was used as a cytoplasmic (C) marker protein and lamin A/C (LMNA) as a marker of the nucleus (N). As confirmation of a productive infection, fractions were assayed for the expression of HRV16 RNA-dependent RNA polymerase 3D and its precursor 3CD. Glyceraldehyde-3-phosphate dehydrogenase (GAPDH) was used as loading control. Hpi: hours post-infection.

The above procedure was performed in biological duplicate leading to replicate cytoplasmic and replicate nuclear 8hpi:mock abundance ratios for tryptic peptides (**Figure 3.2A and 3.2B**, respectively). To determine which proteins relocalize to and/or increase in abundance in the cytoplasm of HRV16-infected cells, peptides with 8hpi:mock abundance ratios in nuclear fractions reproducibly 0.9 or less (**Figure 3.2C**) were recorded and screened, accession-by-accession, for their 8hpi:mock abundance ratios in the cytoplasmic fractions (**Figure 3.2D**). A substantial number of accessions with nuclear 8hpi:mock ratios that were suppressed had correspondingly elevated

cytoplasmic 8hpi:mock ratios, strongly suggesting a coordinated redistribution of these proteins from nucleus to cytoplasm by 8 hours post-infection with HRV16. It should be noted that this cytoplasmic enrichment screen could also identify proteins that are blocked from nuclear import following biogenesis in the cytoplasm, due to the breakdown of nucleocytoplasmic transport during infection. In this way, newly synthesized nuclear proteins would be inhibited from nuclear entry and therefore accumulate in the cytoplasm of HRV16-infected HeLa cells.

Proteins that were reproducibly identified as decreasing in abundance in the nucleus and correspondingly increasing in abundance in the cytoplasm, due to efflux from the nucleus and/or inhibition of nuclear import, are listed in **Table 3.1**. These proteins represent those that fulfilled our most stringent criteria for nucleocytoplasmic re-equilibration: abundance ratios below or above 1 for nuclear or cytoplasmic datasets, respectively, and which had these opposing ratios in both datasets of each biological replicate experiment. All 277 proteins that passed our stringent screening but for which tryptic peptides did not necessarily appear in all four datasets (i.e., not reproducibly) are shown in the **Appendix**. **Figure 3.3** presents the biological process gene ontology (GO) terms that are associated with the proteins listed in **Table 3.1**. A plurality of proteins that decrease in abundance in the nucleus and increase in abundance in the cytoplasm during HRV16 infection are involved with RNA splicing, and proteins involved in mRNA transcription, RNA metabolism, and RNA localization are also represented. The fact that many proteins identified in our screen are overrepresented in RNA-related functions, compared to a random sampling from the human proteome (*p*-value: ~2×10^{-7} calculated from PANTHER database overrepresentation algorithm), suggests that this functional

class of proteins is targeted for cytoplasmic enrichment as infection proceeds (Mi et al., 2016).

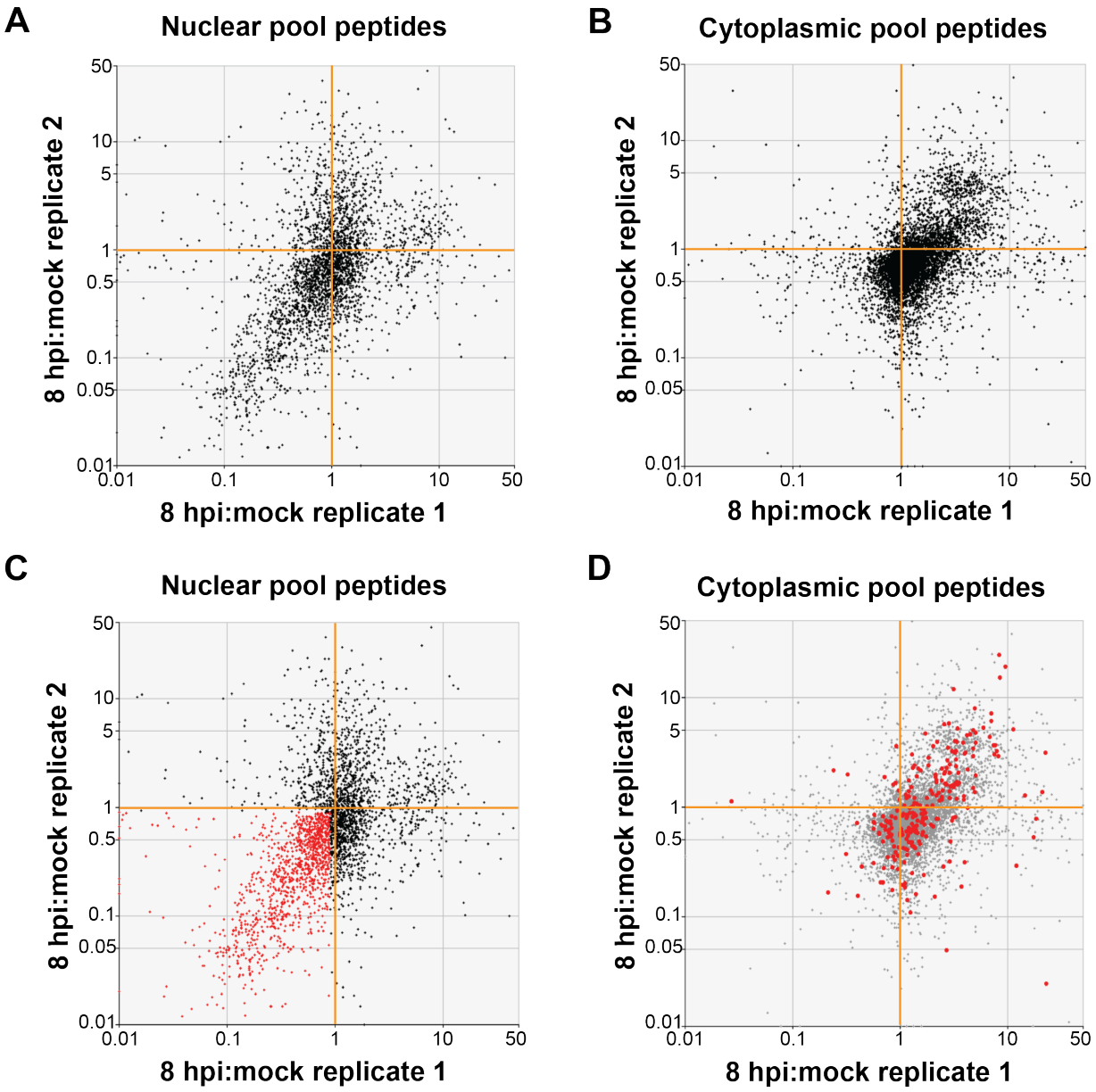

Figure 3.2. HRV16 induces a coordinated redistribution of proteins into the cytoplasm of infected cells. Scatter plots show 8hpi:mock abundance ratios for all tryptic peptides detected in replicate in (**A**) nuclear and (**B**) cytoplasmic fractions. On the theoretical diagonal line of reproducibility (lower-left to upper-right), the apparent overrepresentation of in the lower-left quadrant with respect to the upper-right for nuclear tryptic peptides is consistent with a net efflux of proteins from the nucleus, and the corresponding apparent overrepresentation of the upper-right quadrant for cytoplasmic tryptic peptides is consistent with a net influx of proteins into the cytoplasm. (**C**) Tryptic peptides scoring < 0.9, reproducibly, in nuclear 8hpi:mock abundance ratio were recorded (red) and the subset shared with both cytoplasmic replicates were then highlighted (bold red) on the cytoplasmic scatter plot (**D**), indicating a clear coordination between nuclear depletion and cytoplasmic enrichment.

Table 3.1. Proteins that increase in abundance in the cytoplasm and decrease in abundance in the nucleus of HRV16-infected HeLa cells. Values under each of the four datasets ('Nuc1', 'Nuc2', 'Cyto1', 'Cyto2') take the form 'x/y/z' in which an 8hr:mock abundance ratio of x (geometric mean of relevant, quantifiable tryptic peptides) was based on z tryptic peptide species, y of which tracked the direction (< 1 or > 1) of x.

Accession	Description	Nuc1	Nuc2	Cyto1	Cyto2
ANXA2	Annexin A2	0.4317/21/23	0.1666/8/8	2.0875/14/16	1.2723/18/18
ANXA6	Annexin A6	0.132/7/7	0.0816/6/6	2.7491/6/6	1.3958/7/7
CD44	CD44 antigen	0.6967/1/4	0.2408/1/1	2.2396/4/4	1.269/4/5
COR1B	Coronin-1B	0.2592/5/5	0.0277/1/1	2.2832/3/3	2.1327/3/3
COR1C	Coronin-1C	0.1418/7/7	0.0432/3/3	25.9097/5/5	1.335/6/6
CPSF2	Cleavage and polyadenylation specificity factor subunit 2	0.2228/4/5	0.1982/2/2	2.005/1/1	4.5298/6/6
CSTF3	Cleavage stimulation factor subunit 3	0.5483/5/5	0.3508/2/2	10.25/1/1	7.0256/4/4
DHX9	ATP-dependent RNA helicase A	0.2869/32/34	0.2458/8/9	2.2561/8/9	1.6309/18/18
DREB	Drebrin	0.2133/9/9	0.1965/3/3	3.1428/3/3	1.2084/4/4
FLNA	Filamin-A	0.2329/56/59	0.044/22/22	3.6386/50/50	1.7896/50/52
FLNB	Filamin-B	0.266/36/37	0.0552/7/7	2.113/27/27	1.2044/38/43
HNRPL	Heterogeneous nuclear ribonucleoprotein L	0.4883/15/18	0.4397/4/4	4.6695/3/3	3.1403/6/6
HNRPM	Heterogeneous nuclear ribonucleoprotein M	0.1427/22/22	0.0963/10/10	3.1112/2/2	1.8638/9/9
MATR3	Matrin-3	0.2173/22/22	0.27/8/9	4.1396/3/3	2.0742/12/12
MTA2	Metastasis-associated protein MTA2	0.5761/14/16	0.3655/5/5	353.4703/4/4	1.7301/3/5
MTA3	Metastasis-associated protein MTA3	0.5277/6/6	0.3368/1/1	2.428/1/1	2.876/1/1
NONO	Non-POU domain-containing octamer-binding protein	0.2521/20/21	0.144/8/9	5.015/2/2	1.9679/5/5
OGT1	UDP-N-acetylglucosamine-peptide N-acetylglucosaminyltransfera-se 110 kDa subunit	0.5653/2/2	0.5655/1/1	47.43/1/1	26.1288/2/7
PABP2	Polyadenylate-binding protein 2	0.5335/7/7	0.2987/2/2	2.481/1/1	1.1887/3/3
PLEC	Plectin	0.2751/190/196	0.1086/72/74	4.4278/42/47	2.7159/77/79
PLOD3	Procollagen-lysine,2-oxoglutarate 5-dioxygenase 3	0.5699/10/11	0.4759/2/2	3.154/5/5	1.1828/8/11
PSPC1	Paraspeckle component 1	0.4501/10/12	0.2438/1/1	9.3991/3/3	2.0014/2/2
RBMX	RNA-binding motif protein, X chromosome	0.7064/13/15	0.285/1/1	6.884/1/1	3.2891/5/5
RBP2	E3 SUMO-protein ligase RanBP2	0.4485/31/38	0.3809/9/10	12.0081/4/4	1.5007/12/13
ROA1	Heterogeneous nuclear ribonucleoprotein A1	0.5264/14/15	0.0832/6/6	4.5871/5/5	1.3267/8/10
ROA2	Heterogeneous nuclear ribonucleoproteins A2/B1	0.543/17/19	0.3519/8/10	2.9374/7/7	2.2725/11/11
SAFB1	Scaffold attachment factor B1	0.5182/15/17	0.2757/6/6	6.238/4/4	3.6845/4/4
SF3A1	Splicing factor 3A subunit 1	0.5655/11/19	0.4464/8/9	3.1441/1/1	1.3703/11/12
SF3B1	Splicing factor 3B subunit 1	0.7293/23/31	0.5508/11/11	5.4408/3/3	1.9732/24/24
SFPQ	Splicing factor, proline- and glutamine-rich	0.372/26/26	0.0761/6/6	6.0995/8/8	2.5987/7/7
SPT6H	Transcription elongation factor SPT6	0.1824/20/20	0.3019/5/5	6.2192/3/3	1.2091/12/17
SPTN1	Spectrin alpha chain, non-erythrocytic 1	0.1479/82/83	0.0281/47/47	2.3006/26/28	1.4219/33/36
SYMPK	Symplekin	0.6877/4/4	0.2639/1/1	2.2432/1/1	1.6576/4/4
SYNE2	Nesprin-2	0.4411/8/12	0.3828/2/2	2.539/1/1	1.42/1/1

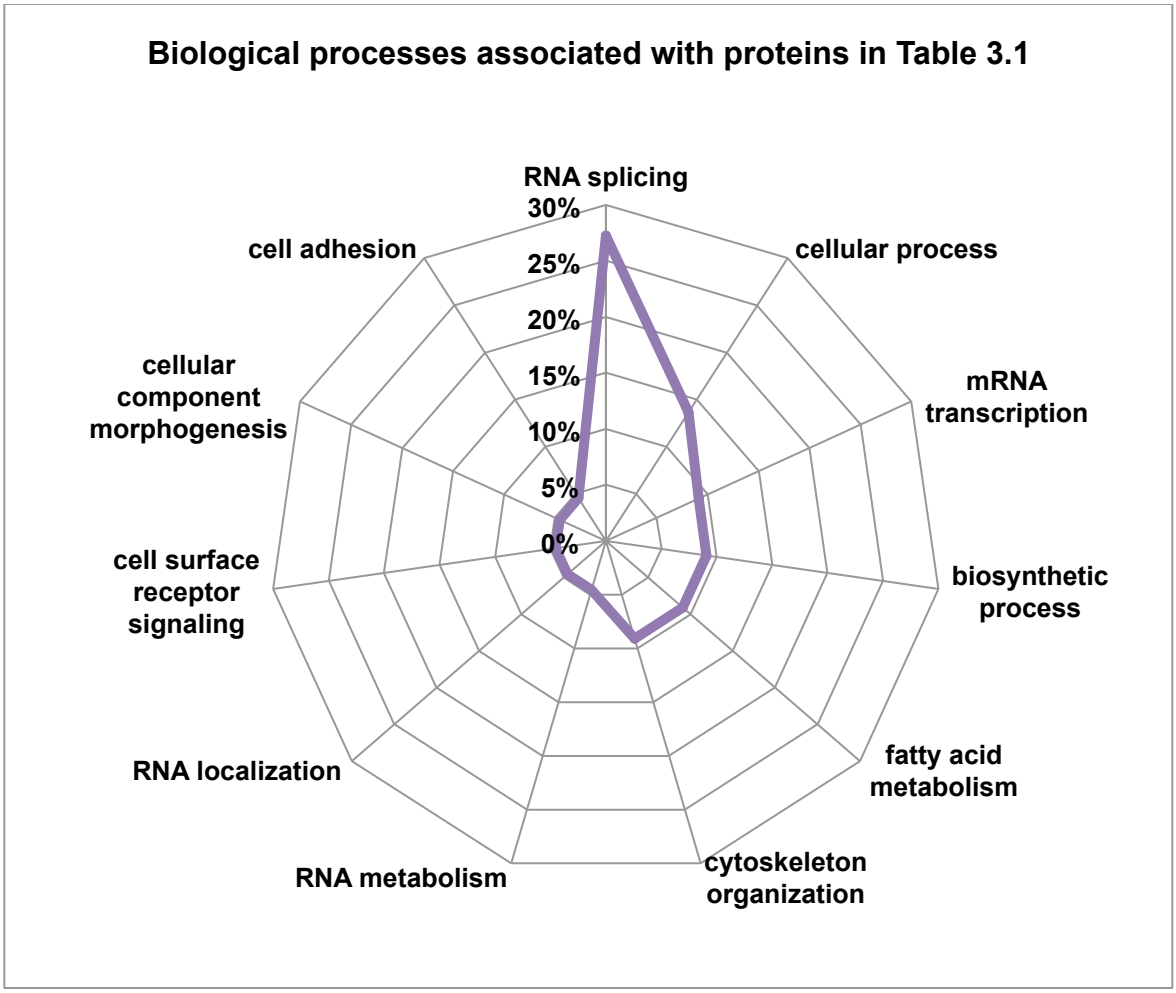

Figure 3.3. Biological process gene ontology terms associated with proteins in Table 3.1. Radar plot showing the percentage of proteins from Table 3.1 that correspond to a particular biological process, for those that have annotated biological process gene ontology (GO) terms associated with them. GO slim terms were compiled using the PANTHER database http://pantherdb.org/ (Mi et al., 2016).

Validation of mass spectrometry approach

The above analysis identified factors that have recently been identified as being involved in enterovirus replication (hnRNP M, NONO) but excluded other proteins with known roles in the infectious cycle, such as PCBP2 (Jagdeo et al., 2015; Lenarcic et al., 2013). This was likely a result of our screening process taking into account the relative abundance of particular proteins in the compartments of uninfected cells. For example, because PCBP2 is present in the cytoplasm of uninfected cells due to its function as a

nuclear shuttling protein, it may have been unable to pass the thresholds that we imposed to identify cytoplasmic enrichment. Based on our analysis it seems the abundance of PCBP2 in HRV16-infected HeLa cells did not significantly change in either the cytoplasm or the nucleus compared to uninfected cells. In this way, our screen emphasized more dramatic protein movements, through changes in normal distribution patterns.

To validate our proteomics-based approach, we selected heterogeneous nuclear ribonucleoprotein M (hnRNP M) as a positive control due to recent work demonstrating that it relocalizes to the cytoplasm during poliovirus infection (Jagdeo et al., 2015). Peptides corresponding to hnRNP M within our nuclear and cytoplasmic fraction datasets demonstrated a clear relocalization event by 8 hours post-infection with HRV16 (**Figure 3.4A**). We confirmed this redistribution via confocal immunofluorescence microscopy (**Figure 3.4B**) and Western blot analysis (**Figure 3.4C**). Very similar to observations made during poliovirus infection, HRV16 infection resulted in cleavage of hnRNP M, likely as a result of viral 3CD/3C proteinase activity (Jagdeo et al., 2015). Additionally, we observed colocalization between HRV16 2C and hnRNP M. This is suggestive of a role for hnRNP M in the HRV16 replication since 2C functions in viral RNA replication through supporting interactions between viral RNA and cellular membranes.

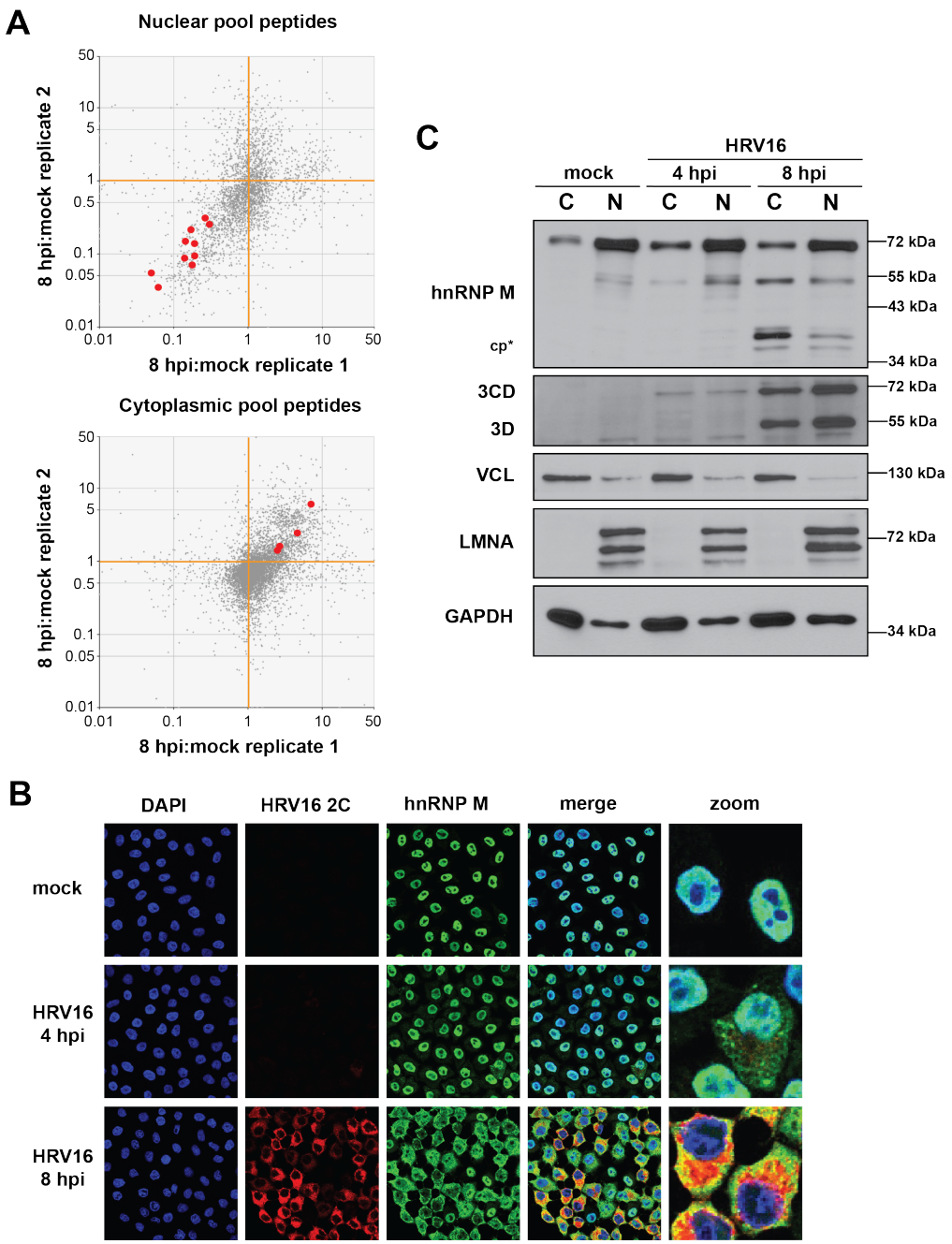

Figure 3.4. Heterogeneous nuclear ribonucleoprotein M (hnRNP M) redistributes to the cytoplasm of HRV16-infected HeLa cells. (**A**) Tryptic peptides in Figure 3.2 that correspond to hnRNP M are highlighted red, clearly reflecting the nucleocytoplasmic redistribution of this protein 8 hours post infection (hpi) by HRV16. (**B**) HeLa cells were mock- or HRV16-infected (MOI 10) then fixed 4 or 8 hpi. Cells were permeabilized then probed, via indirect immunofluorescence, for HRV16 2C (red), a marker of HRV16 RNA replication sites, and cellular protein hnRNP M (green). DNA was counterstained with DAPI to indicate location of nuclei (blue). Cells were then imaged using confocal microscopy. (**C**) HeLa cells were mock- or HRV16-infected (MOI 10), fractionated at the indicated times, and fractions were analyzed by Western blot. Cleaved hnRNP M was observed 8 hpi in both the cytoplasmic and nuclear fractions (cp*). HRV16 3D and its precursor 3CD were used as markers of infection. VCL and LMNA were used as markers of the cytoplasmic (C) and nuclear fractions (N), respectively, and GAPDH was used as a general loading control.

Our proteomics analysis excluded proteins that did not increase in abundance in the cytoplasm during HRV16 infection, so we selected a negative control protein based on previous work with rhinoviruses. Immunofluorescence-based studies have demonstrated that serine and arginine rich splicing factor 2 (SRSF2, also known as SC35) retains its nuclear localization during infection with HRV14 or HRV16 (Gustin and Sarnow, 2002; Walker et al., 2013). Although SRSF2 was not identified in our enrichment screen, tryptic peptides corresponding to this protein were retrieved from our nuclear datasets but not from our cytoplasmic datasets, suggestive of the nuclear retention of this protein throughout infection. We analyzed the distribution of SRSF2 via immunofluorescence microscopy and our results supported the nuclear retention of SRSF2 during HRV16 infection (**Figure 3.5**). We also performed a Western blot analysis to confirm the distribution of SRSF2 throughout the course of HRV16 infection and while there was no change in the relative abundance of SRSF2 in the nucleus and cytoplasm at each time-point, we did observe the presence of SRSF2 in all cytoplasmic fractions (data not shown). These results suggested that an epitope of SRSF2 may become masked during *in situ* formaldehyde cross-linking prior to imaging, or that due to a diffuse cytoplasmic distribution SRF2 may have been below the detection threshold of immunofluorescence. Together, these results highlight the semi-selective redistribution of nuclear proteins during HRV16 infection of HeLa cells.

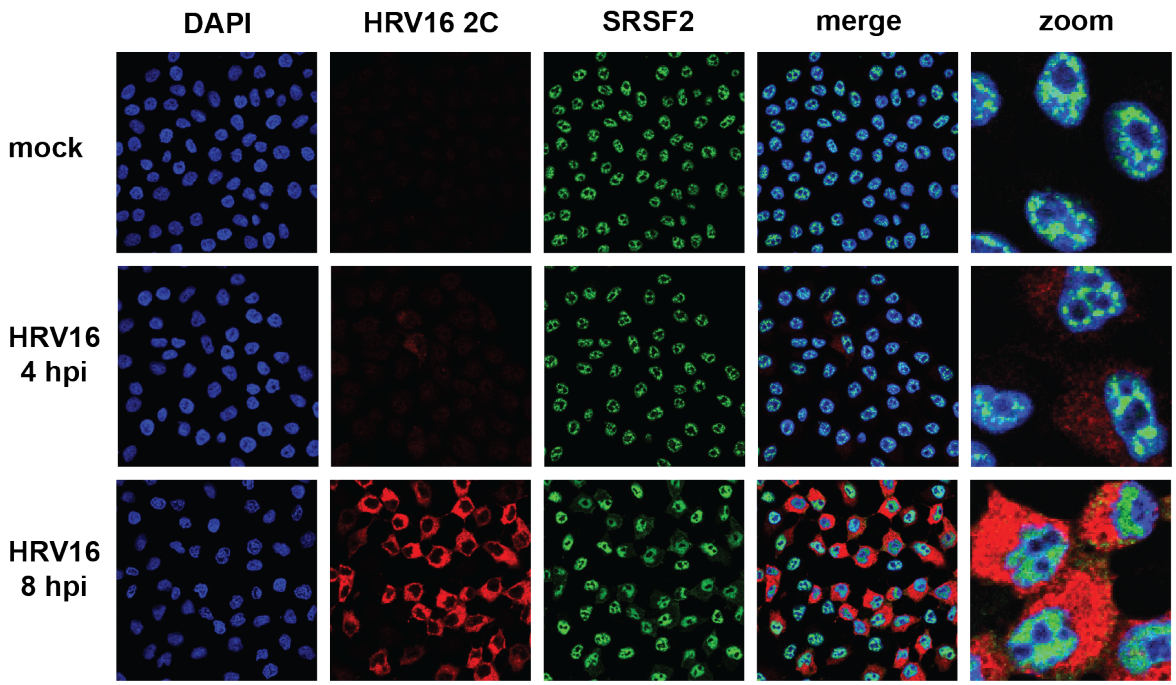

Figure 3.5. Serine and arginine rich splicing factor 2 (SRSF2) remains within the nucleus of HRV16-infected HeLa cells. HeLa cells were mock- or HRV16-infected (MOI 10) then fixed on coverslips at the indicated times post-infection. HRV16 2C (red) and SRSF2 (green) were labeled by indirect immunofluorescence. DNA was counterstained with DAPI to indicate the location of nuclei (blue). Cells were imaged using confocal microscopy.

Splicing factor proline and glutamine rich redistributes to the cytoplasm of HRV16-infected HeLa cells

Based on the compelling evidence for nuclear-cytoplasmic relocalization of splicing factor proline and glutamine-rich (SFPQ) from our proteomics data (**Figure 3.6A**) and the large number of tryptic peptides identified corresponding to SFPQ in all datasets following screening (see **Table 3.1**), we chose to validate the redistribution pattern of this protein. Immunofluorescence microscopy confirmed the strong nuclear localization of SFPQ in uninfected HeLa cells and its partial redistribution 8 hours post-infection with HRV16, with SFPQ distributed throughout the cell cytoplasm and nucleus at this time (**Figure 3.6B**). Fractionation and Western blot analysis of mock- or HRV16-infected HeLa cells revealed that the form of SFPQ that had relocalized to the

cytoplasm was a cleavage fragment of the full-length protein (**Figure 3.6C**). SFPQ appears as two bands within the nucleus by 4 hours post-infection, only the smaller of which was observed in the cytoplasm at 8 hours post-infection. A second possible cleavage product of SFPQ was detected in the nucleus by 8 hours post-infection. The antibody used in these studies was raised against residues 581-660 of SFPQ, which allowed us to track the C-terminal portion of the 707-amino-acid protein. Due to the apparent cleavage of SFPQ at a time when 3CD proteinase was present in the nucleus (as confirmed by immunofluorescence microscopy, data not shown), we inspected the primary amino acid sequence of SFPQ for potential 3CD recognition sites. Over ten potential sites were found, including five of the preferred glutamine-glycine (QG) dipeptides (**Figure 3.6D**). Moreover, utilizing the NetPicoRNA server (http://www.cbs.dtu.dk/services/NetPicoRNA/) which scores predicted cleavage sites based on sequence and surface exposure, the possible 3CD cleavage sites were narrowed to four QG dipeptides (Blom et al., 1996). Residue Q257 showed the highest score for predicted cleavage and surface exposure, and cleavage at this site would yield fragments consistent in size with those identified by Western blot analysis. Although SFPQ has an approximate molecular mass of 76 kDa, via SDS-PAGE it has an electrophoretic mobility more consistent with a protein of ~100 kDa. The high probability of SFPQ cleavage by the NetPicoRNA algorithm, combined with the observation of C-terminal fragments of SFPQ by Western blot analysis suggested that viral proteinase 3CD targets SFPQ for cleavage in the nucleus of HRV16-infected HeLa cells.

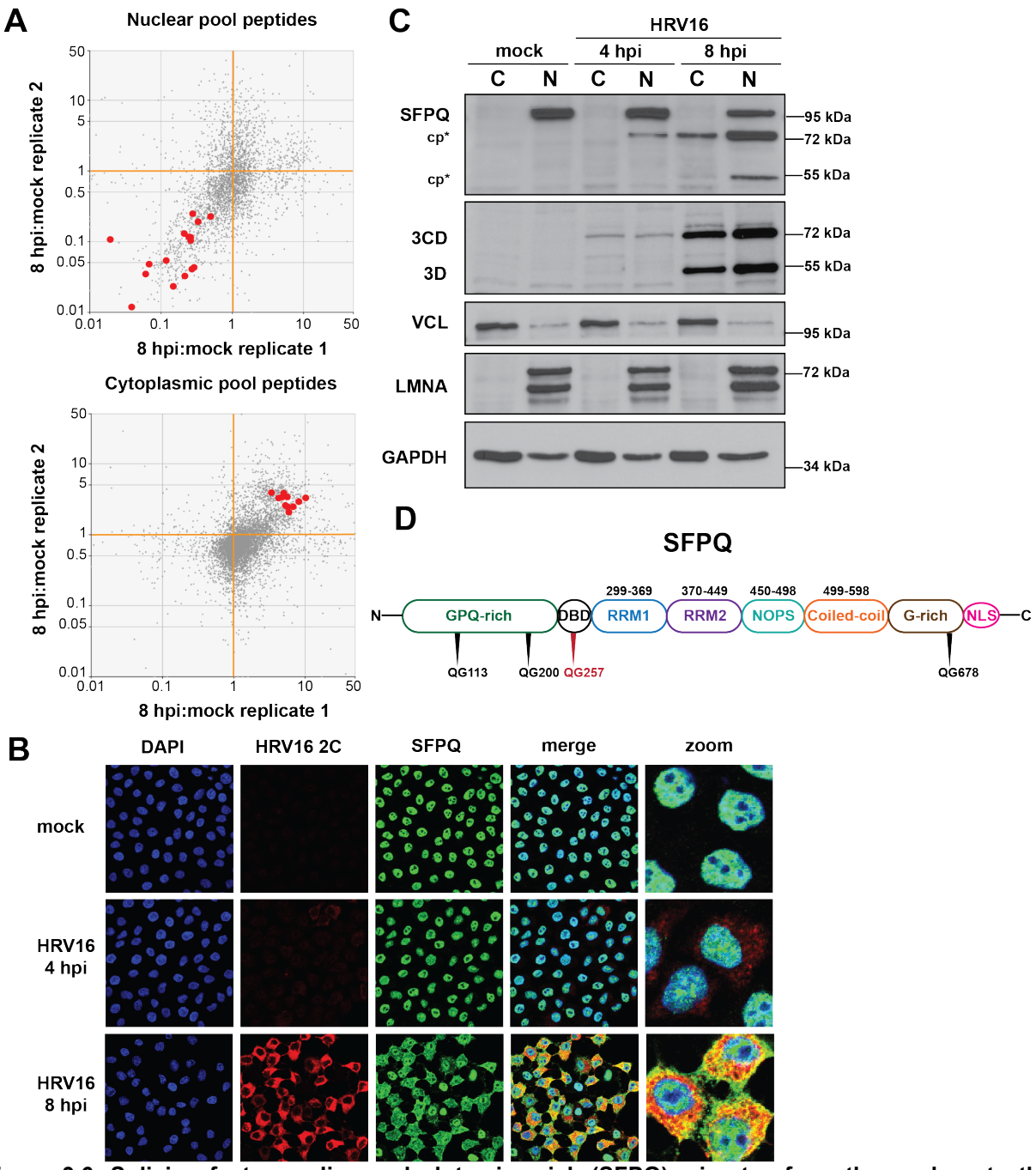

Figure 3.6. Splicing factor proline and glutamine rich (SFPQ) migrates from the nucleus to the cytoplasm following HRV16 infection. (**A**) Tryptic peptides in Figure 3.2 that correspond to SFPQ are highlighted red as described under Figure 3.4. (**B**) HeLa cells were mock- or HRV16-infected (MOI 10) and fixed then imaged as described in Figure 3.4. (**C**) Western blot analysis of cytoplasmic (C) and nuclear (N) fractions of mock- or HRV16-infected HeLa cells. A C-terminal cleavage product (cp*) was detected in the cytoplasm at 8 hpi. A second cleavage fragment of SFPQ was detected in the nucleus at 8 hpi (cp*). HRV16 3D/3CD,VCL, LMNA, and GAPDH used as in Figure 3.4. (**D**) Schematic of SFPQ domains [adapted from (Knott et al., 2016)] with putative 3CD/3C cleavage sites. The proposed 3CD/3C cleavage site resulting in the fragment observed 4 hpi is indicated in red. The N-terminal portion of SFPQ includes the glycine, proline, and glutamine-rich (GPQ-rich) and DNA-binding domain (DBD). The C-terminal portion contains two RNA-recognition motifs (RRM1 and RRM2), a NonA/paraspeckle (NOPS) domain, a coiled-coiled domain, glycine-rich (G-rich) region, and nuclear localization signal (NLS).

SFPQ is differentially cleaved during HRV16 or poliovirus infection and independently of caspase activity

To explore whether SFPQ is a target of the enterovirus 3CD proteinase, we first tested if infection with poliovirus resulted in a similar SFPQ cleavage pattern. Western blot analysis of lysates from HRV16- or poliovirus-infected HeLa cells revealed a consistent C-terminal cleavage product (apparent molecular mass of ~72 kDa) produced by both HRV16 and poliovirus 6 hours post-infection. Poliovirus infection did not, however, lead to detectable amounts of the smaller cleavage product (apparent molecular mass of ~55 kDa) observed at 10 hours post-infection with HRV16 (**Figure 3.7A and B**). This secondary cleavage product was detected after 8 hours of HRV16 infection in the nucleus of fractionated HeLa cells (**Figure 3.6C**). The 3CD/3C proteinases of HRV16 and poliovirus have distinguishable specificities, consistent with the distinct SFPQ cleavage patterns observed during infection [reviewed in (Chase and Semler, 2012)]. If a cellular protease were targeting SFPQ during enterovirus infection, the cleavage pattern for SFPQ would be expected to be independent of the infecting virus species.

Infection with enteroviruses, specifically poliovirus, has been shown to promote apoptosis, which can result in degradation of cellular proteins by executioner caspases (Belov et al., 2003; Croft et al., 2017; Goldstaub et al., 2000; Tolskaya et al., 1995). To determine if SFPQ cleavage was the result of apoptotic induction and subsequently the target of caspases, HeLa cells were infected with HRV16 in the presence or absence of the cell-permeable pan-caspase inhibitor benzyloxycarbonyl-Val-Ala-Asp-(OMe) fluoromethyl ketone (zVAD-FMK) and lysates generated 0, 4, and 8 hours post-

infection. In the absence of zVAD-FMK, apoptotic induction was observed by 4 hours post-infection, through the cleavage of activated caspase substrate poly(ADP-ribose) polymerase 1 (PARP1) (Lazebnik et al., 1994) (**Figure 3.7C**). PARP1 remained intact in zVAD-FMK treated cells, indicating apoptotic cascades were blocked in the presence of this inhibitor. Following zVAD-FMK treatment of HRV16-infected cells, the major SFPQ cleavage product (~75 kDa) was detected (**Figure 3.7C**), suggesting that SFPQ was not cleaved through the action of caspases. The overall proportion of cleaved relative to full-length SFPQ was reduced in the presence of zVAD-FMK, likely due to the fact that this caspase inhibitor can also suppress viral 2A proteinase activity (Deszcz et al., 2004). Inhibition of 2A proteinase activity could lead to decreased proteolytic processing of the viral polyprotein and reduced levels of mature viral proteins. Caspase-inhibited, HRV16-infected cells resulted in decreased levels of the 3CD proteinase and 3D polymerase, consistent with an inhibition of 2A proteinase activity, and as a result, slight reductions in levels of SFPQ cleavage (**Figure 3.7C**). Since SFPQ is cleaved in the presence of a pan-caspase inhibitor and displays a differential cleavage pattern during HRV16 and poliovirus infection, it is likely to be a target of the viral proteinase 3CD/3C during infection.

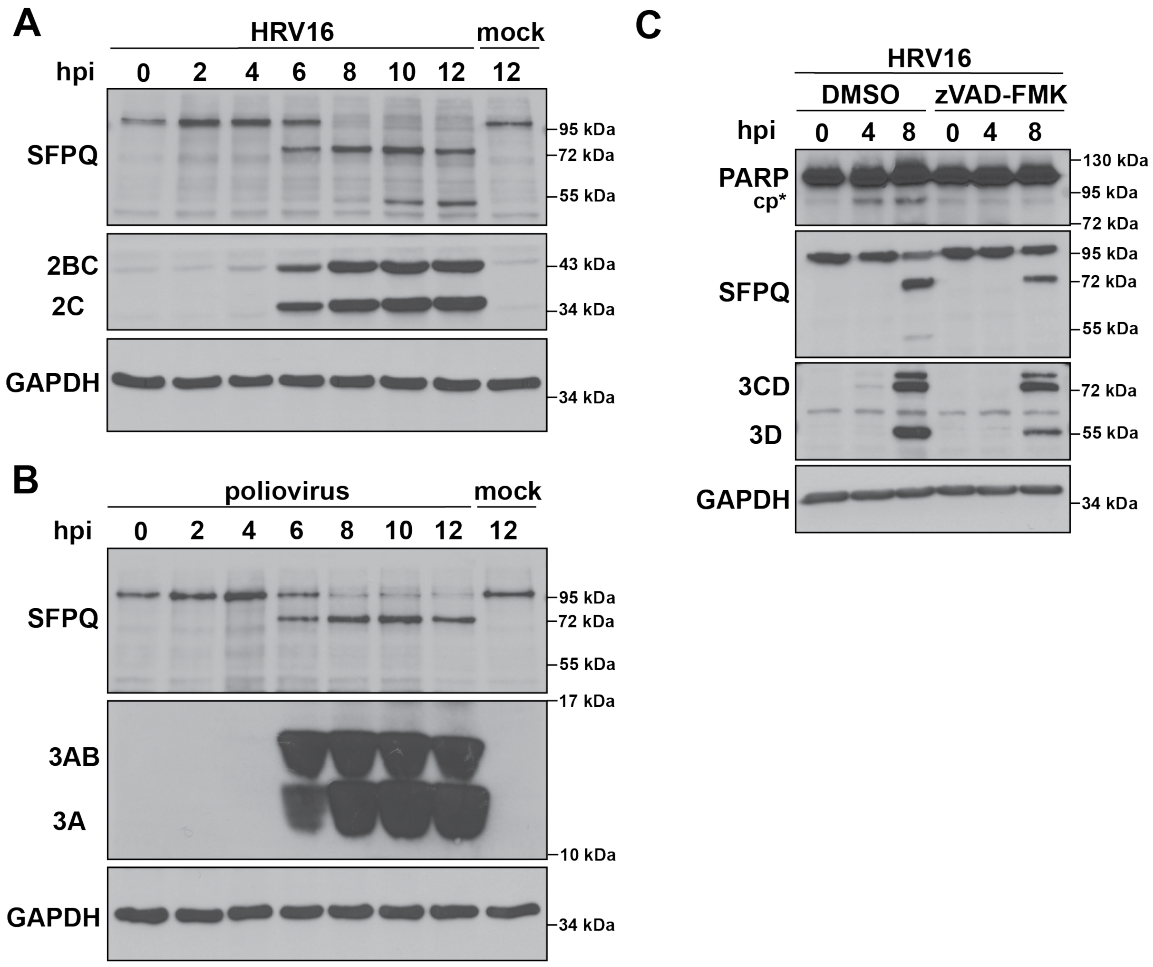

Figure 3.7. SFPQ is differentially cleaved during HRV16 or poliovirus infection of HeLa cells and cleavage is independent of caspase activity. (**A**) HeLa cells were mock- or HRV16-infected (MOI 10), cell lysates were generated at the indicated times, and lysates were subjected to Western blot analysis. HRV16 2C and its precursor 2BC were used as indicators of infection and GAPDH was used as a loading control. (**B**) HeLa cells were mock- or poliovirus-infected (MOI 10) followed by the generation of cell lysates at the indicated times, and which were then subjected to Western blot analysis. Poliovirus 3A and its precursor 3AB served as markers of infection and GAPDH was used as above. Poliovirus and HRV16 infections were both carried out at 34°C. (**C**) HeLa cells were infected with HRV16 in the presence or absence of 50 μM zVAD-FMK after which lysates were generated at the indicated times and subjected to Western blot analysis. SFPQ cleavage was observed with or without zVAD-FMK. HRV16 3D/3CD and GAPDH were used as above. Cleavage product of poly(ADP-ribose) polymerase 1 (PARP) is indicated (cp*). Data are representative of at least two independent experiments.

Knockdown of SFPQ correlates with reduced viral protein production, RNA accumulation, and HRV16 titers

To determine if SFPQ plays a functional role within the HRV16 infectious cycle, we next explored the effect of siRNA-mediated knockdown of SFPQ on HRV16

replication. Transfection of HeLa cells with an siRNA pool targeting SFPQ (siSFPQ) had no significant effect on cell viability compared to transfection of a non-targeting siRNA pool (siNT) (**Figure 3.8A**). Virus growth analyses were then performed on siRNA-transfected cells to measure the effect of SFPQ knockdown on HRV16 replication (**Figure 3.8B and C**). Significant reductions in viral titers were observed in SFPQ knockdown cells infected with HRV16 at low and high multiplicity of infection (MOI). In siSFPQ-treated cells, virus yield was suppressed ~20-fold between 8 and 30 hours post-infection at low MOI. Single-cycle growth analysis of high MOI infections resulted in similar reductions in virus yield: ~20-fold at 6 and 8 hours post-infection, and ~5-fold at 10 and 12 hours post-infection suggesting a delay in the HRV16 replication cycle. Western blot analysis of viral protein production revealed a dramatic reduction in the expression of viral protein 2C and its precursor 2BC in SFPQ knockdown cells (**Figure 3.8D and E**). The reduction in viral protein expression was consistent with the observed decrease in virus titer. Expression of 2BC/2C at 30 hours after low MOI infection of SFPQ knockdown cells was similar to levels of 2BC/2C protein observed early in infection (8-12 hours post-infection) of control cells, indicating that SFPQ knockdown resulted in a significant delay in viral protein production. Similarly, during high MOI infection of siSFPQ-treated cells, 2BC/2C production at the end of the infectious cycle (10-12 hours post-infection) was similar to that observed 6 hours post-infection in siNT-treated cells. Detection of SFPQ cleavage was observed to be concurrent with, or slightly after apparent viral protein production, consistent with our claim that SFPQ is targeted by a viral proteinase (12-24 hours post-infection at low MOI and 6-8 hours post-infection at high MOI). Additionally, the effect of SFPQ on viral RNA accumulation

was measured by reverse transcription polymerase chain reaction (RT-PCR) on HRV16-infected siSFPQ- and siNT-treated cells. Consistent with viral titers and protein production, HRV16 RNA accumulation was reduced and delayed in cells lacking SFPQ (**Figure 3.8F and G**). Collectively, these results point to a proviral role for SFPQ during the HRV16 replication cycle in HeLa cells.

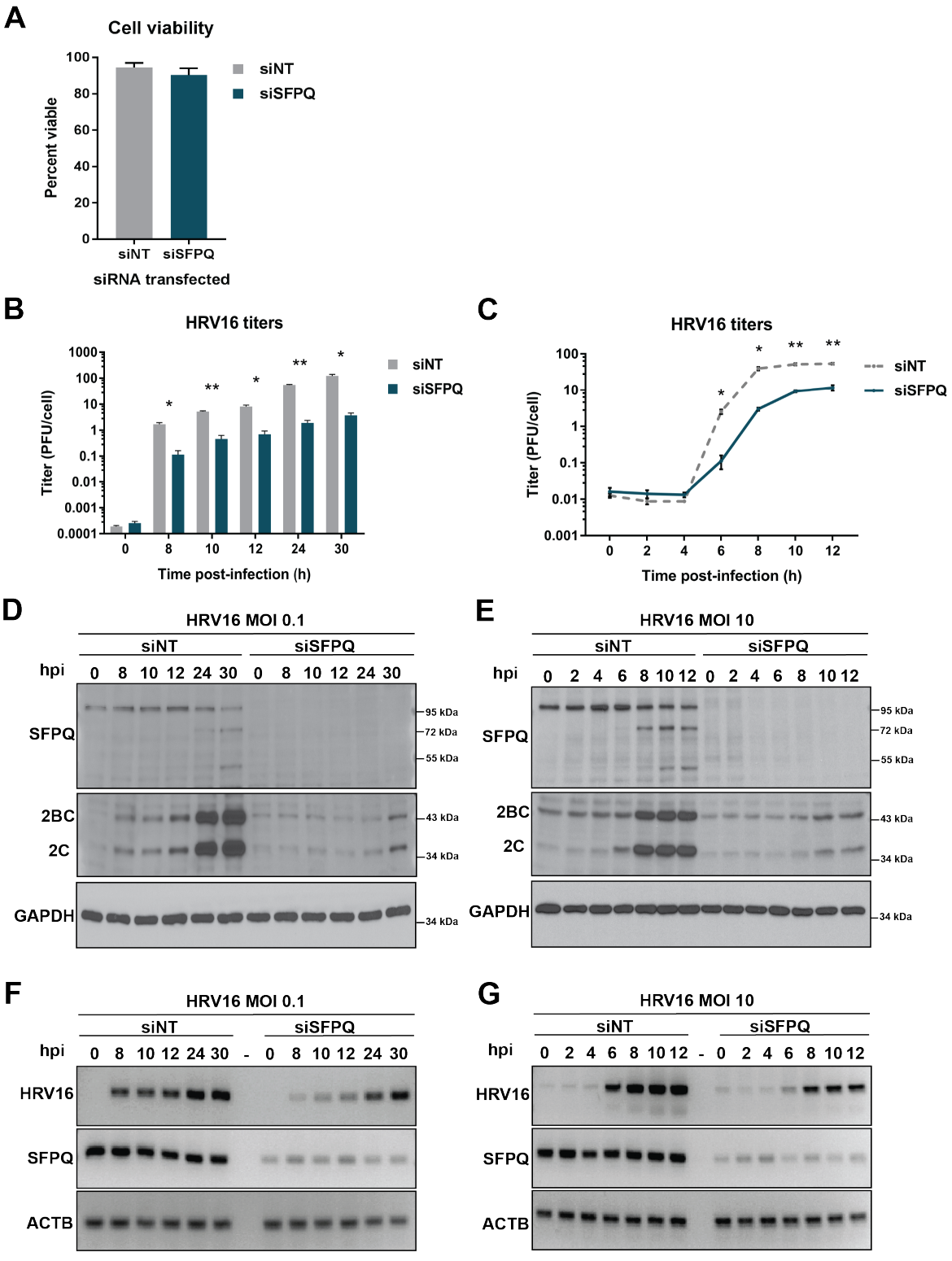

Figure 3.8. SFPQ knockdown correlates with reduced HRV16 replication. (**A**) Transfection of non-targeting siRNA (siNT) or SFPQ-targeting siRNA (siSFPQ) did not result in statistically significant differences in cell viability 96 h post-transfection, as assessed by trypan blue exclusion prior to infection ($P > 0.05$). Mean percent viable values are displayed with error bars representing one standard deviation. **(Continued on next page)**

Figure 3.8. (Continued) (**B**) HeLa cells transfected with siRNA for 96 h were infected with HRV16 (MOI 0.1) and cells and cell culture fluids were harvested at the indicated times. Virus titer was determined by plaque assay. Data represent the means of three biological replicate experiments with error bars indicating standard error of the means (SEM) (* $P < 0.005$, ** $P < 0.0005$). (**C**) Single cycle growth analysis of HRV16 from siRNA-treated and HRV16-infected HeLa cells (MOI 10). As in panel B, data represent the means of three biological replicate experiments with error bars displaying SEM (* $P < 0.005$, ** $P < 0.0005$). (**D**) siRNA-transfected and HRV16-infected HeLa cell lysates corresponding to the time-points in panel B (MOI 0.1) were generated and subjected to Western blot analysis. Knockdown of SFPQ was confirmed and levels of 2C and precursor (2BC) represented viral protein production. GAPDH was used as a loading control. (**E**) Western blot analysis of lysates from siRNA-transfected and HRV16-infected HeLa cells corresponding to time points in panel C (MOI 10). Western blots in panels D and E are representative results from three biological replicate experiments. (**F**) RNA isolated from siRNA-transfected and HRV16-infected HeLa cells at time-points corresponding to panel B (MOI 0.1) was subjected to RT-PCR. Primers for PCR were specific for HRV16 RNA, SFPQ mRNA, or actin (ACTB) mRNA. PCR products were separated by agarose gel electrophoresis. (**G**) RT-PCR analysis of RNA isolated from siRNA-transfected and HRV16-infected HeLa cells at time-points corresponding to panel C (MOI 10). Data in panels F and G are representative results from biological duplicate experiments.

SFPQ is unlikely to play a direct role in viral translation but associates with HRV16 RNA

During HRV16 infection, the positive sense RNA genome serves as a template for both translation and genome replication, resulting in the close coupling of the two processes. In an attempt to better understand the role that SFPQ could be playing during the infectious cycle, we compared the timing of SFPQ redistribution with that of the known IRES trans-acting factor (ITAF) PTBP1. As expected, PTBP1 was detected in cytoplasmic extracts of uninfected and infected cells (**Figure 3.9A**). This is consistent with its role in HRV16 IRES-dependent translation, an early step in the replication cycle. Aside from acting as an ITAF, PTBP1 is also involved in mediating the RNA template usage switch that occurs during enterovirus infection, after the accumulation of sufficient levels of viral protein. Because ribosomes and the RNA-directed RNA polymerase, 3D, travel in opposite directions along the viral mRNA, this template must be cleared of ribosomes prior to the initiation of RNA replication (Barton et al., 1999). Cleavage of PTBP1 (in combination with cleavage of another ITAF, PCBP2) by the viral 3CD/3C proteinase has been proposed to facilitate this clearing event. The cleaved form of

PTBP1, which may be deficient in ribosome recruitment activity, could preclude the binding of intact PTBP1, impeding continued translation (Back et al., 2002). We detected cleavage of PTBP1 by 8 hours post-infection, at a time when viral protein production is at a maximum based on 3CD/3D protein accumulation, which is consistent with a switch in template usage at later times during HRV16 infection. In direct contrast to PTBP1, only the cleaved form of SFPQ was detected in the cytoplasm by 6 hours post-infection, after the initiation of viral protein production. The fact that SFPQ is not present in the subcellular compartment where viral translation takes place until after protein production has initiated, combined with the fact that the highest levels of cleaved SFPQ are not present in the cytoplasm until 8 hours post-infection, suggests that SFPQ is not required for viral translation.

The presence of SFPQ in to the cytoplasm of HRV16-infected HeLa cells at 6 hours post-infection, a time at which RNA replication has initiated (**Figure 3.8G**), together with persistence of the cleavage fragment until at least 10 hours post-infection, is compatible with a role for SFPQ in HRV16 RNA replication. Moreover, the SFPQ C-terminal fragment arising from cleavage at the putative 3CD/3C target site (Q257) retains both RNA recognition motifs (RRMs) identified within the protein (**Figure 3.6D**), suggesting the C-terminal fragment of SFPQ may retain RNA-binding capabilities. Recently, the RNA sequence UAANGGCU(A/G) was proposed as an SFPQ consensus-binding sequence through a process that combined systematic evolution of ligands by exponential enrichment (SELEX) and cross-linking immunoprecipitation (CLIP) (Choi et al., 2017). We identified portions of this consensus-binding sequence within the 5'-NCR as well as the VP4, VP2, 2C, and 3C coding regions of the HRV16 genome (Lee and

Wang, 2003; Lee et al., 1995). To test whether SFPQ interacts with HRV16 RNA, we compared interactions of SFPQ from mock- and HRV16-infected HeLa cells to biotinylated, full-length RNA corresponding to the HRV16 genome and a negative control RNA *in vitro*. We consistently observed an association between the cleaved form of SFPQ that is present in lysates 8 hours post-infection, with HRV16 RNA (**Figure 3.9B and C**). Biotinylated HRV16 RNA was also bound by AU-rich element RNA binding protein 1 (AUF1, also known as hnRNP D) from infected cells, a previously identified HRV16 5'-NCR-binding protein (Rozovics et al., 2012). Together, these results suggest that the C-terminal cleavage product of SFPQ interacts, directly or through another protein partner, with HRV16 RNA during the later stages of infection.

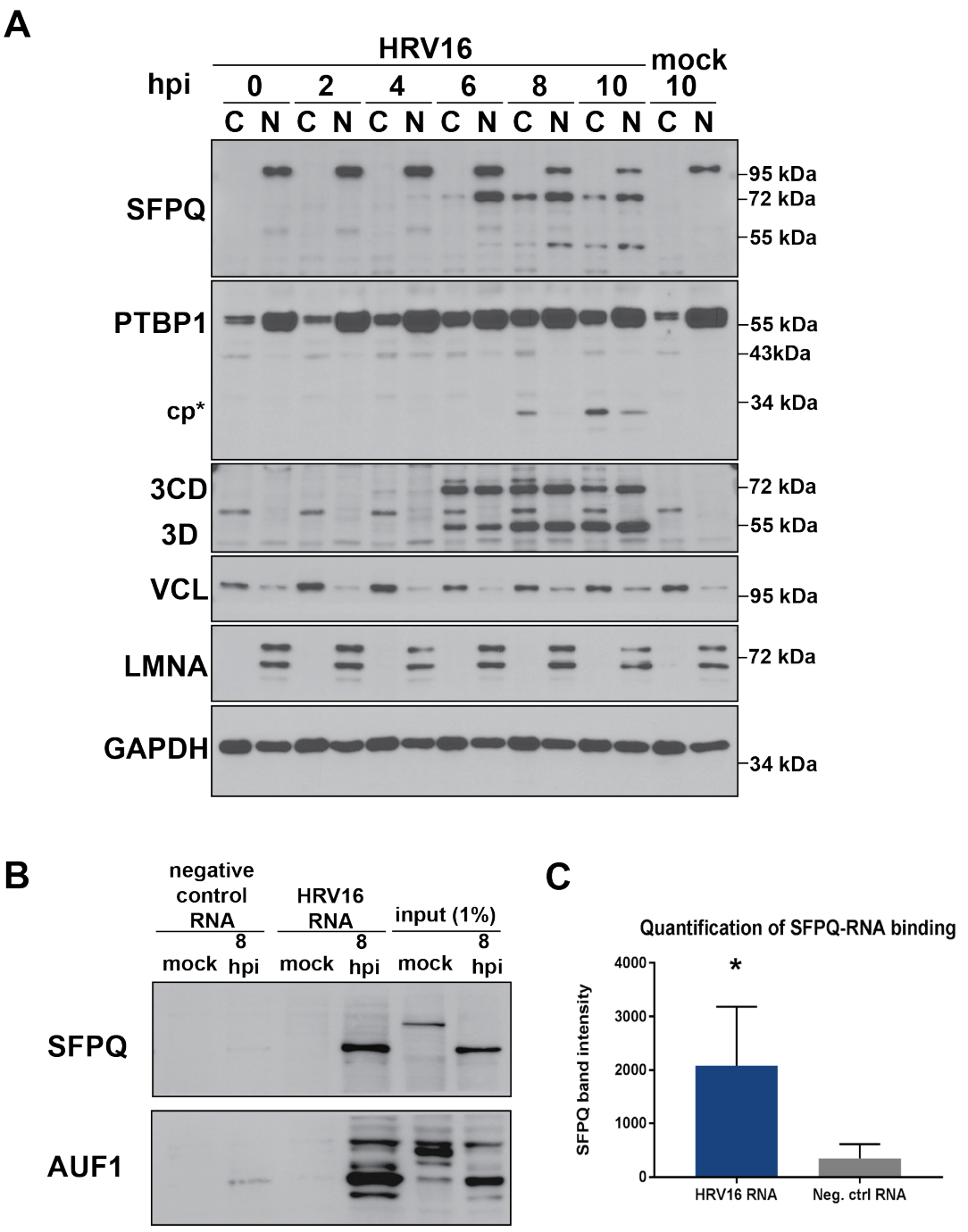

Figure 3.9. An SFPQ cleavage product associates with *in vitro* transcribed HRV16 RNA. (**A**) HeLa cells were mock- or HRV16 infected, fractionated at 2 h intervals, and the subcellular distribution of proteins was analyzed by Western blot. The cleavage product (cp*) of polypyrimidine tract binding protein 1 (PTBP1) is indicated and HRV16 3D and its precursor 3CD served as markers of infection. VCL and LMNA served as markers for the cytoplasm (C), nucleus (N); GAPDH was used as a general loading control. (**B**) Biotinylated, *in vitro* transcribed control or HRV16 RNA were assayed for binding to cellular proteins present in HeLa cell lysates following mock infection or 8 hours post-infection (hpi) with HRV16 by Western blot analysis. A representative experiment is shown. (**C**) Quantification of four separate RNA affinity experiments was carried out using Quantity One software. Means are shown and error bars represent standard deviations (* $P < 0.05$).

Discussion

In this study we have outlined an approach for the identification of proteins that become enriched at the site of HRV16 replication. Through quantitative protein mass spectrometry we have demonstrated a coordinated redistribution of proteins, many of which normally function in RNA-related processes such as splicing, from the nucleus to the cytoplasm by 8 hours post-HRV16 infection of HeLa cells (**Figure 3.2, Figure 3.3,** and **Table 3.1**). It should be noted that although the majority of the proteins listed in Table 3.1 have a significant presence in the nucleus of uninfected cells, some are predominantly cytoplasmic (e.g., cytoskeletal-associated coronin proteins). Whether this points to previously unidentified functions these proteins carry out in the nucleus or possible IRES regions with their mRNAs allowing for their translation to continue during infection, remains to be seen.

Although a number of proteins appeared to re-equilibrate to the cytoplasm following infection with HRV16 in HeLa cells, there does appear to be some specificity in this process, insofar as SRSF2, for example, remains within the nucleus throughout the course of infection (**Figure 3.5**). We identified the multifunctional nuclear resident protein SFPQ as a probable target of the HRV16 3CD/3C proteinase in the nucleus of infected cells and showed that the C-terminal cleavage product moves into the cytoplasm of HRV16-infeced cells (**Figure 3.6 and 3.7**). Interestingly, SFPQ has been shown to be a transcriptional repressor of the cytokine interleukin-8, and virus infection can localize SFPQ to paraspeckles via interactions with a long noncoding RNA, allowing for transcriptional activation of interleukin-8 (Imamura et al., 2014). In agreement with this, the distribution of SFPQ within the nucleus 4 hours post-HRV16 infection was

observed to change from diffuse to points of concentration (puncta), suggesting that SFPQ is mislocalized within the nucleus, possibly to promote an innate immune response, before it is targeted by 3DC/3C (**Figure 3.6B**). However, SFPQ has also been shown to concentrate in nuclear foci upon treatment with actinomycin D, suggesting that the HRV16-induced transcriptional repression could also account for nuclear puncta formation 4 hours post infection (Dye and Patton, 2001).

siRNA-mediated knockdown of SFPQ resulted in decreased viral titers, viral protein production, and viral RNA accumulation independent of MOI, suggesting that SFPQ acts as a proviral factor (**Figure 3.8**). Mechanistically, SFPQ appears to exert its proviral function subsequent to viral translation, as it does not relocate from the nucleus until around the time PTBP1 is cleaved and viral RNA synthesis has commenced, about 6-8 hours post-infection (**Figure 3.8E**). Notably, although only a small proportion of total PTBP1 appears to be cleaved 6-8 hours-post infection, it is likely that the majority of PTBP1 is not associated with viral replication in infected cells and only PTBP1 found in HRV16 replication complexes would be targeted for cleavage, allowing for local concentration effects to drive functionality (**Figure 3.9A**). Finally, we demonstrated that the C-terminal cleavage product of SFPQ associates with *in vitro* transcribed HRV16 RNA, directly or through associated factors, suggesting a direct role for SFPQ in HRV16 replication (**Figure 3.9B and C**). Interestingly, we did not observe full-length SFPQ from mock-infected HeLa cells associating with HRV16 RNA. This suggests that factors that bind SFPQ in uninfected cells preclude interactions between intact SFPQ and HRV16 RNA and/or a viral factor functions in promoting the association of cleaved SFPQ and HRV16 RNA during infection. Through alterations to normal protein distribution patterns

HRV16 is able to increase the functional repertoire of proteins available at the site of replication and to promote viral amplification, including through manipulation of SFPQ (**Figure 3.10**).

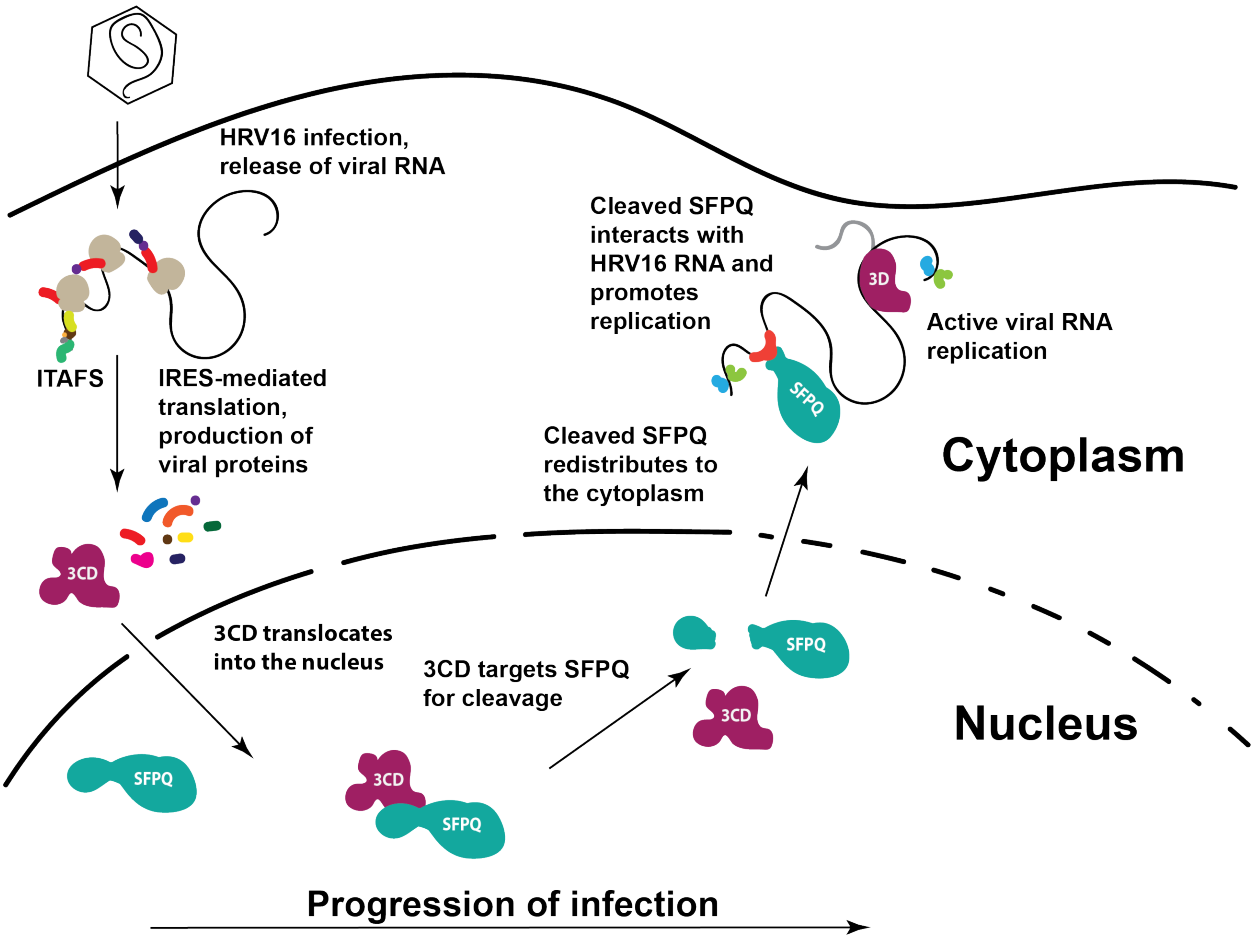

Figure 3.10. Proposed model of HRV16-SFPQ interactions during the infectious cycle. Following translation of viral proteins, HRV16 3CD/3C enters the nucleus where it targets SFPQ for cleavage at Q257 within the N-terminus. Cleavage releases SFPQ from interactions with nuclear resident anchors such as DNA and allows the C-terminal fragment to migrate to the cytoplasm through degraded nuclear pore complexes. Once in the cytoplasm, the SFPQ fragment interacts with HRV16 RNA, directly or through other protein partners, to promotes replication.

Aside from the strong evidence for redistribution of SFPQ during HRV16 infection (**Figure 3.6** and **Table 3.1**), SFPQ is a compelling candidate for involvement in HRV16 replication due to its association with PTBP1 in uninfected cells. It is possible, for example, that once it has migrated to the cytoplasm of HRV16-infected HeLa cells, the

C-terminal fragment of SFPQ sequesters PTBP1 and precludes direct interactions between PTBP1 and HRV16 RNA. In this way, SFPQ could provide another level of regulation to the viral RNA template usage switch from translation to RNA replication that occurs at later times during the infectious cycle. SFPQ itself has also been reported to be an ITAF of cellular mRNAs. SFPQ can bind and promote IRES-mediated translation of the MYC proto-oncogene, tumor suppressor protein p53, and lymphoid enhancer binding factor 1 (LEF1) (Cobbold et al., 2008; Sharathchandra et al., 2012; Tsai et al., 2011). Relocalization of SFPQ to the cytoplasm to carry out this function was also specifically demonstrated for the translation of proteins that are expressed during apoptosis (King et al., 2014). We show here that the redistribution of SFPQ as a result of HRV16 infection does not occur until after peak times of viral protein production during the infections cycle (**Figure 3.9A**). The fact that knocking down SFPQ affects both HRV16 translation and replication is consistent with the close coupling of these processes: with fewer RNA templates available, less viral protein can be produced. Because siRNA-mediated knockdown of SFPQ suggests a proviral role for SFPQ during infection (**Figure 3.8**), SFPQ may aid in viral RNA replication (directly or through recruitment of other proteins), in maintaining the stability of viral RNA, and/or in viral RNA packaging or virion morphogenesis (all of which occur in the later stages of the infectious cycle). As a first step toward describing the role of SFPQ during HRV16 infection, we demonstrated that a C-terminal cleavage product of this protein produced during infection associates specifically with *in vitro* transcribed, biotinylated HRV16 RNA (**Figure 3.9B and C**). This C-terminal fragment of SFPQ is generated in the nucleus of infected cells, where SFPQ is likely a target of the viral 3CD/3C proteinase, and then

relocalizes to the cytoplasm (**Figure 3.6**). SFPQ cleavage may also preclude it from performing its wide-ranging roles in the nucleus, redirecting the cell to processes favoring viral replication. For example, all arginine-glycine-glycine (RGG) box motifs present within SFPQ (discussed further below) and the putative DNA-binding domain within the GPQ-rich region are found in the N-terminal portion of the protein, upstream of the putative 3CD/3C cleavage site at Q257. Cleavage of SFPQ may therefore result in a loss of DNA-binding activity, and the ability of SFPQ to function in transcription and DNA repair may be inhibited. Furthermore, the disruption of DNA association may promote the relocalization of cleaved SFPQ into the cytoplasm upon HRV16 infection, as DNA remains within the nucleus throughout the infectious cycle.

Rhinoviruses are known to cause inhibition of the import pathway that utilizes the classical NLS so it's possible that both disruptions in associations with DNA, as well as retention of newly synthesized SFPQ in the cytoplasm combine to increase the abundance of SFPQ in the cytoplasm of HRV16-infected HeLa cells (Gustin and Sarnow, 2002). Importantly, the C-terminal fragment of SFPQ that is present in the cytoplasm of HRV16-infected HeLa cells retains the protein's two RRMs, presumably allowing SFPQ to bind HRV16 RNA. Aside from the recently identified consensus-binding sequence of SFPQ (UAANGGCU(A/G)), SFPQ has been reported to bind GU-rich sequences, GA-rich sequences, structured RNAs, and pyrimidine-rich RNAs, suggesting that SFPQ is somewhat promiscuous in its interactions with RNA, and the SFPQ binding site within HRV16 RNA remains to be determined (Cho et al., 2014; Greco-Stewart et al., 2006; Melton et al., 2007; Patton et al., 1993; Peng et al., 2002; Ray et al., 2011).

SFPQ has been shown to be involved in the replication cycles of viruses outside of the *Picornaviridae* family. It mediates the post-transcriptional regulation of HIV-1, both inhibiting the production of HIV-1 transcripts through binding *cis*-acting instability elements within gag mRNA and enhancing the production of viral transcripts by binding HIV-1 pre-mRNA (Kula et al., 2013; Zolotukhin et al., 2003). SFPQ is also involved in the transcription of influenza A virus RNAs and promotes virus replication (Landeras-Bueno et al., 2011). SFPQ also binds the terminal stem-loop regions of hepatitis delta virus RNA of both polarities (Greco-Stewart et al., 2006).

Recent work has pointed to the involvement of SFPQ in the replication cycles of enteroviruses. SFPQ has been suggested to bind poliovirus RNA along with another DBHS protein, non-POU domain containing octamer binding protein (NONO) (Lenarcic et al., 2013). No validation or functional characterization of SFPQ was performed in these studies, but the authors demonstrated that NONO-knockdown led to reduced virus yields and that NONO is likely involved in poliovirus RNA replication but not IRES-mediated translation. Coxsackievirus B3 (CVB3), another enterovirus, has recently been shown to utilize SFPQ to promote replication, although the mechanism proposed for its proviral role is distinct from what we report here for HRV16 (Dave et al., 2017). SFPQ was shown to bind the 5'-NCR of CVB3 RNA and enhance IRES-mediated translation. The authors suggested that SFPQ relocalizes to the cytoplasm during CVB3 infection through an indirect mechanism involving the phosphorylation of Tyrosine 293 (Y293) and dephosphorylation of Threonine 687 (T687). Other studies have linked phosphorylation of Y293 to mislocalization of SFPQ in the cytoplasm of cancer cells that express a chimeric kinase, but whether phosphorylation at this residue affects SFPQ

distribution during HRV16 infection is an open question (Galietta et al., 2007; Lukong et al., 2009). During CVB3 infection, SFPQ expression was also demonstrated to be upregulated, likely via an IRES present within the SFPQ mRNA (Dave et al., 2017). However, no cleavage of SFPQ was observed during CVB3 infection, suggesting that although HRV16 and CVB3 both utilize SFPQ for replication, the mechanisms by which it is hijacked are distinct. Interestingly, a Mycobacterium tuberculosis protein has been shown to cleave SFPQ following infection, suggesting that SFPQ is targeted by a range of pathogens, either to exploit its extensive functional capabilities or to alter host-cell homeostasis to favor pathogen replication (Danelishvili et al., 2010). Additionally, SFPQ has been shown to remain intact during apoptosis, which, in combination with the results presented here, lends further evidence for HRV16 3CD/3C targeting SFPQ specifically (Shav-Tal et al., 2001).

SFPQ was first identified as a pre-mRNA splicing factor that interacts with PTBP1 and is required for spliceosome formation. Accordingly, it was given the alias PTB-associated splicing factor (PSF) (Patton et al., 1993). SFPQ is a member of the Drosophila behavior human splicing (DBHS) family, which also includes NONO and paraspeckle component 1 (PSPC1). The DBHS proteins are highly multifunctional nuclear factors that are defined through a conserved domain arrangement that comprises tandem RNA-recognition motifs (RRM1 and RRM2), a nonA/paraspeckle (NOPS) domain, and a coiled-coiled domain (**Figure 3.6D**). The RRM2, NOPS, and coiled-coil domains are required for the formation of homodimers, heterodimers, and extended polymers of the DBHS members, allowing for interactions that result in a molecular scaffolding that can mediate diverse cellular functions in pre-mRNA splicing,

translation, and DNA repair, among others. The ability of these proteins to perform such a variety of functions is likely a result of regulation by post-translational modifications and co-associated factors. [reviewed in (Knott et al., 2016; Yarosh et al., 2015)]. Significantly, our cytoplasmic enrichment screen identified all three members of the DBHS protein family (SFPQ, NONO, and PSPC1).

SFPQ contains five RGG box domains, with two RGG regions separated by 4 residues, a motif known as a di-RGG box, which have been shown to be involved in DNA interactions and DNA repair (Ha et al., 2011; Morozumi et al., 2009; Salton et al., 2010; Thandapani et al., 2013; Yarosh et al., 2015). A classical nuclear localization signal (NLS) is present in seven C-terminal residues of SFPQ, but a second, more complex, overlapping bipartite NLS has been proposed between amino acids 547-574. Interestingly, RRM2 also appears to be required for the nuclear distribution of SFPQ (Dye and Patton, 2001). SFPQ is considered an essential protein, though we have shown here that significant knockdown of SFPQ with a pool of commercially available siRNAs can result in viable HeLa cells up to 96 hours after treatment. It is possible that adequate levels of SFPQ remain in knocked-down cells to allow for essential functions to proceed or that other DBHS proteins compensate for the loss of SFPQ in these cells (Li et al., 2014).

In addition to the well-characterized alterations in nucleocytoplasmic trafficking that occur during enterovirus infections, the subcellular location of viral protein 3CD has significant implications for the productivity of an infection. Cellular transcription driven by the three DNA-directed RNA polymerases (I, II, and III) in mammalian cells is inhibited during infection with enteroviruses. The viral proteinase 3CD/3C inhibits RNA

polymerase I-dependent transcription through cleavage of a factor associated with TATA-box binding protein (TBP), RNA polymerase II-dependent transcription through direct alterations of TBP, and RNA polymerase III-dependent transcription by degradation of general transcription factor IIIC subunit 1 (GTF3C1) (Banerjee et al., 2005; Clark et al., 1991; Rubinstein et al., 1992; Shen et al., 1996; Yalamanchili et al., 1996). The proteinase activity of 3CD/3C also causes cleavage of transcription factors CAMP responsive element binding protein 1 (CREB1), POU class 2 homeobox 1 (POU2F1, also known as Oct-1), and cleavage stimulation factor subunit 2 (CSTF2, also known as CstF-64), with consequences to host cell mRNA production and polyadenylation (Weng et al., 2009; Yalamanchili et al., 1997b; Yalamanchili et al., 1997c). Furthermore 3D of poliovirus has been shown to associate with pre-mRNA processing factor 8 (PRPF8), interfering with splicing and further impacting cellular gene expression (Liu et al., 2014). For 3CD and mature 3C and 3D to perform these functions, they must enter the nucleus of infected cells (Amineva et al., 2004). The data presented here strongly suggest that HRV16 3CD also targets the cellular protein SFPQ for proteolysis in the nucleus.

More than 40 years ago it was shown that poliovirus replication was compromised in enucleated cells and many subsequent studies have reinforced the idea that enteroviruses are dependent upon the functions of nuclear proteins for replication (Pollack and Goldman, 1973). Upon infection with HRV16, heterogeneous nuclear ribonucleoprotein C (hnRNP C); KH RNA binding domain containing, signal transduction associated 1 (Sam68); hnRNP A1; serine and arginine rich splicing factor 3 (SRSF3/SRp20); and AUF1 have previously been shown to relocalize to the cytoplasm

of infected cells. Other proteins that have been shown to relocalize during infection with other enteroviruses may also do so during HRV16 infection (Fitzgerald et al., 2013; Spurrell et al., 2005; Walker et al., 2015; Walker et al., 2013). Not all of these proteins necessarily relocalize to the extent observed for SFPQ, as some shuttle between the nucleus and cytoplasm to carry out their normal cellular functions and may explain why we did not identify these proteins in our cytoplasmic enrichment screen. The multifunctional, DBHS family member SFPQ can now also be added to the growing list of proteins that are involved in enterovirus replication, providing additional evidence for the role of nuclear proteins in the replication cycle of a family of RNA viruses that has been historically considered prototypically cytoplasmic.

Materials and Methods

Cell culture and virus stocks

HeLa cells were grown as monolayers in Dulbecco's Modified Eagles Medium (DMEM) supplemented with amphotericin, penicillin, streptomycin, and 8% newborn calf serum (NCS) (complete medium). Cells were maintained in 5% CO2 at 37°C. Virus was generated in HeLa cells transfected with *in vitro* transcribed RNA produced from infectious cDNA clones. Plasmids pRV16.11 (a gift from Dr. Wai-Ming Lee) and pT7PV1 were used to generate HRV16 and Mahoney strain poliovirus, respectively (Haller and Semler, 1992; Lee and Wang, 2003). High titer stocks of virus were generated by serially propagating virus through HeLa cell monolayers (HRV16) or HeLa cells in suspension (poliovirus).

Virus infections

Stock HRV16 was adsorbed on HeLa cells at the indicated multiplicity of infection (MOI) for 1 h in serum-free DMEM (inoculum) at room temperature. Following adsorption, cells were washed with phosphate buffered saline (PBS). Monolayers were then overlaid with complete medium containing 10 mM MgCl2 and 20 mM HEPES (pH 7.4) (overlay). Immediately following the addition of overlay was regarded as 0 h post-infection. Infected cells were then incubated at 34°C, 5% CO2. Poliovirus infections were performed in the same manner except that adsorption was carried out for 30 minutes. Mock infections were performed simultaneously using serum-free DMEM as inoculum. For caspase inhibition experiments, the HRV16 inoculum and overlay contained 50 μM benzyloxycarbonyl-Val-Ala-Asp-(OMe) fluoromethyl ketone (zVAD-FMK, UBPBio) in DMSO or DMSO alone. At the indicated time-points, cells were washed with PBS and then collected for protein or RNA analysis, or cells and cell culture supernatants were collected for titration by plaque assay.

For plaque assays, cells and culture media were freeze-thawed five times prior to serial dilution in serum-free DMEM and infections were carried out as described above, except that overlay contained 0.45% agarose (Lonza). 72 h following infection a second volume of overlay containing 0.45% agarose was added to cells followed by a further 24 h incubation at 34°C. 96 h after infection, cells were fixed with 10% trichloroacetic acid and then stained with 0.1% crystal violet. Plaques were counted and calculated titers were normalized to the cell count of transfected cells prior to infection (see below). Data are presented as plaque forming units per cell.

Subcellular fractionation

Cellular fractions of uninfected or infected HeLa cells for mass spectrometry analysis were generated as previously described (Penman, 1966). Briefly, cell monolayers were washed, scraped, pelleted by centrifugation, and then incubated on ice in reticulocyte standard buffer (RSB; 10 mM NaCl, 10 mM Tris-HCl [pH 7.4], 1.5 mM MgCl2) for 5 minutes. Cells were then ruptured by Dounce homogenization. The resulting cell homogenate was subjected to centrifugation (1600 rcf), and the supernatant collected as the cytoplasmic fraction. The pellet was washed with RSB, centrifugation was repeated as above, and this supernatant combined with the cytoplasmic fraction. The remaining pellet (nuclear material) was washed with RSB containing mixed detergent solution (0.4% sodium deoxycholate, 0.9% NP-40) and subjected to centrifugation (1600 rcf). The supernatant was removed and the pelleted nuclei were resuspended in high salt buffer (HSB; 0.5 M NaCl, 50 mM MgCl2, 10 mM Tris-HCl [pH7.4]) containing DNase I, resulting in the nuclear fraction (crude lysate). In parallel, nucleocytoplasmic fractionation was carried out using NE-PER™ Nuclear and Cytoplasmic Extraction Reagents (ThermoFisher Scientific) to analyze subcellular distribution of proteins by Western blot.

Mass spectrometry analysis (Performed by Dr. Paul D. Gershon, University of California, Irvine)

Tryptic peptides

From each of three cultures (mock-infected, 4 h-infected, 8 h-infected) a total of 9.2×10^7 HeLa R19 cells were harvested. This number was corrected 7.5×10^7 cells/culture (allowing for ~20% loss during infection and harvesting). From harvested cell pellets, cytoplasmic extracts were made in RSB and nuclear extracts were made in

HSB as described above. The resulting six fractions from the three cultures provided material for two quantitative mass spectrometry experiments: One employing the three cytoplasmic extracts, the other the three nuclear extracts. Proteins were precipitated from the above extracts directly by adding 5 volumes of acetone followed by incubation at -20^{o}C for 60 min then centrifugation at 13,000 rpm at 4^{o}C for 60 min. Acetone pellets were re-dissolved in equivalent volumes of 8 M Urea, 0.1 M triethylammonium bicarbonate (TEAB), 10 mM tris(2-carboxyethyl)phosphine (TCEP). Following bicinchonic acid (BCA) protein assay, an aliquot corresponding to approximately 0.33 mg protein was taken from each of the six samples followed by addition of iodoacetamide to a final concentration of 20–50 mM and 30 min incubation at room temperature in the dark. Dilution to 6 M Urea with 0.1 M TEAB was then followed by addition of LysC (1:100 trypsin:substrate mass ratio) and incubation at 37°C overnight. After dilution with 0.1 M TEAB to 1 M urea, samples were treated with trypsin (1:50 trypsin:substrate mass ratio) overnight then stimulated for 3 h with an equivalent aliquot of trypsin. After mass spectrometric assay for the extent of trypsinization in a small aliquot from each sample, reactions were re-stimulated if necessary with fresh trypsin until fewer than 11% of the identified peptides had missed cleavages. Tryptic digestion products were purified using Sep-Pak C18 (Waters Inc.), eluting with 80% CH_3CN/0.1% formic acid (FA), and then evaporating to dryness under vacuum. After re-dissolving in 0.1 M TEAB, peptides were labeled with light, intermediate and heavy dimethyl isotopes (Boersema et al., 2009) for the 4h, 8h and mock cultures, respectively (cytoplasmic) or mock, 4h and 8h cultures, respectively (nuclear), followed by quenching with ammonium hydroxide then neutralizing with FA. The three differentially-labeled samples were then

combined and the mixture subjected to C18 solid-phase extraction using Sep-Pak C18 as above. Tryptics were re-dissolved in strong cation exchange (SCX) solvent A (30% CH_3CN, 0.05% H3PO4, KOH to pH 2.7) for loading on a Polysulfoethyl A (200 x 4.6 mm, 5-um particle size, 200 Å pore size) column (PolyLC Inc.) that had been thoroughly pre-equilibrated with solvent A using a Waters 600E multisolvent delivery system and monitoring with Clarity chromatography software (DataApex Inc.). After washing with SCX solvent A until the OD280 approached zero, the column was eluted with a linear gradient of 6 – 24% SCX solvent B (solvent A plus 500 mM KCl) over 144 min, collecting 2 mL fractions. The volume of each fraction was reduced under vacuum to 0.1 – 0.2 mL prior to 5-stack C18 stage-tipping (Ishihama et al., 2006). Each stage-tip elution was dried then re-dissolved in 0.1% FA in water for injection, via an Easy-nLC 1000 (ThermoFisher, Inc.), to a 250 x 0.075 mm (ID) nanospray tip packed with ReproSil-Pur C18-AQ (1.9 µm diameter; Dr. Maisch GmbH) pre-equilibrated with 0.1% FA in water.

NanoLC-MS/MS

Spectra were acquired using an LTQ Orbitrap Velos Pro (ThermoFisher, Inc.) while running a bipartite linear gradient of 5 – 23 % C18 solvent B (CN3CN in 0.1% FA/water) over 205 min followed by 23 – 35% C18 solvent B over 30 min at a flow rate of 250 nL/min. In each precursor spectrum (profile, resolution = 60000) the 20 most intense ions above a threshold of 1000 counts with charge of +2 or greater were subjected to CID activation in the ion trap followed by the generation of a rapid trap-scan centroid fragmentation spectrum. Ions otherwise eligible for fragmentation a second time within a period of 40 sec were added to a 500 member (maximum)

exclusion list for a period of 30 sec unless expiring from the list earlier on the basis of either priority or an increase in signal:noise (S:N) by a factor of 2.0.The above experiment was repeated (in biological replicate), using light, intermediate and heavy dimethyl isotopes for 8 h, mock and 4 h cultures, respectively (both cytoplasmic and nuclear fractions). Data: Target/decoy searches of raw data files were against SwissProt (taxonomy: Human, Rhinovirus Type 16) plus a database of common contaminants with trypsin specificity, allowing 1 missed cleavage, charge state of +2 to +4, Carbamidomethyl (C) as fixed modification and Oxidation(M), deamidated (NQ) as variable modifications, with precursor and product mass tolerances of ±20.00 ppm and ±0.50 Da, respectively. Search results from all fractions of a single SCX gradient (above) were combined, then thresholded to < 5% false discovery rate (FDR), and the identified peptide ions in precursor spectra were quantitated using Mascot Distiller 2.5 with 'Dimethylation [MD]' quantitation method allowing N-terminal and lysine labeling with light, medium and heavy reagent. Using in-house software, quant data exports from Mascot Distiller were filtered for good quantitation statistics (> 80% correlation between experimental peak and triple channel peak model, < 40% of total intensity within the triple channel window of a time-integrated ion peak that did not fit the model, < 0.4 in std. error for plots of modeled single channel intensity vs. partner channel intensity for all precursor spectra covering an extracted ion peak). From the filtered data, scatter plots were generated of 8hpi:mock isotope intensity ratios for all tryptics common to the duplicate nuclear datasets. Tryptics for which both 8hpi:mock relative quant ratios were < 0.9 (<~50th percentile in the ascending distributions of all ratios) were recorded. After generating a scatter plot from the replicate cytoplasmic data, as above, tryptics were

highlighted in the latter plot corresponding to the recorded nuclear tryptics and/or all tryptics from their corresponding accessions.

Western blot analysis

HeLa whole cell lysates were generated using radioimmunoprecipitation assay (RIPA) buffer (150 mM NaCl, 1% NP-40, 0.5% sodium deoxycholate, 0.1% sodium dodecyl sulfate, 50 mM Tris-HCl [pH 8.0], Pierce™ Protease Inhibitor Tablet EDTA-free [ThermoFisher Scientific]) after harvesting and pelleting in PBS (4°C, 1200 rcf, 5 minutes). Protein concentration in lysates was determined using the RC DC™ protein assay (Bio-Rad Laboratories) and equivalent amounts of protein were boiled for 3 minutes in 1x Laemmli sample buffer (LSB) and resolved by 12.5% sodium dodecyl sulfate polyacrylamide gel electrophoresis (SDS-PAGE). Proteins were transferred to an Immobilon-P membrane (Millipore), cut for analysis with multiple primary antibodies simultaneously, and blocked with 5% non-fat milk in phosphate buffered saline containing 0.1% Tween-20 (PBST). Membranes were then incubated for 1 h with primary antibody diluted in PBST containing 5% bovine serum albumin (BSA), washed with PBST, then incubated for 1 h with 1:7500 dilution of goat anti-rabbit or goat anti-mouse horseradish peroxidase (HRP)-conjugated IgG-heavy and light chain secondary antibody (Bethyl Laboratories) diluted in PBST. Membranes were washed with PBST then exposed to Pierce™ ECL Western Blotting Substrate (ThermoFisher Scientific) and exposed to Blue Autoradiography Film (USA Scientific) and developed. When necessary, membranes were stripped with harsh stripping buffer (2% SDS, 62.5 mM Tris-HCl [pH 6.8], 0.8% 2-mercaptoethanol), washed extensively with water and PBST, then subjected to the same Western blotting procedure described above.

The primary antibodies and corresponding dilutions used were as follows: 1:10,000 vinculin (Abcam ab129002), 1:10,000 GAPDH (Abcam ab181602), 1:2000 lamin-A (Bethyl A303-432A), 1:1000 HRV16 3D (Chase and Semler, 2014), 1:750 hnRNP M (Santa Cruz Biotechnology sc20002), 1:750 PSF/SFPQ (Santa Cruz Biotechnology sc374502), 1:15,000 HRV16 2C (antisera provided Dr. Roberto Solari), 1:2000 poliovirus 3A (a gift from Dr. George Belov), 1:1000 PARP (Abcam ab32071), 1:1000 PTBP1 (Abcam ab30317), and 1:10,000 AUF1 (Millipore 07-206).

Confocal Immunofluorescence microscopy

HeLa cells were seeded on glass coverslips and subsequently infected with HRV16 as described above. At the specified time following infection, cells were fixed with 3.7% formaldehyde in PBS for 15 minutes then washed with PBS. Cells were permeabilized with 0.5% NP-40 in PBS for 5 minutes, rinsed with 1% NCS in PBS, then blocked with 5% fetal bovine serum in PBS. Permeabilized cells were then incubated with a mixture of primary antibodies targeting cellular and viral proteins (1:50 hnRNP M [Santa Cruz Biotechnology sc20002], 1:50 PSF/SFPQ [Santa Cruz Biotechnology sc374502], or 1:500 SC35/SRSF2 [Sigma-Aldrich s4045] and 1:2500 HRV16 2C [antisera provided Dr. Roberto Solari]) diluted in PBS containing 5% BSA. Cells were washed with 1% NCS in PBS then incubated with a mixture of secondary antibodies in 1% BSA (1:250 goat anti-rabbit IgG-heavy and light chain DyLight 650-conjugated and 1:250 goat anti-mouse IgG-heavy and light chain DyLight 488-conjugated [Bethyl]). Following washes with 1% NCS in PBS, nuclei were counterstained with 0.4% 4',6-diamidino-2-phenylindole (DAPI), mounted on slides with Fluoro-Gel (Electron Microscopy Sciences) and allowed to dry overnight. Cells were visualized with a laser

scanning confocal microscope (Zeiss LSM 700), and images were processed using Zen software (Zeiss).

siRNA transfections

HeLa cells were transfected using DharmaFECT 1 transfection reagent (Dharmacon T-2001) at 25–33% confluence, 24 h after seeding (Chen, 2012). Briefly, a pool of siRNAs targeting SFPQ (Dharmacon M-006455-02) or a pool of non-targeting siRNAs (Dharmacon D-001206-13) was incubated with transfection reagent in OPTI-MEM (Gibco) at room temperature for 20 minutes before diluting siRNA to a final concentration of 5 nM in DMEM containing 8% NCS and no antibiotics, then overlaying on PBS-washed HeLa cells. Transfected cells were incubated for 96 h (5% CO2 and 37°C), trypsinized from representative wells, counted using a hemocytometer, and the remaining wells were infected at the indicated MOI as outlined above.

Reverse transcription polymerase chain reaction

TRIzol (Invitrogen) was added to siRNA-transfected, HRV16-infected cells at the indicated times post-infection, followed by RNA extraction. Complementary DNA (cDNA) was generated from 1 µg of total RNA using either oligo(dT)18 or an HRV16-specific reverse primer listed below and AMV reverse transcriptase (Life Sciences Advanced Technologies). The resulting cDNA was used as a template for polymerase chain reaction (PCR) and indirect analysis of HRV16, SFPQ, and actin beta (ACTB) mRNA levels with 24, 30, or 30 thermal cycler amplification cycles, respectively (Applied Biosystems SimpliAmp).

HRV16- or gene-specific primers used were (Ta: annealing temperature):

HRV16-1975-fwd: 5’-CGGGACTGCAAACACTACCT-3’,

HRV16-2281-rev: 5’-CCGAAGGCAAAAGTCCTTGC-3’ (58°C Ta),

SFPQ-884-fwd: 5’-AGCGATGTCGGTTGTTTGTTG-3’,

SFPQ-1096-rev: 5’-AGCGAACTCGAAGCTGTCTAC-3’ (56°C Ta),

ACTBh1-fwd: 5’-CATGTACTGTGCTATCCAGGC-3’, and

ACTBh1-rev: 5’-CTCCTTAATGTCACGCACGAT-3’ (56°C Ta).

PCR products were separated by agarose gel electrophoresis and visualized via ethidium bromide staining.

Affinity pulldown of biotinylated RNA

Detection of proteins interacting with HRV16 RNA was carried out as described previously (Panda et al., 2016a; Panda et al., 2016b). Plasmids pRV16.11 and pRstF, a bicistronic luciferase reporter construct, were linearized with EcoICRI or StuI, respectively (Jang et al., 2004). DNA was phenol-chloroform extracted and precipitated in ethanol. Linearized templates were transcribed using the MEGAscript™ T7 Transcription Kit (ThermoFisher Scientific) in the presence of biotin-14-CTP and unlabeled-CTP (1:9) resulting in biotinylated RNA corresponding to the HRV16 genome (~7,200 nt) and a biotinylated negative control RNA (~5,200 nt). Mock- or HRV16-infected HeLa cell lysates were generated with polysome extraction buffer (PEB) (20 mM Tris-HCl [pH 7.5], 100 mM KCl, 5 mM MgCl2, 0.5% NP-40, Pierce™ Protease Inhibitor Tablet EDTA-free [ThermoFisher Scientific]). 10 µg biotinylated RNA was renatured by incubating in 2x Tris, EDTA, NaCl, Triton (TENT) buffer (20 mM Tris-HCl [pH 8.0], 2 mM EDTA [pH 8.0], 500 mM NaCl, 1% Triton X-100) at 56°C for 5 minutes, 37°C for 5 minutes, then at room temperature for 5 minutes. Renatured, biotinylated RNA was then combined with 500 µg of cell lysate in the presence of ribonuclease

inhibitor (Promega™ Recombinant RNasin™) and incubated with intermittent mixing for 1 h. 125 µL of TENT-washed hydrophilic streptavidin magnetic beads (New England Biolabs) were added to mixture and incubation continued for 1 h with intermittent mixing. Beads were washed three times in 1x TENT buffer using a magnetic stand, 40 µL of 1x LSB was added, and beads were heated at 95 °C for 5 minutes. The entire sample was then separated by SDS-PAGE followed by Western blot analysis as described above. Quantity One software (Bio-Rad Laboratories) was used to quantify the relative intensity of bands using the volume analysis function.

Statistical analysis

Statistical analyses employed GraphPad software. All virus titer graphs represent the means of at least 3 biological replicate experiments analyzed in technical triplicate and error is presented as the standard error of the mean (SEM). Cell viability and affinity assay quantification represent the mean and standard deviation (SD) associated with five or four separate assays, respectively. *P*-values were determined using an unpaired Student's t test, and statistical significance was established as $P < 0.05$.

Chapter 4

Final conclusions and overall significance

Despite being one of the most extensively studied virus families, picornaviruses have infectious cycles that are incompletely understood. For example, we do not have a comprehensive accounting of the cellular factors co-opted by any particular virus during infection. In an effort to more completely characterize the replication cycles of enteroviruses, we attempted two proteomics-based approaches to identify host proteins which may be involved in this process, as described in this this dissertation. In Chapter 2, we used a direct approach in an attempt to determine which proteins bind to viral RNA molecules throughout the course of infection. Due to technical limitations in the biochemical isolation of viral RNA that became apparent in these studies, we were unable to isolate specific proteins bound to poliovirus RNA from infected cells. As discussed below, if isolation techniques can be improved, mass spectrometry analysis of proteins co-isolated with viral RNA would increase the known catalog of proteins that may play a role in viral replication processes. In Chapter 3, we used an indirect, unbiased strategy to determine what proteins become enriched in the cytoplasm, the site of viral replication, during the infectious cycle of HRV16. This allowed us to identify proteins that may be involved in different aspects of the viral life cycle, but do not necessarily associate with viral RNA. Our goal with this approach was to better understand the role that nuclear proteins play in enterovirus replication, as recent evidence suggests that many of the functional characteristics of these nuclear proteins (e.g., nucleic acid-binding capabilities) are important for a productive infection (refer to Chapter 1). Together, our proteomics-based approaches intended to provide

complementary methods for identifying novel factors in enterovirus replication. Additional molecular biology approaches will be required to define what role these novel proteins may have in the infectious cycle, as was initiated for SFPQ and HRV16 replication in Chapter 3. This Chapter will outline future studies, that build from those previously discussed, to promote a more thorough characterization of the enterovirus infectious cycle, as well as attempt to put the experimental results presented in previous chapters into the broader context of enterovirus-host interactions.

As mentioned in Chapter 2, during our attempts to isolate aptamer-tagged viral RNAs from infected cells, a technique known as thiouracil cross-linking mass spectrometry (TUX-MS) was described to identify proteins bound to poliovirus RNA (Lenarcic et al., 2013). This method utilized a cell line stably expressing uracil phosphoribosyltransferase, which incorporates 4-thiouridine (4sU) into all newly synthesized RNA, specifically poliovirus RNA, when actinomycin D is present during infection. The inclusion of 4sU into poliovirus RNA then allowed the authors to UV-crosslink viral RNA and bound proteins that, together, were subsequently isolated with oligo(dT) magnetic beads. Mass spectrometry analysis allowed for the identification of 66 host factors not previously implicated in poliovirus replication. Interestingly, SFPQ and a number of other nuclear resident proteins were members of this list, providing some corroboration of the data in Chapter 3. Although the TUX-MS method has demonstrated value in identifying novel proteins involved in viral replication, the recombinant virus approach discussed in Chapter 2 may provide a useful complement to the TUX-MS approach. Due to the isolation of poly(A) RNAs in the TUX-MS approach, it is not clear if any negative-strand intermediate RNAs were co-isolated with

positive-sense RNAs (e.g., as part of a replication intermediate). Even if these anti-genomic RNA molecules were isolated, it is not possible to segregate proteins that bind the different species of viral RNA. Our recombinant viruses, on the other hand, could be capable of stand-specific isolation since the aptamer sequences can be specifically engineered into positive- or negative-strands. Obviously, aptamers that allow more specific and reproducible isolation of RNA are a prerequisite for any study that aims to corroborate the associations identified by TUX-MS, as well as to further delineate binding partners.

It is possible that simple substitution of a different aptamer tag into the site where the S1 and D8 tags were engineered (nucleotide position 702 of the 5'-NCR) may enhance biochemical isolation. A recent study has reported the isolation of the yeast U1 snRNP complex through incorporation of an aptamer known as mango into the highly structured, 568 nucleotide U1 snRNA (Panchapakesan et al., 2017). The mango aptamer purification scheme took advantage of nanomolar affinity (K_d ~5 × 10^{-9} M) of the 39-nucleotide aptamer to thiazole orange derivatives and was performed using extracts of yeast expressing the mango-tagged U1 snRNA to isolate native complexes. It is not clear if viral RNA and associated proteins could be isolated without a crosslinking step, as performed by Panchapakesan and colleagues. Alternatively, aptamer-tagged viral RNA molecules (possibly with aptamer present on the apical point of a known stem-loop structure) could be transcribed *in vitro*, bound to respective matrix, incubated with uninfected or infected cell extracts, and then bound proteins could be eluted and analyzed. However, this type of experiment would not allow for full recapitulation of the dynamic nature of viral RNA structures and binding partners

present during infection of a host cell. This type of *in vitro* technique could be useful for verification of particular interactions, but whether it would be superior to standard techniques, such as *in vitro* transcription of biotinylated RNAs followed by streptavidin isolation, is not clear.

In addition to their utility in biochemical isolation, recombinant viruses containing aptamer-tagged genomes could also be used to visualize strand-specific RNA accumulation in infected cells. Fluorescently labeled oligonucleotides complementary to inserted tag sequences to analyze viral RNA distribution in cells (*in situ* hybridization) has been demonstrated previously, and could be especially useful for high-resolution imaging throughout the course of infection (Walker et al., 2011). Utilizing this *in situ* hybridization approach in combination with antibody-based indirect immunofluorescence of proteins could reveal unique spatial arrangements of viral RNA and host proteins and help to clarify how the discreet steps of the infectious cycle progress. Even more useful for observations of the dynamic spatial arrangements associated with viral RNA replication would be the use of recombinant polioviruses containing the mango or baby spinach aptamer. These aptamers fluoresce when bound to fluorophores and could be used for live-cell imaging with cell-permeable thiazole orange containing derivatives or 3,5-difluoro-4-hydroxybenzylidene imidazolinone (DFHBI), in combination with the mango or baby spinach aptamers, respectively (Paige et al., 2011; Warner et al., 2014).

Although we have been unable to utilize recombinant polioviruses containing affinity-tagged genomes for our original objective– the isolation of viral RNP complexes directly from infected cells– these viruses may have utility in future studies. Importantly, we were able to show that a particular location within the 5'-NCR of poliovirus is

amenable to short exogenous sequence insertions, with little effect on replication kinetics and viral progeny production. It is possible that different biochemical “handles” could improve isolation, and these viruses serve as a template for production of a second generation of recombinant polioviruses. Furthermore, the recombinant polioviruses we have on hand could immediately be used for microscopy-based studies of strand-specific RNA accumulation in infected cells.

The quantitative proteomics-based approach discussed in Chapter 3 provided unique insight into the global changes in protein distribution that occur during HRV16 infection. We show that HRV16 infection of HeLa cells results in a coordinated redistribution of nuclear proteins into the cytoplasm and that these proteins are enriched in RNA-related GO processes such as splicing (**Figure 3.2, Table 3.1, and Figure 3.3**). This suggests that HRV16 infection results in the enrichment of a specific functional class of proteins at the site of replication that has conceivable effects on the replication of an RNA virus. We identified the nuclear protein SFPQ as increasing in abundance in the cytoplasm of HRV16-infected HeLa cells through this proteomics approach. Subsequent work indicated that SFPQ is the target of proteolysis in the nucleus of HRV16-infected cells, which is likely carried out by the viral proteinase 3CD/3C, and that SFPQ then relocalizes to the cytoplasm where it interacts with HRV16 RNA. Although we provide evidence of a proviral role for SFPQ and suggest that it promotes viral replication in a step subsequent to viral translation based on its subcellular localization during peak viral protein production, more work will be required to identify the specific function of SFPQ in the HRV16 infectious cycle.

Both ongoing and future experiments are focused on verifying the results we present in Chapter 3. We are currently working to show that the viral proteinase 3CD/3C does, in fact, directly target SFPQ for cleavage. Although we have shown that cleavage of SFPQ during infection was not the result of caspase-mediated cleavage following activation of apoptosis, we have not shown that cleavage is a direct result of viral proteinase activity. This will be addressed through an *in vitro* cleavage assay combining HeLa cell lysates with purified recombinant wild type HRV16 3CD or catalytically inactive 3CD C146A (Chase and Semler, 2014). Additionally, we showed that siRNA-mediated knockdown of SFPQ resulted in reduced HRV16 titers, protein production, and RNA accumulation. To extend this finding, future studies could generate plasmids encoding SFPQ resistant to these siRNAs. These plasmids could then be transfected into SFPQ-knockdown cells and then infected to determine if SFPQ expression could rescue HRV16 replication. Care would have to be taken to ensure that siRNA-resistant SFPQ does not alter normal protein localization and/or functions as this could effect how SFPQ is utilized in HRV16 replication.

Due to the negative effects associated with multiple rounds of transfection and the transient nature of siRNA-mediated protein knockdown, these kinds of overexpression experiments may be more useful in stable knockdown cells through the use of SFPQ-targeting shRNA. Alternatively, *in vitro* replication/translation assays in the presence of recombinant SFPQ could be useful for depletion/rescue and overexpression experiments to verify the proviral effects of SFPQ (Perera et al., 2007). Immunofluorescence assays demonstrated partial colocalization between SFPQ and viral protein 2C or its precursors (**Figure 3.6B**). An association between SFPQ and 2C

could be validated by co-immunoprecipitation assays. Observed interactions between 2C and SFPQ would implicate SFPQ in HRV16 RNA replication because 2C is crucial for RNA replication, the induction of cytoplasmic vesicles on which RNA replication takes place, and possible linking of viral RNA to these vesicles (Aldabe et al., 1996; Cho et al., 1994; Li and Baltimore, 1988; Paul et al., 1994; Pfister et al., 2000; Pincus et al., 1986; Rodrguez and Carrasco, 1995; Teterina et al., 1997). Finally, utilizing guanidine hydrochloride (GuHCl), a known inhibitor of enterovirus RNA replication through effects on 2C, could help to further tease apart in which stage of the HRV16 replication cycle SFPQ is involved.

Recombinant viruses that encode a luciferase gene have proven useful in identifying the effect host proteins have on virus replication. Although an HRV16 replicon encoding luciferase in place of the P1 region of the genome is available, direct transfection of this construct into cells treated with siNT or siSFPQ is not ideal for several reasons (Mello et al., 2014). A major problem associated with the use of replicons in place of viruses is that transfection is biologically distinct from receptor-mediated targeting, as during an infection. For example, following transfection of an HRV16 replicon, nuclear protein relocalization may be dissimilar to that observed during HRV16 infection, since the overall infectious cycle may be altered. Because SFPQ relocalization appears to be required for its proviral effect, experiments using HRV16 replicons would require validation of SFPQ redistribution. Alternatively, an HRV16 virus encoding a luciferase gene immediately upstream of the P1 region could be generated [as previously described for poliovirus (Lanke et al., 2009)]. This virus could then be used to infect siNT- or siSFPQ-treated cells, in the presence or absence of GuHCl. If

SFPQ impinges on RNA replication, there would be no expected difference in luciferase activity from siNT- and siSFPQ-treated cells in the presence of GuHCl, as translation would remain unaffected.

Because SFPQ can bind HRV16 RNA (**Figure 3.9B and C**), it is also possible that this protein functions in stabilizing viral RNA. To test whether HRV16 is degraded more quickly in the absence of SFPQ, siNT- and siSFPQ-treated cells could be infected in the presence of GuHCl, to inhibit viral RNA replication. At different times following infection, the levels of viral RNA in these cells could be assayed either by Northern blot analysis or RT-PCR. If levels of RNA were decreased in siSFPQ-treated cells compared to siNT-treated cells, one explanation would be that SFPQ promotes viral RNA stability in infected cells (Jagdeo et al., 2015). In this scenario, GuHCl treatment would have to occur following SFPQ relocalization into the cytoplasm, or about 6 hours post-infection with HRV16. Another approach for determining viral RNA half-life is 5'-bromo-uridine immunoprecipitation (BrU immunoprecipitation) (Tani et al., 2012). In this method, BrU is used to pulse-label RNA followed by RT-PCR on immunoprecipitated BrU-RNA. BrU-labeled HRV16 RNA isolated from siNT- or siSFPQ-treated cells at different times of infection, following GuHCl treatment, could be compared as above.

As repeatedly pointed out in this dissertation, it is difficult to determine the precise role of a specific protein in the replication cycle of enteroviruses because all steps are closely coupled. Knocking down the expression of a cellular protein involved in any aspect of viral replication will likely have effects on translation, RNA replication, and virion morphogenesis. For example, if a protein has a role in viral translation, its knockdown would result in reduced expression of the viral proteins required for RNA

synthesis. Similarly, knockdown of a cellular protein involved in viral RNA replication will reduce the number of RNA templates available for translation. Furthermore, inhibition of either step impacts morphogenesis since virion assembly is dependent upon expression levels of viral structural proteins and viral RNA abundance. Indeed, many studies have linked viral RNA replication and encapsidation of these genomes directly (Caliguiri and Compans, 1973; Caliguiri and Mosser, 1971; Pfister et al., 1995; Pfister et al., 1992).

Based on the lack of SFPQ in the cytoplasm during peak HRV16 protein production, the involvement of SFPQ in viral translation is unlikely. To further narrow down the possible roles for SFPQ during the HRV16 infectious cycle we can examine how the data in Chapter 3, specifically **Figure 3.8**, were collected. Plaque assays were performed on freeze/thawed collections of cells and culture fluids, so viral titer measurements represent a combination of both intracellular and released infectious virions. Western blot analyses and RT-PCR, on the other hand, represent viral protein and RNA present within infected cells, as cell culture fluids were removed prior to collection for these analyses. Although a direct role for SFPQ in RNA encapsidation was not examined, the fact that relative levels of intracellular viral RNA accumulation in SFPQ knockdown cells roughly correlates with virus titers throughout the time-course suggests that there is not a defect in encapsidation. If SFPQ were involved in encapsidation directly, it would be expected that a lack of SFPQ may not necessarily impact viral RNA replication, but viral titers would be reduced due to a block in mature virion production. It is conceivable that SFPQ could be involved in virion morphogenesis, as perturbations to any one step within the tightly regulated infectious cycle may cause reduced overall replication efficiency and would be borne out by

reduced viral protein and RNA production. However, a more straightforward interpretation of the data presented in Chapter 3 suggests that SFPQ is not involved in encapsidation directly. Overall, the data indicate that the most likely role of SFPQ during the HRV16 infectious cycle is in RNA replication. Since the normal cellular role of SFPQ involves binding nucleic acids and other proteins to form bimolecular structures that can then carry out specific functions, it is reasonable to hypothesize that SFPQ may act as some kind of chaperone to recruit other cellular factors involved in RNA replication, independent of whether it binds HRV16 RNA directly.

As discussed in Chapter 3, SFPQ is targeted for cleavage in the nucleus of HRV16-infected cells and subsequently relocalizes to the cytoplasm where it may have proviral roles. Although it has been demonstrated that enterovirus 3CD/3C causes the degradation of various transcription factors in the nucleus (to effect host-cell transcriptional shutoff), the fact that SFPQ is cleaved prior to its role in virus replication is novel for enterovirus infection. Interestingly, a very similar phenomenon has been observed with the aphthovirus FMDV and cellular protein Sam68. As mentioned in Chapter 1, the 3CD proteinase of FMDV enters the nucleus of infected cells, via an NLS present in the 3D amino acid sequence, and cleaves the nuclear resident protein Sam68 (Lawrence et al., 2012; Sanchez-Aparicio et al., 2013). The Sam68 cleavage fragment then relocalizes to the cytoplasm of FMDV-infected cells. Full-length Sam68 was also shown to bind the viral IRES, and Sam68 knockdown resulted in both reduced luciferase expression from FMDV replicons and diminished FMDV titers. Consequently, there is some precedent to direct alteration of a nuclear protein prior to its use in picornavirus replication. It should be noted again that FMDV proteinases do not target

Nups for degradation and therefore cleavage of Sam68 may be a strategy for cytoplasmic redistribution of this protein to overcome the barrier of an intact NPC.

Other predominantly nuclear proteins have been shown to be involved in enterovirus replication. HnRNP C1/C2 is known to redistribute to the cytoplasm of poliovirus-infected cells and has been shown to promote RNA replication *in vitro* (Brunner et al., 2010; Brunner et al., 2005; Ertel et al., 2010). Similarly, hnRNP M relocalizes to the cytoplasm of poliovirus-infected cells, is cleaved by 3CD/3C, and promotes viral replication, although the precise step of the infectious cycle in which the function of hnRNP M is exploited is not clear (Jagdeo et al., 2015). Ultimately, SFPQ joins a growing number of proteins that influence the replication of cytoplasmic RNA viruses despite being excluded from the cytoplasmic environment in uninfected cells.

While Chapter 3 focused on the characterization of a single host protein during HRV16 infection, future studies may associate other proteins from our cytoplasmic enrichment screen with roles in HRV16 replication. We performed the same type of validation experiments presented in **Figure 3.8** on another protein that had decreased abundance in the nucleus and increased abundance in the cytoplasm 8 hours post-infection with HRV16: DExH-Box Helicase 9 (DHX9). This helicase functions in unwinding double-stranded nucleic acid, a function that could be useful in both translation and RNA replication during the infectious cycle of an RNA virus such as HRV16. Furthermore, DHX9 has been suggested to have a proviral role in the FMDV infectious cycle, possibly at the RNA replication step (Lawrence and Rieder, 2009). As shown in **Figure 4.1**, siRNA-mediated knockdown of DHX9 did not have a significant impact on HRV16 titers or protein production. This suggests that some proteins that

redistribute to the cytoplasm of HRV16-infected cells do not have an active role in viral replication, and may simple relocalize as a result of NPC degradation. This illustrates the importance of assaying each protein identified in the redistribution screen for roles in virus replication as some, like DHX9, are bound to be bystander proteins.

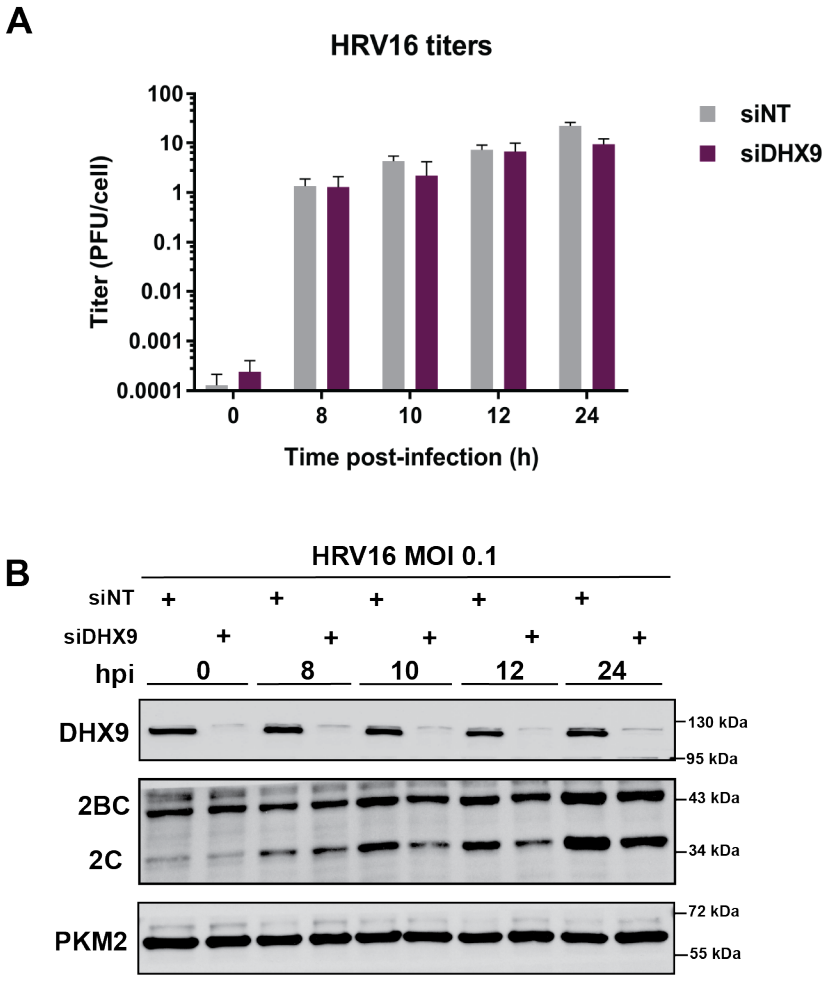

Figure 4.1. Knockdown of DHX9 has no significant effect on HRV16 replication. (A) HeLa cells transfected with non-targeting siRNA (siNT) or DHX9-targeting siRNA (siDHX9) for 96 h were infected with HRV16 (MOI 0.1) and cells and cell culture fluids were harvested at the indicated times. Virus titer was determined by plaque assay. Data represents means and standard deviations from two independent experiments. DHX9 knockdown did not result in statistically significant differences in cell viability as assessed by trypan blue exclusion prior to infection (P>0.05) (not shown). **(B)** siRNA-transfected and HRV16-infected HeLa cell lysates corresponding to the time-points in panel A (MOI 0.1) were generated and subjected to Western blot analysis. Knockdown of DHX9 was confirmed and levels of 2C and precursor (2BC) represented viral protein production. Pyruvate kinase, muscle (PKM2) protein was used as a loading control. The Western blot in panel B is representative of results from two biological replicate experiments.

In lieu of meticulous analysis to ascribe or refute virus-centric functions to each protein that we identified as decreasing in abundance in the nucleus and increasing in abundance in the cytoplasm of HRV16-infected cells (**Table 3.1**), subsequent work could aim to limit the scope of those proteins that should be taken into consideration. For example, identifying the specific tryptic peptides that are found in one subcellular compartment but not the other could further refine the mass spectrometry data. For example, tryptic peptides corresponding to SFPQ within the cytoplasmic dataset should not contain an intact 3CD cleavage site sequence, but tryptic peptides corresponding to SFPQ in the nuclear dataset should, since this protein appears to be targeted for cleavage in the nucleus. Determining the differences in the tryptic fragments corresponding to each identified protein in the separate datasets could reveal other cleavage events that take place in either the cytoplasm or nucleus of infected cells. Focusing on those proteins that may have direct interactions with the infecting virus (e.g., with the 3CD/3C proteinase), in addition to becoming enriched within the cytoplasm during infection, would aid in narrowing down candidate proteins for subsequent analysis.

In addition to further scrutiny of the datasets we have generated related to HRV16-induced cytoplasmic enrichment of proteins, future work could also focus on a different subcellular fraction of infected cells. The cell fractionation protocol we followed included a step that washed the nuclear material with a mixture of detergents after the removal of the cytoplasmic fraction, resulting in a “peri-nuclear” fraction. As mentioned in Chapter 1, the outer nuclear membrane is continuous with endoplasmic reticulum (ER), and therefore this third cellular fraction most likely contains the ER and associated

proteins. This fraction could be particularly rich with information because it is known that the membranous replication complexes on which RNA replication takes place are at least partially derived from the ER (Bienz et al., 1987; Egger and Bienz, 2005; Rust et al., 2001; Schlegel et al., 1996; Tershak, 1984). Prior to performing the same quantitative mass spectrometry analysis on the peri-nuclear fractions that we have generated, the presence of the ER in the fractions could be confirmed by Western blot analysis using an antibody targeting a known ER-resident protein such as KDEL endoplasmic reticulum protein retention receptor 1 (KDEL). Analyzing the relative changes in abundance of cellular proteins in this subcellular location throughout the infectious cycle would not only aid in identification of proteins directly involved in HRV16 RNA replication but also in those cellular proteins that may have roles in the formation of membranous replication complexes.

Finally, our quantitative protein mass spectrometry-based approach could be useful in defining cell-type specific redistribution events that occur during HRV16 infection. HeLa cells have been demonstrated to be a very good model for HRV16 infection in primary human bronchial epithelial cells in that replication kinetics, accumulation of viral biomolecules, and Nup protein cleavage are very similar in both cell types. However, it is possible that the cohorts of proteins that are utilized by the virus during infection of these and other, more physiologically relevant, cells are distinct (Amineva et al., 2011). For example, as explored in Chapter 1, the subset of proteins exploited by picornaviruses for IRES-driven translation are known to be cell-type specific. It is also possible that differences in infection kinetics observed in different cell types could be related to the abundance of particular proteins in the cytoplasm at

specific times during the infectious cycle, i.e., whether a protein is present in the subcellular region in which its function is required by the virus. Adding even more complexity to the issue of cell-type dependence is the fact that many proteins have been shown to have distinct distribution patterns across different cell lines (Thul et al., 2017). The abundance and spatial distribution of cellular proteins encountered by an infecting virus will have obvious consequences on the infectious cycle, since the efficiency and rate of replication is likely to be driven by the subset of protein functions that are available for immediate use by the virus. By identifying cell-type-specific protein redistribution/cytoplasmic enrichment events, our methodology could allow for a more comprehensive accounting of the nuclear proteome that engages in enterovirus replication.

We have performed preliminary experiments in a lung-derived cell line (WisL) to begin to better understand the differences in proteins that are utilized by HRV16 in a cell-type specific manner. As shown in **Figure 4.2A**, hnRNP M is not cleaved in WisL cells even though cleavage of this protein was observed 8 hours post-infection of HeLa cells (**Figure 3.4**). Furthermore, the cleavage of SFPQ that was observed 4 hours post-infection in HeLa cells is not observed until 8 hours post-infection WisL cells. The fact that SFPQ is not cleaved until later in infection in WisL cells is consistent with the limited expression of viral proteins 3CD and 3D at earlier times of infection in these cells (**Figure 3.6**). Notably, SFPQ does relocalize to the cytoplasm 8 hours post-infection in WisL cells (**Figure 4.2B**). Whether these kinetic differences are a result of protracted infection cycles in WisL cells or related to an overall reduction in infection efficiency remains to be seen. It is clear, however, that promulgating broad statements related to

enterovirus biology based on studies conducted in a single cell type does a disservice to the field and offers only a narrow view of the replication cycle. Our fractionation analysis method outlined in Chapter 3 could be applied to multiple cell types and different enteroviruses to provide a broad representation of the redistribution/re-equilibration proteome.

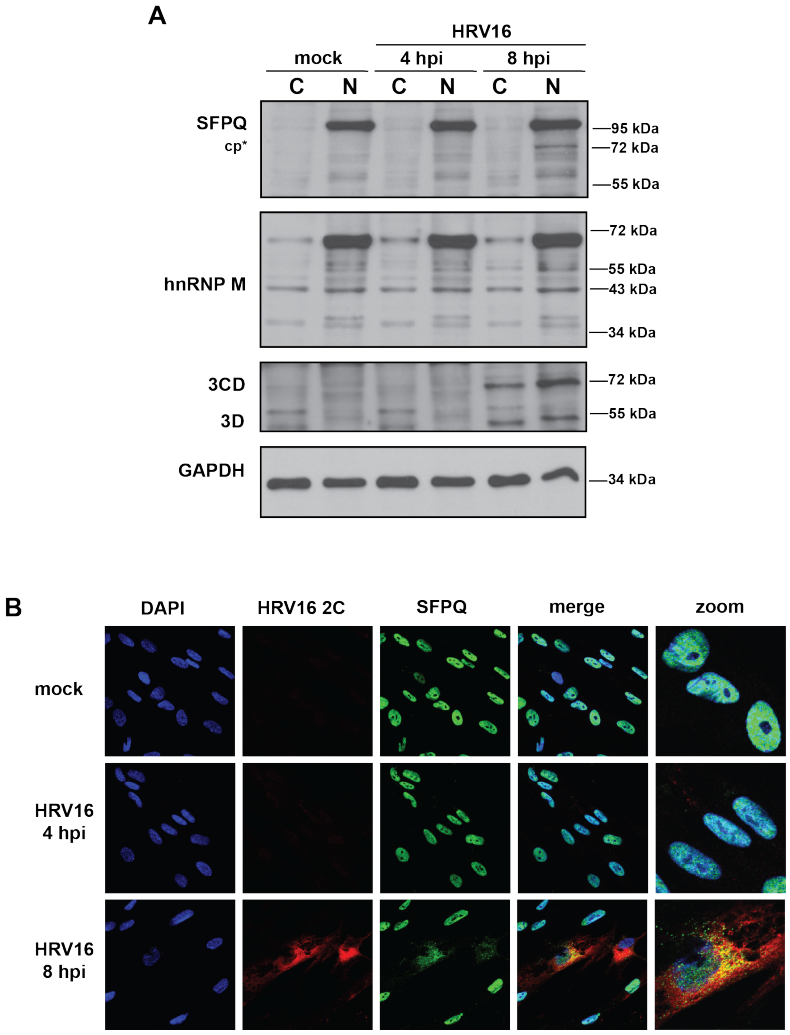

Figure 4.2. SFPQ relocalizes to the cytoplasm of HRV16-infected WisL cells but cleavage kinetics are slowed compared to infection of HeLa cells. (A) Cytoplasmic (C) or nuclear (N) fractions of mock- or HRV16-infected WisL cells were analyzed by Western blot. Cleavage of SFPQ was observed 8 hpi in the nucleus (cp*). No cleavage of hnRNP M was observed in either fraction throughout the course of infection. HRV16 3D/3CD was used as a marker of infection and GAPDH as a loading control (**B**) WisL cells were mock- or HRV16-infected (MOI 10) and fixed 4 or 8 hpi. HRV16 2C (red), a marker of HRV16 RNA replication sites and cellular protein SFPQ (green) were labeled by indirect immunofluorescence. DNA was counterstained with DAPI to indicate location of nuclei (blue). Cells were analyzed via confocal microscopy.

Although not the focus of the research presented here, expanded work to better understand how enteroviral proteins enter the nucleus of infected cells could be useful in developing antiviral therapies. As discussed in previous sections, enteroviral 3CD/3C enters the nucleus to limit host gene expression and promote virus production, so inhibiting the nuclear import of 3CD/3C may attenuate viral replication. Indeed, if 3CD/3C was blocked from entering the nucleus, SFPQ may not relocalize to the cytoplasm and perform proviral functions. Some nuclear localization sequences have been proposed for enteroviral 3CD/3C, but they most closely resemble those that are utilized by the classical import pathway, a pathway that is inhibited during infection (Amineva et al., 2004; Gustin and Sarnow, 2001, 2002; Sharma et al., 2004). If future studies can more specifically characterize the mechanism of 3CD/3C entry into the nucleus it is possible that small molecule inhibitors that target viral and host protein interfaces within this pathway can act as antiviral drugs. This is exemplified by work done with dengue virus: Ivermectin was shown to interfere with interactions between the viral non-structural protein 5 (NS5) and importin α/β, inhibiting NS5 transport to the nucleus and resulting in reduced viral titers (Tay et al., 2013; Wagstaff et al., 2012). Similar strategies to limit enterovirus replication would have to target specific interfaces within import pathways that remain functional during enterovirus infection.

Overall, both the direct and indirect methods discussed in this dissertation have the potential to reveal novel aspects of enterovirus biology. Although the direct approach did not yield the types of results that we had anticipated, it was useful as a proof-of-concept for subsequent work involving recombinant viruses with genomes that can be biochemically isolated from infected cells throughout the course of infection. Our

indirect approach emphasized the importance of nuclear protein relocalization events, and revealed SFPQ as a player in HRV16 replication. As is often the case, this research has provoked questions to be addressed in future studies that will draw from the datasets and methodologies that were generated through the work presented here. Furthermore, these two approaches could also be used in complementary fashion by identifying proteins that both increase in abundance in the cytoplasm and bind enterovirus RNA. Candidates identified through both approaches would have a strong likelihood of impacting the replication cycle of one or more enteroviruses. If employed together, these procedures could provide unique spatiotemporal dissection of the entire infectious cycle of different enteroviruses in a variety of relevant cell lines. The characterization of co-opted cellular factors has produced an ever-expanding list of proteins, though this endeavor remains incomplete. The approaches and results we have discussed here will enrich our understanding of enterovirus biology.

Despite extensive study and a generally successful eradication campaign against a major disease-causing member, picornaviruses remain relevant pathogens across the globe. Aside from the serious morbidity that rhinoviruses can cause in asthmatics, the elderly, and immunocompromised, it has been estimated that non-influenza respiratory tract infections cost about $40 billion dollars annually in the United States alone (Fendrick et al., 2003). Additionally, efforts to completely eradicate poliovirus will continue to be hampered by the use of the oral poliovirus vaccine as this live, attenuated Sabin strain can revert or even recombine with the closely related and naturally present enterovirus C (Kew et al., 2005). There is no doubt that continued basic research, such as that presented in this dissertation, is required to tease apart the

elegant ways in which picornaviruses hijack their cellular hosts. Subsequent studies in the picornavirus field would be well served to embrace a more inclusive view of the way in which these traditionally-considered cytoplasmic viruses interact with host biomolecules within different subcellular locations, and indeed the cell as whole. Only through a comprehensive understanding of even the most seemingly trivial aspects of virus replication can we develop strategies to overcome the economic and health burdens that these viruses bear upon society.

1. Afonina, E., Stauber, R., and Pavlakis, G.N. (1998). The human poly (A)-binding protein 1 shuttles between the nucleus and the cytoplasm. J Biol Chem *273*, 13015-13021.
2. Agol, V.I., Belov, G.A., Bienz, K., Egger, D., Kolesnikova, M.S., Raikhlin, N.T., Romanova, L.I., Smirnova, E.A., and Tolskaya, E.A. (1998). Two types of death of poliovirus-infected cells: caspase involvement in the apoptosis but not cytopathic effect. Virology *252*, 343-353.
3. Aldabe, R., Barco, A., and Carrasco, L. (1996). Membrane permeabilization by poliovirus proteins 2B and 2BC. J Biol Chem *271*, 23134-23137.
4. Almstead, L.L., and Sarnow, P. (2007). Inhibition of U snRNP assembly by a virus-encoded proteinase. Genes Dev *21*, 1086-1097.
5. Altan-Bonnet, N. (2016). Extracellular vesicles are the Trojan horses of viral infection. Current opinion in microbiology *32*, 77-81.
6. Alvarez, E., Castello, A., Carrasco, L., and Izquierdo, J.M. (2013). Poliovirus 2A protease triggers a selective nucleo-cytoplasmic redistribution of splicing factors to regulate alternative pre-mRNA splicing. PLoS One *8*, e73723.
7. Álvarez, E., Castelló, A., Carrasco, L., and Izquierdo, J.M. (2011). Alternative splicing, a new target to block cellular gene expression by poliovirus 2A protease. Biochem Biophys Res Commun *414*, 142-147.
8. Ambros, V., Pettersson, R.F., and Baltimore, D. (1978). An enzymatic activity in uninfected cells that cleaves the linkage between poliovirion RNA and the 5′ terminal protein. Cell *15*, 1439-1446.
9. Aminev, A.G., Amineva, S.P., and Palmenberg, A.C. (2003a). Encephalomyocarditis viral protein 2A localizes to nucleoli and inhibits cap-dependent mRNA translation. Virus Res *95*, 45-57.
10. Aminev, A.G., Amineva, S.P., and Palmenberg, A.C. (2003b). Encephalomyocarditis virus (EMCV) proteins 2A and 3BCD localize to nuclei and inhibit cellular mRNA transcription but not rRNA transcription. Virus Res *95*, 59-73.
11. Amineva, S., Aminev, A., Gern, J., and Palmenberg, A. (2011). Comparison of rhinovirus A infection in human primary epithelial and HeLa cells. J Gen Virol *92*, 2549-2557.
12. Amineva, S., Aminev, A., Palmenberg, A., and Gern, J. (2004). Rhinovirus 3C protease precursors 3CD and 3CD′ localize to the nuclei of infected cells. J Gen Virol *85*, 2969-2979.
13. Andino, R., Rieckhof, G.E., Achacoso, P.L., and Baltimore, D. (1993). Poliovirus RNA synthesis utilizes an RNP complex formed around the 5'-end of viral RNA. EMBO J *12*, 3587.
14. Andino, R., Rieckhof, G.E., and Baltimore, D. (1990). A functional ribonucleoprotein complex forms around the 5′ end of poliovirus RNA. Cell *63*, 369-380.
15. Apriletti, J.W., and Penhoet, E. (1978). Cellular RNA synthesis in normal and mengovirus-infected L-929 cells. J Biol Chem *253*, 603-611.
16. Back, S.H., Kim, Y.K., Kim, W.J., Cho, S., Oh, H.R., Kim, J.-E., and Jang, S.K. (2002). Translation of polioviral mRNA is inhibited by cleavage of polypyrimidine tract-binding proteins executed by polioviral 3Cpro. J Virol *76*, 2529-2542.
17. Bacot-Davis, V.R., Ciomperlik, J.J., Basta, H.A., Cornilescu, C.C., and Palmenberg, A.C. (2014). Solution structures of Mengovirus Leader protein, its phosphorylated derivatives, and in complex with nuclear transport regulatory protein, RanGTPase. Proc Natl Acad Sci U S A *111*, 15792-15797.
18. Bacot-Davis, V.R., and Palmenberg, A.C. (2013). Encephalomyocarditis virus Leader protein hinge domain is responsible for interactions with Ran GTPase. Virology *443*, 177-185.
19. Balandin, I.G., and Franklin, R.M. (1964). The effect of Mengovirus infection on the activity of the DNA-dependent RNA polymerase of L-cells. II. Preliminary data on the inhibitory factor. Biochem Biophys Res Commun *15*, 27-32.
20. Baltimore, D., and Franklin, R. (1962). The effect of Mengovirus infection on the activity of the DNA-dependent RNA polymerase of L-cells. Proc Natl Acad Sci U S A *48*, 1383.
21. Banerjee, R., Weidman, M.K., Navarro, S., Comai, L., and Dasgupta, A. (2005). Modifications of both selectivity factor and upstream binding factor contribute to poliovirus-mediated inhibition of RNA polymerase I transcription. J Gen Virol *86*, 2315-2322.
22. Bardina, M.V., Lidsky, P.V., Sheval, E.V., Fominykh, K.V., van Kuppeveld, F.J., Polyakov, V.Y., and Agol, V.I. (2009). Mengovirus-induced rearrangement of the nuclear pore complex: hijacking cellular phosphorylation machinery. J Virol *83*, 3150-3161.
23. Bardwell, V.J., and Wickens, M. (1990). Purification of RNA and RNA-protein complexes by an R17 coat protein affinity method. Nucleic Acids Res *18*, 6587-6594.
24. Barnett, S.F., Friedman, D.L., and LeStourgeon, W.M. (1989). The C proteins of HeLa 40S nuclear ribonucleoprotein particles exist as anisotropic tetramers of (C1) 3 C2. Mol Cell Biol *9*, 492-498.

25. Barton, D.J., and Flanegan, J.B. (1993). Coupled translation and replication of poliovirus RNA in vitro: synthesis of functional 3D polymerase and infectious virus. J Virol *67*, 822-831.
26. Barton, D.J., Morasco, B.J., and Flanegan, J.B. (1999). Translating ribosomes inhibit poliovirus negative-strand RNA synthesis. J Virol *73*, 10104-10112.
27. Barton, D.J., O'Donnell, B.J., and Flanegan, J.B. (2001). 5′ cloverleaf in poliovirus RNA is a cis-acting replication element required for negative-strand synthesis. EMBO J *20*, 1439-1448.
28. Basta, H.A., Bacot-Davis, V.R., Ciomperlik, J.J., and Palmenberg, A.C. (2014). Encephalomyocarditis virus leader is phosphorylated by CK2 and Syk as a requirement for subsequent phosphorylation of cellular nucleoporins. J Virol *88*, 2219-2226.
29. Basta, H.A., and Palmenberg, A.C. (2014). AMP-activated protein kinase phosphorylates EMCV, TMEV and SafV leader proteins at different sites. Virology *462*, 236-240.
30. Bedard, K.M., Daijogo, S., and Semler, B.L. (2007). A nucleo-cytoplasmic SR protein functions in viral IRES-mediated translation initiation. EMBO J *26*, 459-467.
31. Bedard, K.M., and Semler, B.L. (2004). Regulation of picornavirus gene expression. Microbes and Infection *6*, 702-713.
32. Belov, G.A., Evstafieva, A.G., Rubtsov, Y.P., Mikitas, O.V., Vartapetian, A.B., and Agol, V.I. (2000). Early alteration of nucleocytoplasmic traffic induced by some RNA viruses. Virology *275*, 244-248.
33. Belov, G.A., Lidsky, P.V., Mikitas, O.V., Egger, D., Lukyanov, K.A., Bienz, K., and Agol, V.I. (2004). Bidirectional increase in permeability of nuclear envelope upon poliovirus infection and accompanying alterations of nuclear pores. J Virol *78*, 10166-10177.
34. Belov, G.A., Nair, V., Hansen, B.T., Hoyt, F.H., Fischer, E.R., and Ehrenfeld, E. (2012). Complex dynamic development of poliovirus membranous replication complexes. J Virol *86*, 302-312.
35. Belov, G.A., Romanova, L.I., Tolskaya, E.A., Kolesnikova, M.S., Lazebnik, Y.A., and Agol, V.I. (2003). The major apoptotic pathway activated and suppressed by poliovirus. J Virol *77*, 45-56.
36. Ben-Efraim, I., and Gerace, L. (2001). Gradient of increasing affinity of importin β for nucleoporins along the pathway of nuclear import. J Cell Biol *152*, 411-418.
37. Bienz, K., Egger, D., and Pasamontes, L. (1987). Association of polioviral proteins of the P2 genomic region with the viral replication complex and virus-induced membrane synthesis as visualized by electron microscopic immunocytochemistry and autoradiography. Virology *160*, 220-226.
38. Bienz, K., Egger, D., Rasser, Y., and Bossart, W. (1982). Accumulation of poliovirus proteins in the host cell nucleus. Intervirology *18*, 189-196.
39. Blair, W.S., and Semler, B.L. (1991). Role for the P4 amino acid residue in substrate utilization by the poliovirus 3CD proteinase. J Virol *65*, 6111-6123.
40. Blom, N., Hansen, J., Brunak, S., and Blaas, D. (1996). Cleavage site analysis in picornaviral polyproteins: discovering cellular targets by neural networks. Protein Science *5*, 2203-2216.
41. Blyn, L.B., Chen, R., Semler, B.L., and Ehrenfeld, E. (1995). Host cell proteins binding to domain IV of the 5'noncoding region of poliovirus RNA. J Virol *69*, 4381-4389.
42. Blyn, L.B., Swiderek, K.M., Richards, O., Stahl, D.C., Semler, B.L., and Ehrenfeld, E. (1996). Poly (rC) binding protein 2 binds to stem-loop IV of the poliovirus RNA 5'noncoding region: identification by automated liquid chromatography-tandem mass spectrometry. Proc Natl Acad Sci U S A *93*, 11115-11120.
43. Blyn, L.B., Towner, J.S., Semler, B.L., and Ehrenfeld, E. (1997). Requirement of poly (rC) binding protein 2 for translation of poliovirus RNA. J Virol *71*, 6243-6246.
44. Boersema, P.J., Raijmakers, R., Lemeer, S., Mohammed, S., and Heck, A.J. (2009). Multiplex peptide stable isotope dimethyl labeling for quantitative proteomics. Nature protocols *4*, 484.
45. Bonderoff, J.M., LaRey, J.L., and Lloyd, R.E. (2008). Cleavage of poly (A)-binding protein by poliovirus 3C proteinase inhibits viral internal ribosome entry site-mediated translation. J Virol *82*, 9389-9399.
46. Bossart, W., Egger, D., Rasser, Y., and Bienz, K. (1982). Poliovirus-induced inhibition of host RNA synthesis studied in isolated HEp-2 cell nuclei. J Gen Virol *63*, 131-140.
47. Brown, D.M., Cornell, C.T., Tran, G.P., Nguyen, J.H., and Semler, B.L. (2005). An authentic 3′ noncoding region is necessary for efficient poliovirus replication. J Virol *79*, 11962-11973.
48. Brown, D.M., Kauder, S.E., Cornell, C.T., Jang, G.M., Racaniello, V.R., and Semler, B.L. (2004). Cell-dependent role for the poliovirus 3′ noncoding region in positive-strand RNA synthesis. J Virol *78*, 1344-1351.
49. Brunner, J.E., Ertel, K.J., Rozovics, J.M., and Semler, B.L. (2010). Delayed kinetics of poliovirus RNA synthesis in a human cell line with reduced levels of hnRNP C proteins. Virology *400*, 240-247.

50. Brunner, J.E., Nguyen, J.H., Roehl, H.H., Ho, T.V., Swiderek, K.M., and Semler, B.L. (2005). Functional interaction of heterogeneous nuclear ribonucleoprotein C with poliovirus RNA synthesis initiation complexes. J Virol *79*, 3254-3266.
51. Buckley, B., and Ehrenfeld, E. (1987). The cap-binding protein complex in uninfected and poliovirus-infected HeLa cells. J Biol Chem *262*, 13599-13606.
52. Buendia, B., Santa-Maria, A., and Courvalin, J. (1999). Caspase-dependent proteolysis of integral and peripheral proteins of nuclear membranes and nuclear pore complex proteins during apoptosis. J Cell Sci *112*, 1743-1753.
53. Buenz, E.J., and Howe, C.L. (2006). Picornaviruses and cell death. Trends Microbiol *14*, 28-36.
54. Burrill, C.P., Strings, V.R., and Andino, R. (2013a). Poliovirus: generation, quantification, propagation, purification, and storage. Curr Protoc Microbiol, 15H. 11.11-15H. 11.27.
55. Burrill, C.P., Westesson, O., Schulte, M.B., Strings, V.R., Segal, M., and Andino, R. (2013b). Global RNA structure snalysis of poliovirus identifies a conserved RNA structure involved in viral replication and infectivity. J Virol *87*, 11670-11683.
56. Cáceres, J.F., Screaton, G.R., and Krainer, A.R. (1998). A specific subset of SR proteins shuttles continuously between the nucleus and the cytoplasm. Genes Dev *12*, 55-66.
57. Caliguiri, L., and Compans, R. (1973). The formation of poliovirus particles in association with the RNA replication complexes. J Gen Virol *21*, 99-108.
58. Caliguiri, L.A., and Mosser, A.G. (1971). Proteins associated with the poliovirus RNA replication complex. Virology *46*, 375-386.
59. Caliguiri, L.A., and Tamm, I. (1969). Membranous structures associated with translation and transcription of poliovirus RNA. Science *166*, 885-886.
60. Callan, H., Randall, J., and Tomlin, S. (1949). An electron microscope study of the nuclear membrane. Nature *163*, 280.
61. Cammas, A., Pileur, F., Bonnal, S., Lewis, S.M., Lévêque, N., Holcik, M., and Vagner, S. (2007). Cytoplasmic relocalization of heterogeneous nuclear ribonucleoprotein A1 controls translation initiation of specific mRNAs. Mol Biol Cell *18*, 5048-5059.
62. Capozzo, A., Burke, D., Fox, J., Bergmann, I., La Torre, J., and Grigera, P. (2002). Expression of foot and mouth disease virus non-structural polypeptide 3ABC induces histone H3 cleavage in BHK21 cells. Virus Res *90*, 91-99.
63. Castello, A., Fischer, B., Eichelbaum, K., Horos, R., Beckmann, B.M., Strein, C., Davey, N.E., Humphreys, D.T., Preiss, T., and Steinmetz, L.M. (2012). Insights into RNA biology from an atlas of mammalian mRNA-binding proteins. Cell *149*, 1393-1406.
64. Castelló, A., Izquierdo, J.M., Welnowska, E., and Carrasco, L. (2009). RNA nuclear export is blocked by poliovirus 2A protease and is concomitant with nucleoporin cleavage. J Cell Sci *122*, 3799-3809.
65. Cathcart, A.L., Rozovics, J.M., and Semler, B.L. (2013). Cellular mRNA decay protein AUF1 negatively regulates enterovirus and human rhinovirus infections. J Virol *87*, 10423-10434.
66. Cathcart, A.L., and Semler, B.L. (2014). Differential restriction patterns of mRNA decay factor AUF1 during picornavirus infections. J Gen Virol *95*, 1488-1492.
67. Cautain, B., Hill, R., Pedro, N., and Link, W. (2015). Components and regulation of nuclear transport processes. FEBS J *282*, 445-462.
68. Chang, K., Brown, E.A., and Lemon, S.M. (1993). Cell type-specific proteins which interact with the 5'nontranslated region of hepatitis A virus RNA. J Virol *67*, 6716-6725.
69. Chase, A.J., Daijogo, S., and Semler, B.L. (2014). Inhibition of poliovirus-induced cleavage of cellular protein PCBP2 reduces the levels of viral RNA replication. J Virol *88*, 3192-3201.
70. Chase, A.J., and Semler, B.L. (2012). Viral subversion of host functions for picornavirus translation and RNA replication. Future virology *7*, 179-191.
71. Chase, A.J., and Semler, B.L. (2014). Differential cleavage of IRES trans-acting factors (ITAFs) in cells infected by human rhinovirus. Virology *449*, 35-44.
72. Chatel, G., and Fahrenkrog, B. (2011). Nucleoporins: leaving the nuclear pore complex for a successful mitosis. Cell Sig *23*, 1555-1562.
73. Chen, L.-L., Kung, Y.-A., Weng, K.-F., Lin, J.-Y., Horng, J.-T., and Shih, S.-R. (2013). Enterovirus 71 infection cleaves a negative regulator for viral internal ribosomal entry site-driven translation. J Virol *87*, 3828-3838.
74. Chen, Y. (2012). Dharmacon siRNA Transfection of Hela Cells. Bio-protocol *2*.

75. Chinsangaram, J., Koster, M., and Grubman, M.J. (2001). Inhibition of L-deleted foot-and-mouth disease virus replication by alpha/beta interferon involves double-stranded RNA-dependent protein kinase. J Virol *75*, 5498-5503.
76. Cho, M.W., Teterina, N., Egger, D., Bienz, K., and Ehrenfeld, E. (1994). Membrane rearrangement and vesicle induction by recombinant poliovirus 2C and 2BC in human cells. Virology *202*, 129-145.
77. Cho, S., Moon, H., Loh, T.J., Oh, H.K., Williams, D.R., Liao, D.J., Zhou, J., Green, M.R., Zheng, X., and Shen, H. (2014). PSF contacts exon 7 of SMN2 pre-mRNA to promote exon 7 inclusion. Biochimica et Biophysica Acta (BBA)-Gene Regulatory Mechanisms *1839*, 517-525.
78. Choi, S., Park, C., Kim, K.E., and Kim, K.K. (2017). An in vitro technique to identify the RNA binding-site sequences for RNA-binding proteins. BioTechniques *63*, 28-33.
79. Ciomperlik, J.J., Basta, H.A., and Palmenberg, A.C. (2015). Three cardiovirus Leader proteins equivalently inhibit four different nucleocytoplasmic trafficking pathways. Virology *484*, 194-202.
80. Ciomperlik, J.J., Basta, H.A., and Palmenberg, A.C. (2016). Cardiovirus Leader proteins bind exportins: Implications for virus replication and nucleocytoplasmic trafficking inhibition. Virology *487*, 19-26.
81. Clark, M.E., and Dasgupta, A. (1990). A transcriptionally active form of TFIIIC is modified in poliovirus-infected HeLa cells. Mol Cell Biol *10*, 5106-5113.
82. Clark, M.E., Hämmerle, T., Wimmer, E., and Dasgupta, A. (1991). Poliovirus proteinase 3C converts an active form of transcription factor IIIC to an inactive form: a mechanism for inhibition of host cell polymerase III transcription by poliovirus. EMBO J *10*, 2941.
83. Clark, M.E., Lieberman, P.M., Berk, A.J., and Dasgupta, A. (1993). Direct cleavage of human TATA-binding protein by poliovirus protease 3C in vivo and in vitro. Mol Cell Biol *13*, 1232-1237.
84. Cobbold, L.C., Spriggs, K.A., Haines, S.J., Dobbyn, H.C., Hayes, C., De Moor, C.H., Lilley, K.S., Bushell, M., and Willis, A.E. (2008). Identification of internal ribosome entry segment (IRES)-trans-acting factors for the Myc family of IRESs. Mol Cell Biol *28*, 40-49.
85. Cohen, S., Etingov, I., and Panté, N. (2012). Effect of Viral Infection on the Nuclear Envelope and Nuclear Pore Complex. In Int Rev of Cell and Molec Biol, K.W. Jeon, ed. (Amsterdam: Elsevier), pp. 117-159.
86. Cordes, S., Kusov, Y., Heise, T., and Gauss-Müller, V. (2008). La autoantigen suppresses IRES-dependent translation of the hepatitis A virus. Biochem Biophys Res Commun *368*, 1014-1019.
87. Corne, J.M., Marshall, C., Smith, S., Schreiber, J., Sanderson, G., Holgate, S.T., and Johnston, S.L. (2002). Frequency, severity, and duration of rhinovirus infections in asthmatic and non-asthmatic individuals: a longitudinal cohort study. The Lancet *359*, 831-834.
88. Costa-Mattioli, M., Svitkin, Y., and Sonenberg, N. (2004). La autoantigen is necessary for optimal function of the poliovirus and hepatitis C virus internal ribosome entry site in vivo and in vitro. Mol Cell Biol *24*, 6861-6870.
89. Coyle, J.H., Guzik, B.W., Bor, Y.-C., Jin, L., Eisner-Smerage, L., Taylor, S.J., Rekosh, D., and Hammarskjöld, M.-L. (2003). Sam68 enhances the cytoplasmic utilization of intron-containing RNA and is functionally regulated by the nuclear kinase Sik/BRK. Mol Cell Biol *23*, 92-103.
90. Craig, A., Svitkin, Y.V., Lee, H.S., Belsham, G.J., and Sonenberg, N. (1997). The La autoantigen contains a dimerization domain that is essential for enhancing translation. Mol Cell Biol *17*, 163-169.
91. Crawford, N., Fire, A., Samuels, M., Sharp, P.A., and Baltimore, D. (1981). Inhibition of transcription factor activity by poliovirus. Cell *27*, 555-561.
92. Croft, S.N., Walker, E.J., and Ghildyal, R. (2017). Picornaviruses and Apoptosis: Subversion of Cell Death. Mbio *8*, e01009-01017.
93. Cronshaw, J.M., Krutchinsky, A.N., Zhang, W., Chait, B.T., and Matunis, M.J. (2002). Proteomic analysis of the mammalian nuclear pore complex. J Cell Biol *158*, 915-927.
94. Danelishvili, L., Yamazaki, Y., Selker, J., and Bermudez, L.E. (2010). Secreted Mycobacterium tuberculosis Rv3654c and Rv3655c proteins participate in the suppression of macrophage apoptosis. PLoS One *5*, e10474.
95. Das, S., and Dasgupta, A. (1993). Identification of the cleavage site and determinants required for poliovirus 3CPro-catalyzed cleavage of human TATA-binding transcription factor TBP. J Virol *67*, 3326-3331.
96. Dave, P., George, B., Sharma, D.K., and Das, S. (2017). Polypyrimidine tract-binding protein (PTB) and PTB-associated splicing factor in CVB3 infection: an ITAF for an ITAF. Nucleic Acids Res.
97. Davies, M., Pelletier, J., Meerovitch, K., Sonenberg, N., and Kaufman, R. (1991). The effect of poliovirus proteinase 2Apro expression on cellular metabolism. Inhibition of DNA replication, RNA polymerase II transcription, and translation. J Biol Chem *266*, 14714-14720.

98. De Los Santos, T., de Avila Botton, S., Weiblen, R., and Grubman, M.J. (2006). The leader proteinase of foot-and-mouth disease virus inhibits the induction of beta interferon mRNA and blocks the host innate immune response. J Virol *80*, 1906-1914.
99. De Los Santos, T., Diaz-San Segundo, F., and Grubman, M.J. (2007). Degradation of nuclear factor kappa B during foot-and-mouth disease virus infection. J Virol *81*, 12803-12815.
100. De Los Santos, T., Diaz-San Segundo, F., Zhu, J., Koster, M., Dias, C.C., and Grubman, M.J. (2009). A conserved domain in the leader proteinase of foot-and-mouth disease virus is required for proper subcellular localization and function. J Virol *83*, 1800-1810.
101. De Palma, A.M., Vliegen, I., De Clercq, E., and Neyts, J. (2008). Selective inhibitors of picornavirus replication. Medicinal research reviews *28*, 823-884.
102. Deddouche, S., Goubau, D., Rehwinkel, J., Chakravarty, P., Begum, S., Maillard, P.V., Borg, A., Matthews, N., Feng, Q., and van Kuppeveld, F.J. (2014). Identification of an LGP2-associated MDA5 agonist in picornavirus-infected cells. Elife *3*, e01535.
103. Delhaye, S., Van Pesch, V., and Michiels, T. (2004). The leader protein of Theiler's virus interferes with nucleocytoplasmic trafficking of cellular proteins. J Virol *78*, 4357-4362.
104. Deszcz, L., Seipelt, J., Vassilieva, E., Roetzer, A., and Kuechler, E. (2004). Antiviral activity of caspase inhibitors: effect on picornaviral 2A proteinase. FEBS Lett *560*, 51-55.
105. Detjen, B.M., Lucas, J., and Wimmer, E. (1978). Poliovirus single-stranded RNA and double-stranded RNA: differential infectivity in enucleate cells. J Virol *27*, 582-586.
106. Dienstbier, M., Boehl, F., Li, X., and Bullock, S.L. (2009). Egalitarian is a selective RNA-binding protein linking mRNA localization signals to the dynein motor. Genes Dev *23*, 1546-1558.
107. Dildine, S.L., and Semler, B.L. (1989). The deletion of 41 proximal nucleotides reverts a poliovirus mutant containing a temperature-sensitive lesion in the 5'noncoding region of genomic RNA. J Virol *63*, 847-862.
108. Dix, C.I., Soundararajan, H.C., Dzhindzhev, N.S., Begum, F., Suter, B., Ohkura, H., Stephens, E., and Bullock, S.L. (2013). Lissencephaly-1 promotes the recruitment of dynein and dynactin to transported mRNAs. J Cell Biol *202*, 479-494.
109. Dougherty, J.D., Park, N., Gustin, K., and Lloyd, R. (2010). Interference with cellular gene expression. In The Picornaviruses, E. Ehrenfeld, E. Domingo, and R.P. Roos, eds. (Washington, DC: ASM Press), pp. 165-180.
110. Drahos, J., and Racaniello, V.R. (2009). Cleavage of IPS-1 in cells infected with human rhinovirus. J Virol *83*, 11581-11587.
111. Dreyfuss, G., Matunis, M.J., Pinol-Roma, S., and Burd, C.G. (1993). hnRNP proteins and the biogenesis of mRNA. Annual review of biochemistry *62*, 289-321.
112. Dye, B.T., and Patton, J.G. (2001). An RNA recognition motif (RRM) is required for the localization of PTB-associated splicing factor (PSF) to subnuclear speckles. Exp Cell Res *263*, 131-144.
113. Egger, D., and Bienz, K. (2005). Intracellular location and translocation of silent and active poliovirus replication complexes. J Gen Virol *86*, 707-718.
114. Ertel, K.J., Brunner, J.E., and Semler, B.L. (2010). Mechanistic consequences of hnRNP C binding to both RNA termini of poliovirus negative-strand RNA intermediates. J Virol *84*, 4229-4242.
115. Eyre, N.S., Johnson, S.M., Eltahla, A.A., Aloi, M., Aloia, A.L., McDevitt, C.A., Bull, R.A., and Beard, M.R. (2017). Genome-wide mutagenesis of dengue virus reveals plasticity of the NS1 protein and enables generation of infectious tagged reporter viruses. J Virol *91*, e01455-01417.
116. Faleiro, L., and Lazebnik, Y. (2000). Caspases disrupt the nuclear-cytoplasmic barrier. J Cell Biol *151*, 951-960.
117. Falk, M., Grigera, P., Bergmann, I., Zibert, A., Multhaup, G., and Beck, E. (1990). Foot-and-mouth disease virus protease 3C induces specific proteolytic cleavage of host cell histone H3. J Virol *64*, 748-756.
118. Fendrick, A.M., Monto, A.S., Nightengale, B., and Sarnes, M. (2003). The economic burden of non–influenza-related viral respiratory tract infection in the United States. Archives of internal medicine *163*, 487-494.
119. Feng, Q., Hato, S.V., Langereis, M.A., Zoll, J., Virgen-Slane, R., Peisley, A., Hur, S., Semler, B.L., van Rij, R.P., and van Kuppeveld, F.J. (2012). MDA5 detects the double-stranded RNA replicative form in picornavirus-infected cells. Cell reports *2*, 1187-1196.
120. Fernández-Tomás, C. (1982). The presence of viral-induced proteins in nuclei from poliovirus-infected HeLa cells. Virology *116*, 629-634.

121. Fitzgerald, K.D., Chase, A.J., Cathcart, A.L., Tran, G.P., and Semler, B.L. (2013). Viral proteinase requirements for the nucleocytoplasmic relocalization of cellular splicing factor SRp20 during picornavirus infections. J Virol *87*, 2390-2400.
122. Fitzgerald, K.D., and Semler, B.L. (2011). Re-localization of cellular protein SRp20 during poliovirus infection: bridging a viral IRES to the host cell translation apparatus. PLoS Pathog *7*, e1002127.
123. Flather, D., Cathcart, A.L., Cruz, C., Baggs, E., Ngo, T., Gershon, P.D., and Semler, B.L. (2016). Generation of Recombinant Polioviruses Harboring RNA Affinity Tags in the 5′ and 3′ Noncoding Regions of Genomic RNAs. Viruses *8*, 39.
124. Flather, D., and Semler, B.L. (2015). Picornaviruses and nuclear functions: targeting a cellular compartment distinct from the replication site of a positive-strand RNA virus. Frontiers in Microbiology *6*.
125. Florez, P.M., Sessions, O.M., Wagner, E.J., Gromeier, M., and Garcia-Blanco, M.A. (2005). The polypyrimidine tract binding protein is required for efficient picornavirus gene expression and propagation. J Virol *79*, 6172-6179.
126. Follett, E., Pringle, C., and Pennington, T. (1975). Virus development in enucleate cells: echovirus, poliovirus, pseudorabies virus, reovirus, respiratory syncytial virus and Semliki Forest virus. J Gen Virol *26*, 183-196.
127. Fradkin, L., Yoshinaga, S., Berk, A., and Dasgupta, A. (1987). Inhibition of host cell RNA polymerase III-mediated transcription by poliovirus: inactivation of specific transcription factors. Mol Cell Biol *7*, 3880-3887.
128. Franklin, R.M., and Baltimore, D. (1962). Patterns of macromolecular synthesis in normal and virus-infected mammalian cells. Paper presented at: Patterns of macromolecular synthesis in normal and virus-infected mammalian cells (Cold Spring Harbor symposia on quantitative biology.: Cold Spring Harbor Laboratory Press).
129. Frenkiel-Krispin, D., Maco, B., Aebi, U., and Medalia, O. (2010). Structural analysis of a metazoan nuclear pore complex reveals a fused concentric ring architecture. J Mol Biol *395*, 578-586.
130. Fried, H., and Kutay, U. (2003). Nucleocytoplasmic transport: taking an inventory. Cellular and Molecular Life Sciences CMLS *60*, 1659-1688.
131. Fung, G., Shi, J., Deng, H., Hou, J., Wang, C., Hong, A., Zhang, J., Jia, W., and Luo, H. (2015). Cytoplasmic translocation, aggregation, and cleavage of TDP-43 by enteroviral proteases modulate viral pathogenesis. Cell Death & Diff *22*, 2087-2097.
132. Galietta, A., Gunby, R.H., Redaelli, S., Stano, P., Carniti, C., Bachi, A., Tucker, P.W., Tartari, C.J., Huang, C.-J., and Colombo, E. (2007). NPM/ALK binds and phosphorylates the RNA/DNA-binding protein PSF in anaplastic large-cell lymphoma. Blood *110*, 2600-2609.
133. Gamarnik, A., and Andino, R. (1997). Two functional complexes formed by KH domain containing proteins with the 5'noncoding region of poliovirus RNA. RNA *3*, 882.
134. Gamarnik, A.V., and Andino, R. (1998). Switch from translation to RNA replication in a positive-stranded RNA virus. Genes Dev *12*, 2293-2304.
135. Gamarnik, A.V., and Andino, R. (2000). Interactions of viral protein 3CD and poly (rC) binding protein with the 5′ untranslated region of the poliovirus genome. J Virol *74*, 2219-2226.
136. García-Briones, M., Rosas, M.F., González-Magaldi, M., Martín-Acebes, M.A., Sobrino, F., and Armas-Portela, R. (2006). Differential distribution of non-structural proteins of foot-and-mouth disease virus in BHK-21 cells. Virology *349*, 409-421.
137. Gern, J.E., Calhoun, W., Swenson, C., Shen, G., and Busse, W.W. (1997). Rhinovirus infection preferentially increases lower airway responsiveness in allergic subjects. American journal of respiratory and critical care medicine *155*, 1872-1876.
138. Ghetti, A., Pinol-Roma, S., Michael, W.M., Morandi, C., and Dreyfuss, G. (1992). hnRNP 1, the polyprimidine tract-binding protein: distinct nuclear localization and association with hnRNAs. Nucleic Acids Res *20*, 3671-3678.
139. Ghildyal, R., Jordan, B., Li, D., Dagher, H., Bardin, P.G., Gern, J.E., and Jans, D.A. (2009). Rhinovirus 3C protease can localize in the nucleus and alter active and passive nucleocytoplasmic transport. J Virol *83*, 7349-7352.
140. Giachetti, C., and Semler, B.L. (1991). Role of a viral membrane polypeptide in strand-specific initiation of poliovirus RNA synthesis. J Virol *65*, 2647-2654.
141. Goldstaub, D., Gradi, A., Bercovitch, Z., Grosmann, Z., Nophar, Y., Luria, S., Sonenberg, N., and Kahana, C. (2000). Poliovirus 2A protease induces apoptotic cell death. Mol Cell Biol *20*, 1271-1277.

142. Görlach, M., Wittekind, M., Beckman, R., Mueller, L., and Dreyfuss, G. (1992). Interaction of the RNA-binding domain of the hnRNP C proteins with RNA. EMBO J *11*, 3289.
143. Görlich, D., Pante, N., Kutay, U., Aebi, U., and Bischoff, F. (1996). Identification of different roles for RanGDP and RanGTP in nuclear protein import. EMBO J *15*, 5584.
144. Gosert, R., Chang, K.H., Rijnbrand, R., Yi, M., Sangar, D.V., and Lemon, S.M. (2000a). Transient expression of cellular polypyrimidine-tract binding protein stimulates cap-independent translation directed by both picornaviral and flaviviral internal ribosome entry sites in vivo. Mol Cell Biol *20*, 1583-1595.
145. Gosert, R., Egger, D., and Bienz, K. (2000b). A cytopathic and a cell culture adapted hepatitis A virus strain differ in cell killing but not in intracellular membrane rearrangements. Virology *266*, 157-169.
146. Graff, J., Cha, J., Blyn, L.B., and Ehrenfeld, E. (1998). Interaction of poly (rC) binding protein 2 with the 5′ noncoding region of hepatitis A virus RNA and its effects on translation. J Virol *72*, 9668-9675.
147. Gratacós, F.M., and Brewer, G. (2010). The role of AUF1 in regulated mRNA decay. Wiley Interdiscip Rev RNA *1*, 457-473.
148. Graveley, B.R. (2000). Sorting out the complexity of SR protein functions. RNA *6*, 1197-1211.
149. Greco-Stewart, V.S., Thibault, C.S.-L., and Pelchat, M. (2006). Binding of the polypyrimidine tract-binding protein-associated splicing factor (PSF) to the hepatitis delta virus RNA. Virology *356*, 35-44.
150. Griffis, E.R., Altan, N., Lippincott-Schwartz, J., and Powers, M.A. (2002). Nup98 is a mobile nucleoporin with transcription-dependent dynamics. Mol Biol Cell *13*, 1282-1297.
151. Griffis, E.R., Xu, S., and Powers, M.A. (2003). Nup98 localizes to both nuclear and cytoplasmic sides of the nuclear pore and binds to two distinct nucleoporin subcomplexes. Mol Biol Cell *14*, 600-610.
152. Griger, P.R., and Tisminetzky, S.G. (1984). Histone H3 modification in BHK cells infected with foot-and-mouth disease virus. Virology *136*, 10-19.
153. Groppo, R., Brown, B.A., and Palmenberg, A.C. (2011). Mutational analysis of the EMCV 2A protein identifies a nuclear localization signal and an eIF4E binding site. Virology *410*, 257-267.
154. Grossman, E., Medalia, O., and Zwerger, M. (2012). Functional architecture of the nuclear pore complex. Annu Rev Biophys *41*, 557-584.
155. Gustin, K.E., and Sarnow, P. (2001). Effects of poliovirus infection on nucleo-cytoplasmic trafficking and nuclear pore complex composition. EMBO J *20*, 240-249.
156. Gustin, K.E., and Sarnow, P. (2002). Inhibition of nuclear import and alteration of nuclear pore complex composition by rhinovirus. J Virol *76*, 8787-8796.
157. Ha, K., Takeda, Y., and Dynan, W.S. (2011). Sequences in PSF/SFPQ mediate radioresistance and recruitment of PSF/SFPQ-containing complexes to DNA damage sites in human cells. DNA repair *10*, 252-259.
158. Haller, A.A., and Semler, B.L. (1992). Linker scanning mutagenesis of the internal ribosome entry site of poliovirus RNA. J Virol *66*, 5075-5086.
159. Hellen, C., Witherell, G.W., Schmid, M., Shin, S.H., Pestova, T.V., Gil, A., and Wimmer, E. (1993). A cytoplasmic 57-kDa protein that is required for translation of picornavirus RNA by internal ribosomal entry is identical to the nuclear pyrimidine tract-binding protein. Proc Natl Acad Sci U S A *90*, 7642-7646.
160. Henke, A., Nestler, M., Strunze, S., Saluz, H.-P., Hortschansky, P., Menzel, B., Martin, U., Zell, R., Stelzner, A., and Munder, T. (2001). The apoptotic capability of coxsackievirus B3 is influenced by the efficient interaction between the capsid protein VP2 and the proapoptotic host protein Siva. Virology *289*, 15-22.
161. Herold, J., and Andino, R. (2001). Poliovirus RNA replication requires genome circularization through a protein–protein bridge. Mol Cell *7*, 581-591.
162. Hicks, L.A., Shepard, C.W., Britz, P.H., Erdman, D.D., Fischer, M., Flannery, B.L., Peck, A.J., Lu, X., Thacker, W.L., and Benson, R.F. (2006). Two outbreaks of severe respiratory disease in nursing homes associated with rhinovirus. Journal of the American Geriatrics Society *54*, 284-289.
163. Hinshaw, J.E., Carragher, B.O., and Milligan, R.A. (1992). Architecture and design of the nuclear pore complex. Cell *69*, 1133-1141.
164. Hoelz, A., Debler, E.W., and Blobel, G. (2011). The structure of the nuclear pore complex. Annual review of biochemistry *80*, 613-643.
165. Holcik, M., and Liebhaber, S.A. (1997). Four highly stable eukaryotic mRNAs assemble 3′ untranslated region RNA–protein complexes sharing cis and trans components. Proc Natl Acad Sci U S A *94*, 2410-2414.

166. Huang, M., Rech, J., Northington, S., Flicker, P., Mayeda, A., Krainer, A., and LeStourgeon, W. (1994). The C-protein tetramer binds 230 to 240 nucleotides of pre-mRNA and nucleates the assembly of 40S heterogeneous nuclear ribonucleoprotein particles. Mol Cell Biol *14*, 518-533.
167. Huang, P.-N., Lin, J.-Y., Locker, N., Kung, Y.-A., Hung, C.-T., Lin, J.-Y., Huang, H.-I., Li, M.-L., and Shih, S.-R. (2011). Far upstream element binding protein 1 binds the internal ribosomal entry site of enterovirus 71 and enhances viral translation and viral growth. Nucleic Acids Res *39*, 9633-9648.
168. Huang, Y., Gattoni, R., Stévenin, J., and Steitz, J.A. (2003). SR splicing factors serve as adapter proteins for TAP-dependent mRNA export. Mol Cell *11*, 837-843.
169. Huang, Y., and Steitz, J.A. (2001). Splicing factors SRp20 and 9G8 promote the nucleocytoplasmic export of mRNA. Mol Cell *7*, 899-905.
170. Hunt, S.L., and Jackson, R.J. (1999). Polypyrimidine-tract binding protein (PTB) is necessary, but not sufficient, for efficient internal initiation of translation of human rhinovirus-2 RNA. RNA *5*, 344-359.
171. Iioka, H., Loiselle, D., Haystead, T.A., and Macara, I.G. (2011). Efficient detection of RNA–protein interactions using tethered RNAs. Nucleic Acids Res, gkq1316.
172. Imamura, K., Imamachi, N., Akizuki, G., Kumakura, M., Kawaguchi, A., Nagata, K., Kato, A., Kawaguchi, Y., Sato, H., and Yoneda, M. (2014). Long noncoding RNA NEAT1-dependent SFPQ relocation from promoter region to paraspeckle mediates IL8 expression upon immune stimuli. Mol Cell *53*, 393-406.
173. Ishihama, Y., Rappsilber, J., and Mann, M. (2006). Modular stop and go extraction tips with stacked disks for parallel and multidimensional peptide fractionation in proteomics. Journal of proteome research *5*, 988-994.
174. Izumi, R.E., Valdez, B., Banerjee, R., Srivastava, M., and Dasgupta, A. (2001). Nucleolin stimulates viral internal ribosome entry site-mediated translation. Virus Res *76*, 17-29.
175. Jackson, R., Hunt, S., Reynolds, J., and Kaminski, A. (1995). Cap-dependent and cap-independent translation: operational distinctions and mechanistic interpretations. In Cap-Independent Translation (Springer), pp. 1-29.
176. Jackson, W.T., Giddings Jr, T.H., Taylor, M.P., Mulinyawe, S., Rabinovitch, M., Kopito, R.R., and Kirkegaard, K. (2005). Subversion of cellular autophagosomal machinery by RNA viruses. PLoS Biol *3*, e156.
177. Jacobs, S.E., Lamson, D.M., George, K.S., and Walsh, T.J. (2013). Human rhinoviruses. Clinical microbiology reviews *26*, 135-162.
178. Jagdeo, J.M., Dufour, A., Fung, G., Luo, H., Kleifeld, O., Overall, C.M., and Jan, E. (2015). Heterogeneous nuclear ribonucleoprotein M facilitates enterovirus infection. J Virol *89*, 7064-7078.
179. Jang, G.M., Leong, L.E.-C., Hoang, L.T., Wang, P.H., Gutman, G.A., and Semler, B.L. (2004). Structurally distinct elements mediate internal ribosome entry within the 5′-noncoding region of a voltage-gated potassium channel mRNA. J Biol Chem *279*, 47419-47430.
180. Jang, S., Pestova, T., Hellen, C., Witherell, G., and Wimmer, E. (1989). Cap-independent translation of picornavirus RNAs: structure and function of the internal ribosomal entry site. Enzyme *44*, 292-309.
181. Jang, S.K., and Wimmer, E. (1990). Cap-independent translation of encephalomyocarditis virus RNA: structural elements of the internal ribosomal entry site and involvement of a cellular 57-kD RNA-binding protein. Genes Dev *4*, 1560-1572.
182. Jelachich, M.L., and Lipton, H.L. (2001). Theiler's murine encephalomyelitis virus induces apoptosis in gamma interferon-activated M1 differentiated myelomonocytic cells through a mechanism involving tumor necrosis factor alpha (TNF-α) and TNF-α-related apoptosis-inducing ligand. J Virol *75*, 5930-5938.
183. Joachims, M., Van Breugel, P.C., and Lloyd, R.E. (1999). Cleavage of poly (A)-binding protein by enterovirus proteases concurrent with inhibition of translation in vitro. J Virol *73*, 718-727.
184. Kafasla, P., Lin, H., Curry, S., and Jackson, R.J. (2011). Activation of picornaviral IRESs by PTB shows differential dependence on each PTB RNA-binding domain. RNA *17*, 1120-1131.
185. Kafasla, P., Morgner, N., Pöyry, T.A., Curry, S., Robinson, C.V., and Jackson, R.J. (2009). Polypyrimidine tract binding protein stabilizes the encephalomyocarditis virus IRES structure via binding multiple sites in a unique orientation. Mol Cell *34*, 556-568.
186. Kafasla, P., Morgner, N., Robinson, C.V., and Jackson, R.J. (2010). Polypyrimidine tract-binding protein stimulates the poliovirus IRES by modulating eIF4G binding. EMBO J *29*, 3710-3722.
187. Kallman, F., Williams, R.C., Dulbecco, R., and Vogt, M. (1958). Fine structure of changes produced in cultured cells sampled at specified intervals during a single growth cycle of polio virus. J Biophys Biochem Cytol *4*, 301-308.

188. Kaminski, A., Hunt, S.L., Patton, J., and Jackson, R.J. (1995). Direct evidence that polypyrimidine tract binding protein (PTB) is essential for internal initiation of translation of encephalomyocarditis virus RNA. RNA *1*, 924.
189. Kaminski, A., and Jackson, R.J. (1998). The polypyrimidine tract binding protein (PTB) requirement for internal initiation of translation of cardiovirus RNAs is conditional rather than absolute. RNA *4*, 626-638.
190. Kanda, T., Gauss-Müller, V., Cordes, S., Tamura, R., Okitsu, K., Shuang, W., Nakamoto, S., Fujiwara, K., Imazeki, F., and Yokosuka, O. (2010). Hepatitis A virus (HAV) proteinase 3C inhibits HAV IRES-dependent translation and cleaves the polypyrimidine tract-binding protein. J Viral Hepatitis *17*, 618-623.
191. Kataoka, N., Bachorik, J.L., and Dreyfuss, G. (1999). Transportin-SR, a nuclear import receptor for SR proteins. J Cell Biol *145*, 1145-1152.
192. Kato, H., Takeuchi, O., Sato, S., Yoneyama, M., Yamamoto, M., Matsui, K., Uematsu, S., Jung, A., Kawai, T., and Ishii, K.J. (2006). Differential roles of MDA5 and RIG-I helicases in the recognition of RNA viruses. Nature *441*, 101-105.
193. Kempf, B.J., and Barton, D.J. (2008). Poly (rC) binding proteins and the 5′ cloverleaf of uncapped poliovirus mRNA function during de novo assembly of polysomes. J Virol *82*, 5835-5846.
194. Kerekatte, V., Keiper, B.D., Badorff, C., Cai, A., Knowlton, K.U., and Rhoads, R.E. (1999). Cleavage of Poly (A)-binding protein by coxsackievirus 2A protease in vitro and in vivo: another mechanism for host protein synthesis shutoff? J Virol *73*, 709-717.
195. Keryer-Bibens, C., Barreau, C., and Osborne, H.B. (2008). Tethering of proteins to RNAs by bacteriophage proteins. Biol Cell *100*, 125-138.
196. Kew, O.M., Sutter, R.W., de Gourville, E.M., Dowdle, W.R., and Pallansch, M.A. (2005). Vaccine-derived polioviruses and the endgame strategy for global polio eradication. Annu Rev Microbiol *59*, 587-635.
197. Kim, Y.K., and Jang, S.K. (1999). La protein is required for efficient translation driven by encephalomyocarditis virus internal ribosomal entry site. J Gen Virol *80*, 3159-3166.
198. King, H., Cobbold, L., Pichon, X., Pöyry, T., Wilson, L., Booden, H., Jukes-Jones, R., Cain, K., Lilley, K., and Bushell, M. (2014). Remodelling of a polypyrimidine tract-binding protein complex during apoptosis activates cellular IRESs. Cell Death & Diff *21*, 161-171.
199. Kliewer, S., and Dasgupta, A. (1988). An RNA polymerase II transcription factor inactivated in poliovirus-infected cells copurifies with transcription factor TFIID. Mol Cell Biol *8*, 3175-3182.
200. Kliewer, S., Muchardt, C., Gaynor, R., and Dasgupta, A. (1990). Loss of a phosphorylated form of transcription factor CREB/ATF in poliovirus-infected cells. J Virol *64*, 4507-4515.
201. Knott, G.J., Bond, C.S., and Fox, A.H. (2016). The DBHS proteins SFPQ, NONO and PSPC1: a multipurpose molecular scaffold. Nucleic Acids Res *44*, 3989-4004.
202. Kobayashi, M., Arias, C., Garabedian, A., Palmenberg, A.C., and Mohr, I. (2012). Site-specific cleavage of the host poly (A) binding protein by the encephalomyocarditis virus 3C proteinase stimulates viral replication. J Virol *86*, 10686-10694.
203. Koloteva-Levine, N., Amichay, M., and Elroy-Stein, O. (2002). Interaction of hnRNP-C1/C2 proteins with RNA: analysis using the yeast three-hybrid system. FEBS Lett *523*, 73-78.
204. Kolupaeva, V., Hellen, C., and Shatsky, I. (1996). Structural analysis of the interaction of the pyrimidine tract-binding protein with the internal ribosomal entry site of encephalomyocarditis virus and foot-and-mouth disease virus RNAs. RNA *2*, 1199.
205. Kotla, S., and Gustin, K.E. (2015). Proteolysis of MDA5 and IPS-1 is not required for inhibition of the type I IFN response by poliovirus. Virology journal *12*, 158.
206. Kotla, S., Peng, T., Bumgarner, R.E., and Gustin, K.E. (2008). Attenuation of the type I interferon response in cells infected with human rhinovirus. Virology *374*, 399-410.
207. Kuge, S., Kawamura, N., and Nomoto, A. (1989). Genetic variation occurring on the genome of an in vitro insertion mutant of poliovirus type 1. J Virol *63*, 1069-1075.
208. Kuge, S., and Nomoto, A. (1987). Construction of viable deletion and insertion mutants of the Sabin strain of type 1 poliovirus: function of the 5' noncoding sequence in viral replication. J Virol *61*, 1478-1487.
209. Kula, A., Gharu, L., and Marcello, A. (2013). HIV-1 pre-mRNA commitment to Rev mediated export through PSF and Matrin 3. Virology *435*, 329-340.
210. Kundu, P., Raychaudhuri, S., Tsai, W., and Dasgupta, A. (2005). Shutoff of RNA polymerase II transcription by poliovirus involves 3C protease-mediated cleavage of the TATA-binding protein at an alternative site: incomplete shutoff of transcription interferes with efficient viral replication. J Virol *79*, 9702-9713.

211. Kuo, R.-L., Kao, L.-T., Lin, S.-J., Wang, R.Y.-L., and Shih, S.-R. (2013). MDA5 plays a crucial role in enterovirus 71 RNA-mediated IRF3 activation. PLoS One *8*, e63431.
212. Kuyumcu-Martinez, N.M., Joachims, M., and Lloyd, R.E. (2002). Efficient cleavage of ribosome-associated poly (A)-binding protein by enterovirus 3C protease. J Virol *76*, 2062-2074.
213. Landeras-Bueno, S., Jorba, N., Pérez-Cidoncha, M., and Ortín, J. (2011). The splicing factor proline-glutamine rich (SFPQ/PSF) is involved in influenza virus transcription. PLoS Pathog *7*, e1002397.
214. Langereis, M.A., Feng, Q., Nelissen, F.H., Virgen-Slane, R., van der Heden van Noort, G.J., Maciejewski, S., Filippov, D.V., Semler, B.L., van Delft, F.L., and van Kuppeveld, F.J. (2013). Modification of picornavirus genomic RNA using 'click'chemistry shows that unlinking of the VPg peptide is dispensable for translation and replication of the incoming viral RNA. Nucleic Acids Res *42*, 2473-2482.
215. Lanke, K.H., van der Schaar, H.M., Belov, G.A., Feng, Q., Duijsings, D., Jackson, C.L., Ehrenfeld, E., and van Kuppeveld, F.J. (2009). GBF1, a guanine nucleotide exchange factor for Arf, is crucial for coxsackievirus B3 RNA replication. J Virol *83*, 11940-11949.
216. Lawrence, P., Conderino, J.S., and Rieder, E. (2014). Redistribution of demethylated RNA helicase A during foot-and-mouth disease virus infection: role of Jumonji C-domain containing protein 6 in RHA demethylation. Virology *452*, 1-11.
217. Lawrence, P., and Rieder, E. (2009). Identification of RNA helicase A as a new host factor in the replication cycle of foot-and-mouth disease virus. J Virol *83*, 11356-11366.
218. Lawrence, P., Schafer, E.A., and Rieder, E. (2012). The nuclear protein Sam68 is cleaved by the FMDV 3C protease redistributing Sam68 to the cytoplasm during FMDV infection of host cells. Virology *425*, 40-52.
219. Lazebnik, Y.A., Kaufmann, S.H., Desnoyers, S., Poirier, G., and Earnshaw, W. (1994). Cleavage of poly (ADP-ribose) polymerase by a proteinase with properties like ICE. Nature *371*, 346-347.
220. Lee, W.-M., and Wang, W. (2003). Human rhinovirus type 16: mutant V1210A requires capsid-binding drug for assembly of pentamers to form virions during morphogenesis. J Virol *77*, 6235-6244.
221. Lee, W.-M., Wang, W., and Rueckert, R.R. (1995). Complete sequence of the RNA genome of human rhinovirus 16, a clinically useful common cold virus belonging to the ICAM-1 receptor group. Virus genes *9*, 177-181.
222. Leffers, H., Dejgaard, K., and Celis, J.E. (1995). Characterisation of two major cellular poly (rC)-binding human proteins, each containing three K-homologous (KH) domains. Eur J Biochem *230*, 447-453.
223. Lenarcic, E.M., Landry, D.M., Greco, T.M., Cristea, I.M., and Thompson, S.R. (2013). Thiouracil cross-linking mass spectrometry: a cell-based method to identify host factors involved in viral amplification. J Virol *87*, 8697-8712.
224. Leonov, A.A., Sergiev, P.V., Bogdanov, A.A., Brimacombe, R., and Dontsova, O.A. (2003). Affinity purification of ribosomes with a lethal G2655C mutation in 23 S rRNA that affects the translocation. J Biol Chem *278*, 25664-25670.
225. Leppek, K., and Stoecklin, G. (2014). An optimized streptavidin-binding RNA aptamer for purification of ribonucleoprotein complexes identifies novel ARE-binding proteins. Nucleic Acids Res *42*, e13.
226. Li, J.-P., and Baltimore, D. (1988). Isolation of poliovirus 2C mutants defective in viral RNA synthesis. J Virol *62*, 4016-4021.
227. Li, S., Li, Z., Shu, F.-J., Xiong, H., Phillips, A.C., and Dynan, W.S. (2014). Double-strand break repair deficiency in NONO knockout murine embryonic fibroblasts and compensation by spontaneous upregulation of the PSPC1 paralog. Nucleic Acids Res *42*, 9771-9780.
228. Li, Y., and Altman, S. (2002). Partial reconstitution of human RNase P in HeLa cells between its RNA subunit with an affinity tag and the intact protein components. Nucleic Acids Res *30*, 3706-3711.
229. Lidsky, P.V., Hato, S., Bardina, M.V., Aminev, A.G., Palmenberg, A.C., Sheval, E.V., Polyakov, V.Y., van Kuppeveld, F.J., and Agol, V.I. (2006). Nucleocytoplasmic traffic disorder induced by cardioviruses. J Virol *80*, 2705-2717.
230. Lin, J.-Y., Brewer, G., and Li, M.-L. (2015). HuR and Ago2 bind the internal ribosome entry site of enterovirus 71 and promote virus translation and replication. PLoS One *10*, e0140291.
231. Lin, J.-Y., Li, M.-L., and Brewer, G. (2014). mRNA Decay Factor AUF1 Binds the Internal Ribosomal Entry Site of Enterovirus 71 and Inhibits Virus Replication. PLoS One *9*, e103827.
232. Lin, J.-Y., Li, M.-L., Huang, P.-N., Chien, K.-Y., Horng, J.-T., and Shih, S.-R. (2008). Heterogeneous nuclear ribonuclear protein K interacts with the enterovirus 71 5′ untranslated region and participates in virus replication. J Gen Virol *89*, 2540-2549.

233. Lin, J.-Y., Li, M.-L., and Shih, S.-R. (2009a). Far upstream element binding protein 2 interacts with enterovirus 71 internal ribosomal entry site and negatively regulates viral translation. Nucleic Acids Res *37*, 47-59.
234. Lin, J.-Y., Shih, S.-R., Pan, M., Li, C., Lue, C.-F., Stollar, V., and Li, M.-L. (2009b). hnRNP A1 interacts with the 5′ untranslated regions of enterovirus 71 and Sindbis virus RNA and is required for viral replication. J Virol *83*, 6106-6114.
235. Liu, Y., Wang, C., Mueller, S., Paul, A.V., Wimmer, E., and Jiang, P. (2010). Direct interaction between two viral proteins, the nonstructural protein 2C ATPase and the capsid protein VP3, is required for enterovirus morphogenesis.
236. Liu, Y.-C., Kuo, R.-L., Lin, J.-Y., Huang, P.-N., Huang, Y., Liu, H., Arnold, J.J., Chen, S.-J., Wang, R.Y.-L., Cameron, C.E.*, et al.* (2014). Cytoplasmic Viral RNA-Dependent RNA Polymerase Disrupts the Intracellular Splicing Machinery by Entering the Nucleus and Interfering with Prp8. PLoS Pathog *10*, e1004199.
237. Lukong, K.E., Huot, M.-É., and Richard, S. (2009). BRK phosphorylates PSF promoting its cytoplasmic localization and cell cycle arrest. Cell Sig *21*, 1415-1422.
238. Luz, N., and Beck, E. (1991). Interaction of a cellular 57-kilodalton protein with the internal translation initiation site of foot-and-mouth disease virus. J Virol *65*, 6486-6494.
239. Maciejewski, S., Nguyen, J.H., Gómez-Herreros, F., Cortés-Ledesma, F., Caldecott, K.W., and Semler, B.L. (2016). Divergent requirement for a DNA repair enzyme during enterovirus infections. Mbio *7*, e01931-01915.
240. Mäkelä, M.J., Puhakka, T., Ruuskanen, O., Leinonen, M., Saikku, P., Kimpimäki, M., Blomqvist, S., Hyypiä, T., and Arstila, P. (1998). Viruses and bacteria in the etiology of the common cold. Journal of clinical microbiology *36*, 539-542.
241. Mallia, P., Message, S.D., Gielen, V., Contoli, M., Gray, K., Kebadze, T., Aniscenko, J., Laza-Stanca, V., Edwards, M.R., and Slater, L. (2011). Experimental rhinovirus infection as a human model of chronic obstructive pulmonary disease exacerbation. American journal of respiratory and critical care medicine *183*, 734-742.
242. Martin, U., Jarasch, N., Nestler, M., Rassmann, A., Munder, T., Seitz, S., Zell, R., Wutzler, P., and Henke, A. (2007). Antiviral effects of pan-caspase inhibitors on the replication of coxsackievirus B3. Apoptosis *12*, 525-533.
243. Martínez-Salas, E., Francisco-Velilla, R., Fernandez-Chamorro, J., Lozano, G., and Diaz-Toledano, R. (2015). Picornavirus IRES elements: RNA structure and host protein interactions. Virus Res, In Press.
244. McAfee, J., Shahied-Milam, L., Soltaninassab, S., and LeStourgeon, W. (1996). A major determinant of hnRNP C protein binding to RNA is a novel bZIP-like RNA binding domain. RNA *2*, 1139.
245. McBride, A., Schlegel, A., and Kirkegaard, K. (1996). Human protein Sam68 relocalization and interaction with poliovirus RNA polymerase in infected cells. Proc Natl Acad Sci U S A *93*, 2296-2301.
246. McIntyre, C.L., Knowles, N.J., and Simmonds, P. (2013). Proposals for the classification of human rhinovirus species A, B and C into genotypically assigned types. J Gen Virol *94*, 1791-1806.
247. McLean, G.R. (2014). Developing a vaccine for human rhinoviruses. Journal of vaccines & immunization *2*, 16.
248. Medvedkina, O., Scarlat, I., Kalinina, N., and Agol, V. (1974). Virus-specific proteins associated with ribosomes of Krebs-II cells infected with encephalomyocarditis virus. FEBS Lett *39*, 4-8.
249. Meerovitch, K., Pelletier, J., and Sonenberg, N. (1989). A cellular protein that binds to the 5'-noncoding region of poliovirus RNA: implications for internal translation initiation. Genes Dev *3*, 1026-1034.
250. Meerovitch, K., Svitkin, Y., Lee, H., Lejbkowicz, F., Kenan, D., Chan, E., Agol, V., Keene, J., and Sonenberg, N. (1993). La autoantigen enhances and corrects aberrant translation of poliovirus RNA in reticulocyte lysate. J Virol *67*, 3798-3807.
251. Mello, C., Aguayo, E., Rodriguez, M., Lee, G., Jordan, R., Cihlar, T., and Birkus, G. (2014). Multiple classes of antiviral agents exhibit in vitro activity against human rhinovirus type C. Antimicrobial agents and chemotherapy *58*, 1546-1555.
252. Melton, A.A., Jackson, J., Wang, J., and Lynch, K.W. (2007). Combinatorial control of signal-induced exon repression by hnRNP L and PSF. Mol Cell Biol *27*, 6972-6984.
253. Merrill, M.K., Dobrikova, E.Y., and Gromeier, M. (2006). Cell-type-specific repression of internal ribosome entry site activity by double-stranded RNA-binding protein 76. J Virol *80*, 3147-3156.
254. Merrill, M.K., and Gromeier, M. (2006). The double-stranded RNA binding protein 76: NF45 heterodimer inhibits translation initiation at the rhinovirus type 2 internal ribosome entry site. J Virol *80*, 6936-6942.

255. Mi, H., Huang, X., Muruganujan, A., Tang, H., Mills, C., Kang, D., and Thomas, P.D. (2016). PANTHER version 11: expanded annotation data from Gene Ontology and Reactome pathways, and data analysis tool enhancements. Nucleic Acids Res *45*, D183-D189.
256. Michael, W.M., Eder, P.S., and Dreyfuss, G. (1997). The K nuclear shuttling domain: a novel signal for nuclear import and nuclear export in the hnRNP K protein. EMBO J *16*, 3587-3598.
257. Molla, A., Paul, A.V., and Wimmer, E. (1991). Cell-free, de novo synthesis of poliovirus. Science *254*, 1647-1651.
258. Monie, T.P., Perrin, A.J., Birtley, J.R., Sweeney, T.R., Karakasiliotis, I., Chaudhry, Y., Roberts, L.O., Matthews, S., Goodfellow, I.G., and Curry, S. (2007). Structural insights into the transcriptional and translational roles of Ebp1. EMBO J *26*, 3936-3944.
259. Monto, A.S. (1994). Studies of the community and family: acute respiratory illness and infection. Epidemiologic reviews *16*, 351-373.
260. Morozumi, Y., Takizawa, Y., Takaku, M., and Kurumizaka, H. (2009). Human PSF binds to RAD51 and modulates its homologous-pairing and strand-exchange activities. Nucleic Acids Res *37*, 4296-4307.
261. Mueller, S., and Wimmer, E. (1998). Expression of foreign proteins by poliovirus polyprotein fusion: analysis of genetic stability reveals rapid deletions and formation of cardioviruslike open reading frames. J Virol *72*, 20-31.
262. Nagashima, S., Sasaki, J., and Taniguchi, K. (2008). Interaction between polypeptide 3ABC and the 5′-terminal structural elements of the genome of Aichi virus: implication for negative-strand RNA synthesis. J Virol *82*, 6161-6171.
263. Nakielny, S., and Dreyfuss, G. (1996). The hnRNP C proteins contain a nuclear retention sequence that can override nuclear export signals. J Cell Biol *134*, 1365-1373.
264. Nakielny, S., Shaikh, S., Burke, B., and Dreyfuss, G. (1999). Nup153 is an M9-containing mobile nucleoporin with a novel Ran-binding domain. EMBO J *18*, 1982-1995.
265. Nateri, A.S., Hughes, P.J., and Stanway, G. (2002). Terminal RNA replication elements in human parechovirus 1. J Virol *76*, 13116-13122.
266. Neznanov, N., Kondratova, A., Chumakov, K.M., Angres, B., Zhumabayeva, B., Agol, V.I., and Gudkov, A.V. (2001). Poliovirus protein 3A inhibits tumor necrosis factor (TNF)-induced apoptosis by eliminating the TNF receptor from the cell surface. J Virol *75*, 10409-10420.
267. Nicklin, M.J., Toyoda, H., Murray, M.G., and Wimmer, E. (1986). Proteolytic processing in the replication of polio and related viruses. Nature Biotechnology *4*, 33-42.
268. Niepmann, M. (1996). Porcine polypyrimidine tract-binding protein stimulates translation initiation at the internal ribosome entry site of foot-and-mouth-disease virus. FEBS Lett *388*, 39-42.
269. Niranjanakumari, S., Lasda, E., Brazas, R., and Garcia-Blanco, M.A. (2002). Reversible cross-linking combined with immunoprecipitation to study RNA–protein interactions in vivo. Methods *26*, 182-190.
270. Novak, J.E., and Kirkegaard, K. (1991). Improved method for detecting poliovirus negative strands used to demonstrate specificity of positive-strand encapsidation and the ratio of positive to negative strands in infected cells. J Virol *65*, 3384-3387.
271. Novak, J.E., and Kirkegaard, K. (1994). Coupling between genome translation and replication in an RNA virus. Genes Dev *8*, 1726-1737.
272. Ogram, S.A., Spear, A., Sharma, N., and Flanegan, J.B. (2010). The 5′ CL-PCBP RNP complex, 3′ poly (A) tail and 2A pro are required for optimal translation of poliovirus RNA. Virology *397*, 14-22.
273. Oh, Y., Hahm, B., Kim, Y., Lee, H., Lee, J., Song, O., Tsukiyama-Kohara, K., Kohara, M., Nomoto, A., and Jang, S. (1998). Determination of functional domains in polypyrimidine-tract-binding protein. Biochem J *331*, 169-175.
274. Ohlmann, T., Rau, M., Morley, S.J., and Pain, V.M. (1995). Proteolytic cleavage of initiation factor elF-4γ in the reticulocyte lysate inhibits translation of capped mRNAs but enhances that of uncapped mRNAs. Nucleic Acids Res *23*, 334-340.
275. Ohlmann, T., Rau, M., Pain, V.M., and Morley, S.J. (1996). The C-terminal domain of eukaryotic protein synthesis initiation factor (eIF) 4G is sufficient to support cap-independent translation in the absence of eIF4E. EMBO J *15*, 1371.
276. Pacheco, A., de Quinto, S.L., Ramajo, J., Fernández, N., and Martínez-Salas, E. (2008a). A novel role for Gemin5 in mRNA translation. Nucleic Acids Res *37*, 582-590.

277. Pacheco, A., Reigadas, S., and Martínez-Salas, E. (2008b). Riboproteomic analysis of polypeptides interacting with the internal ribosome-entry site element of foot-and-mouth disease viral RNA. Proteomics *8*, 4782-4790.
278. Paige, J.S., Wu, K.Y., and Jaffrey, S.R. (2011). RNA mimics of green fluorescent protein. Science *333*, 642-646.
279. Palmenberg, A., Neubauer, D., and Skern, T. (2010). Genome Organization and Encoded Proteins. In The picornaviruses, E. Ehrenfeld, E. Domingo, and R.P. Roos, eds. (ASM Press, Washington, DC), pp. 3-17.
280. Panchapakesan, S.S.S., Ferguson, M.L., Hayden, E.J., Chen, X., Hoskins, A.A., and Unrau, P.J. (2017). Ribonucleoprotein purification and characterization using RNA Mango. RNA *23*, 1592-1599.
281. Panda, A.C., Abdelmohsen, K., Martindale, J.L., Di Germanio, C., Yang, X., Grammatikakis, I., Noh, J.H., Zhang, Y., Lehrmann, E., and Dudekula, D.B. (2016a). Novel RNA-binding activity of MYF5 enhances Ccnd1/Cyclin D1 mRNA translation during myogenesis. Nucleic Acids Res *44*, 2393-2408.
282. Panda, A.C., Martindale, J.L., and Gorospe, M. (2016b). Affinity Pulldown of Biotinylated RNA for Detection of Protein-RNA Complexes. Bio-protocol *6*.
283. Panda, D., Pascual-Garcia, P., Dunagin, M., Tudor, M., Hopkins, K.C., Xu, J., Gold, B., Raj, A., Capelson, M., and Cherry, S. (2014). Nup98 promotes antiviral gene expression to restrict RNA viral infection in Drosophila. Proc Natl Acad Sci U S A *111*, E3890-E3899.
284. Papi, A., and Contoli, M. (2011). Rhinovirus vaccination: the case against. European Respiratory Journal *37*, 5-7.
285. Park, N., Katikaneni, P., Skern, T., and Gustin, K.E. (2008). Differential targeting of nuclear pore complex proteins in poliovirus-infected cells. J Virol *82*, 1647-1655.
286. Park, N., Schweers, N.J., and Gustin, K.E. (2015). Selective removal of FG repeat domains from the nuclear pore complex by enterovirus 2Apro. J Virol *89*, 11069-11079.
287. Park, N., Skern, T., and Gustin, K.E. (2010). Specific cleavage of the nuclear pore complex protein Nup62 by a viral protease. J Biol Chem *285*, 28796-28805.
288. Parsley, T., Towner, J., Blyn, L., Ehrenfeld, E., and Semler, B. (1997). Poly (rC) binding protein 2 forms a ternary complex with the 5'-terminal sequences of poliovirus RNA and the viral 3CD proteinase. RNA *3*, 1124-1134.
289. Patton, J.G., Porro, E., Galceran, J., Tempst, P., and Nadal-Ginard, B. (1993). Cloning and characterization of PSF, a novel pre-mRNA splicing factor. Genes Dev *7*, 393-406.
290. Paul, A.V., Molla, A., and Wimmer, E. (1994). Studies of a putative amphipathic helix in the N-terminus of poliovirus protein 2C. Virology *199*, 188-199.
291. Peng, R., Dye, B.T., Pérez, I., Barnard, D.C., Thompson, A.B., and Patton, J.G. (2002). PSF and p54 nrb bind a conserved stem in U5 snRNA. RNA *8*, 1334-1347.
292. Penman, S. (1966). RNA metabolism in the HeLa cell nucleus. J Mol Biol *17*, 117IN114-130.
293. Perera, R., Daijogo, S., Walter, B.L., Nguyen, J.H., and Semler, B.L. (2007). Cellular protein modification by poliovirus: the two faces of poly (rC)-binding protein. J Virol *81*, 8919-8932.
294. Pestova, T.V., Hellen, C., and Shatsky, I.N. (1996). Canonical eukaryotic initiation factors determine initiation of translation by internal ribosomal entry. Mol Cell Biol *16*, 6859-6869.
295. Pfister, T., Egger, D., and Bienz, K. (1995). Poliovirus subviral particles associated with progeny RNA in the replication complex. J Gen Virol *76*, 63-71.
296. Pfister, T., Jones, K.W., and Wimmer, E. (2000). A Cysteine-Rich Motif in Poliovirus Protein 2CATPaseIs Involved in RNA Replication and Binds Zinc In Vitro. J Virol *74*, 334-343.
297. Pfister, T., Pasamontes, L., Troxler, M., Egger, D., and Bienz, K. (1992). Immunocytochemical localization of capsid-related particles in subcellular fractions of poliovirus-infected cells. Virology *188*, 676-684.
298. Pilipenko, E.V., Gmyl, A.P., Maslova, S.V., Svitkin, Y.V., Sinyakov, A.N., and Agol, V.I. (1992a). Prokaryotic-like cis elements in the cap-independent internal initiation of translation on picornavirus RNA. Cell *68*, 119-131.
299. Pilipenko, E.V., Maslova, S.V., Sinyakov, A.N., and Agol, V.I. (1992b). Towards identification of cis-acting elements involved in the replication of enterovirus and rhinovirus RNAs: a proposal for the existence of tRNA-like terminal structures. Nucleic Acids Res *20*, 1739-1745.
300. Pilipenko, E.V., Pestova, T.V., Kolupaeva, V.G., Khitrina, E.V., Poperechnaya, A.N., Agol, V.I., and Hellen, C.U. (2000). A cell cycle-dependent protein serves as a template-specific translation initiation factor. Genes Dev *14*, 2028-2045.

301. Pilipenko, E.V., Viktorova, E.G., Guest, S.T., Agol, V.I., and Roos, R.P. (2001). Cell-specific proteins regulate viral RNA translation and virus-induced disease. EMBO J *20*, 6899-6908.
302. Pincus, S.E., Diamond, D.C., Emini, E.A., and Wimmer, E. (1986). Guanidine-selected mutants of poliovirus: mapping of point mutations to polypeptide 2C. J Virol *57*, 638-646.
303. Piñeiro, D., Fernández, N., Ramajo, J., and Martínez-Salas, E. (2012a). Gemin5 promotes IRES interaction and translation control through its C-terminal region. Nucleic Acids Res, 1-12.
304. Piñeiro, D., Ramajo, J., Bradrick, S.S., and Martínez-Salas, E. (2012b). Gemin5 proteolysis reveals a novel motif to identify L protease targets. Nucleic Acids Res *40*, 4942-4953.
305. Piñol-Roma, S., and Dreyfuss, G. (1992). Shuttling of pre-mRNA binding proteins between nucleus and cytoplasm. Nature *355*, 730-732.
306. Piñol-Roma, S., and Dreyfuss, G. (1993). hnRNP proteins: localization and transport between the nucleus and the cytoplasm. Trends Cell Biol *3*, 151-155.
307. Pollack, R., and Goldman, R. (1973). Synthesis of infective poliovirus in BSC-1 monkey cells enucleated with cytochalasin B. Science *179*, 915-916.
308. Porter, F.W., Bochkov, Y.A., Albee, A.J., Wiese, C., and Palmenberg, A.C. (2006). A picornavirus protein interacts with Ran-GTPase and disrupts nucleocytoplasmic transport. Proc Natl Acad Sci U S A *103*, 12417-12422.
309. Porter, F.W., Brown, B., and Palmenberg, A.C. (2010). Nucleoporin phosphorylation triggered by the encephalomyocarditis virus leader protein is mediated by mitogen-activated protein kinases. J Virol *84*, 12538-12548.
310. Porter, F.W., and Palmenberg, A.C. (2009). Leader-induced phosphorylation of nucleoporins correlates with nuclear trafficking inhibition by cardioviruses. J Virol *83*, 1941-1951.
311. Powers, M.A., Forbes, D.J., Dahlberg, J.E., and Lund, E. (1997). The vertebrate GLFG nucleoporin, Nup98, is an essential component of multiple RNA export pathways. J Cell Biol *136*, 241-250.
312. Racaniello, V.R. (2013). Picornaviridae: The Viruses and Their Replication. In Fields Virology, D.M. Knipe, and P.M. Howley, eds. (Lippincott Williams & Wilkins), pp. 453-489.
313. Rai, D.K., Lawrence, P., Kloc, A., Schafer, E., and Rieder, E. (2015). Analysis of the interaction between host factor Sam68 and viral elements during foot-and-mouth disease virus infections. Virology journal *12*, 224.
314. Ray, P., Kar, A., Fushimi, K., Havlioglu, N., Chen, X., and Wu, J.Y. (2011). PSF suppresses tau exon 10 inclusion by interacting with a stem-loop structure downstream of exon 10. Journal of Molecular Neuroscience *45*, 453.
315. Ray, P.S., and Das, S. (2002). La autoantigen is required for the internal ribosome entry site-mediated translation of Coxsackievirus B3 RNA. Nucleic Acids Res *30*, 4500-4508.
316. Reichelt, R., Holzenburg, A., Buhle, E., Jarnik, M., Engel, A., and Aebi, U. (1990). Correlation between structure and mass distribution of the nuclear pore complex and of distinct pore complex components. J Cell Biol *110*, 883-894.
317. Rexach, M., and Blobel, G. (1995). Protein import into nuclei: association and dissociation reactions involving transport substrate, transport factors, and nucleoporins. Cell *83*, 683-692.
318. Ribbeck, K., and Görlich, D. (2001). Kinetic analysis of translocation through nuclear pore complexes. EMBO J *20*, 1320-1330.
319. Ricour, C., Borghese, F., Sorgeloos, F., Hato, S.V., van Kuppeveld, F.J., and Michiels, T. (2009a). Random mutagenesis defines a domain of Theiler's virus leader protein that is essential for antagonism of nucleocytoplasmic trafficking and cytokine gene expression. J Virol *83*, 11223-11232.
320. Ricour, C., Delhaye, S., Hato, S.V., Olenyik, T.D., Michel, B., van Kuppeveld, F.J., Gustin, K.E., and Michiels, T. (2009b). Inhibition of mRNA export and dimerization of interferon regulatory factor 3 by Theiler's virus leader protein. J Gen Virol *90*, 177-186.
321. Rodrguez, P.L., and Carrasco, L. (1995). Poliovirus protein 2C contains two regions involved in RNA binding activity. J Biol Chem *270*, 10105-10112.
322. Roehl, H.H., and Semler, B.L. (1995). Poliovirus infection enhances the formation of two ribonucleoprotein complexes at the 3'end of viral negative-strand RNA. J Virol *69*, 2954-2961.
323. Rohde, G. (2011). Rhinovirus vaccination: the case in favour (Eur Respiratory Soc), pp. 3-4.
324. Romanelli, M.G., Weighardt, F., Biamonti, G., Riva, S., and Morandi, C. (1997). Sequence determinants for hnRNP I protein nuclear localization. Exp Cell Res *235*, 300-304.

325. Romanova, L.I., Lidsky, P.V., Kolesnikova, M.S., Fominykh, K.V., Gmyl, A.P., Sheval, E.V., Hato, S.V., van Kuppeveld, F.J., and Agol, V.I. (2009). Antiapoptotic activity of the cardiovirus leader protein, a viral "security" protein. J Virol *83*, 7273-7284.
326. Royston, L., and Tapparel, C. (2016). Rhinoviruses and respiratory enteroviruses: not as simple as ABC. Viruses *8*, 16.
327. Rozovics, J.M., Chase, A.J., Cathcart, A.L., Chou, W., Gershon, P.D., Palusa, S., Wilusz, J., and Semler, B.L. (2012). Picornavirus modification of a host mRNA decay protein. Mbio *3*, e00431-00412.
328. Rubinstein, S.J., Hammerle, T., Wimmer, E., and Dasgupta, A. (1992). Infection of HeLa cells with poliovirus results in modification of a complex that binds to the rRNA promoter. J Virol *66*, 3062-3068.
329. Russell, J., and Zomerdijk, J.C. (2006). The RNA polymerase I transcription machinery. Paper presented at: Biochemical Society symposium (Europe PMC Funders).
330. Rust, R.C., Landmann, L., Gosert, R., Tang, B.L., Hong, W., Hauri, H.-P., Egger, D., and Bienz, K. (2001). Cellular COPII proteins are involved in production of the vesicles that form the poliovirus replication complex. J Virol *75*, 9808-9818.
331. Ryan, K.J., and Wente, S.R. (2000). The nuclear pore complex: a protein machine bridging the nucleus and cytoplasm. Current opinion in cell biology *12*, 361-371.
332. Salton, M., Lerenthal, Y., Wang, S.-Y., Chen, D.J., and Shiloh, Y. (2010). Involvement of Matrin 3 and SFPQ/NONO in the DNA damage response. Cell Cycle *9*, 1568-1576.
333. Sanchez-Aparicio, M.T., Rosas, M.F., and Sobrino, F. (2013). Characterization of a nuclear localization signal in the foot-and-mouth disease virus polymerase. Virology *444*, 203-210.
334. Sanford, J.R., Gray, N.K., Beckmann, K., and Cáceres, J.F. (2004). A novel role for shuttling SR proteins in mRNA translation. Genes Dev *18*, 755-768.
335. Sarnow, P. (1989). Role of 3'-end sequences in infectivity of poliovirus transcripts made in vitro. J Virol *63*, 467-470.
336. Sawicka, K., Bushell, M., Spriggs, K., and Willis, A. (2008). Polypyrimidine-tract-binding protein: a multifunctional RNA-binding protein. Biochem Soc Trans *36*, 641-647.
337. Schlegel, A., Giddings, T.H., Ladinsky, M.S., and Kirkegaard, K. (1996). Cellular origin and ultrastructure of membranes induced during poliovirus infection. J Virol *70*, 6576-6588.
338. Schwoebel, E.D., Talcott, B., Cushman, I., and Moore, M.S. (1998). Ran-dependent signal-mediated nuclear import does not require GTP hydrolysis by Ran. J Biol Chem *273*, 35170-35175.
339. Sean, P., Nguyen, J.H., and Semler, B.L. (2009). Altered interactions between stem-loop IV within the 5′ noncoding region of coxsackievirus RNA and poly (rC) binding protein 2: effects on IRES-mediated translation and viral infectivity. Virology *389*, 45-58.
340. Semler, B.L., and Waterman, M.L. (2008). IRES-mediated pathways to polysomes: nuclear versus cytoplasmic routes. Trends Microbiol *16*, 1-5.
341. Shah, S., Tugendreich, S., and Forbes, D. (1998). Major binding sites for the nuclear import receptor are the internal nucleoporin Nup153 and the adjacent nuclear filament protein Tpr. J Cell Biol *141*, 31-49.
342. Sharathchandra, A., Lal, R., Khan, D., and Das, S. (2012). Annexin A2 and PSF proteins interact with p53 IRES and regulate translation of p53 mRNA. RNA biology *9*, 1429-1439.
343. Sharma, R., Raychaudhuri, S., and Dasgupta, A. (2004). Nuclear entry of poliovirus protease-polymerase precursor 3CD: implications for host cell transcription shut-off. Virology *320*, 195-205.
344. Shav-Tal, Y., Cohen, M., Lapter, S., Dye, B., Patton, J.G., Vandekerckhove, J., and Zipori, D. (2001). Nuclear relocalization of the pre-mRNA splicing factor PSF during apoptosis involves hyperphosphorylation, masking of antigenic epitopes, and changes in protein interactions. Mol Biol Cell *12*, 2328-2340.
345. Shen, Y., Igo, M., Yalamanchili, P., Berk, A.J., and Dasgupta, A. (1996). DNA binding domain and subunit interactions of transcription factor IIIC revealed by dissection with poliovirus 3C protease. Mol Cell Biol *16*, 4163-4171.
346. Shiroki, K., Isoyama, T., Kuge, S., Ishii, T., Ohmi, S., Hata, S., Suzuki, K., Takasaki, Y., and Nomoto, A. (1999). Intracellular redistribution of truncated La protein produced by poliovirus 3Cpro-mediated cleavage. J Virol *73*, 2193-2200.
347. Silvera, D., Gamarnik, A.V., and Andino, R. (1999). The N-terminal K homology domain of the poly (rC)-binding protein is a major determinant for binding to the poliovirus 5′-untranslated region and acts as an inhibitor of viral translation. J Biol Chem *274*, 38163-38170.
348. Simons, F.H., Broers, F.J., van Venrooij, W.J., and Pruijn, G.J. (1996). Characterization ofcis-Acting Signals for Nuclear Import and Retention of the La (SS-B) Autoantigen. Exp Cell Res *224*, 224-236.

349. Siomi, H., Choi, M., Siomi, M.C., Nussbaum, R.L., and Dreyfuss, G. (1994). Essential role for KH domains in RNA binding: impaired RNA binding by a mutation in the KH domain of FMR1 that causes fragile X syndrome. Cell *77*, 33-39.
350. Song, Y., Tzima, E., Ochs, K., Bassili, G., Trusheim, H., Linder, M., Preissner, K.T., and Niepmann, M. (2005). Evidence for an RNA chaperone function of polypyrimidine tract-binding protein in picornavirus translation. RNA *11*, 1809-1824.
351. Spector, D.H., and Baltimore, D. (1974). Requirement of 3′-terminal poly (adenylic acid) for the infectivity of poliovirus RNA. Proc Natl Acad Sci U S A *71*, 2983-2987.
352. Spriggs, K., Bushell, M., Mitchell, S., and Willis, A. (2005). Internal ribosome entry segment-mediated translation during apoptosis: the role of IRES-trans-acting factors. Cell Death & Diff *12*, 585-591.
353. Spurrell, J.C., Wiehler, S., Zaheer, R.S., Sanders, S.P., and Proud, D. (2005). Human airway epithelial cells produce IP-10 (CXCL10) in vitro and in vivo upon rhinovirus infection. American Journal of Physiology-Lung Cellular and Molecular Physiology *289*, L85-L95.
354. Srisawat, C., and Engelke, D.R. (2001). Streptavidin aptamers: affinity tags for the study of RNAs and ribonucleoproteins. RNA *7*, 632-641.
355. Srisawat, C., and Engelke, D.R. (2002). RNA affinity tags for purification of RNAs and ribonucleoprotein complexes. Methods *26*, 156-161.
356. Srisawat, C., Goldstein, I.J., and Engelke, D.R. (2001). Sephadex-binding RNA ligands: rapid affinity purification of RNA from complex RNA mixtures. Nucleic Acids Res *29*, e4-e4.
357. Stefano, J.E. (1984). Purified lupus antigen La recognizes an oligouridylate stretch common to the 3′ termini of RNA polymerase III transcripts. Cell *36*, 145-154.
358. Suhy, D.A., Giddings, T.H., and Kirkegaard, K. (2000). Remodeling the endoplasmic reticulum by poliovirus infection and by individual viral proteins: an autophagy-like origin for virus-induced vesicles. J Virol *74*, 8953-8965.
359. Svitkin, Y.V., Hahn, H., Gingras, A.-C., Palmenberg, A.C., and Sonenberg, N. (1998). Rapamycin and wortmannin enhance replication of a defective encephalomyocarditis virus. J Virol *72*, 5811-5819.
360. Svitkin, Y.V., and Sonenberg, N. (2003). Cell-free synthesis of encephalomyocarditis virus. J Virol *77*, 6551-6555.
361. Sweeney, T.R., Abaeva, I.S., Pestova, T.V., and Hellen, C.U. (2014). The mechanism of translation initiation on Type 1 picornavirus IRESs. EMBO J *33*, 76-92.
362. Sweeney, T.R., Dhote, V., Yu, Y., and Hellen, C.U. (2012). A distinct class of internal ribosomal entry site in members of the Kobuvirus and proposed Salivirus and Paraturdivirus genera of the Picornaviridae. J Virol *86*, 1468-1486.
363. Tamura, T., Fukuhara, T., Uchida, T., Ono, C., Mori, H., Sato, A., Fauzyah, Y., Okamoto, T., Kurosu, T., and Setoh, Y.X. (2018). Characterization of Recombinant Flaviviridae Viruses Possessing a Small Reporter Tag. J Virol *92*, e01582-01517.
364. Tani, H., Mizutani, R., Salam, K.A., Tano, K., Ijiri, K., Wakamatsu, A., Isogai, T., Suzuki, Y., and Akimitsu, N. (2012). Genome-wide determination of RNA stability reveals hundreds of short-lived noncoding transcripts in mammals. Genome research *22*, 947-956.
365. Tay, M., Fraser, J., Chan, W., Moreland, N., Rathore, A., Wang, C., Vasudevan, S., and Jans, D. (2013). Nuclear localization of dengue virus (DENV) 1–4 non-structural protein 5; protection against all 4 DENV serotypes by the inhibitor Ivermectin. Antiviral research *99*, 301-306.
366. Tershak, D. (1984). Association of poliovirus proteins with the endoplasmic reticulum. J Virol *52*, 777-783.
367. Tesar, M., and Marquardt, O. (1990). Foot-and-mouth disease virus protease 3C inhibits cellular transcription and mediates cleavage of histone H3. Virology *174*, 364-374.
368. Teterina, N.L., Gorbalenya, A.E., Egger, D., Bienz, K., and Ehrenfeld, E. (1997). Poliovirus 2C protein determinants of membrane binding and rearrangements in mammalian cells. J Virol *71*, 8962-8972.
369. Teterina, N.L., Levenson, E.A., and Ehrenfeld, E. (2010). Viable polioviruses that encode 2A proteins with fluorescent protein tags. J Virol *84*, 1477-1488.
370. Thandapani, P., O'Connor, T.R., Bailey, T.L., and Richard, S. (2013). Defining the RGG/RG motif. Mol Cell *50*, 613-623.
371. Thul, P.J., Åkesson, L., Wiking, M., Mahdessian, D., Geladaki, A., Blal, H.A., Alm, T., Asplund, A., Björk, L., and Breckels, L.M. (2017). A subcellular map of the human proteome. Science *356*, eaal3321.
372. Tian, W., Cui, Z., Zhang, Z., Wei, H., and Zhang, X. (2011). Poliovirus 2Apro induces the nucleic translocation of poliovirus 3CD and 3C′ proteins. Acta Biochim Biophys Sin *43*, 38-44.

373. Todd, S., Towner, J.S., Brown, D.M., and Semler, B.L. (1997). Replication-competent picornaviruses with complete genomic RNA 3'noncoding region deletions. J Virol *71*, 8868-8874.
374. Tolskaya, E.A., Romanova, L.I., Kolesnikova, M.S., Ivannikova, T.A., Smirnova, E.A., Raikhlin, N.T., and Agol, V.I. (1995). Apoptosis-inducing and apoptosis-preventing functions of poliovirus. J Virol *69*, 1181-1189.
375. Toyoda, H., Franco, D., Fujita, K., Paul, A.V., and Wimmer, E. (2007). Replication of poliovirus requires binding of the poly (rC) binding protein to the cloverleaf as well as to the adjacent C-rich spacer sequence between the cloverleaf and the internal ribosomal entry site. J Virol *81*, 10017-10028.
376. Toyoda, H., Nicklin, M.J., Murray, M.G., Anderson, C.W., Dunn, J.J., Studier, F.W., and Wimmer, E. (1986). A second virus-encoded proteinase involved in proteolytic processing of poliovirus polyprotein. Cell *45*, 761-770.
377. Tsai, B.P., Wang, X., Huang, L., and Waterman, M.L. (2011). Quantitative profiling of in vivo-assembled RNA-protein complexes using a novel integrated proteomic approach. Mol Cell Proteomics *10*, M110. 007385.
378. Tuschall, D.M., Hiebert, E., and Flanegan, J.B. (1982). Poliovirus RNA-dependent RNA polymerase synthesizes full-length copies of poliovirion RNA, cellular mRNA, and several plant virus RNAs in vitro. J Virol *44*, 209-216.
379. Van Pesch, V., Van Eyll, O., and Michiels, T. (2001). The leader protein of Theiler's virus inhibits immediate-early alpha/beta interferon production. J Virol *75*, 7811-7817.
380. Vasudevan, S., and Steitz, J.A. (2007). AU-rich-element-mediated upregulation of translation by FXR1 and Argonaute 2. Cell *128*, 1105-1118.
381. Vasudevan, S., Tong, Y., and Steitz, J.A. (2007). Switching from repression to activation: microRNAs can up-regulate translation. Science *318*, 1931-1934.
382. Verma, B., Bhattacharyya, S., and Das, S. (2010). Polypyrimidine tract-binding protein interacts with coxsackievirus B3 RNA and influences its translation. J Gen Virol *91*, 1245-1255.
383. Virgen-Slane, R., Rozovics, J.M., Fitzgerald, K.D., Ngo, T., Chou, W., Filippov, D.V., Gershon, P.D., and Semler, B.L. (2012). An RNA virus hijacks an incognito function of a DNA repair enzyme. Proc Natl Acad Sci U S A *109*, 14634-14639.
384. Vogt, D.A., and Andino, R. (2010). An RNA element at the 5′-end of the poliovirus genome functions as a general promoter for RNA synthesis. PLoS Pathog *6*, e1000936.
385. Waggoner, S., and Sarnow, P. (1998). Viral ribonucleoprotein complex formation and nucleolar-cytoplasmic relocalization of nucleolin in poliovirus-infected cells. J Virol *72*, 6699-6709.
386. Wagstaff, K.M., Sivakumaran, H., Heaton, S.M., Harrich, D., and Jans, D.A. (2012). Ivermectin is a specific inhibitor of importin α/β-mediated nuclear import able to inhibit replication of HIV-1 and dengue virus. Biochem J *443*, 851-856.
387. Walker, E., Jensen, L., Croft, S., Wei, K., Fulcher, A.J., Jans, D.A., and Ghildyal, R. (2016). Rhinovirus 16 2A protease affects nuclear localization of 3CD during infection. J Virol *90*, 11032-11042.
388. Walker, E.J., Jensen, L.M., Croft, S., and Ghildyal, R. (2015). Variation in the nuclear effects of infection by different human rhinovirus serotypes. Frontiers in microbiology *6*.
389. Walker, E.J., Younessi, P., Fulcher, A.J., McCuaig, R., Thomas, B.J., Bardin, P.G., Jans, D.A., and Ghildyal, R. (2013). Rhinovirus 3C protease facilitates specific nucleoporin cleavage and mislocalisation of nuclear proteins in infected host cells. PLoS One *8*, e71316.
390. Walker, S.C., Good, P.D., Gipson, T.A., and Engelke, D.R. (2011). The dual use of RNA aptamer sequences for affinity purification and localization studies of RNAs and RNA–protein complexes. In RNA Detection and Visualization (Springer), pp. 423-444.
391. Walker, S.C., Scott, F.H., Srisawat, C., and Engelke, D.R. (2008). RNA affinity tags for the rapid purification and investigation of RNAs and RNA–protein complexes. In RNA-Protein Interaction Protocols, R.-J. Lin, ed. (Humana Press), pp. 23-40.
392. Walter, B.L., Nguyen, J.H., Ehrenfeld, E., and Semler, B.L. (1999). Differential utilization of poly (rC) binding protein 2 in translation directed by picornavirus IRES elements. RNA *5*, 1570-1585.
393. Walter, B.L., Parsley, T.B., Ehrenfeld, E., and Semler, B.L. (2002). Distinct poly (rC) binding protein KH domain determinants for poliovirus translation initiation and viral RNA replication. J Virol *76*, 12008-12022.
394. Wan, L., Kim, J.-K., Pollard, V.W., and Dreyfuss, G. (2001). Mutational definition of RNA-binding and protein-protein interaction domains of heterogeneous nuclear RNP C1. J Biol Chem *276*, 7681-7688.

395. Wang, C., Sun, M., Yuan, X., Ji, L., Jin, Y., Cardona, C.J., and Xing, Z. (2017). Enterovirus 71 suppresses interferon responses by blocking Janus kinase (JAK)/signal transducer and activator of transcription (STAT) signaling through inducing karyopherin-α1 degradation. J Biol Chem *292*, 10262-10274.
396. Wang, T., Yu, B., Lin, L., Zhai, X., Han, Y., Qin, Y., Guo, Z., Wu, S., Zhong, X., and Wang, Y. (2012). A functional nuclear localization sequence in the VP1 capsid protein of coxsackievirus B3. Virology *433*, 513-521.
397. Warner, K.D., Chen, M.C., Song, W., Strack, R.L., Thorn, A., Jaffrey, S.R., and Ferré-D'Amaré, A.R. (2014). Structural basis for activity of highly efficient RNA mimics of green fluorescent protein. Nat Struct Mol Biol *21*, 658-663.
398. Watters, K., Inankur, B., Gardiner, J.C., Warrick, J., Sherer, N.M., Yin, J., and Palmenberg, A.C. (2017). Differential disruption of nucleocytoplasmic trafficking pathways by rhinovirus 2A proteases. J Virol *91*, e02472-02416.
399. Watters, K., and Palmenberg, A.C. (2011). Differential processing of nuclear pore complex proteins by rhinovirus 2A proteases from different species and serotypes. J Virol *85*, 10874-10883.
400. Weng, K.-F., Li, M.-L., Hung, C.-T., and Shih, S.-R. (2009). Enterovirus 71 3C protease cleaves a novel target CstF-64 and inhibits cellular polyadenylation. PLoS Pathog *5*, e1000593.
401. Wente, S.R., and Rout, M.P. (2010). The nuclear pore complex and nuclear transport. Cold Spring Harbor Pers in Biol *2*, a000562.
402. Wimmer, E., Hellen, C.U., and Cao, X. (1993). Genetics of poliovirus. Annu Rev Genet *27*, 353-436.
403. Wong, J., Si, X., Angeles, A., Zhang, J., Shi, J., Fung, G., Jagdeo, J., Wang, T., Zhong, Z., and Jan, E. (2013). Cytoplasmic redistribution and cleavage of AUF1 during coxsackievirus infection enhance the stability of its viral genome. FASEB J *27*, 2777-2787.
404. Wong, J., Zhang, J., Yanagawa, B., Luo, Z., Yang, X., Chang, J., McManus, B., and Luo, H. (2012). Cleavage of serum response factor mediated by enteroviral protease 2A contributes to impaired cardiac function. Cell research *22*, 360-371.
405. Xiang, Z., Liu, L., Lei, X., Zhou, Z., He, B., and Wang, J. (2016). 3C protease of enterovirus D68 inhibits cellular defense mediated by interferon regulatory factor 7. J Virol *90*, 1613-1621.
406. Yalamanchili, P., Banerjee, R., and Dasgupta, A. (1997a). Poliovirus-encoded protease 2APro cleaves the TATA-binding protein but does not inhibit host cell RNA polymerase II transcription in vitro. J Virol *71*, 6881-6886.
407. Yalamanchili, P., Datta, U., and Dasgupta, A. (1997b). Inhibition of host cell transcription by poliovirus: cleavage of transcription factor CREB by poliovirus-encoded protease 3Cpro. J Virol *71*, 1220-1226.
408. Yalamanchili, P., Harris, K., Wimmer, E., and Dasgupta, A. (1996). Inhibition of basal transcription by poliovirus: a virus-encoded protease (3Cpro) inhibits formation of TBP-TATA box complex in vitro. J Virol *70*, 2922-2929.
409. Yalamanchili, P., Weidman, K., and Dasgupta, A. (1997c). Cleavage of transcriptional activator Oct-1 by poliovirus encoded protease 3C pro. Virology *239*, 176-185.
410. Yarosh, C.A., Iacona, J.R., Lutz, C.S., and Lynch, K.W. (2015). PSF: nuclear busy-body or nuclear facilitator? Wiley Interdiscip Rev RNA *6*, 351-367.
411. Younessi, P., A Jans, D., and Ghildyal, R. (2012). Modulation of host cell nucleocytoplasmic trafficking during picornavirus infection. Infect Disord Drug Targets *12*, 59-67.
412. Ypma-Wong, M.F., Dewalt, P.G., Johnson, V.H., Lamb, J.G., and Semler, B.L. (1988). Protein 3CD is the major poliovirus proteinase responsible for cleavage of the P1 capsid precursor. Virology *166*, 265-270.
413. Yu, Y., Abaeva, I.S., Marintchev, A., Pestova, T.V., and Hellen, C.U. (2011a). Common conformational changes induced in type 2 picornavirus IRESs by cognate trans-acting factors. Nucleic Acids Res *39*, 4851-4865.
414. Yu, Y., Sweeney, T.R., Kafasla, P., Jackson, R.J., Pestova, T.V., and Hellen, C.U. (2011b). The mechanism of translation initiation on Aichivirus RNA mediated by a novel type of picornavirus IRES. EMBO J *30*, 4423-4436.
415. Zell, R., Ihle, Y., Effenberger, M., Seitz, S., Wutzler, P., and Görlach, M. (2008a). Interaction of poly (rC)-binding protein 2 domains KH1 and KH3 with coxsackievirus RNA. Biochem Biophys Res Commun *377*, 500-503.
416. Zell, R., Ihle, Y., Seitz, S., Gündel, U., Wutzler, P., and Görlach, M. (2008b). Poly (rC)-binding protein 2 interacts with the oligo (rC) tract of coxsackievirus B3. Biochem Biophys Res Commun *366*, 917-921.
417. Zhang, B., Seitz, S., Kusov, Y., Zell, R., and Gauss-Müller, V. (2007). RNA interaction and cleavage of poly (C)-binding protein 2 by hepatitis A virus protease. Biochem Biophys Res Commun *364*, 725-730.

418. Zhang, H., Song, L., Cong, H., and Tien, P. (2015). Nuclear protein Sam68 interacts with the enterovirus 71 internal ribosome entry site and positively regulates viral protein translation. J Virol *89*, 10031-10043.
419. Zheng, Z., Li, H., Zhang, Z., Meng, J., Mao, D., Bai, B., Lu, B., Mao, P., Hu, Q., and Wang, H. (2011). Enterovirus 71 2C protein inhibits TNF-α–mediated activation of NF-κB by suppressing IκB kinase β phosphorylation. The Journal of Immunology *187*, 2202-2212.
420. Zoll, J., Melchers, W.J., Galama, J.M., and van Kuppeveld, F.J. (2002). The mengovirus leader protein suppresses alpha/beta interferon production by inhibition of the iron/ferritin-mediated activation of NF-κB. J Virol *76*, 9664-9672.
421. Zolotukhin, A.S., Michalowski, D., Bear, J., Smulevitch, S.V., Traish, A.M., Peng, R., Patton, J., Shatsky, I.N., and Felber, B.K. (2003). PSF acts through the human immunodeficiency virus type 1 mRNA instability elements to regulate virus expression. Mol Cell Biol *23*, 6618-6630.
422. Zou, G., Xu, H.Y., Qing, M., Wang, Q.-Y., and Shi, P.-Y. (2011). Development and characterization of a stable luciferase dengue virus for high-throughput screening. Antiviral research *91*, 11-19.

APPENDIX

Proteins that decrease in abundance in the nucleus and increase in abundance in the cytoplasm of HRV16-infected HeLa cells

All (277) accessions for which at least one of the replicate 8hr:mock nuclear abundance ratios was < 1, and at least one of the replicate 8hr:mock cytoplasmic abundance ratios for the same accession was > 1. Empty cells correspond to accessions that were either undetected in a particular dataset, or detected but no peptide quants passed quality thresholds. Values under each of the four datasets ('Nuc1', 'Nuc2', 'Cyto1', 'Cyto2') take the form 'x/y/z' in which an 8hr:mock abundance ratio of x (geometric mean of relevant, quantifiable tryptic peptides) was based on z tryptic peptide species, y of which tracked the direction (< 1 or > 1) of x. For example "0.372/26/26" represents an overall 8hpi:mock abundance ratio of 0.372 with 26 tryptic peptides following this trend out of a total of 26 tryptic peptides species identified corresponding to the respective accession within the dataset.

Acce-ssion	Protein name	Nuc1	Nuc2	Cyto1	Cyto2
6PGL	6-phosphogluconolactonase	0.4147/3/3		1.0082/5/7	
ABLM1	Actin-binding LIM protein	0.1907/7/7			1.266/1/1
ACINU	Apoptotic chromatin condensation inducer in the nucleus		0.3979/8/8		3.0097/4/4
ACSL4	Long-chain-fatty-acid--CoA ligase 4	0.0322/2/3	0/1/1	2.0131/4/4	
ACTBL	Beta-actin-like protein 2	0.1351/10/11			2.189/4/9
ACTC	Actin, alpha cardiac muscle 1	0.137/18/19			2.4417/2/9
ADAS	Alkyldihydroxyacetonephosphat e synthase, peroxisomal	0.3047/1/2		6.434/1/1	2.0968/10/11
AL3B1	Aldehyde dehydrogenase family 3 member B1	0.4968/1/1		12.7593/2/2	1.2133/3/3
AL9A1	4-trimethylaminobutyraldehyde dehydrogenase	0.0152/1/1		1.9628/4/4	

Acce-ssion	Protein name	Nuc1	Nuc2	Cyto1	Cyto2
ANX11	Annexin A11	0.473/1/1		2.4844/4/4	1.173/4/7
ANXA2	Annexin A2	0.4317/21/23	0.1666/8/8	2.0875/14/16	1.2723/18/18
ANXA4	Annexin A4	0.578/1/1		2.5252/2/2	1.5649/6/6
ANXA6	Annexin A6	0.132/7/7	0.0816/6/6	2.7491/6/6	1.3958/7/7
ARI4B	AT-rich interactive domain-containing protein 4B	0.1797/2/2			133.3/1/1
ARPC4	Actin-related protein 2/3 complex subunit 4	0.3164/2/2	0.298/2/2	4.0387/3/3	
ARRB1	Beta-arrestin-1	0.3935/1/1			1.2/1/1
ASCC3	Activating signal cointegrator 1 complex subunit 3		0.0002/1/1		4.7205/1/2
AT2C1	Calcium-transporting ATPase type 2C member 1	0.3569/1/1			1.629/1/1
ATAD2	ATPase family AAA domain-containing protein 2	0.7275/5/6	0.3777/1/1		8.775/1/1
ATX10	Ataxin-10	0.6603/2/2		1.0063/1/5	
BCORL	BCL-6 corepressor-like protein 1	0.4972/2/2			3.266/1/1
CALD1	Caldesmon	0.2418/2/2	0.491/1/1		1.4977/2/2
CATC	Dipeptidyl peptidase 1	0.0343/1/2		2.329/1/1	
CAV1	Caveolin-1 OS=Homo sapiens GN=CAV1 PE=1 SV=4	0.5884/2/2			3.225/1/1
CBS	Cystathionine beta-synthase	0.5551/2/2		1.0214/3/5	
CCAR1	Cell division cycle and apoptosis regulator protein 1		0.5382/3/3		1.5844/4/4
CD44	CD44 antigen	0.6967/1/4	0.2408/1/1	2.2396/4/4	1.269/4/5
CENPF	Centromere protein F		0.0541/4/5		2.096/1/1
CF120	UPF0669 protein C6orf120	0.1204/1/1			2.1289/1/1
CHD4	Chromodomain-helicase-DNA-binding protein 4	0.7135/29/29			1.8152/3/3
CHSTE	Carbohydrate sulfotransferase 14	0.0001/1/1			110.7/1/1
CK5P2	CDK5 regulatory subunit-associated protein 2		0.0012/1/1		178.4/1/1
CK5P3	CDK5 regulatory subunit-associated protein 3	0.4037/1/3			1.236/4/4
CMTR1	Cap-specific mRNA (nucleoside-2'-O-)-methyltransferase 1	0.7009/2/2		4.002/1/1	
COBL	Protein cordon-bleu	0.3/1/1	0.1735/1/1		1.5899/2/2
COBL1	Cordon-bleu protein-like 1	0.7396/1/1			1.3172/1/1
COR1B	Coronin-1B	0.2592/5/5	0.0277/1/1	2.2832/3/3	2.1327/3/3
COR1C	Coronin-1C	0.1418/7/7	0.0432/3/3	25.9097/5/5	1.335/6/6
COX41	Cytochrome c oxidase subunit 4 isoform 1, mitochondrial	0.6916/2/4			3.426/1/1
CP250	Centrosome-associated protein CEP250		0.0025/1/1		1.3936/1/3
CP2S1	Cytochrome P450 2S1	0.0002/1/1			1.551/1/1

Acce-ssion	Protein name	Nuc1	Nuc2	Cyto1	Cyto2
CP51A	Lanosterol 14-alpha demethylase	0.1113/1/1			1.285/4/4
CPNE3	Copine-3	0.4697/2/2		2.284/3/3	
CPSF1	Cleavage and polyadenylation specificity factor subunit 1	0.2945/10/10	0.1265/4/4		3.0957/2/2
CPSF2	Cleavage and polyadenylation specificity factor subunit 2	0.2228/4/5	0.1982/2/2	2.005/1/1	4.5298/6/6
CPSF3	Cleavage and polyadenylation specificity factor subunit 3	0.3349/3/3			2.292/1/1
CRIP2	Cysteine-rich protein 2	0.342/2/2			1.1927/2/2
CRNL1	Crooked neck-like protein 1	0.5663/5/5	0.0714/1/1	11.3733/1/1	
CSK	Tyrosine-protein kinase CSK	0.4442/1/1		11.4686/2/2	
CSRP1	Cysteine and glycine-rich protein 1	0.1871/2/2		3.4413/5/5	1.6145/1/1
CSTF1	Cleavage stimulation factor subunit 1	0.2928/5/5		6.4939/3/3	2.0937/2/2
CSTF3	Cleavage stimulation factor subunit 3	0.5483/5/5	0.3508/2/2	10.25/1/1	7.0256/4/4
CTG1B	Cancer/testis antigen 1	0.0017/1/1			61.86/1/1
CYTSB	Cytospin-B	0.1754/2/2			1.3204/2/2
DAZP1	DAZ-associated protein 1	0.3577/2/2			1.1738/2/3
DBLOH	Diablo homolog, mitochondrial	0.2402/1/1			1.364/3/3
DC1L2	Cytoplasmic dynein 1 light intermediate chain 2	0.0053/1/1		2379.5397/1/1	
DDX17	Probable ATP-dependent RNA helicase DDX17	0.3948/22/22	0.3764/5/6	1.9736/8/8	
DESM	Desmin	0.3358/1/6		2.5665/4/4	25.9409/2/2
DHX9	ATP-dependent RNA helicase A	0.2869/32/34	0.2458/8/9	2.2561/8/9	1.6309/18/18
DIDO1	Death-inducer obliterator 1		0.5664/4/4		1.4009/3/3
DJB11	DnaJ homolog subfamily B member 11	0.4968/3/6			7.8136/3/3
DREB	Drebrin	0.2133/9/9	0.1965/3/3	3.1428/3/3	1.2084/4/4
DSC2	Desmocollin-2	0.476/1/1			1.385/1/1
DX39A	ATP-dependent RNA helicase DDX39A	0.5005/5/10		13.5955/6/6	
DX39B	Spliceosome RNA helicase DDX39B	0.6418/6/12		8.5124/7/7	
DZIP1	Zinc finger protein DZIP1	0.0205/1/1		18.23/1/1	
ELAV1	ELAV-like protein 1	0.2898/14/14	0.3304/1/1		1.377/3/4
ELAV2	ELAV-like protein 2	0.1041/3/4			1.295/1/1
FAF2	FAS-associated factor 2	0.0444/1/2		447.1/1/1	2.2276/5/5
FIP1	Pre-mRNA 3'-end-processing factor FIP1	0.2878/11/11	0.121/1/1		3.7514/4/4
FLNA	Filamin-A	0.2329/56/59	0.044/22/22	3.6386/50/50	1.7896/50/52
FLNB	Filamin-B	0.266/36/37	0.0552/7/7	2.113/27/27	1.2044/38/43
FLOT1	Flotillin-1	0.4573/6/6	0.1824/1/1		1.4146/2/2

Acce-ssion	Protein name	Nuc1	Nuc2	Cyto1	Cyto2
FLOT2	Flotillin-2		0.161/1/1	2.8295/2/2	
GLYM	Serine hydroxymethyltransferase, mitochondrial	0.524/2/13		2.9321/4/5	3.0969/10/11
GPTC4	G patch domain-containing protein 4		0.5773/3/3	2.7978/1/1	
H2AY	Core histone macro-H2A.1		0.3803/6/9		2.9678/2/2
HACD3	Very-long-chain (3R)-3-hydroxyacyl-CoA dehydratase 3	0.7072/1/1		5.9696/2/2	1.5852/4/4
HAKAI	E3 ubiquitin-protein ligase Hakai	0.3351/1/1			8.036/1/1
HAUS4	HAUS augmin-like complex subunit 4	0.0423/1/1			57.61/1/1
HCFC1	Host cell factor 1	0.5818/14/15		2.1768/1/1	
HDAC1	Histone deacetylase 1	0.504/6/6			1.694/1/2
HMGN5	High mobility group nucleosome-binding domain-containing protein 5	0.5022/3/5			1.281/1/1
HMOX2	Heme oxygenase 2	0.2554/1/1			2.454/1/1
HNRPK	Heterogeneous nuclear ribonucleoprotein K	0.6974/18/20	0.3529/8/8	2.0237/13/13	
HNRPL	Heterogeneous nuclear ribonucleoprotein L	0.4883/15/18	0.4397/4/4	4.6695/3/3	3.1403/6/6
HNRPM	Heterogeneous nuclear ribonucleoprotein M	0.1427/22/22	0.0963/10/10	3.1112/2/2	1.8638/9/9
HNRPR	Heterogeneous nuclear ribonucleoprotein R		0.414/6/6	2.5436/7/7	1.7018/7/9
HS12A	Heat shock 70 kDa protein 12A		0.3411/1/1		162.5/1/1
HS71L	Heat shock 70 kDa protein 1-like	0.7175/5/9		2.9845/6/12	
IKIP	Inhibitor of nuclear factor kappa-B kinase-interacting protein	0.0036/1/1			1.28/1/1
ILVBL	Acetolactate synthase-like protein	0.7452/1/1			1.7368/5/5
ISY1	Pre-mRNA-splicing factor ISY1 homolog	0.7378/3/3	0.5365/2/2		1.2502/2/2
ITPR2	Inositol 1,4,5-trisphosphate receptor type 2	0.7227/3/3		6.085/1/1	1.3984/4/5
ITPR3	Inositol 1,4,5-trisphosphate receptor type 3	0.6375/11/11		6.085/1/1	1.3919/5/7
IWS1	Protein IWS1 homolog	0.2619/2/2			1.1899/1/2
JPH1	Junctophilin-1	0.0014/1/1			1.187/1/1
KANL1	KAT8 regulatory NSL complex subunit 1		0.0941/1/1	50.79/1/1	
KDIS	Kinase D-interacting substrate of 220 kDa	0.1464/1/1			1.1857/2/2
KHDR1	KH domain-containing, RNA-binding, signal transduction-associated protein 1	0.3958/9/10			1.4948/3/3
KI20A	Kinesin-like protein KIF20A	0.5269/4/6			39.88/1/1
KI67	Antigen KI-67		0.5479/19/21		2.0034/3/6

Acce-ssion	Protein name	Nuc1	Nuc2	Cyto1	Cyto2
L2GL2	Lethal(2) giant larvae protein homolog 2	0.0454/1/1		3.2906/2/2	1.1879/2/2
LAMB1	Laminin subunit beta-1		0/1/1		1.3429/1/1
LAP2A	Lamina-associated polypeptide 2, isoform alpha	0.6326/10/16		4.0755/3/3	2.0451/2/3
LAS1L	Ribosomal biogenesis protein LAS1L	0.7405/3/7			1.6753/1/1
LBR	Lamin-B receptor	0.5617/6/6	0.071/1/1		2.069/1/1
LCA5L	Lebercilin-like protein	0.0248/1/1			6100000000/1/1
LETM1	LETM1 and EF-hand domain-containing protein 1, mitochondrial	0.3333/2/3		15.45/1/1	9.1652/2/2
LIMA1	LIM domain and actin-binding protein 1	0.4822/14/16	0.0364/3/3	2.6793/2/3	
LMBD2	LMBR1 domain-containing protein 2		0.011/1/1		1.279/1/1
LYAR	Cell growth-regulating nucleolar protein	0.7084/4/4	0.4792/2/2		2.723/3/3
LYRIC	Protein LYRIC	0.6414/2/5		7.173/1/1	1.514/4/5
MACD1	O-acetyl-ADP-ribose deacetylase MACROD1		0.452/2/2		2.1598/1/1
MATR3	Matrin-3	0.2173/22/22	0.27/8/9	4.1396/3/3	2.0742/12/12
MCE1	mRNA-capping enzyme		0/1/1		3.036/1/1
MDN1	Midasin	0.684/2/8			1.5617/1/5
MESD	LDLR chaperone MESD	0.1304/1/2		2.876/1/1	
MINT	Msx2-interacting protein	0.5245/3/11	0.5314/4/5		2.084/1/1
MS18A	Protein Mis18-alpha	0.2266/1/1			1.439/1/1
MTA2	Metastasis-associated protein MTA2	0.5761/14/16	0.3655/5/5	353.4703/4/4	1.7301/3/5
MTA3	Metastasis-associated protein MTA3	0.5277/6/6	0.3368/1/1	2.428/1/1	2.876/1/1
MYH14	Myosin-14	0.223/2/2			1.3102/3/4
MYO1C	Unconventional myosin-Ic O	0.249/13/13		8.3738/6/6	
MYO6	Unconventional myosin-VI	0.1233/4/4			2.9159/4/5
NCOA5	Nuclear receptor coactivator 5	0.4769/6/7	0.5738/3/3		2.0237/1/1
NEB1	Neurabin-1	0.2712/2/2			1.287/1/1
NECP2	Adaptin ear-binding coat-associated protein 2	0.5283/1/1		2.869/1/1	
NLE1	Notchless protein homolog 1		0.4597/1/1		1.4582/1/2
NOLC1	Nucleolar and coiled-body phosphoprotein 1		0.5708/5/5		1.9169/1/1
NONO	Non-POU domain-containing octamer-binding protein	0.2521/20/21	0.144/8/9	5.015/2/2	1.9679/5/5
NOP58	Nucleolar protein 58		0.2477/5/6		1.762/3/3
NU205	Nuclear pore complex protein Nup205		0.3089/3/3		1.4282/3/3
NUP50	Nuclear pore complex protein	0.5979/9/11	0.3688/2/2		1.4983/4/5

Acce-ssion	Protein name	Nuc1	Nuc2	Cyto1	Cyto2
	Nup50				
NUSAP	Nucleolar and spindle-associated protein 1		0.5057/1/1		1.9285/2/4
OAT	Ornithine aminotransferase, mitochondrial	0.1563/1/3			2.9896/4/4
ODR4	Protein odr-4 homolog	0.7305/1/1			1.3468/1/1
OGT1	UDP-N-acetylglucosamine--peptide N-acetylglucosaminyltransferase 110 kDa subunit	0.5653/2/2	0.5655/1/1	47.43/1/1	26.1288/2/7
P66A	Transcriptional repressor p66-alpha	0.3862/7/7	0.5681/2/2		2.039/1/1
P66B	Transcriptional repressor p66-beta		0.4723/2/2		1.2926/1/1
PA24A	Cytosolic phospholipase A2	0.3419/3/3		13.4155/2/2	
PABP2	Polyadenylate-binding protein 2	0.5335/7/7	0.2987/2/2	2.481/1/1	1.1887/3/3
PALLD	Palladin	0.2484/4/4	0.245/1/1		1.2619/3/3
PEO1	Twinkle protein, mitochondrial	0.4996/2/2			2.743/1/1
PEPL	Periplakin	0.2069/9/9			1.5202/2/3
PERI	Peripherin		0.024/1/2	2.3328/2/2	1.5297/1/1
PHC2	Polyhomeotic-like protein 2	0.694/1/2			1.316/1/1
PHF14	PHD finger protein 14	0.3017/5/8			3.579/1/1
PHF3	PHD finger protein 3	0.6633/7/8			1.7016/1/2
PININ	Pinin		0.3885/3/3	2.962/1/1	2.576/1/1
PLD3	Phospholipase D3	0.0074/1/1		550.4/1/1	
PLEC	Plectin	0.2751/190/196	0.1086/72/74	4.4278/42/47	2.7159/77/79
PLOD1	Procollagen-lysine,2-oxoglutarate 5-dioxygenase 1		0.5246/2/2	32.0162/4/4	
PLOD2	Procollagen-lysine,2-oxoglutarate 5-dioxygenase 2	0.7113/2/7		4.0662/2/2	
PLOD3	Procollagen-lysine,2-oxoglutarate 5-dioxygenase 3	0.5699/10/11	0.4759/2/2	3.154/5/5	1.1828/8/11
PLST_	Plastin-3	0.5812/2/2		2.2255/6/9	
PP1RA	Serine/threonine-protein phosphatase 1 regulatory subunit 10	0.4128/7/7			1.2322/1/2
PR40A	Pre-mRNA-processing factor 40 homolog A	0.7428/6/11	0.5401/2/2		1.818/1/1
PRDBP	Protein kinase C delta-binding protein	0.4753/1/1		2.256/1/1	2.8853/2/2
PRP17	Pre-mRNA-processing factor 17	0.6081/6/6		7.224/1/1	
PRP8	Pre-mRNA-processing-splicing factor 8	0.6147/30/45			1.3645/29/30
PSIP1	PC4 and SFRS1-interacting protein		0.4043/7/7		15.57/1/1
PSPC1	Paraspeckle component 1	0.4501/10/12	0.2438/1/1	9.3991/3/3	2.0014/2/2
PTBP1	Polypyrimidine tract-binding	0.3694/17/18		3.8305/8/8	

Acce-ssion	Protein name	Nuc1	Nuc2	Cyto1	Cyto2
	protein 1				
PTBP3	Polypyrimidine tract-binding protein 3	0.4766/4/6		230.0245/2/2	
PTPRB	Receptor-type tyrosine-protein phosphatase beta		0/1/1	33.07/1/1	
PUR2	Trifunctional purine biosynthetic protein adenosine-3	0.6698/4/4		2.2445/10/12	
PWP2	Periodic tryptophan protein 2 homolog		0.2552/4/4		4.76/1/1
PXDN	Peroxidasin homolog	0.7407/1/1			1.2256/1/1
QSOX2	Sulfhydryl oxidase 2	0.0009/1/1			3.205/1/1
RAE1L	mRNA export factor		0.193/1/1	2.406/1/1	
RAGP1	Ran GTPase-activating protein 1	0.5214/13/15		2.3872/3/3	1.3636/6/6
RALY	RNA-binding protein Raly		0.5137/2/2	1/1/33	2.03/1/1
RBM14	RNA-binding protein 14	0.2211/13/13	0.0798/1/1		1.6308/2/2
RBM15	Putative RNA-binding protein 15	0.735/8/13	0.4961/3/3		1.4192/6/6
RBM25	RNA-binding protein 25	0.6573/9/13			2.7275/4/4
RBM28	RNA-binding protein 28		0.1884/5/5		1.9047/1/1
RBM33	RNA-binding protein 33	0.7447/1/1	0.0006/2/2		204.7744/2/2
RBMX	RNA-binding motif protein, X chromosome	0.7064/13/15	0.285/1/1	6.884/1/1	3.2891/5/5
RBP2	E3 SUMO-protein ligase RanBP2	0.4485/31/38	0.3809/9/10	12.0081/4/4	1.5007/12/13
REPS1	RalBP1-associated Eps domain-containing protein 1		0/1/1	2.191/1/1	
RGPD8	RANBP2-like and GRIP domain-containing protein 8	0.6834/4/6			2.1672/2/2
RING1	E3 ubiquitin-protein ligase RING1	0.5252/4/4			1.285/1/1
RL38	60S ribosomal protein L38	0.0539/2/2		4.032/2/2	1.761/1/1
RLF	Zinc finger protein Rlf	0.1473/2/3			1.407/1/1
RNPS1	RNA-binding protein with serine-rich domain 1	0.5421/3/6			1.714/1/1
ROA0	Heterogeneous nuclear ribonucleoprotein A0	0.6212/9/11		3.2755/5/5	
ROA1	Heterogeneous nuclear ribonucleoprotein A1	0.5264/14/15	0.0832/6/6	4.5871/5/5	1.3267/8/10
ROA2	Heterogeneous nuclear ribonucleoproteins A2/B1	0.543/17/19	0.3519/8/10	2.9374/7/7	2.2725/11/11
RPA1	DNA-directed RNA polymerase I subunit RPA1		0.5122/6/7		3.0331/3/3
RPA2	DNA-directed RNA polymerase I subunit RPA2	0.5037/4/5	0.397/2/2		2.677/1/1
RPB3	DNA-directed RNA polymerase II subunit RPB3	0.4661/2/3	0.2495/1/1		1.2223/3/3
RPR1A	Regulation of nuclear pre-mRNA domain-containing protein 1A	0.4859/1/1			5.688/1/1

Acce-ssion	Protein name	Nuc1	Nuc2	Cyto1	Cyto2
RPR1B	Regulation of nuclear pre-mRNA domain-containing protein 1B	0.1918/5/5	0.1668/2/2	2.566/1/1	
RPRD2	Regulation of nuclear pre-mRNA domain-containing protein 2	0.4327/7/9	0.2623/1/1	4.823/1/1	
RRP12	RRP12-like protein		0.5659/6/8	2.2896/1/1	1.7852/8/8
RSBN1	Round spermatid basic protein 1	0.3442/5/5	0.0824/1/1	923.3/1/1	
RT05	28S ribosomal protein S5, mitochondrial	0.1371/1/1			4.8673/2/2
RT11	28S ribosomal protein S11, mitochondrial	0.1581/1/1			2.3505/1/1
RU17	U1 small nuclear ribonucleoprotein 70 kDa		0.3888/4/4	3.381/1/1	1.203/4/5
RU1C	U1 small nuclear ribonucleoprotein C	0.3619/1/1		2.134/1/1	
RU2A	U2 small nuclear ribonucleoprotein A'	0.6723/7/8	0.5741/4/4		1.7117/6/6
RUXF	Small nuclear ribonucleoprotein F	0.577/2/2	0.2633/1/1	2.1112/1/1	
RUXGL	Putative small nuclear ribonucleoprotein G-like protein 15	0.4802/2/2	0.4144/1/1		1.2576/2/2
S10AA	Protein S100-A10	0.2157/1/1	0.1809/1/1	4.212/1/1	
S38AA	Putative sodium-coupled neutral amino acid transporter 10	0.0033/1/1			1.69/1/1
SAFB1	Scaffold attachment factor B1	0.5182/15/17	0.2757/6/6	6.238/4/4	3.6845/4/4
SAFB2	Scaffold attachment factor B2		0.3037/7/7	5.1625/2/2	3.5091/3/3
2-Sep	Septin-2	0.74/9/12		3.0232/4/4	
6-Sep	Septin-6	0.6843/4/4		2.2522/2/2	1.1818/2/2
7-Sep	Septin-7	0.633/8/8		3.2879/6/6	
9-Sep	Septin-9	0.6608/12/15		1.9852/2/2	
SF3A1	Splicing factor 3A subunit 1	0.5655/11/19	0.4464/8/9	3.1441/1/1	1.3703/11/12
SF3B1	Splicing factor 3B subunit 1	0.7293/23/31	0.5508/11/11	5.4408/3/3	1.9732/24/24
SF3B3	Splicing factor 3B subunit 3		0.4651/5/5		1.1912/15/16
SF3B5	Splicing factor 3B subunit 5		0.2511/1/1		1.364/1/1
SF3B6	Splicing factor 3B subunit 6	0.2043/3/3			2.2772/3/3
SFPQ	Splicing factor, proline- and glutamine-rich	0.372/26/26	0.0761/6/6	6.0995/8/8	2.5987/7/7
SIN3A	Paired amphipathic helix protein Sin3a	0.4538/10/10			1.503/1/1
SK2L2	Superkiller viralicidic activity 2-like 2	0.6922/9/11		2.1144/2/2	
SKAP	Small kinetochore-associated protein	0.0016/1/1	0.1693/1/1		73.28/1/1
SMD1	Small nuclear ribonucleoprotein Sm D1	0.224/3/3		14952.4839/1/1	

Acce-ssion	Protein name	Nuc1	Nuc2	Cyto1	Cyto2
SMRC1	SWI/SNF complex subunit SMARCC1		0.4367/4/5		1.832/1/1
SMRC2	SWI/SNF complex subunit SMARCC2		0.476/5/5		1.628/3/3
SNR27	U4/U6.U5 small nuclear ribonucleoprotein 27 kDa protein	0.6367/2/3			1.559/1/1
SNR40	U5 small nuclear ribonucleoprotein 40 kDa protein	0.3625/5/7	0.4333/1/1		1.4535/4/4
SNW1	SNW domain-containing protein 1		0.1738/1/1		18.4584/2/4
SON	Protein SON	0.5085/20/22	0.1981/4/5		7.13/1/1
SPAS2	Spermatogenesis-associated serine-rich protein 2	0.4502/2/2			1.228/1/1
SPF27	Pre-mRNA-splicing factor SPF27		0.4125/3/3	2.997/1/1	
SPT6H	Transcription elongation factor SPT6	0.1824/20/20	0.3019/5/5	6.2192/3/3	1.2091/12/17
SPTB2	Spectrin beta chain, non-erythrocytic 1	0.1666/54/55	0.095/29/32	2.8963/15/15	
SPTN1	Spectrin alpha chain, non-erythrocytic 1	0.1479/82/83	0.0281/47/47	2.3006/26/28	1.4219/33/36
SPTN2	Spectrin beta chain, non-erythrocytic 2	0.2107/17/17	0.0779/9/9		1.8848/8/8
SR140	U2 snRNP-associated SURP motif-containing protein	0.7179/5/6	0.4949/3/3		1.6025/5/5
SRRM2	Serine/arginine repetitive matrix protein 2	0.5706/29/31	0.1747/2/2		1.5048/6/7
SRSF6	Serine/arginine-rich splicing factor 6	0.5194/11/12	0.4093/3/3		1.3997/1/2
SRSF7	Serine/arginine-rich splicing factor 7		0.5717/2/2		1.3605/4/4
SUMO1	Small ubiquitin-related modifier 1	0.4085/1/1		2.798/1/1	
SURF4	Surfeit locus protein 4	0.0254/1/2			1.1854/3/3
SYF1	Pre-mRNA-splicing factor SYF1	0.6762/7/7	0.3475/4/4		1.4683/7/7
SYMPK	Symplekin	0.6877/4/4	0.2639/1/1	2.2432/1/1	1.6576/4/4
SYNE2	Nesprin-2	0.4411/8/12	0.3828/2/2	2.539/1/1	1.42/1/1
TADBP	TAR DNA-binding protein 43	0.5841/6/6		2.437/2/2	
TBL3	Transducin beta-like protein 3		0.5119/5/6		1.4917/4/4
TCOF	Treacle protein		0.4322/10/10		1.2528/3/4
TDIF2	Deoxynucleotidyltransferase terminal-interacting protein 2		0.576/3/3		1.4828/2/2
TGON2	Trans-Golgi network integral membrane protein 2		0.3661/1/1		1.295/1/1
THIL	Acetyl-CoA acetyltransferase, mitochondrial		0.4333/1/2	2.576/1/1	3.3883/5/5
TIM13	Mitochondrial import inner membrane translocase subunit	0.0354/1/1			1.7711/1/1

Acce-ssion	Protein name	Nuc1	Nuc2	Cyto1	Cyto2
	Tim13				
TIM8A	Mitochondrial import inner membrane translocase subunit Tim8 A	0.6545/1/1			1.739/1/1
TM165	Transmembrane protein 165	0.0001/1/1			1.917/1/1
TM256	Transmembrane protein 256	0.2387/1/1			4.9234/1/1
TOP3A	DNA topoisomerase 3-alpha	0.6039/2/3	0.2948/1/1		1.48/1/1
TP53B	Tumor suppressor p53-binding protein 1		0.5765/5/5		1.2548/1/2
TPR	Nucleoprotein TPR		0.5281/15/17		1.5198/16/17
TR150	Thyroid hormone receptor-associated protein 3	0.5188/17/19	0.3023/5/6		2.0865/3/3
TRIO	Triple functional domain protein		0.002/2/2		1.1717/1/2
TSG10	Testis-specific gene 10 protein	0.2521/1/1			2810000000 /1/1
U2AF1	Splicing factor U2AF 35 kDa subunit	0.7001/1/2		2.025/1/2	
UHRF1	E3 ubiquitin-protein ligase UHRF1	0.6272/17/19			1.2873/2/2
UTRO	Utrophin	0.1949/1/1			1.2501/4/5
VDR	Vitamin D3 receptor	0.7047/1/1			18.37/1/1
VIME	Vimentin		0.1975/6/8	2.9181/24/24	1.601/28/30
WDR1	WD repeat-containing protein 1	0.4185/2/2		2.0342/7/7	
WDR33	pre-mRNA 3' end processing protein WDR33	0.4458/5/6	0.2841/1/1		4.767/1/1
WDR61	WD repeat-containing protein 61	0.069/2/2		3.0835/4/4	
YKT6	Synaptobrevin homolog YKT6	0.5085/2/2		3543.022/2/2	
ZCH18	Zinc finger CCCH domain-containing protein 18	0.5692/9/9	0.2302/2/2		2.1186/5/5
ZFR	Zinc finger RNA-binding protein	0.3949/10/12	0.2806/3/3		2.3523/3/3
ZN106	Zinc finger protein 106	0.0177/5/5	0.4239/1/1		2.728/1/1
ZN292	Zinc finger protein 292		0.0003/1/1	64.42/1/1	
ZN687	Zinc finger protein 687	0.1434/2/2	0.2096/1/1		1.919/1/1
ZNRF2	E3 ubiquitin-protein ligase ZNRF2		0.0072/1/1		1.8081/1/1
ZO2	Tight junction protein ZO-2	0.2389/2/2			1.3485/1/4